MATHEMATICAL MODELLING OF COVID-19(SARS-CoV-2) PANDEMIC

A THESIS SUBMITTED IN PARTIAL FULFILLMENT OF THE REQUIREMENTS FOR THE DEGREE OF DOCTOR OF PHILOSOPHY

JOAN LALDINPUII
MZU REGISTRATION NUMBER : 1501456
Ph.D. REGISTRATION NO: MZU/Ph.D./1701 of 05.11.2020

DEPARTMENT OF MATHEMATICS AND COMPUTER SCIENCE
SCHOOL OF PHYSICAL SCIENCES
AUGUST, 2024

MATHEMATICAL MODELLING OF COVID-19(SARS-CoV-2) PANDEMIC

by

JOAN LALDINPUII

Department of Mathematics and Computer Science

Supervisor: Prof. Jamal Hussain

Submitted

In partial fulfillment of the requirement of the Degree of Doctor of Philosophy in Mathematics of Mizoram University, Aizawl

Dedicated to,

To my brother and parents.

CERTIFICATE

This is to certify that the thesis entitled "**MATHEMATICAL MODELLING OF COVID-19(SARS-CoV-2) PANDEMIC** ", submitted by **Joan Laldinpuii** (Registration No: *MZU/Ph.D./1701 of 05.11.2020*), for the degree of Doctor of Philosophy (Ph.D) **Department of Mathematics and Computer Science** at **Mizoram University** embodies the record of original investigation carried out by him under my supervision. He has been duly registered and the thesis presented is worthy of being considered for the award of the Ph.D degree. This work has not been submitted for any degree at any other university.

. . . .

Prof. Jamal Hussain,

(Supervisor)

Place: Aizawl

Date: *12.08.2024*

i

DECLARATION

Mizoram University

August, 2024

I, **Joan Laldinpuii**, hereby declare that the subject matter of this thesis entitled "**MATHEMATICAL MODELLING OF COVID-19(SARS-CoV-2) PANDEMIC**" is the record of work done by me, that the contents of this thesis did not form basis of the award of any previous degree to me or to the best of my knowledge to anybody else, and that the thesis has not been submitted by me for any research degree in any other University/Institute.

This is being submitted to the Mizoram University for the degree of Doctor of Philosophy in Mathematics.

(JOAN LALDINPUII),

(Candidate)

(PROF. JAMAL HUSSAIN),	(PROF. M. SUNDARARAJAN),
(Supervisor)	(Head of Department)
Dept. Maths. and Comp. Sc.,	Dept. Maths. and Comp. Sc.,
Mizoram University, Mizoram.	Mizoram University, Mizoram.

ACKNOWLEDGEMENTS

foundly grateful for their enduring presence in my life.

Lastly, I am deeply thankful to the Lord Almighty for blessing me with health, strength, and guidance, enabling me to complete this research work.

Place: Aizawl

Date: *31 July 2024* (JOAN LALDINPUII)

PREFACE

The present thesis, entitled "Mathematical Modelling of COVID-19 (SARS-CoV-2) Pandemic," is a culmination of the research carried out by me under the supervision of Prof. Jamal Hussain. My name is Joan Laldinpuii, and throughout this work, I have sought to contribute to the understanding and control of the COVID-19 pandemic through mathematical modelling.

The COVID-19 pandemic, caused by the SARS-CoV-2 virus, has posed unprecedented challenges globally, affecting millions of lives and overwhelming healthcare systems. The necessity for effective intervention strategies has driven researchers to employ various approaches, including mathematical modeling, to predict and mitigate the spread of the virus. This thesis aims to explore and develop mathematical models that can offer insights into the dynamics of the virus and the impact of different control measures.

The thesis is structured into seven chapters, each building on the previous one to provide a comprehensive analysis of COVID-19 dynamics and intervention strategies.

Chapter 1: *General Introduction* This chapter presents a general introduction to the COVID-19 pandemic and the role of mathematical modelling in understanding its spread and control.

Chapter 2: *Mathematical Modeling of Vaccination Strategies Against SARS-CoV-2: Assessing Coverage and Efficacy* This chapter provided a comprehensive analysis of various vaccination strategies against SARS-CoV-2 using our proposed $SVEII_AR$ model. The results demonstrated that higher vaccination coverage and efficacy significantly reduce the basic reproduction number R_0 and the number of infections. The model highlights the critical role of vaccination in controlling the

spread of COVID-19, emphasizing that achieving high coverage and ensuring effective vaccines are paramount for mitigating the pandemic's impact.

Chapter 3: *Investigating SARS-CoV-2 Dynamics: The Role of Vaccination and Intervention Strategies* This chapter delved into the dynamics of SARS-CoV-2 by incorporating various intervention measures. The $SVEII_AR$ model revealed that combining vaccination with other interventions, such as social distancing and mask-wearing, substantially decreases the transmission rate. This synergistic approach underscores the necessity of a multifaceted strategy to effectively curb the virus's spread and protect public health.

Chapter 4: *Evaluating Precautionary Measures in COVID-19 Spread: A Delay Differential Equation Approach* This chapter explored the impact of precautionary measures on COVID-19 transmission using delay differential equations. The findings illustrated how delays in implementing measures can lead to significant increases in infection rates. Conversely, prompt and sustained interventions are critical in reducing transmission. The delay differential equation $SEII_AQR$ model provided valuable insights into the timing and effectiveness of various precautionary measures, offering a framework for timely decision-making in pandemic response.

Chapter 5: *Optimizing SARS-CoV-2 Control Measures: Innovative Reaction-Diffusion Techniques* This chapter focused on optimizing control measures for SARS-CoV-2. The model demonstrated how spatial heterogeneity and diffusion processes influence the spread of the virus. By incorporating these factors, the model provided a more nuanced understanding of disease dynamics, highlighting the importance of tailored interventions based on regional characteristics. This approach paves the way for more targeted and effective control strategies.

Chapter 6: *Analysis of a Novel Reaction-Diffusion Model for COVID-19: Evaluating Direct and Aerosol Transmission Strategies* In the final analytical chapter, a

novel reaction-diffusion $SEII_AHR$ model was developed to evaluate the dynamics of direct and aerosol transmission of COVID-19. The model revealed that aerosol transmission plays a significant role in the spread of the virus, especially in enclosed spaces. Strategies focusing on improving ventilation and air filtration, alongside traditional direct transmission interventions, were shown to be critical in mitigating overall transmission. This comprehensive model emphasizes the need for integrated approaches addressing both direct and aerosol pathways.

Chapter 7: *Conclusion* This chapter provides a summary and conclusions of the thesis, synthesizing the findings from each chapter and discussing their implications for future research and public health policy.

Throughout this thesis, I have aimed to offer valuable insights for public health policymakers, emphasizing the importance of a multifaceted approach in combating the pandemic. By integrating vaccination strategies, timely precautionary measures, and innovative modelling techniques, this research provides a robust framework for optimizing SARS-CoV-2 control and informs future responses to similar public health crises.

Contents

List of Figures

List of Tables

Chapter 1

General Introduction

1.1 Epidemiology

The term "epidemiology" originates from the Greek words "epi" (meaning "on" or "upon"), "demos" (meaning "people"), and "logos" (meaning "study"). Epidemiology is a branch of science that focuses on studying the incidence, distribution, and control of diseases within populations. This etymology suggests that the field of epidemiology pertains specifically to human populations. The title of "Father of Epidemiology" is frequently attributed to the Greek physician Hippocrates (460–377 B.C.E.), who identified the link between disease and the environment (Jones *et al.*, 1868). The term "epidemiology" seems to have been first used by the Spanish physician de Villalba in 1802 in his work "Epidemiologia Espanola" to describe the study of epidemics (Buck, 1988). Until the twentieth century, epidemiological studies primarily focused on infectious diseases. Among these, lower respiratory infections (such as pneumonia) and HIV are leading causes of death worldwide. Among these, lower respiratory infections (such as pneumonia) and HIV are leading causes of death worldwide. The recent COVID-19 pandemic has further exacerbated this issue, highlighting the vulnerabilities in global health systems. As we continue to battle these infectious diseases, the importance of robust healthcare infrastructure and preventative measures cannot be overstated. Addressing these challenges requires a concerted effort from the international community.

1.2   Basic Definitions in the Epidemiology

1. Epidemic:
An epidemic refers to a sudden increase in the number of cases of a disease above what is normally expected in a specific area or population. In the context of COVID-19, it would be a significant rise in cases within a localized region or community.

2. Pandemic:
A pandemic is an epidemic that has spread over multiple countries or continents, usually affecting a large number of people. COVID-19 was declared a pandemic by the World Health Organization (WHO) in March 2020 due to its widespread and sustained transmission globally.

3. Susceptible Individuals:
Susceptible individuals are those who have not yet been infected with the disease and do not have immunity against it. These individuals are at risk of contracting COVID-19 if they are exposed to the virus.

4. Exposed Individuals:
Exposed individuals are those who have come into contact with the disease but have not yet developed symptoms or tested positive for infection. They are in the period between exposure and the potential onset of symptoms. In mathematical models, it is often assumed that all exposed individuals will eventually develop the disease.

5. Asymptomatic Individuals:
Asymptomatic individuals are those who have been infected with the disease but do not exhibit any symptoms. Despite not showing symptoms, they can still spread the disease to others.

6. Infected Individuals and Infectious Individual:
If the pathogen takes hold in an exposed individual, that person becomes infected. Infected individuals who are capable of spreading the disease are referred to as infectious.

7. Recovered Individuals:
Recovered individuals are those who were previously infected with the disease and have since recovered, either by clearing the disease from their system or having developed immunity. They are no longer symptomatic and are not considered infectious.

8. Latent Period :
These are individuals who are infected but not yet capable of spreading the infection.
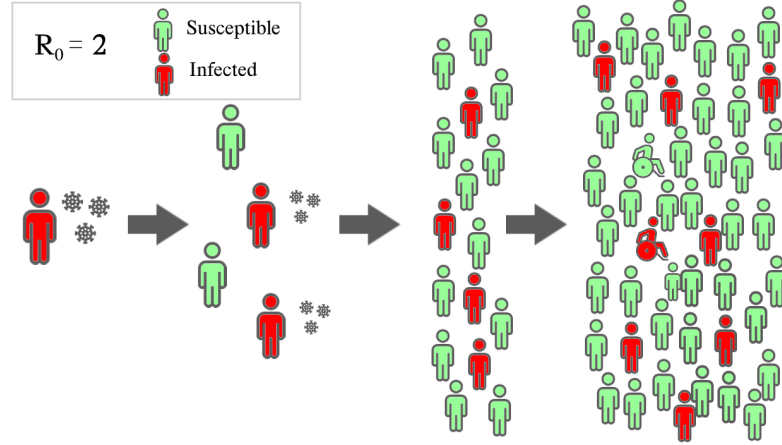
Figure 1.1: Illustration of Basic Reproduction Number when $R_0 = 2$

The latent period is the interval between the time of infection and the point at which the host can transmit the infectious agent to others. For COVID-19, this period can vary, but individuals may start being contagious before they exhibit symptoms.

9. Incubation Period :

The incubation period is the interval between being exposed to the virus and the appearance of symptoms. For COVID-19, this period usually spans from 2 to 14 days, with most individuals developing symptoms approximately 4 to 5 days after exposure.

10. Disease-Induced Mortality:

Disease-induced mortality refers to deaths directly caused by the infection. In the context of COVID-19, this represents the number of people who die as a direct consequence of contracting the virus, commonly measured by the case fatality rate (CFR), which is the ratio of confirmed cases that result in death.

11. Basic Reproduction Number:

In epidemiology, the basic reproduction number, often referred to as R_0, represents the average number of secondarily infected persons infected by one primary infected patient during the infectious period. This metric is crucial for understanding the potential spread of an infectious disease. If $R_0 < 1$, each infected person, on average, produces fewer than one new infection, leading to the eventual decline of the disease. Conversely, if $R_0 > 1$, each infected individual generates more than one new infection on average, allowing the disease to spread through the population. Figure 1.1 shows the illustration of Basic Reproduction number when $R_0 = 2$.

1.3 Epidemiology of SARS-CoV-2

Severe Acute Respiratory Syndrome Coronavirus-2 (SARS-CoV-2), the novel coronavirus responsible for the COVID-19 pandemic, is a highly infectious viral pathogen that has had a profound and far-reaching impact on global health, economies, and daily life. This virus, belonging to the Coronaviridae family, is characterized by its rapid transmission and ability to cause severe respiratory illness in humans. The epidemiology of SARS-CoV-2 encompasses the study of its transmission dynamics, infection rates, distribution patterns, and the effectiveness of public health interventions to mitigate its spread. Understanding the epidemiological characteristics of SARS-CoV2 is crucial for developing effective strategies for prevention, control, and treatment, thereby highlighting the ongoing need for comprehensive research and vigilant public health measures in the management of infectious diseases.

1.3.1 History

Coronavirus, one of the families of Coronaviradae started invading human civilization in the late 20th centuries, it was first discovered in the 1960s, and due to its crown-like spiked proteins found on its surface, it was named 'corona'. Over the years, coronaviruses have caused three significant outbreaks. In 2003, an outbreak occurred in China and was named 'Severe Acute Respiratory Syndrome' (SARS) outbreak, the case-fatality rate for SARS was 9.6 %, the virus infected a total of 8,098 individuals and 774 of these cases were fatal (Killerby et al., 2020). Saudi Arabia in 2012 and South Korea in 2015 were both affected by 'Middle East Respiratory Syndrome' (MERS) outbreak (Willman et al., 2019).

In late 2019, coronaviruses caused their fourth major outbreak, leading to a global crisis. This outbreak was first identified in Wuhan, the capital city of Hubei province in China (Cohen and Normile, 2020). On February 11th, 2020, the disease and its causative virus were officially named coronavirus disease 2019 (COVID-19) and severe acute respiratory syndrome coronavirus 2 (SARS-CoV-2), by the World Health Organization (WHO) DirectorGeneral, Dr Tedros Adhanom Ghebreyesus (Organization et al., 2020c).

The World Health Organization (WHO) designated SARS-CoV-2 as a "public health emergency of international concern" on January 30, 2020 (Y.-D. Li et al., 2020). The virus quickly spread to 113 countries. As of 10:00 AM CET on March

23, 2020, global data reported by national authorities indicated a total of 332,930 confirmed cases and 14,509 deaths due to SARS-CoV-2. The Western Pacific Region reported 95,637 confirmed cases and 3,473 deaths, while the European Region had 171,424 confirmed cases and 8,742 deaths. The South-East Asia Region reported 1,776 confirmed cases and 58 deaths, and the Eastern Mediterranean Region had 25,375 confirmed cases with 1,741 deaths. In the Region of the Americas, there were 37,016 confirmed cases and 465 deaths, and the African Region reported 990 confirmed cases and 23 deaths (Organization *et al.*, 2020a). In response to the rapid transmission of SARS-CoV-2, many governments implemented various lockdowns and social distancing measures to curb the spread of infections (Tobías, 2020). Despite these efforts, new infections continued to rise swiftly, overwhelming healthcare systems. This strain not only compromised the effective treatment of patients but also significantly impacted the physical and mental well-being of healthcare workers (Sanghera *et al.*, 2020).

The severe acute respiratory syndrome coronavirus (SARS-CoV) and the Middle East respiratory syndrome coronavirus (MERS-CoV) shares 79% (Y.-Z. Zhang and Holmes, 2020) and 50% (Adelman *et al.*, 2002) sequence similarity with the wild type of SARS-CoV-2, respectively. The fatality rates for SARS and MERS are approximately 10% and 35%, respectively. In contrast, SARS-CoV-2 has fatality rates that range from 0.1% to 18.1%, depending on the country (Johns Hopkins University of Medicine, March 2023). Furthermore, it is estimated that there were 14.83 million excess deaths due to the SARS-CoV-2 pandemic between January 2020 and December 2021 (Msemburi *et al.*, 2023).

Coronaviruses are categorized into four genera: $\alpha CoVs$, $\beta CoVs$, $\gamma CoVs$ and $\delta CoVs$ Among these, α and β coronaviruses infect only mammals, γ coronaviruses infect avian species, and δ coronaviruses can infect both mammals and birds (Naqvi *et al.*, 2020). SARS-CoV-2 is a novel beta coronavirus with an approximately 30 kb single-stranded positive-sense RNA genome that encodes six functional proteins: replicase (ORF1a/1b), spike protein (S), envelope (E), membrane (M), and nucleocapsid (N), along with seven interspersed non-structural proteins (M.-Y. Wang *et al.*, 2020). Figure 1.2 illustrates the structure of SARS-CoV-2. Many current vaccines include antigens targeting the virus's spike protein, while a few use whole inactivated virus (Creech *et al.*, 2021).

Signs and Symptoms
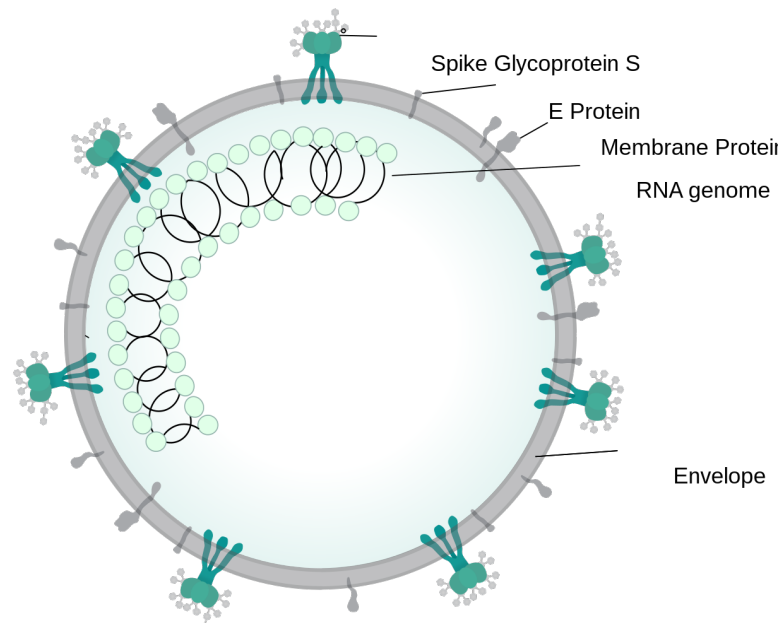
Figure 1.2: SARS-CoV-2 virion (https://en.wikipedia.org/wiki/ COVID-19).

COVID-19, caused by the SARS-CoV-2 virus, presents a wide range of symptoms that can vary significantly from person to person. Symptoms can appear 2-14 days after exposure to the virus and can range from mild to severe. Some individuals may remain asymptomatic but still carry and transmit the virus. Here is a detailed overview of the common and less common signs and symptoms associated with COVID-19:

1. **Common Symptoms**

   - Fever: Elevated body temperature, often accompanied by chills.

   - Cough: A persistent, dry cough is one of the hallmark symptoms.

   - Shortness of Breath: Difficulty breathing or a feeling of breathlessness.

   - Fatigue: Generalized tiredness or lack of energy.

   - Muscle or Body Aches: Pain or discomfort in muscles or joints.

   - Headache: Varying in intensity and frequency.

   - New Loss of Taste or Smell: A sudden change or loss in the ability to taste or smell.

   - Sore Throat: Pain or irritation in the throat.

   - Congestion or Runny Nose: Nasal congestion or increased nasal discharge.

- Nausea or Vomiting: Stomach discomfort leading to nausea or vomiting.

- Diarrhea: Frequent, loose, or watery stools.

2. **Less Common Symptoms**

- Skin Rashes: Various types of rashes, including COVID toes (red or purple discolouration of the toes).

- Conjunctivitis (Pink Eye): Inflammation or infection of the outer membrane of the eyeball and the inner eyelid.

- Loss of Appetite: Decreased desire to eat.

- Confusion: Cognitive impairment or delirium, especially in older adults.

- Chest Pain: Persistent pain or pressure in the chest.

3. **Severe Symptoms**

- Difficulty Breathing: Severe breathlessness or inability to catch breath.

- Persistent Chest Pain or Pressure: Constant pain or tightness in the chest.

- Bluish Lips or Face: A sign of low oxygen levels in the blood.

- New Confusion: Sudden onset of confusion or disorientation.

- Inability to Wake or Stay Awake: Severe fatigue or lethargy.

4. **Complications** COVID-19 can lead to serious complications, especially in individuals with underlying health conditions or those who are immunocompromised. These complications can include:

- Pneumonia: Infection that inflames the air sacs in the lungs.

- Acute Respiratory Distress Syndrome (ARDS): Severe lung damage leading to significant breathing difficulties.

- Thrombosis: Formation of blood clots in the veins and arteries.

- Multi-Organ Failure: Failure of multiple organ systems, which can be fatal.

- Septic Shock: A severe infection leading to dangerously low blood pressure and organ damage.

5. **Long-term Effects (Long COVID)** Some individuals continue to experience symptoms or develop new symptoms after the initial infection has cleared, a condition often referred to as "Long COVID" or "Post-Acute Sequelae of SARS-CoV-2 infection (PASC)." Common long-term effects include:

   - Fatigue

   - Shortness of breath

   - Joint pain

   - Chest pain

   - Cognitive issues, often described as "brain fog"

   - Difficulty sleeping

   - Loss of taste or smell

   - Depression or anxiety

1.3.2   Transmission

SARS-CoV-2 spreads through direct means such as droplet and human-to-human transmission, as well as indirect contact via contaminated objects and airborne contagion. Additionally, personal protective equipment (PPE) has been identified as a potential source of airborne infections (Y. Liu *et al.*, 2020). It has been noted previously that the primary mode of person-to-person transmission of SARS-CoV-2 is through respiratory droplets released when an infected individual coughs, sneezes, talks, or sings. These droplets, which are typically unable to travel more than six feet and linger in the air briefly, can contain intact and infectious SARS-CoV-2 particles less than five microns in diameter, capable of remaining suspended for up to three hours (Van Doremalen *et al.*, 2020). Hence, measures such as airborne isolation, room ventilation, and thorough disinfection, particularly in bathrooms, are crucial to mitigate aerosol transmission of the virus (Santarpia *et al.*, 2020).

COVID-19 can be contracted when a person touches a surface contaminated with SARS-CoV-2 and subsequently touches their eyes, nose, or mouth with contaminated hands (Lotfi *et al.*, 2020). Therefore, it is advisable to regularly wash hands thoroughly with soap and water or use hand sanitisers. The reported rates of contagion from individuals with symptomatic COVID-19 infection vary depending on

geographical location and the effectiveness of infection control measures. According to a collaborative report from the WHO and China, the rate of secondary COVID-19 infections ranged from one to five per cent among tens of thousands of confirmed cases in China (Lotfi *et al.*, 2020).

Similar to SARS-CoV, the virus may also spread through the oral-fecal route. RNA from SARS-CoV-2 has been found in the stool of patients with COVID-19 pneumonia (Holshue *et al.*, 2020), suggesting that sewage could potentially contribute to the transmission of the virus. Consequently, it is important to consider technical treatments like biosorbents that can capture and deactivate the virus (Núñez-Delgado, 2020).

SARS-CoV-2 has been found in the saliva of individuals who are infected (To *et al.*, 2020). This presence is thought to be linked to the fact that ACE2 receptors, which the virus uses to enter cells, are present in the epithelial cells that line the ducts of salivary glands (L. Liu *et al.*, 2011). These receptors serve as entry points for the virus, allowing it to infect and replicate within these cells, potentially contributing to the viral load present in saliva. This finding underscores the potential for saliva to serve as a route of transmission for SARS-CoV-2, particularly through activities such as coughing, sneezing, or talking that generate respiratory droplets containing the virus and saliva.

The RNA of the virus has been detected on various surfaces within the homes of individuals confirmed to have COVID-19, including door handles and cell phones (Han *et al.*, 2020). This discovery underscores the potential for infection through contact with contaminated surfaces. If individuals touch these surfaces and then touch their eyes, mouth, or nose, they may introduce the virus into their bodies, increasing the risk of contracting COVID-19. Therefore, meticulous hand hygiene and regular disinfection of commonly touched surfaces are essential practices to mitigate the spread of the virus in household settings and other environments where people congregate.

Studies have also tested patient urine for SARS-CoV-2 viral RNA, with pooled rates of RNA positivity around 5-6%. However, the duration of viral shedding in urine samples and the potential infectivity of urine are still uncertain (Chan *et al.*, 2020).

The debate over vertical transmission of SARS-CoV-2 continues; initial studies involving nine pregnant women with COVID-19 showed no transmission to their in-
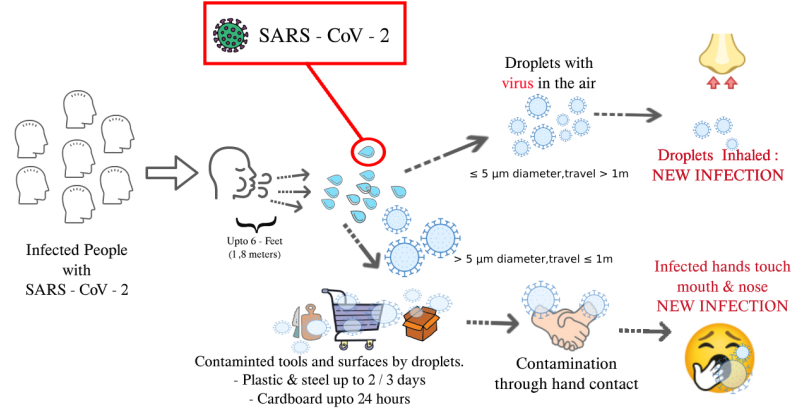
Figure 1.3: Transmission of SARS-CoV-2

fants. Additionally, SARS-CoV-2 was not detected in breast milk, indicating that there is no transmission through breastfeeding (H. Chen *et al.*, 2020). However, there have been reports of a newborn with elevated IgM antibodies against SARS-CoV-2 born to a COVID19-positive mother, suggesting possible in-utero infection despite negative PCR tests on nasopharyngeal swabs (Dong *et al.*, 2020).

Lastly, there is concern that the eyes could serve as a route of transmission for SARS-CoV-2. RNA from the virus was detected in ocular swabs from a confirmed COVID-19 patient, even when nasopharyngeal swabs tested negative by PCR. The virus isolated from ocular swabs was capable of infecting Vero E6 cells, indicating that ocular secretions might be infectious (Colavita *et al.*, 2020). While definitive evidence is lacking, wearing goggles is recommended when examining patients with suspected or confirmed COVID-19 (C. W. Lu *et al.*, 2020). Figure 1.3 shows different transmission of SARS-CoV-2.

1.3.3 Prevention and Vaccination

According to the World Health Organization's infection prevention and control strategies, standard precautions for all patients, which are also suitable for public prevention, include hand and respiratory hygiene, the use of appropriate personal protective equipment, safe injection practices, safe waste management, environmental cleaning, and sterilization of patient-care equipment (Organization *et al.*, 2020b). These strategies aim to reduce transmission rates and prevent outbreaks.

A. Mask-Wearing:

The use of face masks, particularly in indoor and crowded environments, has been proven to decrease virus transmission. According to the Centers for Disease Control and Prevention (CDC), universal mask-wearing can reduce the spread of COVID-19 by as much as 70% in community settings. High-quality masks, such as N95 respirators, provide the highest level of protection.

B. Social Distancing:

Maintaining physical distance, ideally at least 6 feet, is a critical measure to prevent person-to-person transmission. This practice is especially important in areas with high transmission rates.

C. Hand Hygiene:

Regular and thorough hand washing with soap and water for at least 20 seconds, or the use of hand sanitisers with at least 60% alcohol, is vital in minimizing the risk of infection. The World Health Organization (WHO) emphasizes that proper hand hygiene can decrease the likelihood of contracting respiratory infections, including COVID-19, by over 20% (Organization, 2023).

D. Ventilation:

Enhancing indoor ventilation reduces the concentration of airborne viral particles, thereby lowering the risk of transmission. Strategies include opening windows and doors, using exhaust fans, and deploying air purifiers with HEPA filters.

E. Testing and Contact Tracing:

Prompt testing and effective contact tracing are essential for identifying and isolating infected individuals to curb the spread of the virus. Rapid antigen tests and PCR tests are widely used, with PCR tests offering higher sensitivity and specificity. Effective contact tracing can help reduce the reproduction number.

COVID-19 Vaccine

In the history of vaccines, the development of COVID-19 vaccines has progressed at an unprecedented pace. There are 184 vaccine candidates in preclinical development and 104 in clinical stages (COVID, 19). Recent data show that 18 COVID-19 vaccines have been approved and are currently in use worldwide (COVID, 19), (Organization *et al.*, 2021). These vaccines fall into four main categories based on their platforms: 1. whole virus vaccines, 2. protein-based vaccines, 3. viral vector vaccines, and 4. nucleic acid vaccines (Nagy and Alhatlani, 2021).

The efficacy and effectiveness of the COVID-19 vaccines

The systematic review conducted by Ibrahim Mohammed et al. (Mohammed *et al.*,

2022) provides a comprehensive analysis of the efficacy and effectiveness of COVID-19 vaccines in reducing infection rates, disease severity, hospitalization, and mortality. Their findings indicate that the COVID-19 vaccines have significantly contributed to controlling the pandemic across various populations. Among the vaccines studied, the Pfizer/BioNTech vaccine emerged as the most effective, demonstrating over 90% effectiveness against infection, severe infection, hospitalization, and mortality after the second dose. Similarly, the Moderna vaccine showed over 80% effectiveness after the second dose for the same parameters. The AstraZeneca vaccine, while not extensively reported for effectiveness after the second dose, was found to be 80.7% efficacious against infection post-second dose and 74% effective after the first dose. The single-dose J and J vaccine exhibited over 60% effectiveness against infection, severe infection, and hospitalization. For the Sputnik, Novavax, and Sinovac vaccines, efficacy after the second dose was reported as 60.1% and 73.8%, respectively, with specific data on the Sputnik vaccine lacking.

The review highlights that the effectiveness of these vaccines can vary due to the presence of different viral variants in specific populations. Notably, the Pfizer/BioNTech vaccine showed high effectiveness against the B.1.1.7 and B.1.351 variants. Despite the overall high effectiveness of the vaccines, the authors emphasize the need for continued efforts to evaluate their performance against new and emerging variants. This ongoing assessment is crucial to ensure that vaccination strategies remain effective as the virus evolves. The findings of this review underscore the vital role that COVID-19 vaccines have played a role in mitigating the impact of the pandemic, particularly in preventing severe outcomes and reducing the burden on healthcare systems.

Global coverage of COVID-19 vaccination campaigns.

The rapid development, testing, and manufacturing of multiple effective vaccines against SARS-CoV-2 was a groundbreaking achievement in 2020. Historically, it has taken many years or even decades to develop a vaccine for a new pathogen. However, in the case of COVID-19, scientists developed several highly efficacious vaccines within a year. The current challenge is whether the global rollout of these vaccines can match the speed of their development and whether they can be administered quickly and equitably worldwide.

The 'Our World in Data' https://ourworldindata.org/ COVID-19 vaccination dataset offers a comprehensive public collection of global vaccination data. This dataset,
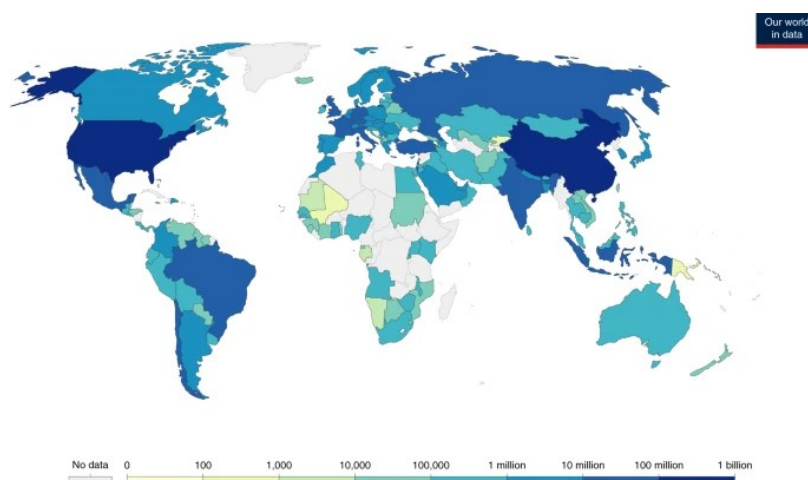
Figure 1.4: Total number of COVID-19 vaccine doses administered as of 7 April 2021(Mathieu *et al.*, 2021)

which has been consistently updated since its initial release on December 13, 2020, captures the progress of vaccination efforts worldwide. As more nations share their official vaccination data, the dataset continues to grow. By April 7, 2021, it included information from 169 countries.

The United Kingdom reported the first COVID-19 vaccinations outside of clinical trials on December 13, 2020. By April 7, 2021, 710 million doses had been administered globally, with 5% of the world's population having received at least one dose of an approved vaccine. This data underscores significant disparities in global vaccine distribution. Figure 1.4 illustrates the number of vaccine doses administered by each country, without adjusting for population size. 'Our World in Data'(Mathieu *et al.*, 2021) shows Cumulative Vaccine Doses Administered per 100 People, from the data we observe the cumulative total vaccine doses administered per 100 people across selected countries from December 13, 2020, to April 7, 2021. The key observations are:

Israel has the highest cumulative doses, approaching 120 doses per 100 people by early April 2021. United Arab Emirates, Chile, United Kingdom, Bahrain, and United States show significant progress, all-surpassing 50 doses per 100 people by early April 2021. Germany, Brazil, China, India, and Indonesia demonstrate slower vaccine rollout, with doses per 100 people not exceeding 20 by the same date.

Also, daily Vaccine Doses Administered per 100 People (7-Day Smoothed), for the same set of countries over the same period. Key observations include:

United States shows a sharp peak in daily doses administered, exceeding 1.5 doses per 100 people at its highest point. United Arab Emirates and United Kingdom also have significant peaks, although not as high as the United States. Other countries, including Brazil, Germany, India, and Indonesia, have relatively lower daily administration rates with less pronounced peaks.

Cumulative Vaccine Doses:

Israel leads significantly in the cumulative number of vaccine doses administered, followed by the United Arab Emirates and Chile. These countries have maintained high cumulative doses per 100 people, indicating a robust vaccination campaign. The United Kingdom, Bahrain, and the United States follow closely, demonstrating their prioritization of mass vaccination.

Daily Vaccine Doses:

The United States shows the most aggressive daily vaccination campaign at its peak, followed by the United Arab Emirates and the United Kingdom. This indicates a focused effort to maximize daily vaccination rates during critical periods. Other countries exhibit more moderate daily vaccination rates, reflecting either a slower rollout or logistical challenges.

The data reveal stark differences in vaccine rollout strategies and efficiencies among countries:

1. Israel's Success: Israel's high cumulative doses and consistent daily vaccination rates underscore its effective vaccination strategy. Factors contributing to this success include strong healthcare infrastructure, effective public communication, and a clear prioritization framework.

2. United States' Peaks: The sharp peaks in the United States' daily vaccination rates suggest periods of intensified vaccination efforts, possibly linked to increased vaccine availability and large-scale vaccination drives.

3. United Arab Emirates and United Kingdom: These countries also exhibit high cumulative and daily rates, reflecting well-coordinated vaccination campaigns.

4. Slower Rollouts in Other Countries: Germany, Brazil, China, India, and Indonesia show slower progress, both cumulatively and daily. These countries might face challenges such as vaccine supply constraints, distribution logistics, and vaccine hesitancy.

5. Strategic Implications: The variation in vaccination rates suggests the importance of tailored strategies. High-income countries with robust healthcare systems have

generally achieved higher rates, while middle and low-income countries may need international support and improved logistical planning.

By mid-2021, over three billion COVID-19 vaccine doses had been given globally, with 24% of the world's population having received at least one dose (Mathieu *et al.*, 2021). During this period, more than 40 million doses were being administered daily worldwide. Countries such as the United Kingdom, Chile, Uruguay, Israel, Bahrain, Hungary, Italy, Spain, Germany, the United States, and France had vaccinated at least 50% of their populations by mid-2021. Conversely, by the end of June 2021, only 1% of individuals in low-income countries had received a dose of the COVID-19 vaccine. In Africa, just 53 million doses had been administered (Mathieu *et al.*, 2021).

In conclusion, the data highlight the critical need for effective vaccine distribution strategies to ensure equitable and rapid global vaccination coverage. Understanding the successes and challenges faced by different countries can inform future public health initiatives and policies to manage ongoing and future pandemics.

1.3.4 Treatment

Depending on the severity of a patient's symptoms and the medical resources available in a region, various treatment sites may be chosen for observing and isolating patients. The general treatment protocols for different cases are as follows:

A. Asymptomatic cases: The primary treatment involves centralized quarantine for 14 days, with further monitoring by the local Public Health Department. If quarantined at home, household members should either stay in a different room or maintain a distance of at least 1 meter from the isolated person.

B. Suspected cases: Patients who are capable of self-care, under 65 years old, and without underlying conditions like respiratory or cardiovascular diseases or mental health issues should voluntarily go to a healthcare facility after providing informed consent. During quarantine observation, they should ideally stay in a single room and not leave it randomly.

C. Mild cases: If available, these patients are treated in a mobile cabin hospital, or at home if hospitalization is not feasible due to the healthcare system's heavy burden. They should be monitored and cared for by family members. If sharing a room, the space between beds should be at least 1.2 meters, and the room should have its own facilities. Family visits and additional nursing should be avoided.

D. Severe/critically ill cases: Patients initially diagnosed as critically ill should

be admitted to the Intensive Care Unit (ICU) immediately. Those whose condition worsens from mild to severe should be transferred to the critical observation and treatment area of a sheltered hospital after hospital triage and expert consultation, and subsequently to a designated hospital for treatment.

1.4   Mathematical Modelling

Mathematical modelling is a representation of the behaviour of real objects and phenomena in mathematics language. It is the best way to quantify the abstract behaviour of some real phenomena. It helps us to understand and explore the meaning of equations or functional relationships.

The objective of mathematical modelling is to analyze systems and make predictions, providing insight into real-world phenomena. This includes forecasting the future, preventing undesired outcomes, and understanding various natural and artificial phenomena. A model aids in explaining a system, studying the effects of different components, and predicting behaviour.

The modelling process, schematically depicted in Figure 1.5, involves translating a biological scenario into a mathematical problem. It typically begins with a detailed description of the processes, based on the scientist's knowledge of the system. Given the complexity of real-world phenomena, it is necessary to make numerous assumptions to simplify these into manageable equations. When translating real-world problems into mathematical equations, it is essential to have a specific purpose or biological question in mind. The verbal description of the system is then encoded into mathematical equations. These equations are solved and analyzed using various mathematical tools. The results are interpreted in layman's terms, and validation follows by comparing the data or results with the actual situation to refine the model or conclude the experiment.

Mathematical epidemiological models have been crucial for understanding infectious disease transmission and assessing the potential impacts of public health interventions. The foundations of mathematical modelling in epidemiology were established in the early 20th century, particularly through the work of (Ross, 1916), (Ross and Hudson, 1917a)(Ross and Hudson, 1917b),(Kermack and McKendrick, 1927), and (Kendall, 1956). Ross's pioneering 1916 study (Ross, 1916) was the first to apply mathematical techniques to analyze malaria transmission. This was further developed
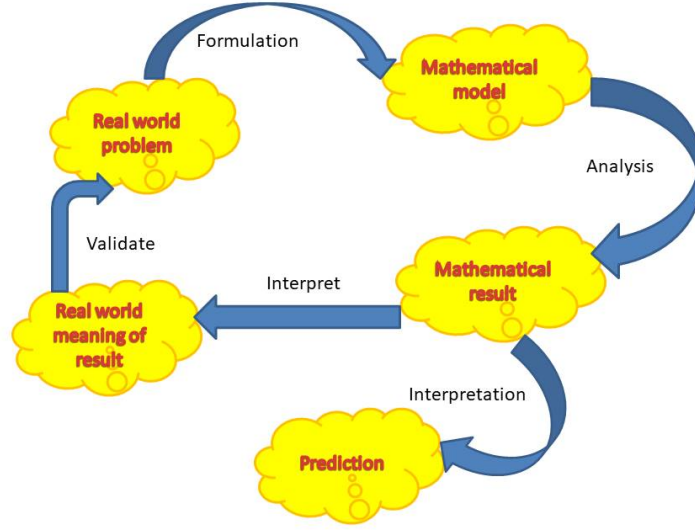
Figure 1.5: A Schematic representation of the Modeling process

by (Ross and Hudson, 1917a)(Ross and Hudson, 1917b), who utilized their models to propose effective mosquito control strategies. The historical evolution of this field is extensively reviewed by (Hethcote, 2000), (Bacaër, 2011), and (Brauer, 2017).

1.5 Classification of Epidemiological Model

The epidemiological Model is classified into two: Deterministic and Stochastic. Deterministic is divided into Discrete time and Continuous time. Hethcote (Hethcote, 1989) introduced three fundamental types of deterministic epidemiological models for infectious diseases: SIS Model, SIR Model with and without vital dynamics .

Deterministic and Stochastic Model : A deterministic model is one where the parameters and initial states of the variables uniquely determine every set of variable states. In contrast, stochastic models incorporate randomness, with variable states described by probability distributions.

Discrete-time and Continuous-time Model: Discrete models represent time or system states as distinct, separate values. In contrast, continuous models treat time and system states as flowing smoothly without interruption.

SIS Model

In an SIS epidemiological model, the total population is divided into two distinct
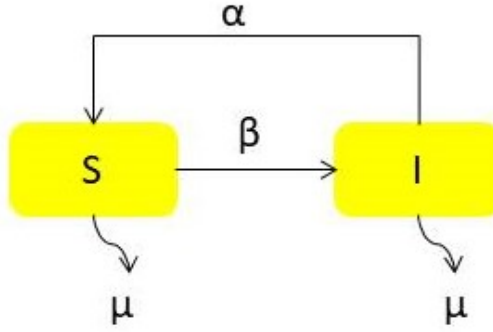
Figure 1.6: Flowchart of the simple SIS Epidemic Model

Figure 1.7: Flowchart of the simple SIR Epidemic Model

classes: Susceptible (S) and Infective (I). This model is used for diseases that do not confer immunity after infection. It is termed the SIS model because individuals move from the susceptible class to the infected class and then back to the susceptible class upon recovery, as seen in diseases such as influenza and malaria. The Flowchart for SIS Model is shown in Figure 1.6.

SIR Model

Kermack and McKendrick proposed SIR model in 1927 (Kermack and McKendrick, 1927). In an SIR epidemiological model, the total population is divided into three distinct classes: Susceptible (S), Infective (I), and Recovered (R). This model is useful for representing diseases that confer permanent immunity. Individuals move from the susceptible class to the infected class and then, upon recovery, to the recovered class. This model is applicable to many infectious diseases, including measles, mumps, and rubella. The Flowchart for SIS Model is shown in Figure 1.7.

SEIR Model

In this model by Carcione *et.al* (Carcione *et al.*, 2020), the total (initial) population, N_0, is categorized into four classes, namely, susceptible, $S(t)$, exposed, $E(t)$, infected-
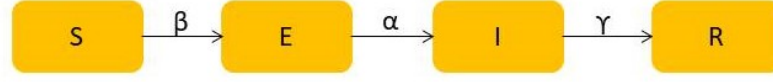
Figure 1.8: Flowchart of the simple $SEIR$ Epidemic Model

infectious, $I(t)$ and recovered, $R(t)$, where t is the time variable with vital dynamics i.e., including birth and death. The Flowchart for $SEIR$ Model is shown in Figure 1.8.

1.6 Mathematical preliminaries

In this section, we provide a concise overview of the mathematical tools and concepts that are utilized throughout the thesis. This includes the key theories, formulas, and methodologies that form the foundation of our analysis and arguments.

1.6.1 Computation of R_0 using next generation matrix method

To compute the basic reproduction number R_0 next generation matrix method is used. The Next Generation Matrix method was proposed by Diekmann et al in 1990 (Diekmann *et al.*, 1990) and van den Driessche and Watmough (Van den Driessche and Watmough, 2002).

The next generation matrix is a non-negative matrix used to determine the basic reproduction number, R_0, which is the spectral radius of this matrix. Consider a heterogeneous population where individuals can be categorized by factors such as age, behavior, spatial location, or disease stage, and grouped into n homogeneous compartments. Let $x = (x_1, x_2, \ldots, x_n)^T$, with each $x_i \geq 0$, represent the number of individuals in each compartment. For clarity, we arrange the compartments so that the first m compartments correspond to infected individuals. The distinction between infected and uninfected compartments must be based on the epidemiological interpretation of the model, as this cannot be deduced from the structure of the equations alone, and multiple interpretations may be possible for some models.

The basic reproduction number, R_0, depends on the definition of infected and uninfected compartments. We define X_s as the set of all disease-free states:

$$X_s = \{x \geq 0 \mid x_i = 0 \text{ for } i = 1, 2, \ldots, m\}.$$

Let $F_i(x)$ be the rate of new infections in compartment i, $V_i^+(x)$ the rate of transfer of individuals into compartment i by all other means, and $V_i^-(x)$ the rate of transfer of individuals out of compartment i. Each function is assumed to be continuously differentiable at least twice in each variable. The disease transmission model consists of non-negative initial conditions along with the following system of equations:

$$\frac{dx_i}{dt} = F_i(x) - V_i(x), \quad i = 1, 2, \ldots, n,$$

To compute F and V matrices, we consider their Jacobians at the disease-free equilibrium:

$$F = \left[\frac{\partial F_i(x_0)}{\partial x_j}\right],$$

$$V = \left[\frac{\partial V_i(x_0)}{\partial x_j}\right],$$

for $1 \leq i, j \leq m$. The matrix F contains the new infection terms, while the matrix V includes the remaining transfer terms. The next generation matrix is then defined as FV^{-1}. Thus, R_0 is the spectral radius (or the largest eigenvalue in magnitude) of the next generation matrix:

$$R_0 = \rho(FV^{-1}).$$

In a compartmental model defined by ordinary differential equations (ODEs), let $x = (x_1, x_2, \ldots, x_n)^T$ be the vector of compartment sizes, with the first $m < n$ compartments containing infected individuals. Assume that the disease-free equilibrium (DFE), denoted x_0, exists and is stable in the absence of the disease. The equations of the model are:

$$\frac{dx_i}{dt} = F_i(x) - V_i(x), \quad i = 1, 2, \ldots, m,$$

where $F_i(x)$ is the rate of new infections in the ith compartment and $V_i(x)$ is the rate of transitions among compartments. Define:

$$\bar{F} = \begin{pmatrix} F_1 \\ F_2 \\ \vdots \\ F_n \end{pmatrix}, \quad \bar{V} = \begin{pmatrix} V_1 \\ V_2 \\ \vdots \\ V_n \end{pmatrix},$$

and:

$$F = \left[\frac{\partial \bar{F}(x_0)}{\partial x_j}\right], \quad V = \left[\frac{\partial \bar{V}(x_0)}{\partial x_j}\right],$$

for $1 \leq i, j \leq m$. The matrix F is entry-wise nonnegative, and V is a nonsingular M-matrix, making V^{-1} entry-wise nonnegative. The (i, j) entry of the matrix FV^{-1} represents the expected number of secondary infections in compartment i produced by an infected individual introduced into compartment j. Hence, FV^{-1} is the next generation matrix, and R_0 is the spectral radius of this matrix:

$$R_0 = \rho(FV^{-1}).$$

1.6.2   Stability

The stability of a critical point indicates whether the solution trajectories of the system will converge to or diverge from that point over time. In the context of COVID-19, understanding the stability of critical points within epidemiological models is essential for predicting the behaviour of the disease under various conditions. This concept can be further categorized into local stability and global stability.

Local stability refers to the behaviour of the system in the immediate vicinity of the critical point. If the critical point is locally stable, small perturbations or deviations from this point will eventually return to it, suggesting that minor changes in the number of infections will not lead to large outbreaks. In contrast, if the critical point is locally unstable, even small deviations can lead to significant divergence, potentially resulting in an outbreak or a change in the disease dynamics.

1.6.3   Local Stability Analysis

Consider the system of ordinary differential equations given by:

$$\frac{dx}{dt} = G(x)$$

Here, $x = (x_1, x_2, \ldots, x_n)^T$ and $G = (G_1, G_2, \ldots, G_n)^T$, with each G_i for $i = 1, 2, \ldots, n$ being a continuous function from $\mathbb{R}^n$ to $\mathbb{R}$.

The equilibrium point of this system is determined by setting $\frac{dx_i}{dt} = 0$ for $i = 1, 2, \ldots, n$, which yields:

$$G_i(\bar{x}_1, \bar{x}_2, \ldots, \bar{x}_n) = 0$$

for $i = 1, 2, \ldots, n$, where $\bar{x} = (\bar{x}_1, \bar{x}_2, \ldots, \bar{x}_n)^T$ in $\mathbb{R}^n$.

To analyze the linear stability of these equilibrium points (steady state solutions), we shift the origin to $\bar{x}$ using the transformation:

$$X_i = x_i - \bar{x}_i, \quad i = 1, 2, \ldots, n$$

With this change of variables and by ignoring higher-order terms in equation (1.2), we obtain the following linearized system:

$$\frac{dX}{dt} = AX$$

where $X = (X_1, X_2, \ldots, X_n)^T$ and $A = \left(\frac{\partial G_i}{\partial x_j}\right)_{x=\bar{x}}$ is the Jacobian matrix of the system.

The equilibrium point $x = \bar{x}$ of the dynamical system is considered linearly asymptotically stable if all the eigenvalues of the Jacobian matrix have negative real parts. Therefore, determining the linear asymptotic stability of an equilibrium point reduces to finding the signs of the roots of the characteristic equation of the corresponding Jacobian matrix.

In this context, the Routh-Hurwitz criterion is particularly useful, providing the necessary and sufficient conditions for a polynomial to have all roots with negative real parts.

Routh-Hurwitz Criterion

Consider $a_1, a_2, \ldots, a_n$ as n real numbers. The equation

$$\lambda^n + a_1\lambda^{n-1} + a_2\lambda^{n-2} + \ldots + a_n = 0$$

has roots with negative real parts if and only if the determinants of the following matrices are positive:

$$H_1 = \begin{pmatrix} a_1 \end{pmatrix}, \quad H_2 = \begin{pmatrix} a_1 & 1 \\ a_3 & a_2 \end{pmatrix}, \quad H_3 = \begin{pmatrix} a_1 & 1 & 0 \\ a_3 & a_2 & a_1 \\ a_5 & a_4 & a_3 \end{pmatrix},$$

$$H_j = \begin{pmatrix} a_1 & 1 & 0 & \cdots & 0 \\ a_3 & a_2 & a_1 & \cdots & 0 \\ a_5 & a_4 & a_3 & \cdots & 0 \\ \vdots & \vdots & \vdots & \ddots & \vdots \\ a_{2j-1} & a_{2j-2} & a_{2j-3} & \cdots & a_j \end{pmatrix},$$

$$H_n = \begin{pmatrix} a_1 & 1 & 0 & \cdots & 0 \\ a_3 & a_2 & a_1 & \cdots & 0 \\ a_5 & a_4 & a_3 & \cdots & 0 \\ \vdots & \vdots & \vdots & \ddots & \vdots \\ 0 & \cdots & \cdots & \cdots & a_n \end{pmatrix}.$$

The (l, m)-th entry of the matrix H_j for $l = 1, 2, \ldots, j$ and $m = 1, 2, \ldots, j$ is given by:

$$\begin{cases} a_{2l-m}, & \text{if } 0 < 2l - m < n; \\ 1, & \text{if } 2l = m; \\ 0, & \text{if } 2l < m \text{ or } 2l > n + m. \end{cases}$$

For quadratic and cubic polynomials, these conditions simplify to:

- $a_1 > 0$, $a_2 > 0$, and

- $a_1 > 0$, $a_3 > 0$, $a_1 a_2 - a_3 > 0$, respectively.

For more details, refer to references (Kot, 2001), (Kuznetsov and Kuznetsov, 2004), and (Perko, 2013).

1.6.4   Lyapunov Stability

Lyapunov stability provides a method for verifying system stability by examining the system's behaviour instead of analyzing its eigenvalues. Lyapunov's Direct Method involves the determination of a Lyapunov function. Here, we present the definition of the Lyapunov function and the theorem for the global stability of an equilibrium point.

Definition: *(Lyapunov Function)* "For a given system of differential equations, say in two variables x, y, a function $E(x, y)$ is said to be a Lyapunov function for the system if the two conditions are satisfied:

(i) $E(x, y)$ is positive definite, and

(ii) $\frac{dE}{dt}$ is negative definite."

Theorem 1.1. *"A critical point of the system is globally stable if the following conditions are satisfied:*

(i) Function $E(x, y)$ is a Lyapunov function, and

(ii) The function $E(x, y)$ must be radially unbounded, i.e. $E(x, y) \to \infty$ as $x, y \to \infty$."

For further details, refer to reference (Korobeinikov and Wake, 2002)

1.6.5   Global Asymptotic Stability of the Disease-Free Equilibrium

In this subsection, we present the result and outline two conditions that ensure the global asymptotic stability of the disease-free state. To study this global stability, we employ a theorem by Castillo-Chavez et al. (Castillo-Chavez, 2002), which is stated as follows:

Theorem 1.2. *If the model system can be expressed in the form:*

$$\begin{cases} X'(t) = F(X, Y), \\ Y'(t) = G(X, Y), \quad G(X, 0) = 0, \end{cases}$$

where $X \in \mathbb{R}_+^m$ represents the number of uninfected individuals and $Y \in \mathbb{R}_+^n$ represents the number of infected individuals (including latent, infectious, etc.). The disease-free equilibrium is denoted by $E_0 = (X_0, 0)$. The following conditions (H1) and (H2) must be met to ensure the global asymptotic stability of E_0:

- **H1:** *For $X'(t) = F(X_0, 0)$, X_0 is globally asymptotically stable (g.a.s.).*

- **H2:** *$G(X, Y) = AY - G_b(X, Y)$, $G_b(X, Y) \geq 0$ for $(X, Y) \in D$, where $A = D_Y G(X_0, 0)$ is an M-matrix (the off-diagonal elements of A are nonnegative) and D is the region where the model is biologically valid.*

If the system meets the above conditions (H1 and H2), then the following theorem holds:

Theorem 1.3. *The fixed point $E_0 = (X_0, 0)$ is a globally asymptotically stable equilibrium of system provided $R_0 < 1$ (locally asymptotically stable) and that the assumptions H1 and H2 are satisfied.*

Theorem 1.4 (Lasalle's Invariance Theorem). *Let $\Omega \subset D$ be a compact set that is positively invariant with respect to the system. Let $V : D \to D$ be a continuously differentiable function such that $\frac{dV}{dt} \leq 0$ in Ω. Let $E = \{x \mid \frac{dV}{dt} = 0, x \in \Omega\}$ and M be the largest invariant set in E. Then every solution starting in Ω approaches M as $t \to \infty$. In particular, if $M = \{0\}$, then the zero solution of (1.2) is asymptotically stable.*

For further details, refer to references (J. La Salle and Lefschetz, 1961) and (J. P. La Salle, 1976).

1.7 Review of Literature

In this section, a review of 55 studies is presented. Given the significant impact of COVID-19, numerous researchers have developed models to understand the transmission of SARS-CoV-2 and evaluated the effectiveness of various intervention strategies in mitigating its spread. According to the WHO, mathematical models are crucial for informed decision-making by health policy-makers. Approaching infectious diseases mathematically can uncover the underlying patterns and potential structures for epidemic control. These models provide valuable insights into disease transmission dynamics and the impact of various public health intervention strategies (Kermack and McKendrick, 1927). Population-level phenomena are often complex and cannot be fully understood by examining individuals alone (Rm, 1991). Statistical analysis of epidemiological data helps describe, quantify, and summarize disease transmission modes in susceptible populations. Additionally, mathematical modelling is a valuable tool for exploring and testing epidemiological hypotheses, especially given the ethical and practical constraints of live human or animal experiments.

The literature was analyzed and categorized based on model type, methods, hypotheses, and distribution of key input parameters. Of the 55 studies reviewed, 33 employed Compartmental models, either Deterministic or Stochastic, to simulate transmission. For clarity, the distribution of the studies, their respective models, and their research findings are summarized in Table 1.1 and 1.2 Of the 33 studies that utilized Compartmental models, 18 were based on the classic SIR model. The remaining 23 studies from a total of 55 employed various other modelling approaches, including the Bayesian method, generalized growth model, agent-based model, and other methodologies.

Agent-Based Model: This stochastic model assesses the impact of universal masking and the likelihood of human-to-human transmission of SARS-CoV-2. Notable studies by (Kai and Guy-PhilippeGoldstein, 2020) and (Koo *et al.*, 2020)provide insights into how widespread masking can mitigate the spread of the virus.

Branching Process Model: Another stochastic approach, the branching process model, evaluates the effectiveness of contact tracing and isolation. (Hellewell *et al.*, 2020) demonstrated the critical role of these measures in controlling outbreaks.

Bayesian Method: This method, which estimates R_0, incubation period, serial interval, and age-stratified CFR and IFR, is useful for comprehensive epidemiological assessments. Studies by (Y.-Z. Zhang and Holmes, 2020), (Verity *et al.*, 2020), and (Ganyani *et al.*, 2020) have utilized this approach to provide detailed COVID-19 dynamics.

Generalized Linear Models: These stochastic models analyze the incubation period and the effect of human mobility and control measures. (Kraemer *et al.*, 2020) explored how movement patterns influence the virus's spread.

Generalized Growth Model: This model examines R_0, the impact of social distancing, and doubling time. Research by (Munayco *et al.*, 2020), (Muniz-Rodriguez *et al.*, 2020), and (Shim *et al.*, 2020) highlights the importance of early intervention in reducing transmission rates.

Linear Growth and Exponential Growth Model: These stochastic models assess how changes in testing rates affect the epidemic growth rate. (Omori *et al.*, 2020) demonstrated the implications of testing strategies on understanding the epidemic trajectory.

Exponential Growth Model: This model focuses on estimating R_0, the number of unreported COVID-19 cases, the risk of sustained transmission, and the impact of reporting rates. Studies by (Thompson, 2020), (S. Zhao, Lin, *et al.*, 2020), and (S. Zhao, Musa, *et al.*, 2020) provide valuable estimates for public health planning.

Second Derivative Model: This model assesses the detection rate of COVID-19 cases. (X. Chen and Yu, 2020) used this approach to evaluate how well the infection is being identified and reported.

Poisson Transmission Model: This stochastic model estimates R_0. (Y. Zhu and Chen, 2020) employed this model to understand the basic reproduction number in different settings.

Segmented Poisson Model: This model determines the turning point, duration, and attack rate of the epidemic. (Y.-Z. Zhang and Holmes, 2020) utilized this model to study the phases of the COVID-19 outbreak.

Analytically Solvable Model: This model provides estimates of the contribution of different transmission routes and generation time. (Ferretti *et al.*, 2020) used it to differentiate between direct and indirect transmission pathways.

Gaussian Distribution Theory: This stochastic model estimates R_0 and the incubation period. (Y.-D. Li *et al.*, 2020) applied it to analyze the distribution of these parameters.

Phenomenological Models: These models predict the short-term cumulative confirmed cases. (Roosa *et al.*, 2020a) and (Roosa *et al.*, 2020b) demonstrated their utility in making near-term forecasts.

Transmission Model with Zoonotic Infections: This model evaluates R_0, doubling time, incubation period, and serial interval, particularly in the context of zoonotic spillovers. (L. Li, Yang, Dang, Meng, Huang, Meng, Wang, *et al.*, 2020) explored these dynamics to understand the initial spread of COVID-19.

Data-Driven and Model-Free Estimations: These approaches predict epidemic trends under various public health interventions and estimate mortality. (Scarabel *et al.*, 2020) employed these methods to provide real-time predictions and scenario analyses.

Basic reproduction number R_0

The basic reproductive number R_0 is a critical epidemiological metric representing the average number of secondary infections generated by one primary infected individual during the infectious period. It is calculated as the product of three factors: $R_0 = cdp$, where c denotes the average contact rate of the infectious source per unit time, d represents the infectious period, and p is the probability of transmission per contact (Halloran, 2001). In COVID-19 epidemic models, R_0 is typically estimated using a combination of epidemiological characteristics, confirmed case reports, population movement data, and other relevant information, varying by study area and time period.

A review of thirty studies reveals that most R_0 estimates for COVID-19 range between 2 and 4 as shown in Figure 1.9, with some studies (B. Tang, Wang, Li, Bragazzi, Tang, Xiao, and Wu, 2020), (Y. Zhu and Chen, 2021) reporting values exceeding 5. Researchers have frequently used daily confirmed case data from the China CDC,
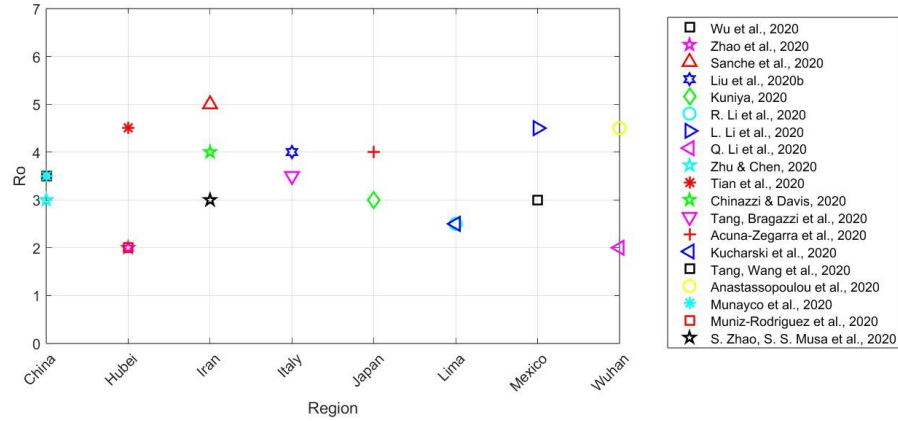
Figure 1.9: Comparison of Basic Reproduction Number R_0 Across Models Using Data from Various Regions

particularly focusing on the initial outbreak in Wuhan, China. For instance, Wang et al. (C. Wang *et al.*, 2020) analyzed confirmed cases in Wuhan, segmenting the epidemic into four periods: before January 11, January 11-22, January 23-February 1, and February 2-18. The corresponding R_0 values declined from 3.88, 3.86, 1.26, to 0.32. Similarly, Li et al. (Kucharski *et al.*, 2020),(R. Li, Pei, Chen, Song, Zhang, Yang, and Shaman, 2020), (L. Li, Yang, Dang, Meng, Huang, Meng, Wang, *et al.*, 2020) conducted phased evaluations based on key events and interventions, finding a significant reduction in R_0 with the implementation of more stringent public health measures.

Asymptomatic Infection

Asymptomatic infections can be categorized into two groups: the first group consists of individuals with no or mild symptoms throughout the infection, while the second group refers to those who are initially asymptomatic but may develop symptoms later during the incubation period. The prevalence and proportion of asymptomatic cases are closely linked to disease control and prevention strategies. This review incorporates findings from over 30 studies on asymptomatic infections related to COVID-19. These studies align with epidemic reports but vary in their hypotheses regarding the infectivity of asymptomatic individuals. For instance, (Hauser, Counotte, Margossian, Konstantinoudis, Low, Althaus, and Riou, 2020) suggested that 82.1% of infected individuals develop symptoms after an average incubation period of 5.9 days, with the remaining being asymptomatic and non-transmitting. Some mild cases may

not exhibit symptoms that significantly impact medical treatment or isolation measures. (Kissler *et al.*, 2020),(C. N. Ngonghala *et al.*, 2020), and (Verity *et al.*, 2020) included mild or asymptomatic infections in their models, whereas (Sanche *et al.*, 2020), (C. N. Ngonghala *et al.*, 2020), and others considered asymptomatic infections as potentially infectious. (Yang *et al.*, 2020) suggested that asymptomatic individuals could either remain without symptoms or develop symptoms later. (S. Mandal *et al.*, 2020) proposed that asymptomatic infections are half as infectious as symptomatic cases, while (Hou *et al.*, 2020) estimated that 50% of asymptomatic infections are infectious.

The asymptomatic infection ratio denotes the proportion of infections where individuals exhibit no symptoms throughout the disease. This parameter plays a crucial role in assessing the true disease burden, evaluating transmission potential, and shaping strategies for infection control, isolation measures, public interventions, and epidemic monitoring. Various models have differed in their assessments and hypotheses regarding this ratio, with none estimating it higher than 50%.

Six studies ((Acuna-Zegarra *et al.*, 2020),(S. E. Eikenberry *et al.*, 2020),(Ferretti *et al.*, 2020),(Koo *et al.*, 2020),(C. N. Ngonghala *et al.*, 2020),(S. Zhao, Lin, *et al.*, 2020)) have proposed different proportions for asymptomatic versus symptomatic infections. For instance, (Koo *et al.*, 2020) suggested an asymptomatic infection ratio of 7.5%, exploring sensitivity analyses ranging from 22.7% to 50.0%. They emphasized that higher asymptomatic rates could substantially diminish the impact of public health interventions, underscoring the need for robust case management, treatment, vaccines, and preventive measures.

Additionally, four studies ((Hauser, Counotte, Margossian, Konstantinoudis, Low, Althaus, and et al., 2020),(Sun and Weng, 2020),(B. Tang, Wang, Li, Bragazzi, Tang, Xiao, and et al., 2020),(C. Wang *et al.*, 2020)) specifically evaluated the proportion of asymptomatic infections. (B. Tang, Wang, Li, Bragazzi, Tang, Xiao, and et al., 2020) estimated this ratio to be less than 20%, whereas (Sun and Weng, 2020) suggested a median proportion of approximately 44.46% (interquartile range: 37.31% - 53.72%).

Impact of intervention on R_0

Qualitative assessments of various interventions' impacts on COVID-19 transmission are summarized above. Figure 1.10 illustrates the comparison of the basic reproduction number R_0 before and after the implementation of public health interventions
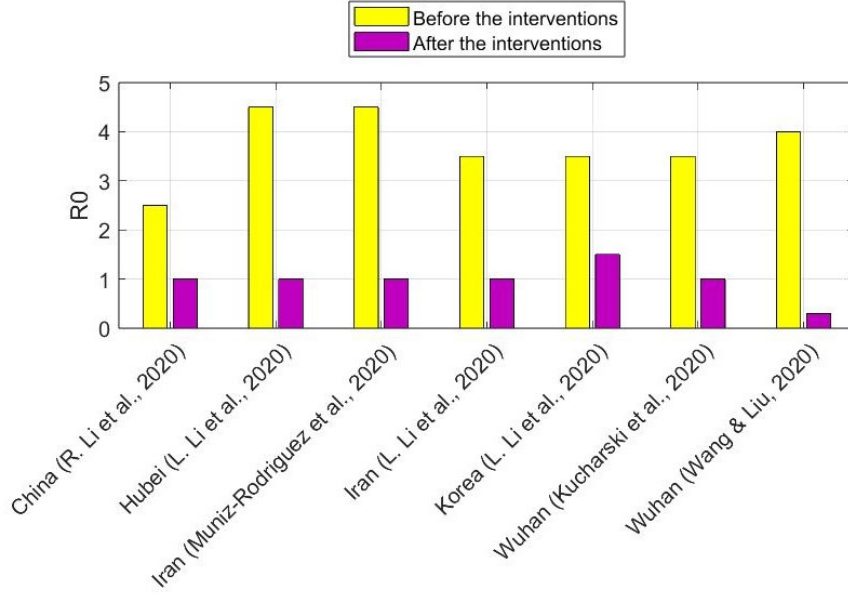
Figure 1.10: Comparison of R_0 Before and After Public Health Interventions Across Various Studies

across different studies. While many studies agree that R_0 decreases following intervention policies, the predicted outcomes vary significantly due to differences in study locations and the nature of interventions. For instance, (Kucharski *et al.*, 2020) predicted a decrease in R_0 from 2.35 to 1.05 after interventions. In contrast,(World Health Organization, 2020) observed a more substantial impact, with R_0 decreasing from 3.86 to 1.26 following the lockdown of Wuhan. Similarly, studies by (L. Li, Yang, Dang, Meng, Huang, Meng, and et al., 2020) and (R. Li, Pei, Chen, Song, Zhang, Yang, and et al., 2020)reported varied results within China, with R_0 decreasing by 1.23 and 2.8 respectively in different regions.

Studies in Iran ((Q. Li *et al.*, 2020), (Muniz-Rodriguez *et al.*, 2020)) showed similar effectiveness of social distancing and other interventions, lowering R_0 from around 4 to near the critical value, indicating effective local control of the epidemic. The most pronounced impact of intervention measures on R_0 was observed in South Korea ((R. Li, Pei, Chen, Song, Zhang, Yang, and Shaman, 2020)), where large-scale epidemic control measures reduced R_0 from 4.1 to 0.1, well below the critical threshold ($R_0 = 1$), suggesting successful containment and potential elimination of the epidemic.

These findings underscore the effectiveness of targeted public health interventions

in reducing R_0 and controlling the spread of COVID-19, albeit with varying degrees of success influenced by local contexts and intervention strategies.

Objective of Research

The Objectives of this Research are given bellow:

- To study the stability of various Mathematical Models.

- To study the effect of delay created by precautionary measures.

- To study the effect of Diffusion on various Models.

Table 1.1: COVID-19 compartmental models.

Models	Model type	Compartments	Results/Findings	References
SEIR	Stochastic	Susceptible (S), exposed (E), Infectious (I), Removed (R)	R_0, mortality, the impact of travel restrictions, the impact of behavioural changes, the impact of interventions, the epidemic risk of imported cases from outside China, the impact of quarantine of Wuhan city, infectious period, prediction of epidemic, doubling time, the impact of transmission control measures, the impact of universal masking	((Chinazzi and Davis, 2020); (Kai and Guy-PhilippeGoldstein, 2020); (Kucharski *et al.*, 2020); (Sanche *et al.*, 2020); (R. Li, Pei, Chen, Song, Zhang, Yang, and Shaman, 2020); (M.-Y. Wang *et al.*, 2020); (J. T. Wu *et al.*, 2020); (Yang *et al.*, 2020); (S. Zhao, Lin, *et al.*, 2020))
SLIR	Deterministic	Susceptible (S), Latent (L), Infectious (I), Removed (R)	Prediction of an epidemic, the impact of universal masking, the impact of travel restrictions, the impact of behavioral changes, the impact of interventions, doubling time, the impact of transmission control measures	((Acuna-Zegarra *et al.*, 2020), (Santarpia *et al.*, 2020); (Boldog *et al.*, 2020); (Hauser, Counotte, Margossian, Konstantinoudis, Low, Althaus, and et al., 2020); (Hou *et al.*, 2020); (Kuniya, 2020); (S. Mandal *et al.*, 2020); (C. N. Ngonghala *et al.*, 2020); (B. Tang, Bragazzi, *et al.*, 2020))
SIRD	Deterministic	Susceptible (S), Infected (I), Recovered (R), Dead (D)	R_0, the prediction of the COVID-19 outbreak, mortality of COVID-19	((Anastassopoulou *et al.*, 2020); (Fanelli and Piazza, 2020))
SEIRS	Stochastic	Susceptible (S), Exposed (E), Infectious (I), Recovered (R), Susceptible (S)	R_0, the transmission dynamics of SARS-CoV-2	((Kissler *et al.*, 2020))
SIR-X	Deterministic	Infected (I), susceptible (S), removed (R), quarantined (X)	R_0, the impact of containment policies	((Maier and Brockmann, 2020))
SEIRU	Deterministic	Susceptible(S), Asymptomatic non-infectious (E), Asymptomatic Infectious(I), Reported symptomatic infectious (R), Unreported symptomatic infectious (U)	R_0, the role of latency period transmission rate	((Z. Liu *et al.*, 2020b))
SIRU	Deterministic	Susceptible(S), Asymptomatic infectious (I), Reported symptomatic infectious(R), Unreported symptomatic infectious (U)	The impact of unreported cases and prediction of cumulative confirmed cases	((Z. Liu *et al.*, 2020c), 2020c; (Magal and Webb, 2020))

Table 1.2: Overview of COVID-19 Compartmental Models (continued)

Models	Model Type	Compartments	Results/Findings	References
SEIIN	Stochastic	Susceptible (S), Exposed (E), documented infected (I), undocumented infected (I), total population (N)	Analysis of R_0, fraction of undocumented infections, and their relative contagiousness, as well as latent and infectious periods	((R. Li, Pei, Chen, Song, Zhang, Yang, and Shaman, 2020))
SEIQR	Deterministic	Susceptible (S), Exposed (E), Hospitalized Infected (I), Quarantined (Q), Recovered or Removed (R)	Short-term prediction models for COVID-19 spread	((M. Mandal *et al.*, 2020))
SEIRQ	Stochastic	Susceptible (S), Exposed (E), Infectious (I), Removed (R), Quarantined (Q)	Short-term predictive capabilities for COVID-19	((Hu *et al.*, 2020))
SCIRA	Stochastic	Susceptible (S), Closely Observed (C), Infected Patients (I), Recovered/Cured/Dead (R), Asymptomatic (A)	Assessment of asymptomatic infection ratios and the impact of asymptomatic and imported cases	((Sun and Weng, 2020))
SEIHR	Deterministic	Susceptible (S), Exposed (E), Symptomatic Infectious (I), Hospitalized (H), Recovered or Dead (R)	Evaluation of R_0 and the effects of interventions on COVID-19 spread	((Choi and Ki, 2020))

Chapter 2

Mathematical Modelling of Vaccination Strategies Against SARS-CoV-2: Assessing Coverage and Efficacy

2.1 Introduction

. The COVID-19 pandemic has presented an unprecedented challenge to global public health, with over 775 million infections and 7 million deaths reported worldwide (World Health Organization, 2024). Vaccination has emerged as a pivotal intervention to curb the spread of SARS-CoV-2, the virus responsible for COVID-19. The rapid development and deployment of vaccines have provided a crucial tool in the fight against this pandemic. However, the effectiveness of vaccination programs depends on several factors, including vaccine coverage, efficacy, and the ability to reach herd immunity thresholds.

The severe acute respiratory syndrome coronavirus (SARS-CoV) and the Middle East respiratory syndrome coronavirus (MERS-CoV) shares 79% (Y.-Z. Zhang and Holmes, 2020) and 50% (Adelman *et al.*, 2002) sequence similarity with the wild type of SARS-CoV-2, respectively. The fatality rates for SARS and MERS are approximately 10% and 35%, respectively. In contrast, SARS-CoV-2 has fatality rates that

range from 0.1% to 18.1%, depending on the country (Johns Hopkins University of Medicine, March 2023). Furthermore, it is estimated that there were 14.83 million excess deaths due to the SARS-CoV-2 pandemic between January 2020 and December 2021 (Msemburi *et al.*, 2023). Because of the severity of the outbreak, vaccines were developed rapidly, utilizing every known technology and method available to humanity. By mid-2021, over three billion COVID-19 vaccine doses had been given globally, with 24% of the world's population having received at least one dose (Mathieu *et al.*, 2021). There are 184 vaccine candidates in preclinical development and 104 in clinical stages (COVID, 19). Recent data show that 18 COVID-19 vaccines have been approved and are currently in use worldwide (COVID, 19), (Organization *et al.*, 2021). These vaccines fall into four main categories based on their platforms: 1. whole virus vaccines, 2. protein-based vaccines, 3. viral vector vaccines, and 4. nucleic acid vaccines (Nagy and Alhatlani, 2021). The systematic review conducted by Ibrahim Mohammed et al. (Mohammed *et al.*, 2022) provides a comprehensive analysis of the efficacy and effectiveness of COVID-19 vaccines in reducing infection rates, disease severity, hospitalization, and mortality. Their findings indicate that the COVID-19 vaccines have significantly contributed to controlling the pandemic across various populations.

Mathematical modelling has been instrumental in understanding the dynamics of infectious diseases and evaluating the potential impact of various interventions. In the context of COVID-19, models have been used to predict the course of the pandemic, assess the effects of social distancing measures, and estimate the potential outcomes of vaccination campaigns. Numerous mathematical models have been developed to unravel the complex dynamics of the novel coronavirus (Fuk-Woo *et al.*, 2020), (B. Tang, Wang, Li, Bragazzi, Tang, Xiao, and Wu, 2020), (Khajanchi *et al.*, 2020), (T. Chen *et al.*, 2020), (Imai *et al.*, 2020), (Z. Liu *et al.*, 2020a), (Nadim *et al.*, 2020), (B. Tang, Bragazzi, *et al.*, 2020), (J. Wu *et al.*, 2020). Chen et al. (T. Chen *et al.*, 2020) formulated a novel model to determine the basic reproduction number of the virus. Imai et al. (Imai *et al.*, 2020) crafted a computational model for COVID-19 focusing on human-to-human transmission in Wuhan, while Tang et al. (Fuk-Woo *et al.*, 2020) introduced a compartmental model incorporating a symptomatic class, revealing a high basic reproduction number of 6.47. Wu et al. (J. Wu *et al.*, 2020) proposed a model with four compartments—susceptible, exposed, infected, and recovered—to analyze human transmission dynamics, estimating a reproduction number of

approximately 2.68. In the absence of therapeutics or vaccines, non-pharmaceutical interventions, such as widespread mask usage, play a crucial role in mitigating community transmission and the overall burden of the COVID-19 pandemic (S. Eikenberry *et al.*, 2020). Ngonghala et al. (C. Ngonghala *et al.*, 2019) also emphasized the significance of non-pharmaceutical interventions in controlling the pandemic. In India, a variety of mathematical models have been devised to explore the transmission dynamics of COVID-19, considering intervention strategies like lockdowns and social distancing, along with economic perspectives (Khajanchi *et al.*, 2020), (Nadim *et al.*, 2020), (A. Das *et al.*, 2020), (Shekatkar *et al.*, 2020), (Agrawal *et al.*, 2020), (Khajanchi and Sarkar, 2020), (Sarkar *et al.*, 2020), (Samui *et al.*, 2020), (Chatterjee *et al.*, 2020), (Rai *et al.*, 2021), (Anggriani *et al.*, 2022), (Singh and Arquam, 2022), (Shiferaw and Lemecha, 2022). Chatterjee et al. (Chatterjee *et al.*, 2020) employed an extended SEIR model using stochastic differential equations to study the pandemic. Few models, such as the one by (Rai *et al.*, 2021), have specifically examined the effects of lockdowns by treating them as a distinct compartment in the Indian context. The epidemic in India has garnered significant interest, with various studies exploring different aspects (Perc *et al.*, 2020). Additionally, the role of media in influencing the outbreak has been acknowledged in modelling infectious diseases (D. Das *et al.*, 2020a), (D. Das *et al.*, 2020b), (Khajanchi *et al.*, 2018), (D. Das *et al.*, 2019). Mujahid et al. (Abbas *et al.*, 2022) performed a decision-making analysis to reduce the mortality rate associated with the COVID-19 pandemic, utilizing the q-rung ortho-pair fuzzy soft Bonferroni mean operator. Mohsen et al. (Khasteh *et al.*, 2022) developed a numerical methodology for analyzing a distributed order time fractional model of COVID-19 contagion, employing a finite difference scheme and the midpoint quadrature approach for problem-solving. Alemzewde et al. (Alemzewde *et al.*, 2023) proposed a deterministic model to evaluate the effectiveness of two therapeutic interventions, vaccination and treatment, for controlling the COVID-19 pandemic. Venkatesh et al. (Venkatesh *et al.*, 2023) developed a multistrain epidemic model with sixteen compartments to reduce the spread of COVID-19 by employing vaccine and treatment measures. Bishal et al. (Chhetri *et al.*, 2022) constructed an optimal control model that incorporates age-specific transmission dynamics of COVID-19, assessing the impact of vaccination and treatment strategies on mitigating the pandemic's burden.

Penn and Donnelly (2023)(Penn and Donnelly, 2023) employed an ODE-based SIR model to investigate the impact of the basic reproduction number R_0 on optimal vaccination strategies. Zhao et al. (2021b)(Z. Zhao $et\ al.$, 2021) utilized three different ODE-based SEIAR models to determine the optimal vaccination strategy against COVID-19 in Wuhan, China, using the effective reproduction number to estimate SARS-CoV-2 transmission among age groups. Stafford et al. (2023)(Stafford $et\ al.$, 2023) developed an age-and-race-stratified ODE-based model to study vaccine distribution in the United States, focusing on non-Hispanic White persons and all other groups. Babus et al. (2023)(Babus $et\ al.$, 2023) formulated a linear programming problem to devise a U.S. vaccination plan aimed at minimizing deaths and the economic cost of stay-at-home orders, considering occupation-based risk exposure across 454 occupations. Galli et al. (2023)(Galli $et\ al.$, 2023) used an ODE-based SIR model to predict COVID-19 dynamics and assess vaccination plans in the Southwest Shewa Zone, Ethiopia, concluding that prioritizing individuals aged 50 and older avoids more critical cases than random vaccine allocation. All these studies employed age-structured mathematical models.

To obtain a better insight into the important factors related to the control of novel coronavirus in a community and throughout the world, we propose a deterministic SVEIIAR model. This model incorporates compartments for Susceptible (S), Vaccinated (V), Exposed (E), Infectious (I), Asymptomatic (A), and Recovered (R) individuals. By including both vaccine efficacy and effectiveness of vaccine coverage, the model aims to capture the dynamics of COVID-19 spread and control under various vaccination strategies.

2.2   Model Formulation

We develop a deterministic compartmental model, denoted as $SVEII_AR$, to describe the transmission mechanism of COVID-19. Let N represent the total population. This population is divided into six compartments: Susceptible (S), Vaccinated (V), Exposed (E), Symptomatic Infection (I), Asymptomatic Infection (I_A), and Recovered or Deceased (R). Additionally, we incorporate vital dynamics, including the natural human natality or recruitment rate (Λ) and the mortality (death) rate (μ).

Susceptible individuals move to the Exposed compartment upon contact with either Symptomatic (I) or Asymptomatic (I_A) individuals at a transmission rate (β).

Reports indicate that the transmission rate from Asymptomatic individuals (I_A) is lower than that from Symptomatic individuals (I) (MoHFW). Therefore, we assume that the transmission from I_A to Susceptible individuals occurs at a reduced rate, represented by η, where $\eta < 1$. The new infection rate is given by $\beta S(I + \eta I_A)$.

Susceptible individuals who are vaccinated move to the Vaccinated compartment at a rate δ. Given that vaccines are not 100% effective (www.cdc.gov), we assume that vaccinated individuals are not completely protected. Vaccinated individuals may become infected and move into the Exposed class at a lower transmission rate ω, where $\omega \in [0, 1]$ represents the reduction in transmission.

Exposed individuals transition to the Infected class, either Symptomatic (I) or Asymptomatic (I_A), at a rate γ. A fraction (r) of the Exposed population moves to the Symptomatic class, while the remaining fraction ($1 - r$) moves to the Asymptomatic class.

Individuals in the Symptomatic and Asymptomatic classes recover at rates α and η, respectively. Both classes may decrease due to natural mortality (μ). Additionally, individuals in the Symptomatic class may succumb to COVID-19 at a higher rate (θ), reflecting the lower survival probability for symptomatic individuals.

The dynamics of the novel coronavirus model are governed by the following system of non-linear ordinary differential equations:

Dynamics of Susceptible Individuals $S(t)$

The susceptible individuals are recruited into the population at a constant rate Λ. They decrease due to several factors: infection at a rate β when they come into contact with infectious (I) and asymptomatic (I_A) individuals (with a reduced transmission rate η for I_A), vaccination at a rate δ, and natural mortality at a rate μ. Thus, the dynamics of susceptible individuals are given by:

$$\frac{dS}{dt} = \Lambda - \beta S(I + \eta I_A) - \delta S - \mu S$$

Dynamics of Vaccinated Individuals $V(t)$

Vaccinated individuals arise from the susceptible population at a rate δ. These individuals experience a reduced risk of infection by a factor ω. They also decrease due to natural mortality at a rate μ. Thus, the dynamics of vaccinated individuals are given by:

$$\frac{dV}{dt} = \delta S - \omega \beta V I - \mu V$$

Dynamics of Exposed Individuals $E(t)$

Exposed individuals are those who have been infected but are not yet infectious. They increase due to the infection of both susceptible and vaccinated individuals at rates $\beta S(I + \eta I_A)$ and $\omega \beta V I$, respectively. They decrease as they transition to the infectious class at a rate γ and due to natural mortality at a rate μ. Thus, the dynamics of exposed individuals are given by:

$$\frac{dE}{dt} = \beta S(I + \eta I_A) + \omega \beta V I - \gamma E - \mu E$$

Dynamics of Symptomatic Infectious Individuals $I(t)$

Symptomatic infectious individuals arise from the exposed class at a fraction r and transition at a rate γ. They decrease due to disease-induced mortality at a rate θ, recovery at a rate α, and natural mortality at a rate μ. Thus, the dynamics of symptomatic infectious individuals are given by:

$$\frac{dI}{dt} = r\gamma E - (\mu + \theta)I - \alpha I$$

Dynamics of Asymptomatic Infectious Individuals $I_A(t)$

Asymptomatic infectious individuals also arise from the exposed class but at a fraction $1 - r$ and transition at a rate γ. They decrease due to recovery at a rate ϵ and natural mortality at a rate μ. Thus, the dynamics of asymptomatic infectious individuals are given by:

$$\frac{dI_A}{dt} = (1 - r)\gamma E - \epsilon I_A - \mu I_A$$

Dynamics of Recovered Individuals $R(t)$

Recovered individuals increase due to the recovery of both symptomatic and asymptomatic infectious individuals at rates α and ϵ, respectively. They decrease due to natural mortality at a rate μ. Thus, the dynamics of recovered individuals are given by:

$$\frac{dR}{dt} = \alpha I + \epsilon I_A - \mu R$$

Based on the biological assumptions and the schematic representation of the coronavirus Fig. 2.1, we develop a mathematical model for the novel coronavirus. The

parameter description is shown in Table 2.1. The model is expressed as the following six-dimensional system of nonlinear ordinary differential equations (ODEs):

$$\frac{dS}{dt} = \Lambda - \beta S(I + \eta I_A) - \delta S - \mu S,$$

$$\frac{dV}{dt} = \delta S - \omega \beta V I - \mu V,$$

$$\frac{dE}{dt} = \beta S(I + \eta I_A) + \omega \beta V I - \gamma E - \mu E, \qquad (2.1)$$

$$\frac{dI}{dt} = r\gamma E - (\mu + \theta)I - \alpha I,$$

$$\frac{dI_A}{dt} = (1 - r)\gamma E - \epsilon I_A - \mu I_A,$$

$$\frac{dR}{dt} = \alpha I + \epsilon I_A - \mu R,$$

with nonnegative initial conditions given by

$$S(0) > 0, \ V(0) > 0, \ E(0) > 0, \ I(0) > 0, \ I_A > 0, \ R(0) > 0. \qquad (2.2)$$

All the parameters of the system (2.1) are assumed to be positive for all time $t > 0$.

Table 2.1: Parameter Description for $SVEII_AR$

Parameter	Description	Value
Λ	Birth rate	$\frac{10000}{59\times365} \ day^{-1}$
μ	Death rate	$\frac{1}{59\times365} \ day^{-1}$
β	Rate of transmission	$1.7399 \ day^{-1}$
γ	Rate of transition from Exposed to infected class	$0.1923 \ day^{-1}$
r	Fraction of population moves from Exposed to symptomatic class	0.4579
$(1\text{-}r)$	Fraction of population moves from Exposed to asymptomatic class	0.5422
α	Recovery rate of symptomatic infected class	$0.004165 \ day^{-1}$
η	Reduction in transmission from asymptomatic, $\eta < 1$	0.1002
ϵ	Recovery rate of asymptomatic infection	$0.13978 \ day^{-1}$
θ	Rate of disease-induced death	$0.0175 \ day^{-1}$
δ	Rate at which susceptible individuals are vaccinated	$0.4 \ day^{-1}$
ω	Rate of reduction in risk of infection due to vaccination	0.2

Figure 2.1: A Schematic representation of SVEII_AR

2.3 Mathematical Model Analysis

2.3.1 Positivity of Solutions

For the COVID-19 model system 2.1 to be epidemiologically realistic, it is necessary to prove that all the state variables remain positive for all time.

Theorem 2.1. *Let the initial data be* $\{(S, V, E, I, I_A, R) \leq 0\} \in \phi$. *Then the solution set* $\{S(t), V(t), E(t), I(t), I_A(t), R(t)\}$ *of the model system is non negative for all time* *t.*

Proof. Considering the non-linear system of the model (2.1), we take the first equation

$$\frac{dS}{dt} = \Lambda - \beta S(I + \eta I_A) - \delta S - \mu S,$$

$$\frac{dS}{dt} \geq -[\beta(I + \eta I_A) + \delta + \mu]S,$$

$$\int \frac{dS}{S} \geq -\int [\beta(I + \eta I_A) + \delta + \mu]dt,$$

$$\ln S \geq -[\beta(I + \eta I_A) + \delta + \mu]t + c,$$

$$S \geq e^{-[\beta(I+\eta I_A)+\delta+\mu]t} + e^c,$$

$$S(t) \geq S(0)e^{-[\beta(I+\eta I_A)+\delta+\mu]t}.$$

Since $S(0) \geq 0$, it follows that $S(t) \geq 0$ for all $t \geq 0$. Similarly, it can also been shown that $V(t) > 0$, $E(t) > 0$, $I(t) > 0$, I_A $R(t) > 0$ for all $t > 0$. Therefore, the disease is uniformly persistent for every positive solution. $\square$

2.3.2 Invariant Region

Theorem 2.2. *For the initial conditions (2.2), the solutions of system (2.1) are contained in the region $\phi \subset R_+^6$ defined by*

$$\phi = [\{S(t), V(t), E(t), I(t), I_A(t), R(t)\} \in R_+^6 : N(t) \leq \frac{\Lambda}{\mu}]$$

Proof. Let, $N = S + V + E + I + I_A + R$

$$\frac{dN}{dt} = \Lambda - (S + V + E + I + I_A + R)\mu - \theta I \tag{2.3}$$

$$\frac{dN}{dt} = \Lambda - \mu N - \theta I \tag{2.4}$$

$$\frac{dN}{dt} \leq \Lambda - \mu N \tag{2.5}$$

$$\frac{dN}{dt} + \mu N \leq \Lambda \tag{2.6}$$

$$N e^{\mu t} \leq \int e^{\mu t} \Lambda + C \tag{2.7}$$

$$N e^{\mu t} \leq \frac{\Lambda e^{\mu t}}{\mu} + C \tag{2.8}$$

$$N \leq \frac{\Lambda}{\mu} + C e^{-\mu t}. \tag{2.9}$$

At $t \longrightarrow \infty$, $N \longrightarrow \frac{\Lambda}{\mu}$. Clearly $\phi = [\{S(t), \ V(t), \ E(t), \ I(t) \ , I_A(t), \ R(t)\} \in R_+^6 :$ $N(t) \leq \frac{\Lambda}{\mu}]$ $\qquad\square$

2.3.3   Analysis of Disease-Free Equilibrium (DFE) E_0

The model gets DFE when the disease has zero induction

Taking the first equation of system (2.1) with $E = I = I_A = R = 0$ into consideration.

$$0 = \Lambda - \beta S(I + \eta I_A) - \delta S - \mu S \tag{2.10}$$

$$0 = \delta S - \omega \beta V I - \mu V \tag{2.11}$$

$$0 = \beta S(I + \eta I_A) + \omega \beta V I - \gamma E - \mu E \tag{2.12}$$

$$0 = r\gamma E - (\mu + \theta)I - \alpha I \tag{2.13}$$

$$0 = (1 - r)\gamma E - \epsilon I_A - \mu I_A \tag{2.14}$$

$$0 = \alpha I + \epsilon I_A - \mu R \tag{2.15}$$

we arrive at

$$S_0 = \frac{\Lambda}{(\delta + \mu)}, V_0 = \frac{\delta \Lambda}{\mu(\delta + \mu)}$$

Then, the disease-free equilibrium (DFE) state E_0 is given by

$$E_0 = [\frac{\Lambda}{(\delta + \mu)}, \frac{\delta\Lambda}{\mu(\delta + \mu)}, 0, 0, 0, 0]$$

2.3.4 Basic Reproductive Number R_0

R_0 refers to the average number of secondarily infected persons infected by one primary infected patient during the infectious period. To obtain the basic reproduction number, we used the next generation matrix method by (Diekmann and Heesterbeek, 2000) and (van den Driessche and Watmough, 2008), where $\mathcal{F}$ is the matrix of the new infection terms and $\mathcal{V}$ is the matrix of the transition terms.

Infected compartments are E, I, I_A, R.
Let $Y = (E, I, I_A, R)$,

$$\frac{dY}{dt} = \begin{bmatrix} \beta S(I + \eta I_A) + \omega \beta V I \\ 0 \\ 0 \\ 0 \end{bmatrix} - \begin{bmatrix} (\gamma + \mu)E \\ -r\gamma E + (\mu + \theta + \alpha)I \\ -(1 - r)\gamma E + (\eta + \mu)I_A \\ -\alpha I - \epsilon I_A + \mu R \end{bmatrix}$$

$$F_1 = \begin{bmatrix} 0 & \beta S + \omega \beta V & \beta \eta S & 0 \\ 0 & 0 & 0 & 0 \\ 0 & 0 & 0 & 0 \\ 0 & 0 & 0 & 0 \end{bmatrix}$$

$$V_1 = \begin{bmatrix} \gamma + \mu & 0 & 0 & 0 \\ -r\gamma & (\mu + \theta + \alpha) & 0 & 0 \\ (r - 1)\gamma & 0 & \epsilon + \mu & 0 \\ 0 & -\alpha & -\epsilon & \mu \end{bmatrix}$$

At disease-free equilibrium

$$E_0 = [\frac{\Lambda}{(\delta + \mu)}, \frac{\delta\Lambda}{\mu(\delta + \mu)}, 0, 0, 0, 0]$$

$$\mathcal{F} = \begin{bmatrix} o & \frac{\beta\Lambda}{(\delta+\mu)} + \frac{\omega\beta\delta\Lambda}{\mu(\delta+\mu)} & \frac{\beta\eta\Lambda}{(\delta+\mu)} & 0 \\ 0 & 0 & 0 & 0 \\ 0 & 0 & 0 & 0 \\ 0 & 0 & 0 & 0 \end{bmatrix} \quad \mathcal{V} = \begin{bmatrix} \gamma+\mu & 0 & 0 & 0 \\ -r\gamma & (\mu+\theta+\alpha) & 0 & 0 \\ -(1-r)\gamma & 0 & \epsilon+\mu & 0 \\ 0 & -\alpha & -\epsilon & \mu \end{bmatrix}$$

Now, $\mathcal{F}\mathcal{V}^{-1} =$

$$\begin{bmatrix} \frac{\gamma r[\frac{\beta\Lambda}{(\mu+\delta)}+\frac{\beta\delta\Lambda\omega}{\mu(\mu+\delta)}]}{(\mu+\gamma)(\alpha+\theta+\mu)} - \frac{\beta\gamma\eta\Lambda(r-1)}{(\mu+\eta)(\mu+\gamma)(\mu+\delta)} & \frac{\frac{\beta\Lambda}{\mu+\delta}+\frac{\beta\delta\Lambda\omega}{\mu(\mu+\delta)}}{(\alpha+\theta+\eta)} & \frac{\beta\eta V}{(\mu+\eta)(\mu+\delta)} & 0 \\ 0 & 0 & 0 & 0 \\ 0 & 0 & 0 & 0 \\ 0 & 0 & 0 & 0 \end{bmatrix}$$

The basic Reproduction number is given by

$$R_0 = \frac{\gamma r[\frac{\beta\Lambda}{(\mu+\delta)} + \frac{\beta\delta\Lambda\omega}{\mu(\mu+\delta)}]}{(\mu+\gamma)(\alpha+\theta+\mu)} - \frac{\beta\gamma\eta\Lambda(r-1)}{(\mu+\eta)(\mu+\gamma)(\mu+\delta)}$$

2.4 Stability analysis of DFE

2.4.1 Local stability of disease-free equilibrium

Theorem 2.3. *The Disease Free Equilibrium DEF is locally asymptotically stable if $R_0 < 1$.*

Proof. The Jacobian matrix wrt system 1 is given by

$$J = \begin{bmatrix} -(\delta+\mu) & 0 & 0 & -\beta S_0 & -\beta\eta S_0 & 0 \\ \delta & -\mu & 0 & -\omega\beta V_0 & 0 & 0 \\ 0 & 0 & -(\gamma+\mu) & \beta S_0 & \beta\eta S_0 & 0 \\ 0 & 0 & r\gamma & -(\mu+\theta+\alpha) & 0 & 0 \\ 0 & 0 & (1-r)\gamma & 0 & -(\epsilon+\mu) & 0 \\ 0 & 0 & 0 & \alpha & \epsilon & -\mu \end{bmatrix}$$

which implies

$J_{DFE} =$

$$\begin{bmatrix} -p & 0 & 0 & -\beta S_0 & -\beta \eta S_0 & 0 \\ \delta & -\mu & 0 & -\omega \beta V_0 & 0 & 0 \\ 0 & 0 & -q & \beta S_0 & \beta \eta S_0 & 0 \\ 0 & 0 & r\gamma & -z & 0 & 0 \\ 0 & 0 & (1-r)\gamma & 0 & -t & 0 \\ 0 & 0 & 0 & \alpha & \epsilon & -\mu \end{bmatrix}$$

Where,
p $= (\delta + \mu)$, $q = (\gamma + \mu)$, $z = (\mu + \theta + \alpha)$, $t = (\epsilon + \mu)$

Clearly, two eigenvalues of the matrix J_{DFE} are negative such as $-\mu$ and $-\mu$. The remaining eigenvalues are the roots of the following Polynomial equation

$$\lambda^4 + a_3\lambda^3 + a_2\lambda^2 + a_1\lambda + a_0 = 0$$

where,

$$a_3 = -(-p - q - z - t) = (p + q + z + t)$$
$$a_2 = [(p + q + z + t)^2 - (p^2 + q^2 + z^2 + t^2)]/2 - \beta\gamma r S_0 - \beta\gamma\eta S_0(1 - r)$$
$$a_1 = [z(z^2 + \beta\gamma r S_0)]/3 - ((p + q + t + z)(p^2 + q^2 + t^2 + z^2 + 2\beta\gamma r S_0$$
$$- 2\beta\gamma\eta S_0(r - 1)))/2 + [(p + q + t + z)^3]/6 + p^3/3 + (t(t^2 - \beta\gamma\eta S_0(r - 1)))/3$$
$$+ (q(q^2 + \beta\gamma r S_0 - \beta\gamma\eta S_0(r - 1)))/3 - (\gamma(\beta\eta q S_0 +$$
$$\beta\eta S_0 t)(r - 1))/3 + (\gamma r(\beta q S_0 + \beta S_0 z))/3$$
$$+ (\beta S_0(\gamma q r + \gamma r z))/3 - (\beta\eta S_0(\gamma q(r - 1)$$
$$+ \gamma t(r - 1)))/3$$
$$a_0 = p(1 - R_0)(qtz - \beta\gamma r S_0 t - \beta\gamma\eta S_0 z + \beta\gamma\eta r S_0 z)$$

According to the Routh-Hurwitz criterion, the above equation will give negative roots or roots with negative real parts if the following condition is satisfied:

$$a_3 > 0, \begin{vmatrix} a_3 & a_1 \\ 1 & a_2 \end{vmatrix} > 0, \begin{vmatrix} a_3 & a_1 & 0 \\ 1 & a_2 & a_0 \\ 0 & a_3 & a_1 \end{vmatrix} > 0$$

Hence, the disease-free equilibrium point E_0 of the system is locally asymptotically stable, when $R_0 < 1$. $\qquad\square$

2.4.2   Global stability of disease-free equilibrium

We now study the global stability of disease-free equilibrium, using the theorem by (Castillo-Chavez, 2002) and (Korobeinikov and Wake, 2002)

Theorem 2.4. *If the given mathematical model can be written in the form:*

$$\frac{dX}{dt} = F(X,Y) \tag{2.16}$$
$$\frac{dY}{dt} = G(X,Y), G(X,Y) = 0$$

where $X = (S,V)^T$, $Y = (E,I,I_A,R)^T$, denoting the number of uninfected individuals and denoting the number of COVID-19-infected people respectively. Let the disease-free equilibrium of this system be

$$U_0 = (X^*, 0) = (\frac{\Lambda}{\delta + \mu}, \frac{\delta\Lambda}{\mu(\delta + \mu)}, 0)$$

where $\mathbf{0}$ is a zero vector.
For the global asymptotically stable, the following condition $(H1)$ and $(H2)$ must be satisfied.

$$(H1) : For\frac{dX}{dt} = F(X,0), \ 0 \ is \ global \ asymptotically \ stable.$$
$$(H2) : G(X,Y) = AY - \hat{G}(X,Y), \hat{G}(X,Y) \geq 0 for(X,Y) \in \Omega$$

where $A = D_Y G(X^*, 0)$ is an M- matrix (the off-diagonal elements of A are non-negative) and Ω is the region where the model makes biological sense. If the given system of differential equations of our model satisfies the given condition in (2) then the fixed point $U_0 = (X^\star, 0)$ is a global asymptotically stable (g.a.s) equilibrium of (2) provided $R_0 < 1$, and the assumption (H1) and (H2) are satisfied.

Theorem 2.5 (global asymptotic stability of DFE)**.** *The DFE E_0 of model (2.1) is global asymptotically stable if $R_0 < 1$.*

Proof. First, we rewrite the system of differential equation of our model (2.1) as $X = (S, V)^T$ and $Y = (E, I, I_A, R)^T$.

Then, the DFE is given by

$$U_0 = (X^\star, 0) = (\frac{\Lambda}{\delta + \mu}, \frac{\delta\Lambda}{\mu(\delta + \mu)}, 0)$$

. and the system $\frac{dX}{dt} = F(X, 0)$ becomes

$$\dot{S} = \Lambda - (\delta + \mu)S$$
$$\dot{V} = \delta S - \mu V \tag{2.17}$$

This equation has a unique equilibrium point

$$X^* = (\frac{\Lambda}{\delta + \mu}, \frac{\delta\Lambda}{\mu(\delta + \mu)}) \tag{2.18}$$

which is globally asymptotically stable. Therefore, condition (H1) is satisfied. We now verify the second condition (H2). For model (2.1), we have

$$G(X,Y) = \begin{bmatrix} \beta S(I + \eta I_A) + \omega\beta VI - \gamma E - \mu E \\ r\gamma E - (\mu + \theta)I - \alpha I \\ (1 - r)\gamma E - \epsilon I_A - \mu I_A \\ \alpha I + \epsilon I_A - \mu R \end{bmatrix}$$

$$D_Y G(X^*, 0) = A = F - V$$
$$= \begin{bmatrix} -(\gamma + \mu) & \beta S_0 + \omega\beta V_0 & \beta\eta S_0 & 0 \\ r\gamma & -(\mu + \theta + \alpha) & 0 & 0 \\ (1 - r)\gamma & 0 & -(\epsilon + \mu) & 0 \\ 0 & \alpha & \epsilon & -\mu \end{bmatrix}$$

Clearly, we see that A is an M-matrix, i,e. all the off-diagonal elements of A are non-negative.

$$\hat{G}(X,Y) = AY - G(X,Y)$$
$$= \begin{bmatrix} [\beta(I + \eta I_A)](S - S_0) + \omega\beta I(V - V_0) \\ 0 \\ 0 \\ 0 \end{bmatrix}$$

which implies that $\hat{G}$(X,Y) ≥ 0 for all (X,Y) $\in \Omega$. Therefore, conditions (H1) and (H2) are satisfied. Hence, disease-free equilibrium is globally asymptotically stable. $\qquad\square$

2.5 Stability analysis of EE

2.5.1 Existence of Endemic Equilibrium point

Let us denote the Endemic Equilibrium by $E_1 = (S^*, V^*, E^*, I^*, I_A^*, R^*)$ The Endemic Equilibrium always satisfies:

$$
\begin{aligned}
0 &= \Lambda - \beta S^*(I^* + \eta I_A^*) - \delta S^* - \mu S^* \\
0 &= \delta S^* - \omega \beta V^* I^* - \mu V^* \\
0 &= \beta S^*(I^* + \eta I_A^*) + \omega \beta V^* I^* - \gamma E^* - \mu E^* \\
0 &= r\gamma E^* - (\mu + \theta)I^* - \alpha I^* \\
0 &= (1 - r)\gamma E^* - \epsilon I_A^* - \mu I_A^* \\
0 &= \alpha I^* + \epsilon I_A^* - \mu R^*
\end{aligned}
\tag{2.19}
$$

which gives

$$
\begin{aligned}
S^* &= \frac{\Lambda}{\beta(I^* + \eta B) + \delta + \mu} = C \\
V^* &= \frac{\delta C}{\omega \beta I^* + \mu} = D \\
E^* &= \frac{(\mu + \theta + \alpha)I^*}{r\gamma} = A \\
I_A^* &= \frac{(1 - r)\gamma A}{(\epsilon + \mu)} = B \\
I^* &= \frac{(\mu + \gamma)(\mu + \delta)(\alpha + \theta + \mu) + \beta\gamma\Lambda r\left[\frac{\eta(r-1)(\alpha+\theta+\mu)}{r(\mu+\epsilon)} - 1\right]}{\beta(\mu + \gamma)\left[\frac{\eta(r-1)(\alpha+\theta+\mu)}{r(\mu+\epsilon)} - 1\right](\alpha + \theta + \mu)}(R_0 - 1) \\
R^* &= \frac{\alpha I^* + \epsilon B}{\mu}
\end{aligned}
$$

2.5.2 Local stability of endemic equilibrium

Theorem 2.6. *The endemic equilibrium E_1 is locally asymptotically stable if $R_0 > 1$, otherwise it is unstable.*

Proof. The Jacobian matrix of the system (2.1) at endemic equilibrium point E_1 is

obtained as follows:

$$
J_{E1} = \begin{bmatrix}
-a & 0 & 0 & -\beta S^* & -\beta \eta S^* & 0 \\
\delta & -d & 0 & -\omega\beta V^* & 0 & 0 \\
a_{31} & \omega\beta I^* & -f & a_{34} & \beta\eta S^* & 0 \\
0 & 0 & r\gamma & -j & 0 & 0 \\
0 & 0 & (1-r)\gamma & 0 & -l & 0 \\
0 & 0 & 0 & \alpha & \epsilon & -\mu
\end{bmatrix}
$$

where

$$
a = [\beta(I^* + \eta I_A^*) + \delta + \mu]
$$
$$
d = [\omega\beta I^* + \mu]
$$
$$
f = (\gamma + \mu)
$$
$$
j = (\mu + \theta + \alpha)
$$
$$
l = (\epsilon + \mu)
$$
$$
a_{31} = \beta(I^* + \eta I_A^*)
$$
$$
a_{34} = \beta S^* + \omega\beta V^*
$$

Clearly, one eigenvalue of the matrix J_{E1} is negative $-\mu$ and the remaining eigenvalues are the roots of the following Polynomial equation:

$$
\lambda^5 + c_4\lambda^4 + c_3\lambda^3 + c_2\lambda^2 + c_1\lambda + c_0 = 0
$$

where

$$
c_4 = a + d + f + j + l
$$
$$
c_3 = [(a + d + f + j - l)^2]/2 - a_{34}r\gamma - a^2/2 - d^2/2 - f^2/2
$$
$$
- j^2/2 - l^2/2 - \beta\eta S^*(1-r)\gamma
$$
$$
c_2 = adf + adj - aa_{34}r\gamma - adl + afj - afl - da_{34}r\gamma
$$
$$
+ dfj - dfl - ajl - djl + a_{34}r\gamma l - fjl + \beta a_{31}r\gamma S^*
$$
$$
+ (\beta)^2 r\gamma I^* v^*(\omega)^2 - a\beta(1-r)\gamma\eta S^* - \beta d(1-r)\gamma\eta S^*
$$
$$
+ \beta a_{31}(1-r)\gamma\eta S^* - \beta j(1-r)\gamma\eta S^*
$$

$$c_1 = adfj - ada_{34}r\gamma - adfl - adjl + aa_{34}r\gamma l - afjl$$
$$+ da_{34}r\gamma l - dfjl + \beta da_{31}r\gamma S^* - \beta a_{31}r\gamma lS^*$$
$$+ (\beta)^2 \delta r\gamma I^* S^* \omega + a(\beta)^2 r\gamma I^* V^* (\omega)^2$$
$$- (\beta)^2 r\gamma I^* lV^* (\omega)^2 - a\beta d(1-r)\gamma\eta S^*$$
$$+ \beta da_{31}(1-r)\gamma\eta S^* - a\beta j(1-r)\gamma\eta S^*$$
$$- \beta dj(1-r)\gamma\eta S^* + \beta a_{31} j(1-r)\gamma\eta S^*$$
$$+ (\beta)^2 \delta I^* (1-r)\gamma\eta S^* \omega$$
$$c_0 = adfjl - ada_{34}r\gamma l + \beta da_{31}r\gamma lS^*$$
$$+ a(\beta)^2 r\gamma I^* lV^* (\omega)^2 + a\beta dj(1-r)\gamma\eta S^*$$
$$- \beta da_{31} j(1-r)\gamma\eta S^* + (\beta)^2 \delta r\gamma I^* S^* l\omega$$
$$- (\beta)^2 \delta I^* j(1-r)\gamma\eta S^* \omega$$

According to the Routh-Hurwitz criterion, the above equation will give negative roots or negative real parts if the following condition is satisfied:

$$c_4 > 0, \begin{vmatrix} c_4 & c_2 \\ 1 & c_3 \end{vmatrix} > 0, \begin{vmatrix} c_4 & c_2 & c_0 \\ 1 & c_3 & c_1 \\ 0 & a_4 & a_2 \end{vmatrix} > 0, \begin{vmatrix} c_4 & c_2 & c_0 & 0 \\ 1 & c_3 & c_1 & 0 \\ 0 & c_4 & c_2 & c_0 \\ 0 & 1 & c_3 & c_1 \end{vmatrix} > 0$$

Hence, the endemic equilibrium point E_1 of the system is locally asymptotically stable when $R_0 > 1$. $\qquad\qquad\qquad\qquad\qquad\qquad\qquad\qquad\qquad\qquad\qquad\square$

2.5.3 Global stability of endemic equilibrium

Theorem 2.7. *The endemic equilibrium $E_1 = (S^*, V^*, E^*, I^*, I_A^*, R^*)$ of our mathematical model is globally asymptotically stable.*

Proof. For the global stability result, we will use the method discussed in Korobeinikov (Korobeinikov and Wake, 2002) and Wake , Li and Muldowney (M. Y. Li and Muldowney, 1995). From (2.1), a person was infected with coronavirus and then fully recovered. After that, we assume that a person has permanent immunity. The first five equations are independent of R in (2.1) and we will study the following sub-

system.

$$\frac{dS}{dt} = \Lambda - \beta S(I + \eta I_A) - \delta S - \mu S$$

$$\frac{dV}{dt} = \delta S - \omega \beta V I - \mu V$$

$$\frac{dE}{dt} = \beta S(I + \eta I_A) + \omega \beta V I - \gamma E - \mu E \qquad (2.20)$$

$$\frac{dI}{dt} = r\gamma E - (\mu + \theta)I - \alpha I$$

$$\frac{dI_A}{dt} = (1 - r)\gamma E - \epsilon I_A - \mu I_A$$

Let

$$x_1 = \frac{S}{S^*}, y_1 = \frac{V}{V^*}, z_1 = \frac{E}{E^*} u_1 = \frac{I}{I^*}, v_1 = \frac{I_A}{I_A^*}$$

The model of the system of equation (2.20) is transformed into the following form

$$\frac{dx_1}{dt} = x_1[\frac{\Lambda}{S^*}(\frac{1}{x_1}) - \beta I^*(u_1 - 1) - \beta \eta I_A^*(v_1 - 1)]$$

$$\frac{dy_1}{dt} = y_1[\frac{\delta S^*}{V^*}(\frac{x_1}{y_1} - 1) - \omega \beta I^*(u_1 - 1)]$$

$$\frac{dz_1}{dt} = z_1[\frac{\beta S^* I^*}{E^*}(\frac{x_1 u_1}{z_1} - 1) + \frac{\beta \eta S^* I_A^*}{E^*}(\frac{x_1 v_1}{z_1} - 1) + \frac{\omega \beta V^* I^*}{E^*}(\frac{y_1 u_1}{z_1} - 1)] \qquad (2.21)$$

$$\frac{du_1}{dt} = u_1 \frac{r\gamma E^*}{I^*}(\frac{z_1}{u_1} - 1)$$

$$\frac{dv_1}{dt} = v_1 \gamma(1 - r)\frac{E^*}{I_A^*}(\frac{z_1}{v_1} - 1)$$

Here it is easy to find that the system of equation (2.21) has unique endemic equilibrium $E_1(1,1,1,1,1)$ and the global stability of $E_1(1,1,1,1,1)$ is same as that of E_1. Thus we investigate the global stability of $E_1(1,1,1,1,1)$ instead of E_1.

Defining the Volterra- type Lyapunov function

$$L(x_1, y_1, z_1, u_1, v_1) = S^*(x_1 - 1 - \ln x_1) + V^*(y_1 - 1 - \ln y_1) + E^*(z_1 - 1 - \ln z_1)$$
$$+ \frac{\beta I^*(S^* + \omega V^*)}{r\gamma E^*}(u_1 - 1 - \ln u_1) +$$
$$\frac{\beta \eta I_A^*(S^* + \omega V^*)}{\gamma(1 - r)E^*}(v_1 - 1 - \ln v_1)$$

From equilibrium state E_1 we have the following equations

$$\Lambda = \beta S^*(I^* + \eta I_A^*) + (\delta + \mu)S^*$$
$$\delta S^* = \omega \beta V^* I^* + \mu V^*$$
$$(\gamma + \mu)E^* = \beta S^*(I^* + \eta I_A^*) + \omega \beta V^* I^*$$
$$r\gamma E^* - (\alpha + \mu)I^*$$
$$\gamma(1 - r)E^* = (\epsilon + \mu)I_A^*$$

Then, differentiating L w.r.t 't' along the solution curve of the system of the equation of model (2.21) and considering the above equation gives

$$\frac{dL}{dt} = S^*(x_1 - 1)\frac{\dot{x}_1}{x_1} + V^*(y_1 - 1)\frac{\dot{y}_1}{y_1} + E^*(z_1 - 1)\frac{\dot{z}_1}{z_1}$$
$$+ \frac{\beta I^*(S^* + \omega V^*)}{r\gamma E^*}(u_1 - 1)\frac{\dot{u}_1}{u_1} + \frac{\beta \eta I_A^*(S^* + \omega V^*)}{\gamma(1 - r)E^*}(v_1 - 1)\frac{\dot{v}_1}{v_1}$$
$$= (x_1 - 1)[\Lambda(\frac{1}{x_1} - 1) - \beta S^* I^*(u_1 - 1) - \beta \eta S^* I_A^*(v_1 - 1)]$$
$$+ (y_1 - 1)[\delta S^*(\frac{x_1}{y_1} - 1) - \omega \beta V^* I^*(u_1 - 1)]$$
$$+ (z_1 - 1)[\beta S^* I^*(\frac{x - 1u_1}{z_1} - 1) + \beta \eta S^* I_A^*(\frac{x - 1v_1}{z_1} - 1) + \omega \beta V^* I^*(\frac{y - 1u_1}{z_1} - 1)]$$
$$+ \beta I^*(S^* + \omega V^*)(u_1 - 1)(\frac{z_1}{u_1} - 1)$$
$$+ \beta \eta I_A^*(S^* + \omega V^*)(v_1 - 1)(\frac{z_1}{v_1} - 1)$$

After some algebraic manipulation, we have

$$\frac{dL}{dt} = \mu S^*(2 - x_1 - \frac{1}{x_1}) + \mu V^*(3 - \frac{1}{x_1} - y_1 - \frac{x_1}{y_1})$$
$$+ \beta S^* I^*(3 - \frac{1}{x_1} - \frac{x_1 u_1}{z_1} - \frac{z_1}{u_1}) + \beta \eta S^* I_A^*(3 - \frac{1}{x_1} - \frac{x_1 v_1}{z_1} - \frac{z_1}{v_1})$$
$$+ \omega \beta V^* I^*(4 - \frac{1}{x_1} - \frac{x_1}{y_1} - \frac{y_1 u_1}{z_1} - \frac{z_1}{u_1})$$

Since the arithmetic mean is greater than or equal to geometric mean, we have

$$(2 - x_1 - \frac{1}{x_1}) \leq 0$$

$$(3 - \frac{1}{x_1} - y_1 - \frac{x_1}{y_1}) \leq 0$$

$$(3 - \frac{1}{x_1} - \frac{x_1 u_1}{z_1} - \frac{z_1}{u_1}) \leq 0$$

$$(3 - \frac{1}{x_1} - \frac{x_1 v_1}{z_1} - \frac{z_1}{v_1}) \leq 0$$

$$(4 - \frac{1}{x_1} - \frac{x_1}{y_1} - \frac{y_1 u_1}{z_1} - \frac{z_1}{u_1}) \leq 0$$

Thus it is easy to observe that $\frac{dL}{dt} \leq 0$ and the equality $\frac{dL}{dt} = 0$ hold for

$$x_1 = y_1 = 1, z_1 = u_1 = v_1$$

which corresponds to the set $[(S,V,E,I,I_A: S=S^*,V\ -V^*, E= E^*,I=I^*,I_A = I_A^*)]$Hence from LaSalle's invariance principle (J. P. La Salle, 1976), the equilibrium E_1 of the given system is globally asymptotically stable for $R_0 > 1$.   □

2.6   Sensitivity Analysis

In this section, we conduct a sensitivity analysis to understand the impact of various parameters on the basic reproduction number, R_0. This analysis helps identify how changes in these parameters can increase or decrease R_0. The goal is to determine which parameters significantly influence R_0 and should therefore be targeted by intervention strategies.

Sensitivity indices measure the relative change in a variable when a parameter changes. We use the forward sensitivity index of a variable with respect to a given parameter, defined as follows:

$$\alpha_\phi^{R_0} = \frac{\partial R_0}{\partial \phi} \frac{\phi}{R_0}$$

where ϕ represents the parameters $[\gamma, \mu, r, \theta, \alpha, \epsilon, \beta, \delta, \omega, \eta, \Lambda]$.

Using this formula, we can analytically calculate the sensitivity of R_0 to each parameter it comprises. Figure 2.2 illustrates the sensitivity indices for parameters $\gamma, \mu, r, \theta, \alpha, \epsilon, \beta, \delta, \omega, \eta$, and Λ with respect to R_0.

Positive indices indicate a direct relationship between the parameter and R_0. This means that an increase in the parameter will result in an increase in R_0, and vice versa. To control COVID-19 in the population, we need to reduce the basic reproduction number. This can be achieved by reducing the parameters that have positive indices, namely γ, r, β, ω, η, and Λ. Among these, the birth rate (Λ) and the transmission rate (β) are the most sensitive parameters of R_0. Since it is not feasible to control the birth rate, we focus on reducing the transmission rate. This reduction can be accomplished by limiting contact rates, hence the implementation of measures like quarantine and social distancing. Additionally, as the reduction in infection risk due to vaccination (ω) increases, R_0 decreases. Therefore, increasing vaccination coverage can effectively reduce the basic reproduction number.

Negative indices indicate an inverse relationship between the parameter and R_0. This means that a decrease in the parameter will lead to an increase in R_0, and vice versa. Parameters μ, θ, α, ϵ, and δ have negative indices. Among these, μ (the death rate) is the most sensitive. An increase in the death rate results in a decrease in R_0.
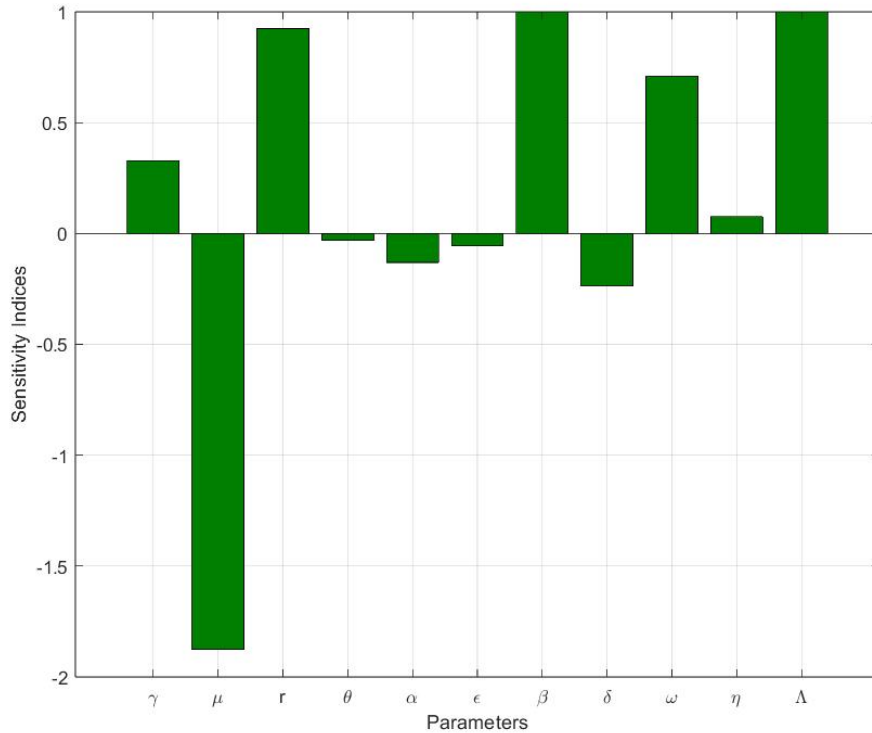
Figure 2.2: Forward sensitivity of R_0

The sensitivity analysis of our mathematical model provides critical insights into the dynamics of COVID-19 transmission and control, highlighting the impact of various parameters on the basic reproduction number (R_0). This analysis guides effective intervention strategies by identifying key parameters that significantly influence R_0.

From our analysis (Figure 2.3), we observe that increasing the vaccination rate (δ) leads to a decrease in R_0. Conversely, higher transmission rates (β) result in higher values of R_0. However, effective vaccination can mitigate this effect. This finding underscores the importance of mass vaccination programs in controlling the pandemic, even in scenarios with high transmission rates. Vaccination significantly reduces the potential for the virus to spread by lowering the basic reproduction number.
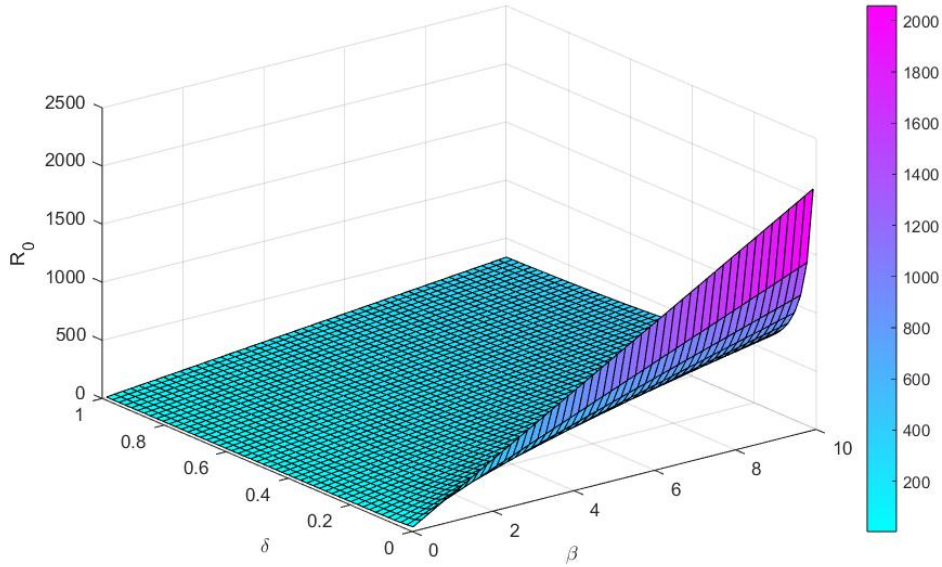
Figure 2.3: The numerical result exhibit that the dependence of R_0 of system on the rate of transmission β and Vaccination rate δ

Further examination (Figure 2.4) reveals that both higher vaccination rates and higher vaccine efficacy (ω) lead to a substantial reduction in R_0. The interplay between these parameters shows how both coverage and effectiveness of vaccines are critical in controlling the spread of COVID-19. Policies should focus on rapid vaccine deployment and ensuring high efficacy to achieve significant control over the pandemic.
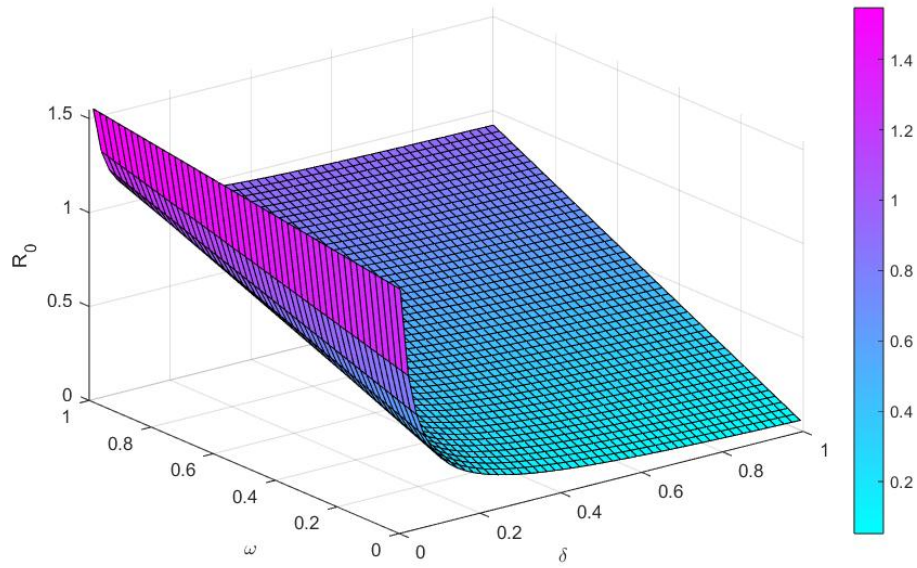
Figure 2.4: The numerical result exhibit that the dependence of R_0 of system on Vaccination rate δ and Efficacy of Vaccine ω

In addition, our findings (Figure 2.5) indicate that while higher transmission rates increase R_0, reducing transmission from asymptomatic individuals (η) can mitigate this effect. The presence of asymptomatic carriers with reduced transmission still contributes to controlling R_0. This emphasizes the importance of vaccination and public health strategies that target asymptomatic spread through widespread testing and vaccination.
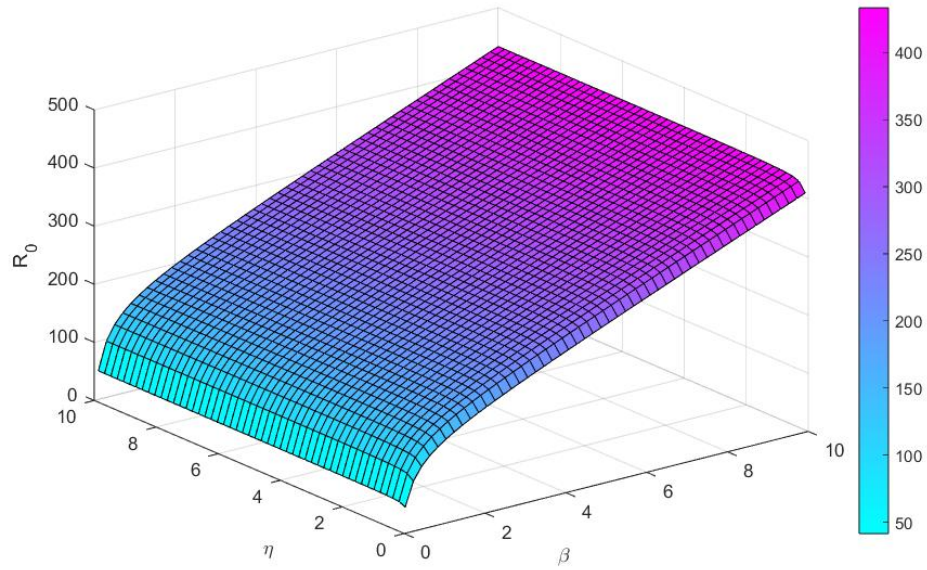
Figure 2.5: The numerical result exhibit that the dependence of R_0 of system on the rate of transmission β and Reduction in the transmission from asymptomatic η
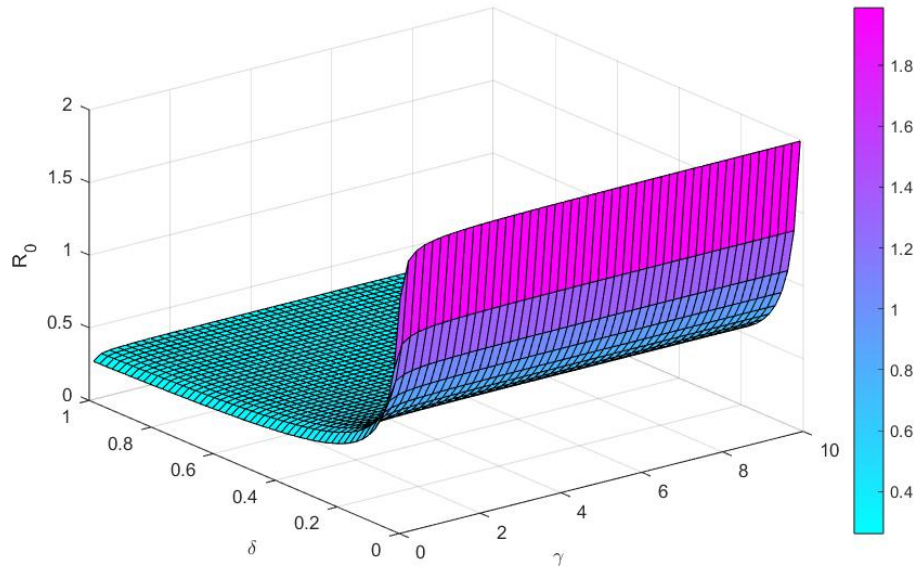
Figure 2.6: The numerical result exhibit that the dependence of R_0 of system on the rates of transition to infected states γ and Vaccination rate δ

Moreover, our analysis (Figure 2.6) suggests that higher rates of transition to

infected states (γ) increase R_0, but this can be counteracted by increasing the vaccination rate (δ). Effective vaccination lowers R_0 despite faster progression from exposed to infected states. Therefore, efforts to vaccinate quickly and efficiently are key to managing outbreaks and controlling the spread of COVID-19.

Overall, our numerical simulations validate these findings, highlighting the critical role of vaccination in controlling the pandemic. By targeting key parameters identified through sensitivity analysis, public health policies can be better informed and more effective in mitigating the spread of COVID-19.

This revised structure presents a comprehensive narrative of your results, integrating the relevant figures and their implications. This approach ensures that the results section is detailed and addresses the reviewers' concerns about insufficient detail.

2.7 Numerical Simulation

For the numerical simulation of the proposed model, we utilize the MATLAB program to illustrate the mathematical findings. The parameter values used in the simulation are listed in the table and depicted in Figures 2.7 and 2.8.
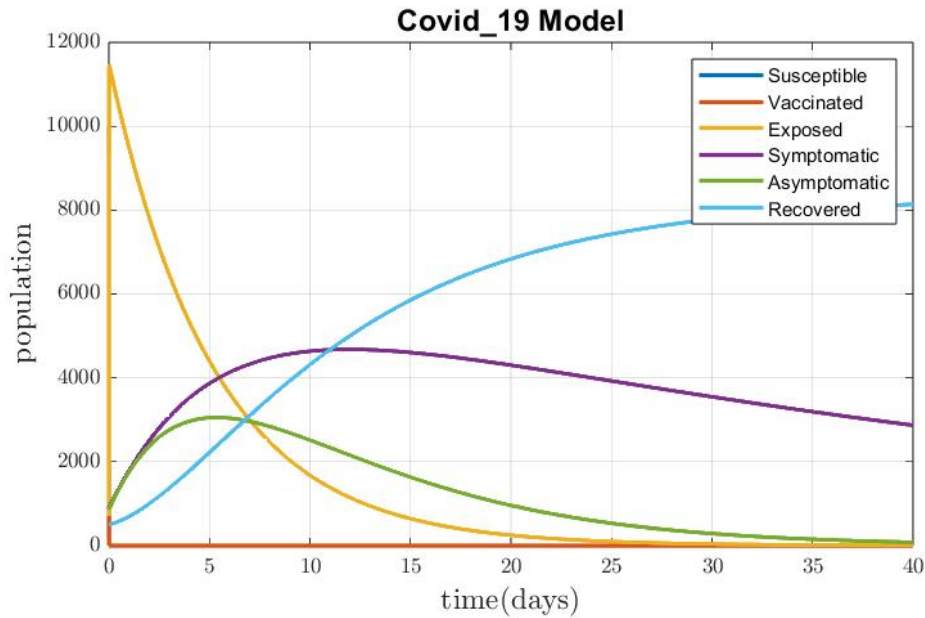
Figure 2.7: Variation of $SVEII_AR$ with time corresponding to $R_0 > 1$ from t=0 to 40
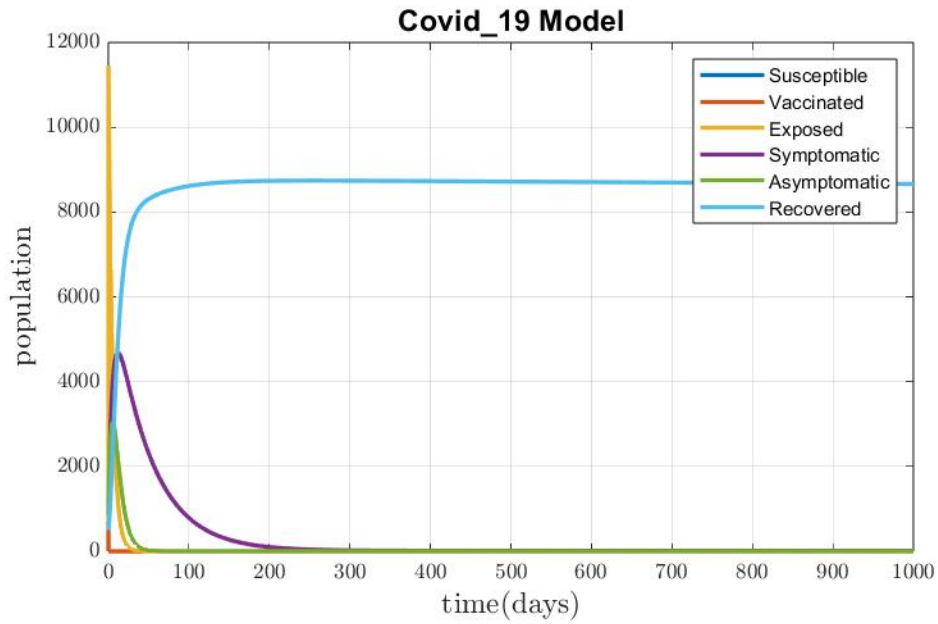
Figure 2.8: Variation of $SVEII_AR$ with time corresponding to $R_0 > 1$ from t=0 to 1000

Next, we consider all parameters on daily basis, the parameter value is considered for Disease-Free Equilibrium as $\Lambda = 20$, $\mu = 0.0245$, $\theta = 0.001$, $\alpha = 0.004165$, $\epsilon = 0.0714$, $\delta = 0.4$, $\eta = 0.0085$, $\gamma = 0.05$, r = 0.0075, $\beta = 0.0065$, $\omega = 0.2$. we get $R_0 = 0.2397 < 1$, if $\omega = 1$, $R_0 = 0.9184$. The stability of Disease-Free Equilibrium $E_0 = (47.1143, 138.6122, 0, 0, 0, 0)$ is stable and is shown in Figure 2.9.
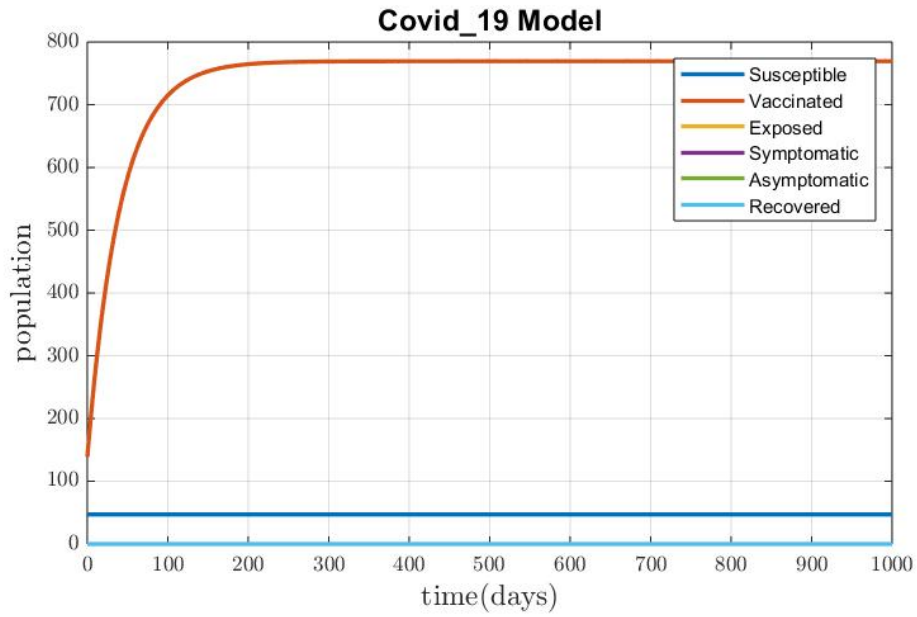
Figure 2.9: Variation of $SVEII_A$R with time showing the stability of Disease-Free Equilibrium with $R_0 = 0.2397$

Figure 2.10 and 2.11 shows the Variation of $SVEII_A$R with time corresponding to the values of $R_0 < 1$ for different values of the initial numbers of each compartment.
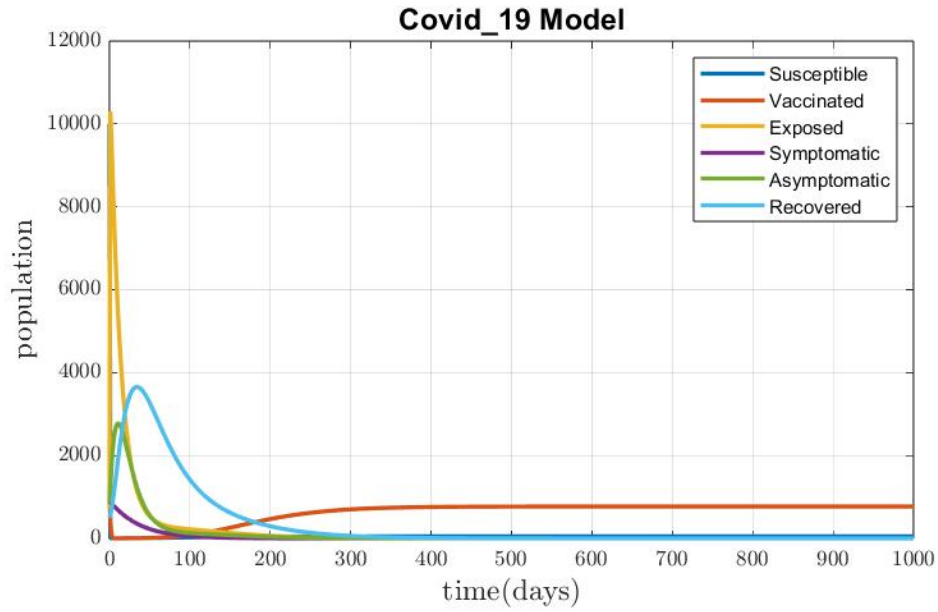
Figure 2.10: Variation of $SVEII_AR$ with time corresponding to the values of R_0 < 1 for different values of initial numbers of each compartment with time t = 0 to 1000
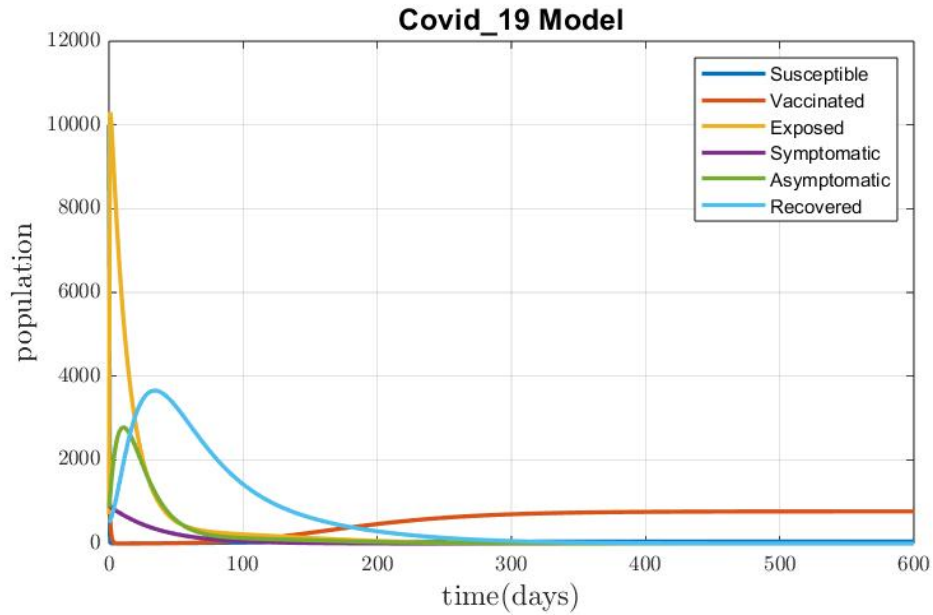
Figure 2.11: Variation of $SVEII_AR$ with time corresponding to the values of R_0 < 1 for different values of initial numbers of each compartment with time t = 0 to 600

The impact of varying the parameters ω and β is illustrated in Figures 2.12 and

2.13. These figures demonstrate that as the values of ω and β decrease, the infected population correspondingly diminishes. This relationship indicates that a lower rate of reduction in the risk of infection due to the vaccine, represented by ω, leads to a decrease in the basic reproduction number, R_0. Consequently, a higher number of vaccinated individuals results in a more substantial decrease in the infection risk induced by the vaccine. By successfully lowering R_0, we can achieve a significant decline in the infected population.

To elaborate, parameter ω represents the efficacy of the vaccine in reducing the risk of infection. When ω is high, the vaccine is highly effective, leading to a significant reduction in the transmission of the virus. As ω decreases, the vaccine's effectiveness diminishes, resulting in a smaller reduction in transmission. Parameter β, on the other hand, represents the transmission rate of the virus. A lower β indicates a lower probability of virus transmission per contact between susceptible and infected individuals.

Figures 2.12 and 2.13 clearly show that reducing ω and β lowers the number of new infections, thereby reducing the overall infected population. This finding underscores the critical importance of maintaining high vaccine efficacy and minimizing the transmission rate to control the spread of the virus effectively. By focusing on strategies that enhance vaccine coverage and efficacy, we can significantly impact the basic reproduction number, R_0, and achieve a substantial reduction in the infected population.
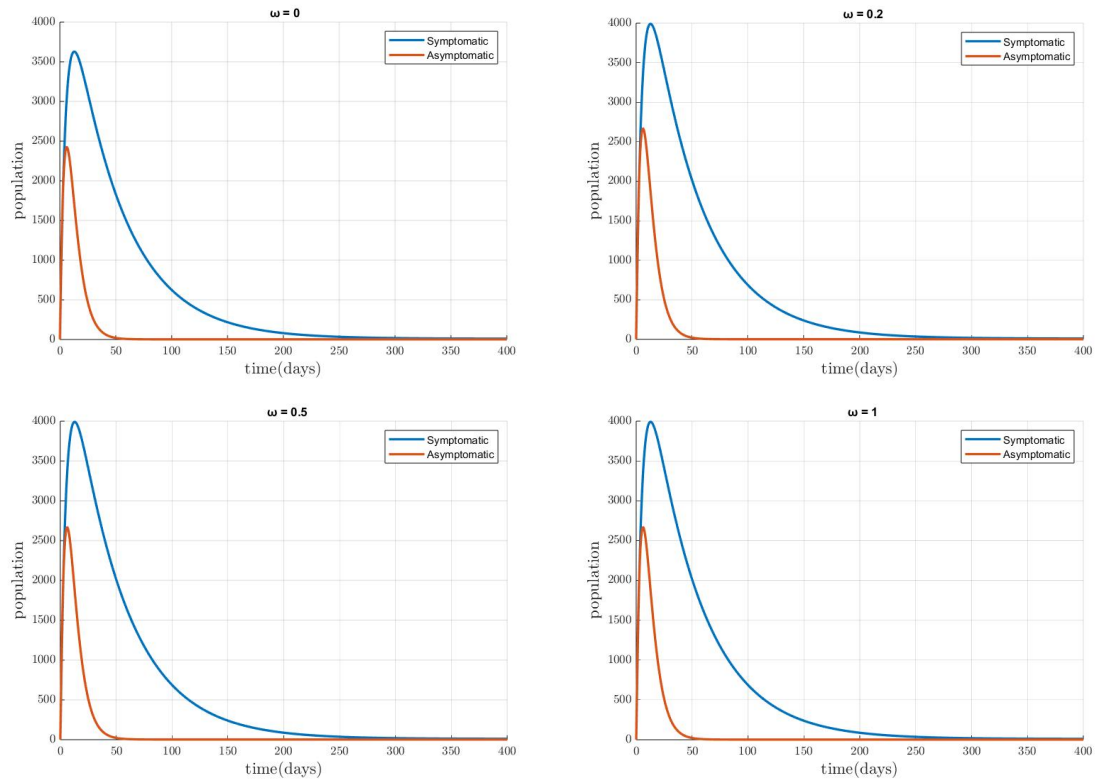
Figure 2.12: Variation of Infected population with time for different value of ω
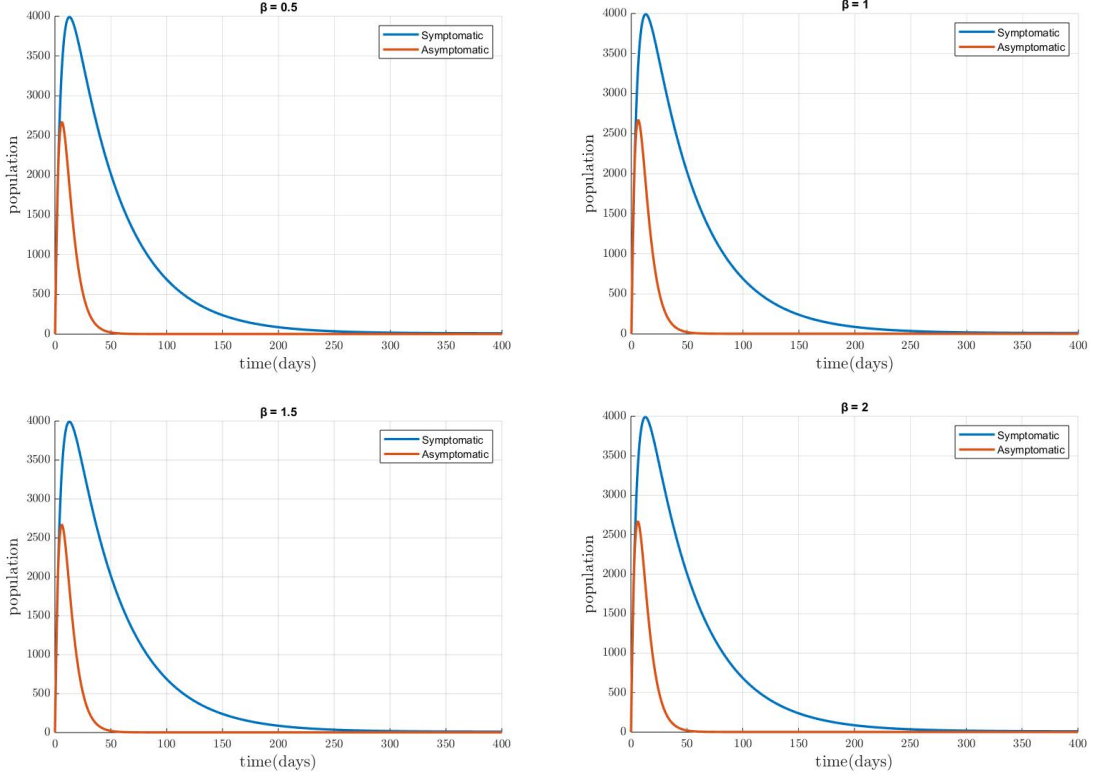
Figure 2.13: Variation of Infected population with time for different value of β

Lastly, we simulate our model to observe the change in the final density of infected individuals with vaccination coverage levels of $\delta = 0$, 20%, 40%, 60%, and 80% in a local population of N = 6000. The numerical results, presented in Figure 2.14, indicate that timely vaccination and expanding vaccination coverage can control both the peak and the final scale of the epidemic more effectively. Notably, 80% vaccination coverage yields optimal results in reducing the number of cases. With maximum vaccine efficacy, the basic reproduction number R_0 is reduced to 0.2397, demonstrating the profound impact of high vaccination coverage. This approach not only achieves faster epidemic control but also significantly diminishes the harm caused by the epidemic and reduces the costs associated with epidemic prevention. Therefore, emphasizing the importance of widespread vaccination coverage is crucial for effective epidemic management. In conclusion, our numerical simulations underscore the critical importance of vaccination coverage. Higher vaccination rates reduce the basic reproduction number and the infected population, highlighting the effectiveness of vaccination strategies in controlling and mitigating the impact of the epidemic.
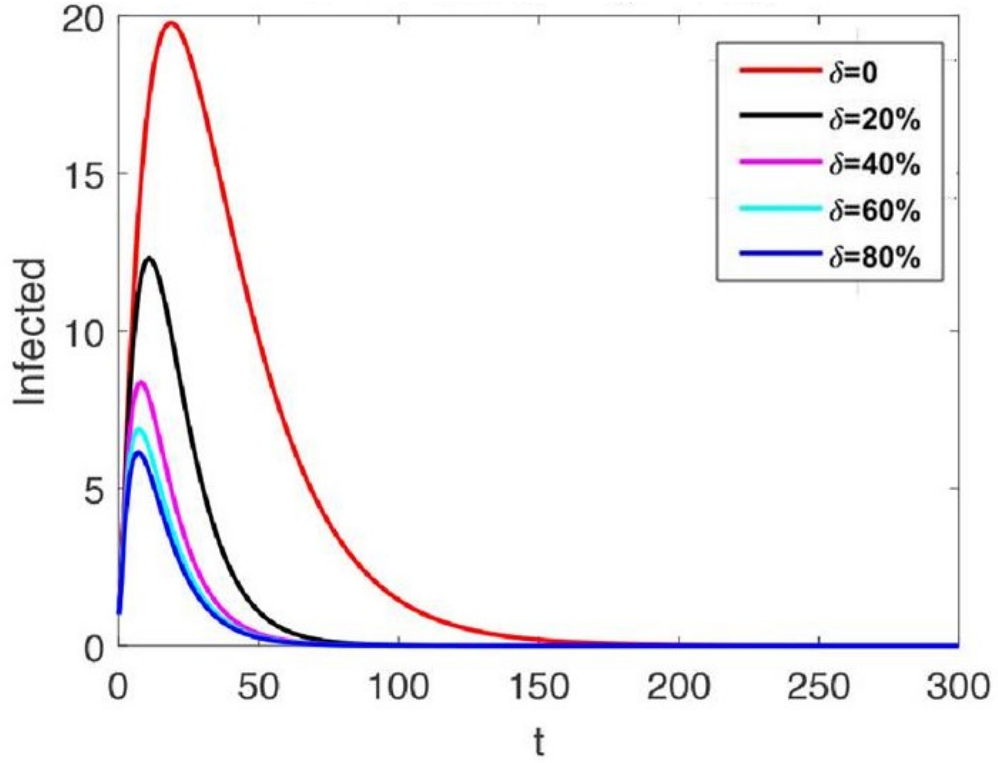
Figure 2.14: Simulation of Infected individuals with different vaccination rate $\delta = 0, 20\%, 40\%, 60\%, 80\%$ show that the higher the COVID-19 vaccination rate, the smaller the peak number of infected patients

2.8   Conclusion

This study presents a comprehensive mathematical model to understand and predict the dynamics of COVID-19 transmission and the impact of various vaccination strategies. By categorizing the population into compartments—Susceptible, Vaccinated, Exposed, Symptomatic Infection, Asymptomatic Infection, and Recovered or Deceased—we captured the complexities of disease spread and the effects of vaccination.

Our stability analysis highlights the importance of the basic reproduction number, R_0. The Disease-Free Equilibrium is stable when R_0 is less than 1, suggesting that the disease can be eradicated under this condition. Conversely, the Endemic Equilibrium remains stable when R_0 exceeds 1, indicating persistent transmission. These findings underscore the critical threshold value of R_0 in determining the long-term behaviour of the epidemic.

Through sensitivity analysis, we identified key parameters influencing R_0. Parameters such as transmission rate, vaccination rate, and vaccine efficacy are crucial in controlling the spread of the virus. Our results indicate that increasing vaccination coverage and efficacy while reducing transmission rates are effective strategies to lower R_0.

Numerical simulations using MATLAB validated these findings, demonstrating how different parameters affect disease dynamics. For instance, increasing the vaccination rate and vaccine efficacy significantly reduces the infected population, even in scenarios with high transmission rates. This reinforces the need for rapid and extensive vaccination campaigns to control the pandemic effectively.

The simulations also illustrated the critical impact of reducing transmission rates and enhancing vaccine efficacy on R_0. Lowering these parameters directly reduces the number of new infections, highlighting the importance of maintaining high vaccine efficacy and minimizing transmission rates.

Lastly, our simulations emphasized the substantial benefits of high vaccination coverage. With a vaccination rate of 80%, the basic reproduction number R_0 was significantly reduced, leading to faster epidemic control and lower infection rates. This demonstrates that widespread vaccination is essential for effective epidemic management.

In conclusion, our study unequivocally demonstrates the critical importance of vaccination in the fight against COVID-19. By targeting the key parameters identified through our sensitivity analysis, public health interventions can be precisely tailored to effectively reduce R_0 and control the epidemic. The insights garnered from this research offer a solid foundation for developing robust strategies to combat COVID-19 and bolster preparedness for future outbreaks. Overall, our study provides valuable insights for public health policymakers and stakeholders, advocating for sustained efforts to maximize vaccination coverage and improve vaccine efficacy.

Chapter 3

Investigating SARS-CoV-2 Dynamics: The Role of Vaccination and Intervention Strategies

3.1 Introduction

The COVID-19 pandemic has presented an unprecedented global health crisis, requiring rapid and effective strategies to mitigate its impact. Mathematical modelling has become a potent tool for comprehending and forecasting the dynamics of infectious diseases, providing insightful data on the modes of transmission, effects of vaccination, and efficacy of intervention strategies. The use of mathematical modelling is essential for guiding evidence-based decision-making in India, a nation with a sizable population and distinctive demographic traits, in order to address COVID-19 effectively.

The first Mathematical model in Epidemiology was the work of Daniel Bernoulli on the effect of variolation against smallpox in increasing life expectancy (Bernoulli, 1760), Since Kermack and McKendrick's pioneering work, mathematical models have been applied to provide a framework for comprehending the dynamics of infectious diseases (Kermack and McKendrick, 1927). A number of mathematical models have also been put forth to comprehend the COVID-19 transmission dynamics in India. Several studies have expanded the SI (Duan *et al.*, 2019), SIS (Y. Xie *et al.*, 2020),

---

SIR (Sene, 2020), SEIR [(Rezapour *et al.*, 2020) by including a number of new compartments such as asymptomatic, isolated, quarantined, protected, death, lock-down, hospitalized, etc. (Bajiya *et al.*, 2020; Gupta *et al.*, 2021; Khajanchi and Sarkar, 2020; Mahajan *et al.*, 2020; Ray *et al.*, 2020; Senapati *et al.*, 2021; Tiwari *et al.*, 2020).

This research aims to investigate the mathematical modelling of COVID-19 in India, with a specific focus on studying the impact of vaccination and intervention measures. In this study, we also consider the period from March 2020 to December 2020 of the COVID-19 outbreak where several preventive measures have been implemented in India to measure the strength of intervention measures. The government of India declares a nationwide lockdown from 24 March 2020 for 21 days (Pulla, 2020). In India vaccine was introduced on 16 January 2021, and India began the administration of COVID-19 vaccines. As of 25 March 2022, India has administered over 1.8 billion doses overall. In India, 90 % of the eligible population has received at least one shot, and 76 % of the eligible population is fully vaccinated(V. M. Kumar *et al.*, 2021). We shall introduce the Vaccine compartment in our model.

The findings will help policymakers, public health professionals, and researchers develop focused strategies to manage the epidemic and ensure the health and well-being of the Indian population. This will support evidence-based decision-making.

3.2 Model Formulation

We create a deterministic compartmental model $SVEII_AR$ to describe the disease transmission mechanism. Let N be the total population of humans. The total population N is divided into six compartments: Susceptible (S), Vaccinated(V), Exposed(E), Symptomatic Infection(I), Asymptomatic Infection(I_A), and individuals that are either recovered or die from COVID-19(R). We also include Vital Dynamics: The natural human natality or recruitment rate denoted by Λ and mortality(death) rate denoted by μ.

Susceptible individuals move to the Exposed compartment when they come into contact with Symptomatic Individuals(I) as well as Asymptomatic Individuals(I_A) at a rate β (rate of transmission). It is reported that I_A has a lower chance of transmission than I (MoHFW). So we assume that transmission of the disease from

Asymptomatic individuals(I_A) to Susceptible individuals is less than that of Symptomatic Individuals to Susceptible.

We denote the reduction in the rate of transmission from Asymptomatic Individuals to Symptomatic as η where $\eta < 1$. The new infection is given by $\beta S(I + \eta I_A)$

Susceptible Individuals who are Vaccinated move to the Vaccinated compartment at the rate δ. Since Vaccines are not 100 % effective(www.cdc.gov), we assume that those in the Vaccination class are not at a complete protective level, and the Vaccinated individuals become infected and move into the Exposed class. We assume that this occurs at a lower transmission rate ω, where $\omega \in [0,1]$ is the decreasing coefficient.

We adapt the model to include several intervention techniques. The use of preventive measures such as lock-downs, media campaigns to raise awareness, effective handwashing techniques, social seclusion, mask use, etc., as part of intervention strategies, slows the spread of disease.

The application of the intervention suggests that there would be a decrease in the rate of disease transmission in terms of model parameters. The strength of the intervention, h where $h \in [0, 1]$, is deemed to have decreased at this rate of transmission.

During the course of implementation, the parameter β is transformed to $(1-h)\beta$ when there is intervention. The Exposed individuals move to the Infected class i.e, I, I_A at a rate γ. A fraction of the population moves from Expose to the Symptomatic class at a rate r, and the remaining fraction moves to the Asymptomatic class at the rate (1-r).

Individuals from Symptomatic and Asymptomatic recover at a rate α, η respectively. Each of these classes may decrease as a result of mortality μ, while an individual who shows COVID-19 Symptoms may have a lower chance of survival, therefore, the Symptomatic class decreases as a result of death from COVID-19 at a rate θ.

Based on the assumption we propose the following model; a system of non-linear differential equations. The Schematic diagram is shown in Figure 3.1.
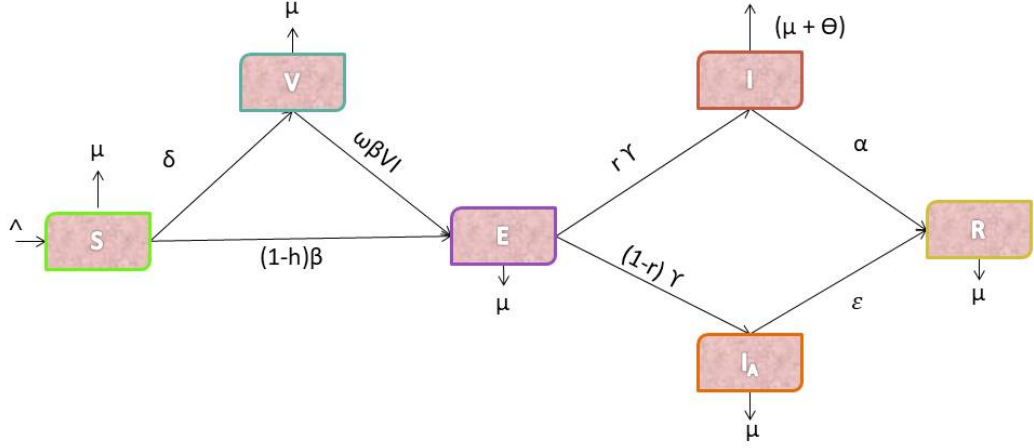
Figure 3.1: Schematic Diagram of $SVEII_AR$

$$\frac{dS}{dt} = \Lambda - (1-h)\beta S(I + \eta I_A) - \delta S - \mu S,$$

$$\frac{dV}{dt} = \delta S - \omega \beta V I - \mu V,$$

$$\frac{dE}{dt} = (1-h)\beta S(I + \eta I_A) + \omega \beta V I - \gamma E - \mu E, \qquad (3.1)$$

$$\frac{dI}{dt} = r\gamma E - (\mu + \theta)I - \alpha I,$$

$$\frac{dI_A}{dt} = (1-r)\gamma E - \epsilon I_A - \mu I_A,$$

$$\frac{dR}{dt} = \alpha I + \epsilon I_A - \mu R,$$

with nonnegative initial conditions given by

$$S(0) > 0, \ V(0) > 0, \ E(0) > 0, \ I(0) > 0, \ I_A > 0, \ R(0) > 0. \qquad (3.2)$$

All the parameters of the system (3.1) are assumed to be positive for all time $t > 0$.

Table 3.1: Parameter Description for $SVEII_AR$

Parameter	Description	Value
Λ	Birth rate	$\frac{10000}{59 \times 365} \ day^{-1}$
μ	Death rate	$\frac{1}{59 \times 365} \ day^{-1}$
β	Rate of transmission	$1.7399 \ day^{-1}$
γ	Rate of transition from Exposed to infected class	$0.1923 \ day^{-1}$
r	Fraction of population moves from Exposed to symptomatic class	0.4579
$(1\text{-}r)$	Fraction of population moves from Exposed to asymptomatic class	0.5422
α	Recovery rate of symptomatic infected class	$0.004165 \ day^{-1}$
η	Reduction in transmission from asymptomatic, $\eta < 1$	0.1002
ϵ	Recovery rate of asymptomatic infection	$0.13978 \ day^{-1}$
θ	Rate of disease-induced death	0.0175
δ	Rate at which susceptible individuals are vaccinated	$0.4 \ day^{-1}$
ω	Rate of reduction in risk of infection due to vaccination	0.2
h	Strength of intervention	$0; 0.5042;$
		$0.6544; 0.7282$

3.3 Mathematical Model Analysis

3.3.1 Positivity of Solutions

For the COVID-19 model system 3.1 to be epidemiologically realistic, it is necessary to prove that all the state variables remain positive for all time.

Theorem 3.1. *Let the initial data be $\{(S, V, E, I, I_A, R) \leq 0\} \in \phi$. Then the solution set $\{S(t), V(t), E(t), I(t), I_A(t), R(t)\}$ of the model system is non negative for all time t.*

Proof. Considering the non-linear system of the model (3.1), we take the first equation

$$\frac{dS}{dt} = \Lambda - (1 - h)\beta S(I + \eta I_A) - \delta S - \mu S,$$

$$\frac{dS}{dt} \geq -[(1 - h)\beta(I + \eta I_A) + \delta + \mu]S,$$

$$\int \frac{dS}{S} \geq -\int [(1-h)\beta(I+\eta I_A) + \delta + \mu]dt,$$

$$\ln S \geq -[(1-h)\beta(I+\eta I_A) + \delta + \mu]t + c,$$

$$S \geq e^{-[(1-h)\beta(I+\eta I_A)+\delta+\mu]t} + e^c,$$

$$S(t) \geq S(0)e^{-[(1-h)\beta(I+\eta I_A)+\delta+\mu]t}.$$

Similarly, it can also been shown that $V(t) > 0$, $E(t) > 0$, $I(t) > 0$, I_A $R(t) > 0$ for all $t > 0$. Therefore, the disease is uniformly persistent for every positive solution. □

3.3.2 Invariant Region

Theorem 3.2. *For the initial conditions (3.2), the solutions of system (3.1) are contained in the region $\phi \subset R_+^6$ defined by*

$$\phi = [\{S(t), V(t), E(t), I(t), I_A(t), R(t)\} \in R_+^6 : N(t) \leq \frac{\Lambda}{\mu}]$$

Proof. Let, $N = S + V + E + I + I_A + R$

$$\frac{dN}{dt} = \Lambda - (S + V + E + I + I_A + R)\mu - \theta I \tag{3.3}$$

$$\frac{dN}{dt} = \Lambda - \mu N - \theta I \tag{3.4}$$

$$\frac{dN}{dt} \leq \Lambda - \mu N \tag{3.5}$$

$$\frac{dN}{dt} + \mu N \leq \Lambda \tag{3.6}$$

$$Ne^{\mu t} \leq \int e^{\mu t}\Lambda + C \tag{3.7}$$

$$Ne^{\mu t} \leq \frac{\Lambda e^{\mu t}}{\mu} + C \tag{3.8}$$

$$N \leq \frac{\Lambda}{\mu} + Ce^{-\mu t}. \tag{3.9}$$

At $t \longrightarrow \infty$, $N \longrightarrow \frac{\Lambda}{\mu}$. Clearly $\phi = [\{S(t), V(t), E(t), I(t), I_A(t), R(t)\} \in R_+^6 : N(t) \leq \frac{\Lambda}{\mu}]$ □

3.3.3   Analysis of Disease-Free Equilibrium (DFE) E_0

The model gets DFE when the disease has zero induction

Taking the first equation of system (3.1) with $E = I = I_A = R = 0$ into consideration.

$$0 = \Lambda - (1 - h)\beta S(I + \eta I_A) - \delta S - \mu S \tag{3.10}$$

$$0 = \delta S - \omega \beta V I - \mu V \tag{3.11}$$

$$0 = (1 - h)\beta S(I + \eta I_A) + \omega \beta V I - \gamma E - \mu E \tag{3.12}$$

$$0 = r\gamma E - (\mu + \theta)I - \alpha I \tag{3.13}$$

$$0 = (1 - r)\gamma E - \epsilon I_A - \mu I_A \tag{3.14}$$

$$0 = \alpha I + \epsilon I_A - \mu R \tag{3.15}$$

we arrive at

$$S_0 = \frac{\Lambda}{(\delta + \mu)}, V_0 = \frac{\delta \Lambda}{\mu(\delta + \mu)}$$

Then, the disease-free equilibrium (DFE) state E_0 is given by

$$E_0 = [\frac{\Lambda}{(\delta + \mu)}, \frac{\delta \Lambda}{\mu(\delta + \mu)}, 0, 0, 0, 0]$$

3.3.4   Basic reproductive number R_0

R_0 refers to the average number of secondarily infected persons infected by one primary infected patient during the infectious period. To obtain the basic reproduction number, we used the next-generation matrix method by (Diekmann and Heesterbeek, 2000) and (van den Driessche and Watmough, 2008), where $\mathcal{F}$ is the matrix of the new infection terms and $\mathcal{V}$ is the matrix of the transition terms.

Infected compartments are $E,\ I,\ I_A\ , R$.

Let $Y\ =\ (E\ , I\ , I_A\ , R)$,

$$\frac{dY}{dt} = \begin{bmatrix} (1-h)\beta S(I + \eta I_A) + \omega \beta V I \\ 0 \\ 0 \\ 0 \end{bmatrix} - \begin{bmatrix} (\gamma + \mu)E \\ -r\gamma E + (\mu + \theta + \alpha)I \\ -(1-r)\gamma E + (\eta + \mu)I_A \\ -\alpha I - \epsilon I_A + \mu R \end{bmatrix}$$

$$F_1 = \begin{bmatrix} 0 & (1-h)\beta S + \omega\beta V & (1-h)\beta\eta S & 0 \\ 0 & 0 & 0 & 0 \\ 0 & 0 & 0 & 0 \\ 0 & 0 & 0 & 0 \end{bmatrix}$$

$$V_1 = \begin{bmatrix} \gamma + \mu & 0 & 0 & 0 \\ -r\gamma & (\mu + \theta + \alpha) & 0 & 0 \\ (r-1)\gamma & 0 & \epsilon + \mu & 0 \\ 0 & -\alpha & -\epsilon & \mu \end{bmatrix} \text{ At disease-free equilibrium}$$

$$E_0 = [\frac{\Lambda}{(\delta + \mu)}, \frac{\delta\Lambda}{\mu(\delta + \mu)}, 0, 0, 0, 0]$$

$$\mathcal{F} = \begin{bmatrix} 0 & \frac{(1-h)\beta\Lambda}{(\delta+\mu)} + \frac{\omega\beta\delta\Lambda}{\mu(\delta+\mu)} & \frac{(1-h)\beta\eta\Lambda}{(\delta+\mu)} & 0 \\ 0 & 0 & 0 & 0 \\ 0 & 0 & 0 & 0 \\ 0 & 0 & 0 & 0 \end{bmatrix}$$

$$\mathcal{V} = \begin{bmatrix} \gamma + \mu & 0 & 0 & 0 \\ -r\gamma & (\mu + \theta + \alpha) & 0 & 0 \\ -(1-r)\gamma & 0 & \epsilon + \mu & 0 \\ 0 & -\alpha & -\epsilon & \mu \end{bmatrix}$$

Now, $\mathcal{F}\mathcal{V}^{-1} =$

$$
\begin{bmatrix}
\dfrac{\gamma r\left[\frac{(1-h)\beta\Lambda}{(\mu+\delta)}+\frac{\beta\delta\Lambda\omega}{\mu(\mu+\delta)}\right]}{(\mu+\gamma)(\alpha+\theta+\mu)} - \dfrac{\beta\gamma\eta\Lambda(r-1)}{(\mu+\eta)(\mu+\gamma)(\mu+\delta)} & \dfrac{\frac{(1-h)\beta\Lambda}{\mu+\delta}+\frac{\beta\delta\Lambda\omega}{\mu(\mu+\delta)}}{(\alpha+\theta+\mu)} & \dfrac{\beta\eta\Lambda}{(\mu+\epsilon)(\mu+\delta)} & 0 \\
0 & 0 & 0 & 0 \\
0 & 0 & 0 & 0 \\
0 & 0 & 0 & 0
\end{bmatrix}
$$

The basic Reproduction number is given by

$$
R_0 = \frac{\gamma r\left[\frac{(1-h)\beta\Lambda}{(\mu+\delta)}+\frac{\beta\delta\Lambda\omega}{\mu(\mu+\delta)}\right]}{(\mu+\gamma)(\alpha+\theta+\mu)} + \frac{\beta\gamma\eta\Lambda(1-r)}{(\mu+\eta)(\mu+\gamma)(\mu+\delta)}
$$

3.4 Stability analysis of DFE

3.4.1 Local stability of disease-free equilibrium

Theorem 3.3. *The Disease Free Equilibrium DEF is locally asymptotically stable if $R_0 < 1$.*

Proof. The Jacobian matrix wrt system 1 is given by

J =

$$
\begin{bmatrix}
-(\delta+\mu) & 0 & 0 & -(1-h)\beta S_0 & -(1-h)\beta\eta S_0 & 0 \\
\delta & -\mu & 0 & -\omega\beta V_0 & 0 & 0 \\
0 & 0 & -(\gamma+\mu) & (1-h)\beta S_0 & (1-h)\beta\eta S_0 & 0 \\
0 & 0 & r\gamma & -(\mu+\theta+\alpha) & 0 & 0 \\
0 & 0 & (1-r)\gamma & 0 & -(\epsilon+\mu) & 0 \\
0 & 0 & 0 & \alpha & \epsilon & -\mu
\end{bmatrix}
$$

which implies

$J_{DFE} =$

$$\begin{bmatrix} -p & 0 & 0 & -(1-h)\beta S_0 & -(1-h)\beta \eta S_0 & 0 \\ \delta & -\mu & 0 & -\omega \beta V_0 & 0 & 0 \\ 0 & 0 & -q & (1-h)\beta S_0 & (1-h)\beta \eta S_0 & 0 \\ 0 & 0 & r\gamma & -z & 0 & 0 \\ 0 & 0 & (1-r)\gamma & 0 & -t & 0 \\ 0 & 0 & 0 & \alpha & \epsilon & -\mu \end{bmatrix}$$

Where,
p $= (\delta + \mu)$, $q = (\gamma + \mu)$, $z = (\mu + \theta + \alpha)$, $t = (\epsilon + \mu)$

Clearly, two eigenvalues of the matrix J_{DFE} are negative such as $-\mu$ and $-\mu$. The remaining eigenvalues are the roots of the following Polynomial equation

$$\lambda^4 + a_3\lambda^3 + a_2\lambda^2 + a_1\lambda + a_0 = 0$$

where,

$a_3 = -(-p - q - z - t) = (p + q + z + t)$

$a_2 = [(p + q + z + t)^2 - (p^2 + q^2 + z^2 + t^2)]/2 - (1 - h)\beta\gamma r S_0 - (1 - h)\beta\gamma\eta S_0(1 - r)$

$a_1 = [z(z^2 + (1 - h)\beta\gamma r S_0)]/3 - ((p + q + t + z)(p^2 + q^2 + t^2 + z^2 + 2(1 - h)\beta\gamma r S_0$

$\quad - 2(1 - h)\beta\gamma\eta S_0(r - 1)))/2 + [(p + q + t + z)^3]/6$

$\quad + p^3/3 + (t(t^2 - (1 - h)\beta\gamma\eta S_0(r - 1)))/3 + (q(q^2 + (1 - h)\beta\gamma r S_0$

$\quad - (1 - h)\beta\gamma\eta S_0(r - 1)))/3 - (\gamma((1 - h)\beta\eta q S_0 +$

$\quad (1 - h)\beta\eta S_0 t)(r - 1))/3 + (\gamma r((1 - h)\beta q S_0 + (1 - h)\beta S_0 z))/3$

$\quad + (\beta S_0(\gamma q r + \gamma r z))/3 - ((1 - h)\beta\eta S_0(\gamma q(r - 1)$

$\quad + \gamma t(r - 1)))/3$

$a_0 = p(1 - R_0)(qtz - (1 - h)\beta\gamma r S_0 t - (1 - h)\beta\gamma\eta S_0 z + (1 - h)\beta\gamma\eta r S_0 z)$

According to the Routh-Hurwitz criterion, the above equation will give negative roots or roots with negative real parts if the following condition is satisfied:

$$a_3 > 0, \begin{vmatrix} a_3 & a_1 \\ 1 & a_2 \end{vmatrix} > 0, \begin{vmatrix} a_3 & a_1 & 0 \\ 1 & a_2 & a_0 \\ 0 & a_3 & a_1 \end{vmatrix} > 0$$

Hence, the disease-free equilibrium point E_0 of the system is locally asymptotically stable, when $R_0 < 1$.   □

3.4.2 Global stability of disease-free equilibrium

We now study the global stability of disease-free equilibrium, using the theorem by Castillo-Chavez et al. (Korobeinikov and Wake, 2002)

Theorem 3.4. *If the given mathematical model can be written in the form:*

$$\frac{dX}{dt} = F(X, Y) \tag{3.16}$$

$$\frac{dY}{dt} = G(X, Y), G(X, Y) = 0$$

where $X = (S, V)^T$, $Y = (E, I, I_A, R)^T$, *denoting the number of uninfected individuals and denoting the number of COVID-19-infected people respectively. Let the disease-free equilibrium of this system be*

$$U_0 = (X^*, 0) = (\frac{\Lambda}{\delta + \mu}, \frac{\delta\Lambda}{\mu(\delta + \mu)}, 0)$$

where $\boldsymbol{0}$ is a zero vector.

For the global asymptotically stable, the following condition $(H1)$ and $(H2)$ must be satisfied.

$$(H1) : For \frac{dX}{dt} = F(X, 0), \ 0 \ is \ global \ asymptotically \ stable.$$
$$(H2) : G(X, Y) = AY - \hat{G}(X, Y), \hat{G}(X, Y) \geq 0 \ for (X, Y) \in \Omega$$

where $A = D_Y G(X^*, 0)$ is an M- matrix (the off-diagonal elements of A are non-negative) and Ω is the region where the model makes biological sense. If the given system of differential equations of our model satisfies the given condition in (2) then the fixed point $U_0 = (X^\star, 0)$ is a global asymptotically stable (g.a.s) equilibrium of (2) provided $R_0 < 1$, and the assumption (H1) and (H2) are satisfied.

Theorem 3.5. *The DFE E_0 of model (3.1) is global asymptotically stable if $R_0 < 1$.*

Proof. First, we rewrite the system of differential equation of our model (3.1) as X = $(S, V)^T$ and Y = $(E, I, I_A, R)^T$.

Then, the DFE is given by

$$U_0 = (X^\star, 0) = (\frac{\Lambda}{\delta + \mu}, \frac{\delta\Lambda}{\mu(\delta + \mu)}, 0)$$

. and the system $\frac{dX}{dt}$ = F(X, 0) becomes

$$\dot{S} = \Lambda - (\delta + \mu)S$$
$$\dot{V} = \delta S - \mu V \tag{3.17}$$

This equation has a unique equilibrium point

$$X^* = (\frac{\Lambda}{\delta + \mu}, \frac{\delta\Lambda}{\mu(\delta + \mu)}) \tag{3.18}$$

which is globally asymptotically stable. Therefore, condition (H1) is satisfied. We now verify the second condition (H2). For model (3.1), we have

$$G(X,Y) = \begin{bmatrix} (1-h)\beta S(I + \eta I_A) + \omega\beta VI - \gamma E - \mu E \\ r\gamma E - (\mu + \theta)I - \alpha I \\ (1-r)\gamma E - \epsilon I_A - \mu I_A \\ \alpha I + \epsilon I_A - \mu R \end{bmatrix}$$

$$D_Y G(X^*, 0) = A = F - V$$

$$= \begin{bmatrix} -(\gamma + \mu) & (1-h)\beta S_0 + \omega\beta V_0 & (1-h)\beta\eta S_0 & 0 \\ r\gamma & -(\mu + \theta + \alpha) & 0 & 0 \\ (1-r)\gamma & 0 & -(\epsilon + \mu) & 0 \\ 0 & \alpha & \epsilon & -\mu \end{bmatrix}$$

Clearly, we see that A is an M-matrix, i,e. all the off-diagonal elements of A are non-negative.

$$\hat{G}(X,Y) = AY - G(X,Y)$$

$$= \begin{bmatrix} [(1-h)\beta(I + \eta I_A)](S - S_0) + \omega\beta I(V - V_0) \\ 0 \\ 0 \\ 0 \end{bmatrix}$$

which implies that $\hat{G}$(X,Y) $\geq$ 0 for all (X,Y) $\in \Omega$. Therefore, conditions (H1) and (H2) are satisfied. Hence, disease-free equilibrium is globally asymptotically stable. $\qquad\square$

3.5 Stability analysis of EE

3.5.1 Existence of Endemic Equilibrium point

Let us denote the Endemic Equilibrium by $E_1 = (S^*, V^*, E^*, I^*, I_A^*, R^*)$ The Endemic Equilibrium always satisfies:

$$0 = \Lambda - (1-h)\beta S^*(I^* + \eta I_A^*) - \delta S^* - \mu S^*$$
$$0 = \delta S^* - \omega\beta V^* I^* - \mu V^*$$
$$0 = (1-h)\beta S^*(I^* + \eta I_A^*) + \omega\beta V^* I^* - \gamma E^* - \mu E^*$$
$$0 = r\gamma E^* - (\mu + \theta)I^* - \alpha I^* \qquad\qquad (3.19)$$
$$0 = (1-r)\gamma E^* - \epsilon I_A^* - \mu I_A^*$$
$$0 = \alpha I^* + \epsilon I_A^* - \mu R^*$$

which gives

$$S^* = \frac{\Lambda}{(1-h)\beta(I^* + \eta B) + \delta + \mu} = C$$

$$V^* = \frac{\delta C}{\omega\beta I^* + \mu} = D$$

$$E^* = \frac{(\mu + \theta + \alpha)I^*}{r\gamma} = A$$

$$I_A^* = \frac{(1-r)\gamma A}{(\epsilon + \mu)} = B$$

$$I^* = \frac{(\mu + \gamma)(\mu + \delta)(\alpha + \theta + \mu) + (1-h)\beta\gamma\Lambda r[\frac{\eta(r-1)(\alpha+\theta+\mu)}{r(\mu+\epsilon)} - 1]}{\beta(1-h)(\mu+\gamma)[\frac{\eta(r-1)(\alpha+\theta+\mu)}{r(\mu+\epsilon)} - 1](\alpha + \theta + \mu)}(R_0 - 1)$$

$$R^* = \frac{\alpha I^* + \epsilon B}{\mu}$$

3.5.2 Local stability of endemic equilibrium

Theorem 3.6. *The endemic equilibrium E_1 is locally asymptotically stable if $R_0 > 1$, otherwise it is unstable.*

Proof. The Jacobian matrix of the system (3.1) at endemic equilibrium point E_1 is obtained as follows:

$$J_{E1} = \begin{bmatrix} -a & 0 & 0 & -(1-h)\beta S^* & -(1-h)\beta\eta S^* & 0 \\ \delta & -d & 0 & -\omega\beta V^* & 0 & 0 \\ a_{31} & \omega\beta I^* & -f & a_{34} & (1-h)\beta\eta S^* & 0 \\ 0 & 0 & r\gamma & -j & 0 & 0 \\ 0 & 0 & (1-r)\gamma & 0 & -l & 0 \\ 0 & 0 & 0 & \alpha & \epsilon & -\mu \end{bmatrix}$$

where

$$a = [(1-h)\beta(I^* + \eta I_A^*) + \delta + \mu]$$

$$d = [\omega\beta I^* + \mu]$$

$$f = (\gamma + \mu)$$

$$j = (\mu + \theta + \alpha)$$

$$l = (\epsilon + \mu)$$

$$a_{31} = (1-h)\beta(I^* + \eta I_A^*)$$

$$a_{34} = (1-h)\beta S^* + \omega\beta V^*$$

Clearly, one eigenvalue of the matrix J_{E1} is negative $-\mu$ and the remaining eigenvalues are the roots of the following Polynomial equation:

$$\lambda^5 + c_4\lambda^4 + c_3\lambda^3 + c_2\lambda^2 + c_1\lambda + c_0 = 0$$

where

$$c_4 = a + d + f + j + l$$

$$c_3 = [(a + d + f + j - l)^2]/2 - a_{34}r\gamma - a^2/2 - d^2/2 - f^2/2$$
$$- j^2/2 - l^2/2 - (1 - h)\beta\eta S^*(1 - r)\gamma$$

$$c_2 = adf + adj - aa_{34}r\gamma - adl + afj - afl - da_{34}r\gamma$$
$$+ dfj - dfl - ajl - djl + a_{34}r\gamma l - fjl + (1 - h)\beta a_{31}r\gamma S^*$$
$$+ \beta^2 r\gamma I^* v^*\omega^2 - a(1 - h)\beta(1 - r)\gamma\eta S^* - (1 - h)\beta d(1 - r)\gamma\eta S^*$$
$$+ (1 - h)\beta a_{31}(1 - r)\gamma\eta S^* - (1 - h)\beta j(1 - r)\gamma\eta S^*$$

$$c_1 = adfj - ada_{34}r\gamma - adfl - adjl + aa_{34}r\gamma l - afjl$$
$$+ da_{34}r\gamma l - dfjl + (1 - h)\beta da_{31}r\gamma S^* - (1 - h)\beta a_{31}r\gamma lS^*$$
$$+ \beta^2\delta r\gamma I^*S^*\omega + a\beta^2 r\gamma I^*V^*\omega^2$$
$$- \beta^2 r\gamma I^*lV^*\omega^2 - a(1 - h)\beta d(1 - r)\gamma\eta S^*$$
$$+ (1 - h)\beta da_{31}(1 - r)\gamma\eta S^* - a(1 - h)\beta j(1 - r)\gamma\eta S^*$$
$$- (1 - h)\beta dj(1 - r)\gamma\eta S^* + (1 - h)\beta a_{31}j(1 - r)\gamma\eta S^*$$
$$+ \beta^2\delta I^*(1 - r)\gamma\eta S^*\omega$$

$$c_0 = adfjl - ada_{34}r\gamma l + (1 - h)\beta da_{31}r\gamma lS^*$$
$$+ a\beta^2 r\gamma I^*lV^*\omega^2 + a(1 - h)\beta dj(1 - r)\gamma\eta S^*$$
$$- (1 - h)\beta da_{31}j(1 - r)\gamma\eta S^* + \beta^2\delta r\gamma I^*S^*l\omega$$
$$- \beta^2\delta I^*j(1 - r)\gamma\eta S^*\omega$$

According to the Routh-Hurwitz criterion, the above equation will give negative roots or negative real parts if the following condition is satisfied:

$$c_4 > 0, \begin{vmatrix} c_4 & c_2 \\ 1 & c_3 \end{vmatrix} > 0, \begin{vmatrix} c_4 & c_2 & c_0 \\ 1 & c_3 & c_1 \\ 0 & a_4 & a_2 \end{vmatrix} > 0, \begin{vmatrix} c_4 & c_2 & c_0 & 0 \\ 1 & c_3 & c_1 & 0 \\ 0 & c_4 & c_2 & c_0 \\ 0 & 1 & c_3 & c_1 \end{vmatrix} > 0$$

Hence, the endemic equilibrium point E_1 of the system is locally asymptotically stable when $R_0 > 1$. $\qquad\square$

3.5.3   Global stability of disease-free equilibrium

Theorem 3.7. *The endemic equilibrium $E_1 = (S^*, V^*, E^*, I^*, I_A^*, R^*)$ of our mathematical model is globally asymptotically stable.*

Proof. For the global stability result, we will use the method discussed in Korobeinikov (Korobeinikov and Wake, 2002) and Wake, Li and Muldowney (M. Y. Li and Muldowney, 1995). From (3.1), a person was infected with coronavirus and then fully recovered. After that, we assume that a person has permanent immunity. The first five equations are independent of R in (3.1) and we will study the following subsystem.

$$\frac{dS}{dt} = \Lambda - (1-h)\beta S(I + \eta I_A) - \delta S - \mu S$$
$$\frac{dV}{dt} = \delta S - \omega \beta V I - \mu V$$
$$\frac{dE}{dt} = (1-h)\beta S(I + \eta I_A) + \omega \beta V I - \gamma E - \mu E \qquad (3.20)$$
$$\frac{dI}{dt} = r\gamma E - (\mu + \theta)I - \alpha I$$
$$\frac{dI_A}{dt} = (1-r)\gamma E - \epsilon I_A - \mu I_A$$

Let

$$x_1 = \frac{S}{S^*}, y_1 = \frac{V}{V^*}, z_1 = \frac{E}{E^*} u_1 = \frac{I}{I^*}, v_1 = \frac{I_A}{I_A^*}$$

The model of the system of equation (3.20) is transformed into the following form

$$\frac{dx_1}{dt} = x_1\left[\frac{\Lambda}{S^*}\left(\frac{1}{x_1}\right) - (1-h)\beta I^*(u_1 - 1) - (1-h)\beta \eta I_A^*(v_1 - 1)\right]$$
$$\frac{dy_1}{dt} = y_1\left[\frac{\delta S^*}{V^*}\left(\frac{x_1}{y_1} - 1\right) - \omega \beta I^*(u_1 - 1)\right]$$
$$\frac{dz_1}{dt} = z_1\left[\frac{(1-h)\beta S^* I^*}{E^*}\left(\frac{x_1 u_1}{z_1} - 1\right) + \frac{(1-h)\beta \eta S^* I_A^*}{E^*}\left(\frac{x_1 v_1}{z_1} - 1\right) + \frac{\omega \beta V^* I^*}{E^*}\left(\frac{y_1 u_1}{z_1} - 1\right)\right]$$

$$\frac{du_1}{dt} = u_1 \frac{r\gamma E^*}{I^*}\left(\frac{z_1}{u_1} - 1\right)$$
$$\frac{dv_1}{dt} = v_1 \gamma(1-r)\frac{E^*}{I_A^*}\left(\frac{z_1}{v_1} - 1\right)$$

Here it is easy to find that the system of equation (3.21) has unique endemic equilibrium $E_1(1,1,1,1,1)$ and the global stability of $E_1(1,1,1,1,1)$ is same as that of E_1.

Thus we investigate the global stability of $E_1(1,1,1,1,1)$ instead of E_1.

Defining the Volterra- type Lyapunov function

$$
\begin{aligned}
L(x_1, y_1, z_1, u_1, v_1) =& S^*(x_1 - 1 - \ln x_1) + V^*(y_1 - 1 - \ln y_1) + E^*(z_1 - 1 - \ln z_1) \\
& + \frac{(1-h)\beta I^*(S^* + \omega V^*)}{r\gamma E^*}(u_1 - 1 - \ln u_1) + \\
& \frac{(1-h)\beta \eta I_A^*(S^* + \omega V^*)}{\gamma(1-r)E^*}(v_1 - 1 - \ln v_1)
\end{aligned}
$$

From equilibrium state E_1 we have the following equations

$$
\Lambda = (1-h)\beta S^*(I^* + \eta I_A^*) + (\delta + \mu)S^*
$$

$$
\delta S^* = \omega \beta V^* I^* + \mu V^*
$$

$$
(\gamma + \mu)E^* = (1-h)\beta S^*(I^* + \eta I_A^*) + \omega \beta V^* I^*
$$

$$
r\gamma E^* - (\alpha + \mu)I^*
$$

$$
\gamma(1-r)E^* = (\epsilon + \mu)I_A^*
$$

Then, differentiating L w.r.t 't' along the solution curve of the system of the equation of model (3.21) and considering the above equation gives

$$
\begin{aligned}
\frac{dL}{dt} =& S^*(x_1 - 1)\frac{\dot{x_1}}{x_1} + V^*(y_1 - 1)\frac{\dot{y_1}}{y_1} + E^*(z_1 - 1)\frac{\dot{z_1}}{z_1} \\
& + \frac{(1-h)\beta I^*(S^* + \omega V^*)}{r\gamma E^*}(u_1 - 1)\frac{\dot{u_1}}{u_1} + \frac{(1-h)\beta \eta I_A^*(S^* + \omega V^*)}{\gamma(1-r)E^*}(v_1 - 1)\frac{\dot{v_1}}{v_1} \\
=& (x_1 - 1)[\Lambda(\frac{1}{x_1} - 1) - (1-h)\beta S^* I^*(u_1 - 1) - (1-h)\beta \eta S^* I_A^*(v_1 - 1)] \\
& + (y_1 - 1)[\delta S^*(\frac{x_1}{y_1} - 1) - \omega \beta V^* I^*(u_1 - 1)] \\
& + (z_1 - 1)[(1-h)\beta S^* I^*(\frac{x - 1u_1}{z_1} - 1) + (1-h)\beta \eta S^* I_A^*(\frac{x - 1v_1}{z_1} - 1) \\
& + \omega \beta V^* I^*(\frac{y - 1u_1}{z_1} - 1)] + (1-h)\beta I^*(S^* + \omega V^*)(u_1 - 1)(\frac{z_1}{u_1} - 1) \\
& + (1-h)\beta \eta I_A^*(S^* + \omega V^*)(v_1 - 1)(\frac{z_1}{v_1} - 1)
\end{aligned}
$$

After some algebraic manipulation, we have

$$\frac{dL}{dt} = \mu S^*(2 - x_1 - \frac{1}{x_1}) + \mu V^*(3 - \frac{1}{x_1} - y_1 - \frac{x_1}{y_1})$$
$$+ (1 - h)\beta S^* I^*(3 - \frac{1}{x_1} - \frac{x_1 u_1}{z_1} - \frac{z_1}{u_1}) + (1 - h)\beta \eta S^* I_A^*(3 - \frac{1}{x_1} - \frac{x_1 v_1}{z_1} - \frac{z_1}{v_1})$$
$$+ \omega \beta V^* I^*(4 - \frac{1}{x_1} - \frac{x_1}{y_1} - \frac{y_1 u_1}{z_1} - \frac{z_1}{u_1})$$

Since the arithmetic mean is greater than or equal to the geometric mean, we have

$$(2 - x_1 - \frac{1}{x_1}) \leq 0$$
$$(3 - \frac{1}{x_1} - y_1 - \frac{x_1}{y_1}) \leq 0$$
$$(3 - \frac{1}{x_1} - \frac{x_1 u_1}{z_1} - \frac{z_1}{u_1}) \leq 0$$
$$(3 - \frac{1}{x_1} - \frac{x_1 v_1}{z_1} - \frac{z_1}{v_1}) \leq 0$$
$$(4 - \frac{1}{x_1} - \frac{x_1}{y_1} - \frac{y_1 u_1}{z_1} - \frac{z_1}{u_1}) \leq 0$$

Thus it is easy to observe that $\frac{dL}{dt} \leq 0$ and the equality $\frac{dL}{dt} = 0$ hold for

$$x_1 = y_1 = 1, z_1 = u_1 = v_1$$

which corresponds to the set [$(S,V,E,I,I_A$: S=S^*,V -V^*, E= E^*,I=I^*,$I_A = I_A^*$)]Hence from LaSalle's invariance principle (J. P. La Salle, 1976), the equilibrium E_1 of the given system is globally asymptotically stable for $R_0 > 1$. □

3.6   Sensitivity Analysis

In this section, We examine the impact of the parameters used to express the basic reproduction number, R_0, through sensitivity analysis.

This demonstrates that an alteration in these parameters results in an alteration in R_0. It is used to identify the variables with a significant impact on R_0 and determine which ones should be the focus of intervention measures. Sensitivity indices make it possible to quantify the proportional change in a variable when a parameter is altered.

The forward sensitivity index of a variable, with regard to a specific parameter, is used for that.

$$\alpha_\phi^{R_0} = \frac{\partial R_0}{\partial \phi} \frac{\phi}{R_0}$$

where $\phi = [\gamma, \mu, r, \theta, \alpha, \epsilon, \beta, \delta, \Lambda, \omega, \eta, h]$. The analytical equation for the sensitivity of R_0 to each parameter it comprises can be calculated using the formula mentioned above. As a result, Figure 3.2 shows the sensitivity index of parameters i.e $\gamma, \mu, r, \theta, \alpha, \epsilon, \beta, \delta, \Lambda, \omega, \eta, h$ respectively on R_0.
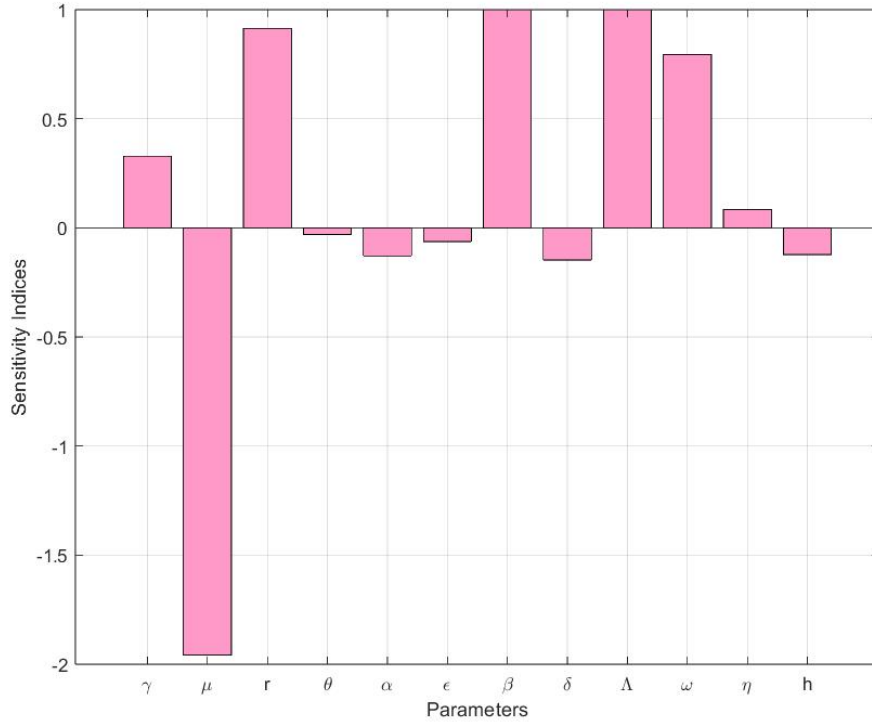
Figure 3.2: Forward sensitivity of R_0

The positive indices indicate a direct relationship between the parameters and R_0, that is if the parameter increases/decrease then the value of R_0 will increase/decrease. Therefore in order to control COVID-19 from the population, we need to reduce the Basic Reproduction number, we can achieve this by reducing the parameters which give positive indices i.e γ, r, β, ω, η, Λ, here birth rate Λ and rate of transmission β are the most sensitive parameters of R_0, since it is not possible to control the birth

rate we are left with the rate of transmission, we can reduce this by limiting our contact rate, which is why there was a suggestion like quarantine, social distancing, etc. If the rate of reduction in risk of infection due to vaccine ω decreases then R_0 also decreases, the higher the number of vaccinated people the lower the Vaccine-induced decrease in infection risk, therefore the Basic Reproduction number can be reduced. The negative indices indicate that there is an inverse relationship between the parameters and R_0, that is if the parameter decrease/increases then the value of R_0 will increase/decrease. μ, θ, α, ϵ, δ, η, h have negative indices, among the μ is the highest sensitive if the death rate increase than R_0 decrease. The strength of intervention h has negative indices which imply that if we implement strict intervention measures then R_0 will decrease which will lead to a decrease in the Infected population.

3.7 Numerical Simulation

For the Numerical Simulation of the proposed model, we illustrate the mathematical findings using the MATLAB program, the value of parameters are listed in the table. Figure 3.3 shows the variation of the infected population with time t for different values of h. First, we take the strength of intervention h to be $h = 0$, which means that there is no intervention measure taken during this period. We consider this period to be from the start of March 2020 till 24 March 2020 when no action has yet been taken by the Government of India.

On 24 March 2020, the Government of India declared a nationwide lockdown for the period of 21 days (Pulla, 2020). After the nationwide lockdown and by the Ministry of Health and Family Welfare, Government of India, many preventive measures for COVID-19 were taken by India. We notice that from COVID-19 case data from the World Health Organization, the infected case curve began to slope down from mid-September 2020 till the first week of February 2021. In order to investigate the impact of intervention strategies, the strength of intervention is assumed as $h = 0.5042$, during the period of March to July 2020, where the early preventive measure has been implemented, the COVID-19 positive case curve keeps on increasing; $h = 0.6544$, during the period from July to September 2020, where the increasing curve has been slow down and $h = 0.7282$, where strict intervention measures have been taken including social distancing, wearing a mask, awareness through various media, etc, it is noticed that the curve has been miraculously kept on decreasing till
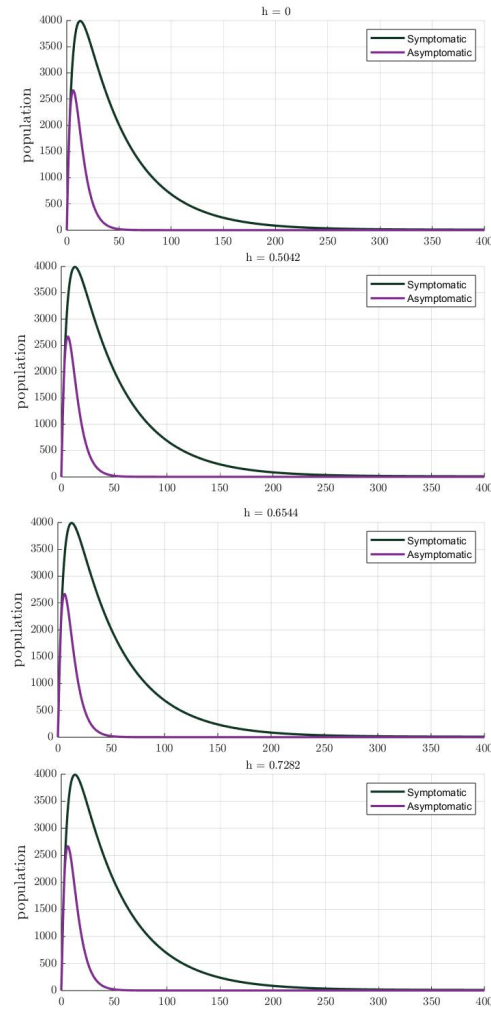
Figure 3.3: Variation of Infected population with time for different values of h

8 February 2021. From Figure 3.3 We can see that by strengthening the intervention strategy i.e. by increasing the strength of intervention h the curve of Symptomatic infection and Asymptomatic infection can be positively decreased.

Figure 3.4 shows the Variation of $SVEII_AR$ with time corresponding to the values of $R_0 < 1$ for different values of initial numbers of each compartment with time $t = 0$ to 1000.
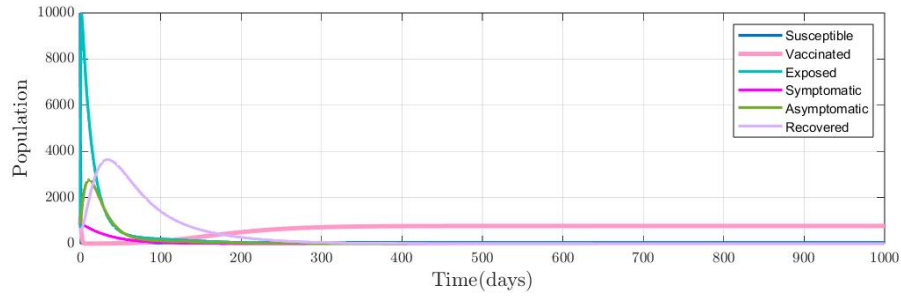
Figure 3.4: Variation of $SVEII_AR$ with time corresponding to the values of $R_0 < 1$ for different values of initial numbers of each compartment with time $t = 0$ to 1000

Figure 3.5 shows Variation of $SVEII_AR$ with time corresponding to $R_0 > 1$ from $t = 0$ to 40.
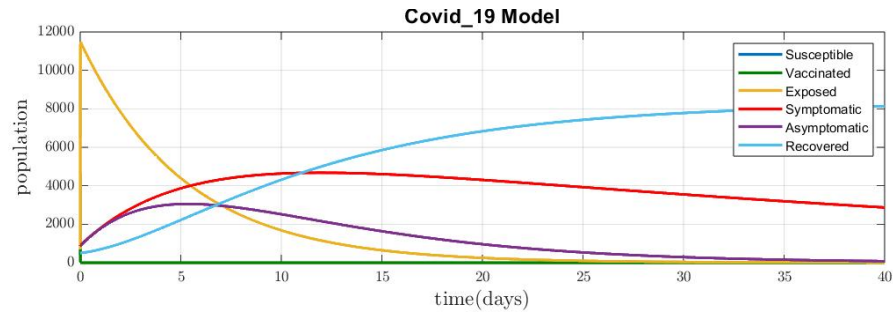
Figure 3.5: Variation of $SVEII_AR$ with time corresponding to $R_0 > 1$ from $t = 0$ to 40

Figure 3.6 shows Variation of $SVEII_AR$ with time corresponding to the values of $R_0 > 1$ from $t = 0$ to 1000.

Figure 3.7 shows the Variation of $SVEII_AR$ with time corresponding to the values of $R_0 < 1$ for different values of initial numbers of each compartment with time $t = 0$ to 600.
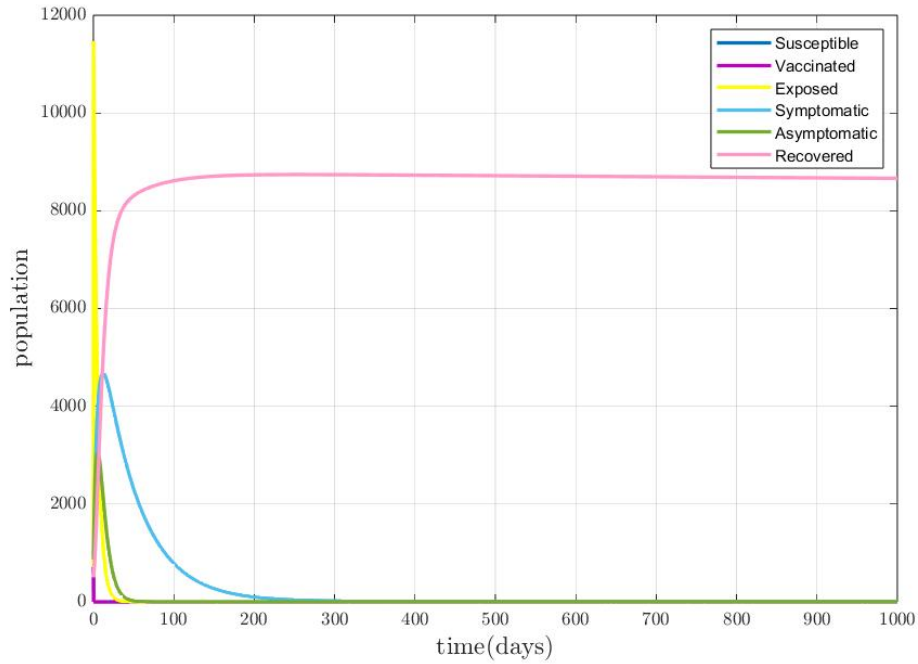
Figure 3.6: Variation of $SVEII_AR$ with time corresponding to $R_0 > 1$ from $t = 0$ to 1000
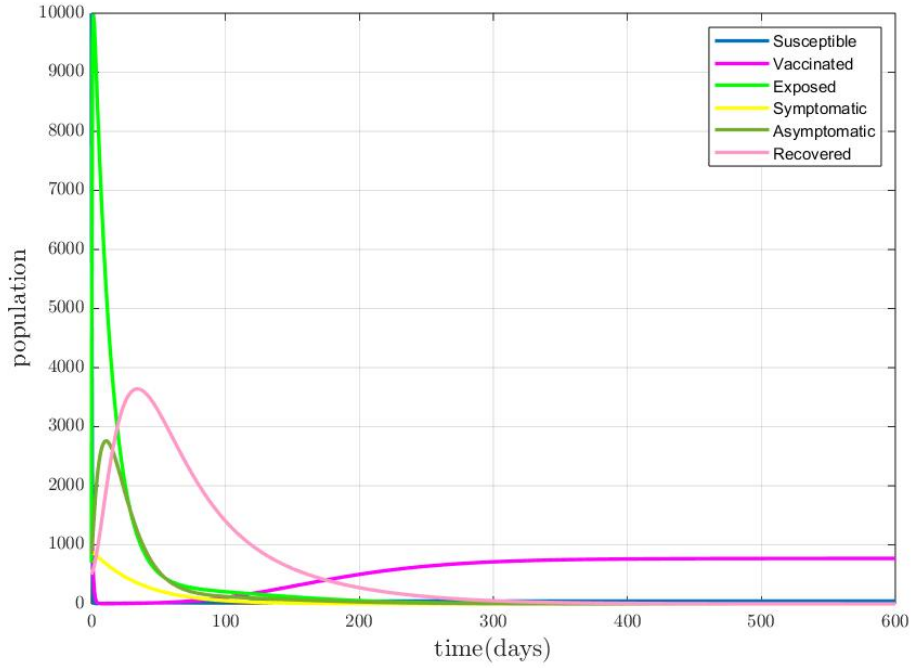
Figure 3.7: Variation of $SVEII_AR$ with time corresponding to the values of $R_0 < 1$ for different values of initial numbers of each compartment with time $t = 0$ to 600.

Figure 3.8 shows the variation of $SVEII_AR$ with time for different values of h. This is to show how *no intervention measure*, *implementation of the intervention*, and *strict intervention* change the cure of Susceptible, Vaccinated, Exposed, Symptomatic, Asymptomatic, and Recovered Population

Figure 3.9 shows the Variation of the Infected population with time for different values of β, ω, and h. We have 4 cases, we choose $\beta = 1.5$, $\omega = 0.5$, $h = 0.6544$; $\beta = 1$, $\omega = 0.2$, $h = 0.0.5042$; $\beta = 0.5$, $\omega = 0$, $h = 0$; $\beta = 2$, $\omega = 1$, $h = 0.7282$, and from here we can suggest that a combination of strict intervention measures and increased vaccination can be the most effective solution in reducing the number of people infected with the coronavirus.
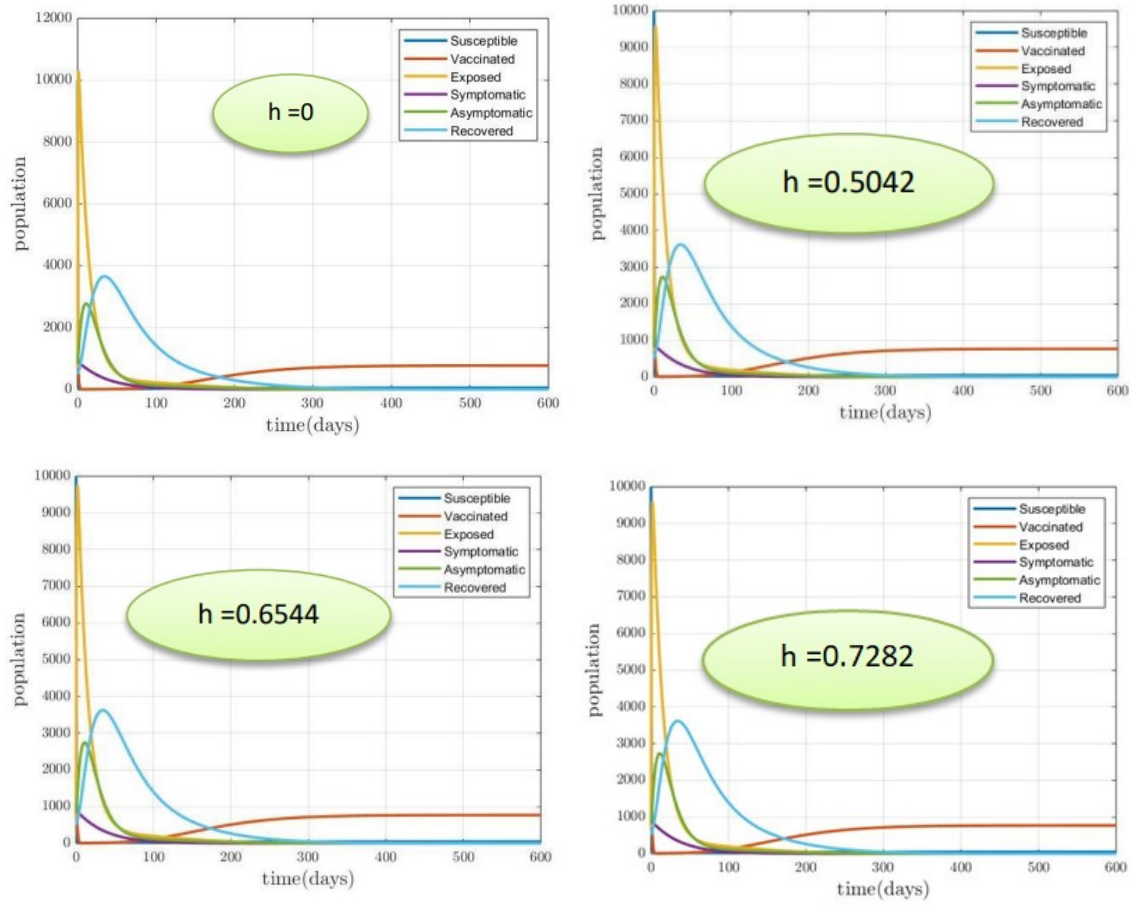
Figure 3.8: Variation of $SVEII_AR$ with time for different values of h
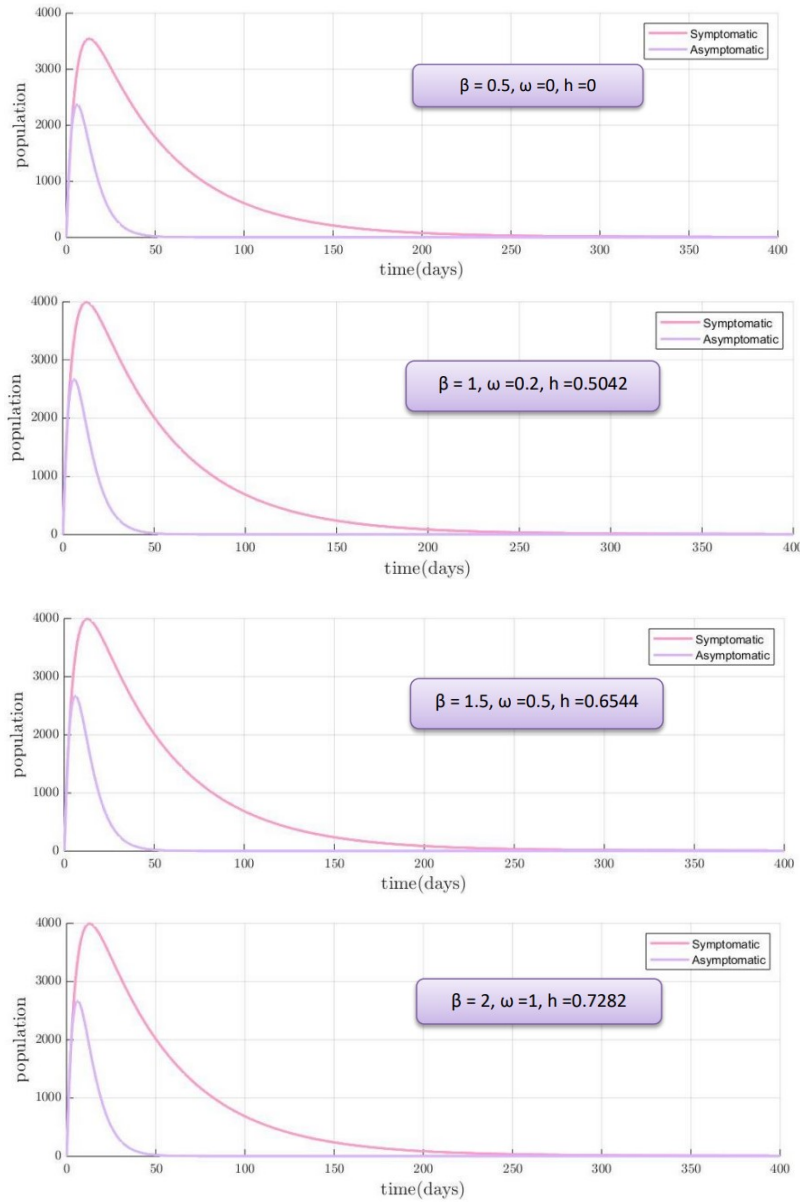
Figure 3.9: Variation of the Infected population with time for different values of β, ω, and h.

3.8 Conclusion

The mathematical modelling of COVID-19 has been explored in depth in this paper, with a focus on examining the effects of vaccination and intervention strategies. The kinetics of COVID-19 transmission and the efficiency of various tactics for controlling

the virus' propagation have been studied using mathematical modelling approaches. We examined how interventions affected the burden of disease. We mainly focused on the preventive measures that essentially slow down the development of the disease, such as lock-down, media awareness campaigns, adequate hand sanitization, social seclusion, wearing masks, etc.

We discussed the existence and stability of Disease-Free Equilibrium and Endemic Equilibrium. Stability analysis of the equilibrium points shows DFE is locally asymptotically stable whenever the basic reproduction number, $R_0 < 1$, and is globally asymptotically stable whenever $R_0 < 1$. Also, EE is locally asymptotically stable whenever the basic reproduction number, $R_0 > 1$, and is globally asymptotically stable whenever $R_0 > 1$.

Sensitivity analysis for the effect of the parameters involved in the expression of basic reproduction number, R_0 is conducted. It shows that changing these factors causes R_0 to change depending on how they change. It is used to identify the parameters that should be the focus of intervention initiatives because they have a significant impact on R_0. The relative change in a variable when a parameter changes can be measured using sensitivity indices.

The forward sensitivity index of a variable with regard to a specific parameter is used for that. The most sensitive parameter is found to be μ, death rate, which is on the negative side, which means it has an inverse relationship with R_0 since it is not possible to control μ another sensitive parameter which we can control in order to control COVID-19 from the population is β, which have a direct relationship with R_0, we can reduce this by limiting our contact rate, which is why there was a suggestion like quarantine, social distancing, etc. Also if the rate of reduction in risk of infection due to vaccine ω decreases then R_0 also decreases, the higher the number of vaccinated people the lower the Vaccine-induced decrease in infection risk, therefore the Basic Reproduction number can be reduced. Parameters like γ, r, β, ω, η, Λ have positive indices and have direct relationship with R_0. μ, θ, α, ϵ, δ, η, h have negative indices and have inverse relationship with R_0. Numerical simulation is also performed using MATLAB.

This study could give policymakers more information to help them decide whether to retain the strictness of an ongoing intervention plan or to let it up. Our study showed that more intensive action is needed to stop the illness outbreak in a shorter

amount of time. Also, our analysis demonstrated that in order to effectively eradicate the condition, the strength of the intervention should not be weakened over time.

In conclusion, we recommend that a combination of strict intervention measures and increased vaccination can be the most effective solution in reducing the number of people infected with the coronavirus.

Chapter 4

Evaluating Precautionary Measures in COVID-19 Spread: A Delay Differential Equation Approach

4.1   Introduction

The unprecedented global health crisis posed by the COVID-19 pandemic demands swift and effective strategies to mitigate its impact. Mathematical modelling has emerged as a powerful tool for understanding and predicting the dynamics of infectious diseases, offering valuable insights into transmission modes, vaccination effects, and the efficacy of intervention strategies. In India, a country with a sizable population and unique demographic characteristics, the use of mathematical modelling is crucial for guiding evidence-based decision-making to address COVID-19 effectively.

The inception of mathematical modelling in epidemiology dates back to Daniel Bernoulli's work on the effect of variolation against smallpox, which highlighted the potential to increase life expectancy (Bernoulli, 1760). Since then, pioneering work by Kermack and McKendrick laid the foundation for applying mathematical models to comprehend infectious disease dynamics (Kermack and McKendrick, 1927). In the context of COVID-19, numerous mathematical models have been developed to

study transmission dynamics in India. Studies have extended classical models like SI (Duan *et al.*, 2019), SIS (Y. Xie *et al.*, 2020), and SIR (Sene, 2020), introducing additional compartments to account for asymptomatic cases, isolated individuals, quarantine, protection, deaths, lockdowns, hospitalizations, and more (Bajiya *et al.*, 2020; Gupta *et al.*, 2021; Khajanchi and Sarkar, 2020; Mahajan *et al.*, 2020; Ray *et al.*, 2020; Senapati *et al.*, 2021; Tiwari *et al.*, 2020). The COVID-19 epidemic has damaged beyond repair society at large, prompting the development of a number of preventative measures to slow its rapid spread. While lockdowns, social isolation, and other treatments have all been successful, they also slow the coronavirus's ability to spread. For effective pandemic response measures to be developed, it is essential to comprehend the effects of these delays. In this research, we explore the field of mathematical modelling and use Delay Differential Equations (DDEs) to investigate the impact of delays brought on by preventative measures on the dynamics of COVID-19. Although several studies have used delay settings, the impact of this parameter on COVID-19 has not been extensively studied(Avila-Vales and Pérez, 2019; Goel *et al.*, 2020; A. Kumar and Nilam, 2019; V. M. Kumar *et al.*, 2021; Tipsri and Chinviriyasit, 2014).

Delay Differential Equations (DDEs) are a powerful mathematical tool that has gained significant importance in various fields of science and engineering. Unlike ordinary differential equations (ODEs), which describe the rate of change of a system with respect to the current time, DDEs account for the influence of past states on the current state. This consideration of delays is particularly pertinent in epidemiology, where the time lag between exposure, infection, and transmission plays a crucial role in disease dynamics (Aguiar *et al.*, 2022; Khajanchi *et al.*, 2021; Lin and Wang, 2012; Sweilam *et al.*, 2020). DDEs have been extensively used to model infectious diseases, providing valuable insights into the impact of time delays on disease spread and control strategies.

A Delay Differential Equation (DDE) is a type of differential equation where the current time derivatives of certain unknown functions depend on the values of these functions at previous points in time. In other words, the evolution of the system at the present moment is influenced not only by its current state but also by its past states. The general form of a DDE can be represented as follows:

$$\frac{dx(t)}{dt} = f(t, x(t), x(t - \tau))$$

where

$$x(t - \tau) = x(\tau) : \tau \leq t$$

gives the trajectory of the solution in the past. Here, the function f is a functional operator from $\mathbb{R} X \mathbb{R}^n X C^1$ to $\mathbb{R}^n$ and $x(t) \in \mathbb{R}^n$ (Banerjee, 2021).

As a consequence of enforcing diverse precautionary measures, such as social distancing, self-isolation, practising personal hygiene, mask-wearing, and widespread media awareness, a delay is anticipated in the time it takes for each susceptible individual to be exposed and potentially infected. In our study, we incorporate the notion of time delay by introducing the parameter τ, which represents the extent of this delay in the susceptibility of individuals to exposure and potential infection. This parameter accounts for the temporal gap resulting from precautionary measures, effectively postponing the transmission of the disease from infected to susceptible individuals.

4.2   Model Formulation

We create a deterministic compartmental model $SEII_AQR$ to describe the disease transmission mechanism. Let N be the total population of humans. The total population N is divided into six compartments: Susceptible (S), Exposed(E), Symptomatic Infection(I), Asymptomatic Infection(I_A), Quarantine(Q) and individuals that are either recovered or die from COVID-19(R). We also include Vital Dynamics: The natural human natality or recruitment rate denoted by Λ and mortality(death) rate denoted by μ. The schematic diagram is shown in Figure 4.1

$$
\begin{aligned}
\frac{dS}{dt} &= \Lambda - \beta S(I + I_A) - \mu S, \\
\frac{dE}{dt} &= \beta S(I + I_A) - \gamma E - \mu E, \\
\frac{dI}{dt} &= p_1 \gamma E - (\mu + \theta)I - \alpha I, \\
\frac{dI_A}{dt} &= p_2 \gamma E - \epsilon I_A - \mu I_A, \\
\frac{dQ}{dt} &= p_3 \gamma E - \sigma Q - \mu Q \\
\frac{dR}{dt} &= \alpha I + \epsilon I_A + \sigma Q - \mu R,
\end{aligned}
\tag{4.1}
$$

with nonnegative initial conditions given by

$$S(0) > 0, \ E(0) > 0, \ I(0) > 0, \ I_A > 0, \ Q(0) > 0, \ R(0) > 0.$$

All the parameters of the system 4.1 are assumed to be positive for all time $t > 0$.

Due to the implementation of various precautionary measures, like social distancing, self-isolation, personal hygiene, wearing masks, media awareness, etc. We assume that there will be some delay in the time taken by each susceptible person to be exposed and likely infected. We introduce the concept of time delay and use parameter τ which takes into account this delay in the delaying of susceptibility to be exposed and likely infected due to measure;τ is the time delay due to delaying in the transmission of the disease from infected to susceptible due to precautionary measures.
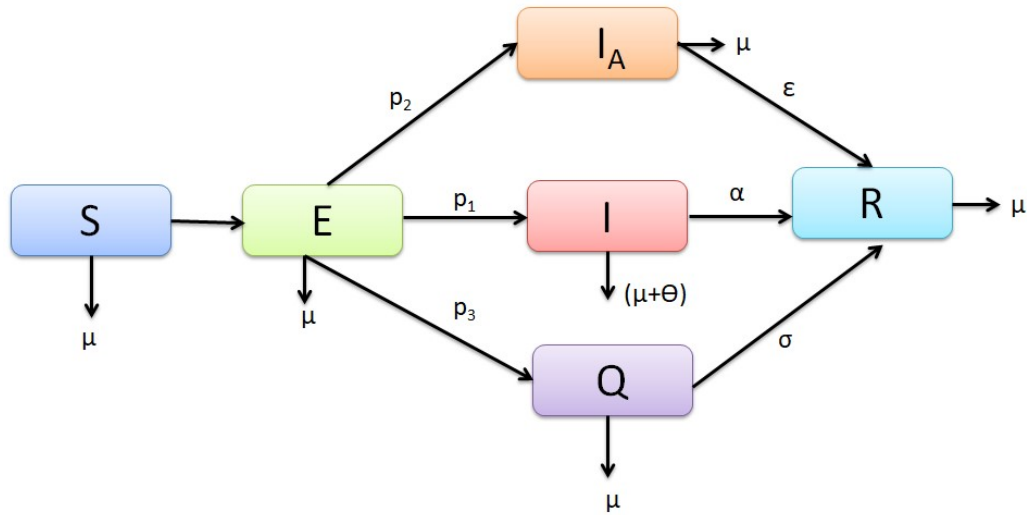
Figure 4.1: Schematic Diagram of $SEII_AQR$

$$\frac{dS}{dt} = \Lambda - \beta \ S \ I(t-\tau) - \beta S \ I_A - \mu S,$$

$$\frac{dE}{dt} = \beta \ S \ I(t-\tau) - \beta S \ I_A - \gamma E - \mu E,$$

$$\frac{dI}{dt} = p_1 \gamma E - (\mu + \theta)I - \alpha I, \qquad (4.2)$$

$$\frac{dI_A}{dt} = p_2 \gamma E - \epsilon I_A - \mu I_A,$$

$$\frac{dQ}{dt} = p_3 \gamma E - \sigma Q - \mu Q$$

$$\frac{dR}{dt} = \alpha I + \epsilon I_A + \sigma Q - \mu R,$$

Consider the initial conditions for system 4.2 are of the form:

$$S(\eta) = f_1(\eta), \ E(\eta) = f_2(\eta), \ I(\eta) = f_3(\eta), \ I_A(\eta) = f_4(\eta), \ Q(\eta) = f_5(\eta), \ R(\eta) = f_6(\eta).$$

where $f_i(\eta) \in C([-\tau, 0], R_+^6)$, which is a Banach space of continuous functions from $[-\tau, 0]$ into R_+^6; such that, $f_\eta \geq 0$ for $\eta \in [-\tau, 0)$, and $f_i(0) > 0$, $\forall i = 1, 2, 3, 4, 5, 6, 7$. Table 4.1 briefly describes all the parameters of the model.

Table 4.1: Parameter Description for $SEII_AQR$

Parameter	Description	Values (Units)
Λ	Birth rate	$52000 \ year^{-1}$
μ	Death rate	$0.0245 \ year^{-1}$
β	Rate of transmission	$1.7399 \ day^{-1}$
γ	Rate of transition from Exposed to I, I_A, and Q	$0.1923 \ day^{-1}$
p_1	Fraction of population moves from Exposed to symptomatic class	0.3362
p_2	Fraction of population moves from Exposed to asymptomatic class	0.4204
p_3	Fraction of population moves from Exposed to quarantine class	0.2434
α	Recovery rate of symptomatic infected class	$0.07 \ day^{-1}$
ϵ	Recovery rate of asymptomatic infection	$0.9 \ day^{-1}$
σ	Recovery rate of quarantine class	$0.9 \ day^{-1}$
θ	Rate of disease-induced death	$0.0001 \ day^{-1}$

4.3 Dynamics of non-delayed system 4.1

4.3.1 Positivity of Solutions

For the COVID-19 model system 4.1 to be epidemiologically realistic, it is necessary to prove that all the state variables remain positive for all time.

Theorem 4.1. *Let the initial data be $\{(S, E, I, I_A, Q, R) \leq 0\} \in \phi$. Then the solution set $\{S(t), E(t), I(t), I_A(t), Q(t), R(t)\}$ of the model system is non negative for all time t.*

Proof. Considering the non-linear system of the model 4.1, we take the first equation

$$\frac{dS}{dt} = \Lambda - \beta S(I + I_A) - \mu S,$$

$$\frac{dS}{dt} \geq -[\beta S(I + I_A) + \mu]S,$$

$$\int \frac{dS}{S} \geq - \int [\beta S(I + I_A) + \mu]dt,$$

$$\ln S \geq -[\beta S(I + I_A) + \mu]t + c,$$

$$S \geq e^{-[\beta S(I+I_A)+\mu]t} + e^c,$$

$$S(t) \geq S(0)e^{-[\beta S(I+I_A)+\mu]t}.$$

Similarly, it can also been shown that $E(t) > 0$, $I(t) > 0$, I_A $Q(t) > 0$, $R(t) > 0$ for all $t > 0$. Therefore, the disease is uniformly persistent for every positive solution $\square$

4.3.2   Invariant Region

Theorem 4.2. *For the initial conditions 4.2, the solutions of system 4.1 are contained in the region $\phi \subset R_+^6$ defined by*

$$\phi = [\{S(t), E(t), I(t), I_A(t), Q(t), R(t)\} \in R_+^6 : N(t) \leq \frac{\Lambda}{\mu}]$$

Proof. Let, $N = S + E + I + I_A + Q + R$

$$\frac{dN}{dt} = \Lambda - (S + E + I + I_A + Q + R)\mu - \theta I$$

$$\frac{dN}{dt} = \Lambda - \mu N - \theta I$$

$$\frac{dN}{dt} \leq \Lambda - \mu N$$

$$\frac{dN}{dt} + \mu N \leq \Lambda$$

$$Ne^{\mu t} \leq \int e^{\mu t}\Lambda + C$$

$$Ne^{\mu t} \leq \frac{\Lambda e^{\mu t}}{\mu} + C$$

$$N \leq \frac{\Lambda}{\mu} + Ce^{-\mu t}.$$

At $t \longrightarrow \infty$, $N \longrightarrow \frac{\Lambda}{\mu}$. Clearly $\phi = [\{S(t), E(t), I(t), I_A(t), Q(t), R(t)\} \in R_+^6 : N(t) \leq \frac{\Lambda}{\mu}]$ $\qquad\square$

4.3.3 Analysis of Disease-Free Equilibrium (DFE) E_0

The model gets DFE when the disease has zero induction
Taking the first equation of system (1) with $E = I = I_A = Q = R = 0$ into consideration.

$$0 = \beta S(I + I_A) - \gamma E - \mu E,$$
$$0 = p_1\gamma E - (\mu + \theta)I - \alpha I,$$
$$0 = p_2\gamma E - \epsilon I_A - \mu I_A,$$
$$0 = p_3\gamma E - \sigma Q - \mu Q$$
$$0 = \alpha I + \epsilon I_A + \sigma Q - \mu R$$

we arrive at

$$S_0 = \frac{\Lambda}{\mu}$$

Then, the disease-free equilibrium (DFE) state E_0 is given by

$$E_0 = [\frac{\Lambda}{\mu}, 0, 0, 0, 0, 0]$$

4.4 Basic reproductive number R_0

R_0 refers to the average number of secondarily infected persons infected by one primary infected patient during the infectious period. To obtain the basic reproduction number, we used the next generation matrix method by (Diekmann and Heesterbeek, 2000) and (van den Driessche and Watmough, 2008), where $\mathcal{F}$ is the matrix of the new infection terms and $\mathcal{V}$ is the matrix of the transition terms.

Infected compartments are $E,\ I,\ I_A,\ Q,\ R$.
Let $Y\ =\ (E,\ I,\ I_A,\ Q,\ ,R)$,

$$\frac{dY}{dt} = \begin{bmatrix} \beta S(I + I_A) \\ 0 \\ 0 \\ 0 \\ 0 \end{bmatrix} - \begin{bmatrix} (\gamma + \mu)E \\ -p_1\gamma E + (\mu + \theta + \alpha)I \\ -p_2\gamma E + (\eta + \mu)I_A \\ -p_3\gamma E + (\sigma + \mu)Q \\ -\alpha I - \epsilon I_A - \sigma Q + \mu R \end{bmatrix}$$

$$F_1 = \begin{bmatrix} 0 & \beta S_0 & \beta S_0 & 0 & 0 \\ 0 & 0 & 0 & 0 & 0 \\ 0 & 0 & 0 & 0 & 0 \\ 0 & 0 & 0 & 0 & 0 \\ 0 & 0 & 0 & 0 & 0 \end{bmatrix}$$

$$V_1 = \begin{bmatrix} \gamma + \mu & 0 & 0 & 0 & 0 \\ -p_1\gamma & (\mu + \theta + \alpha) & 0 & 0 & 0 \\ -p_2\gamma & 0 & \epsilon + \mu & 0 & 0 \\ -p_3\gamma & 0 & 0 & \sigma + \mu & 0 \\ 0 & -\alpha & -\epsilon & -\sigma & \mu \end{bmatrix}$$

At disease-free equilibrium

$$E_0 = [\frac{\Lambda}{(\delta + \mu)}, \frac{\delta\Lambda}{\mu(\delta + \mu)}, 0, 0, 0, 0]$$

$$\mathcal{F} = \begin{bmatrix} o & \frac{\beta\Lambda}{\mu} & \frac{\beta\Lambda}{\mu} & 0 & 0 \\ 0 & 0 & 0 & 0 & 0 \\ 0 & 0 & 0 & 0 & 0 \\ 0 & 0 & 0 & 0 & 0 \\ 0 & 0 & 0 & 0 & 0 \end{bmatrix}$$

$$\mathcal{V} = \begin{bmatrix} \gamma + \mu & 0 & 0 & 0 & 0 \\ -p_1\gamma & (\mu + \theta + \alpha) & 0 & 0 & 0 \\ -p_2\gamma & 0 & \epsilon + \mu & 0 & 0 \\ -p_3\gamma & 0 & 0 & \sigma + \mu & 0 \\ 0 & -\alpha & -\epsilon & -\sigma & \mu \end{bmatrix}$$

Now, $\mathcal{F}\mathcal{V}^{-1} = \begin{bmatrix} \frac{\beta\gamma\Lambda P_1}{\mu(\mu+\gamma)(\alpha+\theta+\mu)} + \frac{\beta\gamma\Lambda P_2}{\mu(\mu+\epsilon)(\mu+\gamma)} & \frac{\beta\Lambda}{\mu(\alpha+\theta+\mu)} & \frac{\beta\Lambda}{\mu(\mu+\epsilon)} & 0 & 0 \\ 0 & 0 & 0 & 0 & 0 \\ 0 & 0 & 0 & 0 & 0 \\ 0 & 0 & 0 & 0 & 0 \\ 0 & 0 & 0 & 0 & 0 \end{bmatrix}$

The basic Reproduction number is given by

$$R_0 = \frac{\beta\gamma\Lambda P_1}{\mu(\mu + \gamma)(\alpha + \theta + \mu)} + \frac{\beta\gamma\Lambda P_2}{\mu(\mu + \epsilon)(\mu + \gamma)}$$

4.5   Stability analysis of DFE

4.5.1   Local stability of disease-free equilibrium

Theorem 4.3. *The Disease Free Equilibrium DEF is locally asymptotically stable if* $R_0 < 1$

Proof. The Jacobian matrix wrt system 4.1 is given by

$$J = \begin{bmatrix} -\mu & 0 & -\beta S_0 & -\beta S_0 & 0 & 0 \\ 0 & -(\gamma + \mu) & \beta S_0 & \beta S_0 & 0 & 0 \\ 0 & p_1\gamma & -(\mu + \theta + \alpha) & 0 & 0 & 0 \\ 0 & p_2\gamma & 0 & -(\epsilon + \mu) & 0 & 0 \\ 0 & p_3\gamma & 0 & 0 & -(\sigma + \mu) & 0 \\ 0 & 0 & \alpha & \epsilon & \sigma & -\mu \end{bmatrix}$$

which implies

$$J_{DFE} = \begin{bmatrix} -l_1 & \beta S_0 & \beta S_0 & 0 \\ p_1\gamma & -l_2 & 0 & 0 \\ p_2\gamma & 0 & -l_3 & 0 \\ p_3\gamma & 0 & 0 & -l_4 \end{bmatrix}$$

Where,
$l_1 = (\gamma + \mu), \ l_2 = (\mu + \theta + \alpha), \ l_3 = (\epsilon + \mu), \ l_4 = \sigma + \mu$

Clearly, two eigenvalues of the matrix J_{DFE} are negative such as $-\mu$ and $-\mu$. The remaining eigenvalues are the roots of the following Polynomial equation

$$\lambda^4 + a_3\lambda^3 + a_2\lambda^2 + a_1\lambda + a_0 = 0$$

where,

$a_3 = -(-l_1 - l_2 - l_3 - l_4) = (l_1 + l_2 + l_3 + l_4)$

$a_2 = (l_1 + l_2 + l_3 + l_4)^2/2 - (l_1^2 + l_2^2 + l_3^2 + l_4^2)/2 - \beta\gamma S_0(p_1 + p_2)$

$a_1 = l_1 l_2 l_3 + l_1 l_2 l_4 + l_1 l_3 l_4 + l_2 l_3 l_4 - \beta\gamma l_2 p_2 S_0 - \beta\gamma l_3 p_1 S_0 - \beta\gamma l_4 p_1 S_0 - \beta\gamma l_4 p_2 S_0$

$a_0 = l_1 l_2 l_3 l_4 - \beta\gamma l_2 l_4 p_2 S_0 - \beta\gamma l_3 l_4 p_1$

According to the Routh-Hurwitz criterion, the above equation will give negative roots or roots with negative real parts if the following condition is satisfied:

$$a_3 > 0, \begin{vmatrix} a_3 & a_1 \\ 1 & a_2 \end{vmatrix} > 0, \begin{vmatrix} a_3 & a_1 & 0 \\ 1 & a_2 & a_0 \\ 0 & a_3 & a_1 \end{vmatrix} > 0$$

Hence, the disease-free equilibrium point E_0 of the system is locally asymptotically stable, when $R_0 < 1$. $\qquad\square$

4.5.2 Global stability of disease-free equilibrium

We now study the global stability of disease-free equilibrium, using the theorem by Castillo-Chavez et al. (Korobeinikov and Wake, 2002)

Theorem 4.4. *If the given mathematical model can be written in the form:*

$$\frac{dX}{dt} = F(X, Y) \tag{4.3}$$
$$\frac{dY}{dt} = G(X, Y), G(X, Y) = 0$$

where $X = S^T$, $Y = (E, I, I_A, Q, R)^T$, denoting the number of uninfected individuals and denoting the number of COVID-19-infected people respectively. Let the disease-free equilibrium of this system be

$$U_0 = (X^*, 0) = (\frac{\Lambda}{\mu}, 0)$$

where $\mathbf{0}$ is a zero vector.
For the global asymptotically stable, the following condition $(H1)$ and $(H2)$ must be satisfied.

$$(H1) : For \frac{dX}{dt} = F(X, 0), \ 0 \ is \ global \ asymptotically \ stable.$$
$$(H2) : G(X, Y) = AY - \hat{G}(X, Y), \hat{G}(X, Y) \geq 0 for (X, Y) \in \Omega$$

where $A = D_Y G(X^*, 0)$ is an M- matrix (the off-diagonal elements of A are non-negative) and Ω is the region where the model makes biological sense. If the given

*system of differential equations of our model satisfies the given condition in (2) then
the fixed point $U_0 = (X^\star, 0)$ is a global asymptotically stable (g.a.s) equilibrium of (2)
provided $R_0 < 1$, and the assumption (H1) and (H2) are satisfied.*

Theorem 4.5. *(global asymptotic stability of DFE)*
The DFE E_0 of model 4.1 is global asymptotically stable if $R_0 < 1$

Proof. First, we rewrite the system of differential equation of our model 4.1 as $X = S^T$ and $Y = (E, I, I_A, Q, R)^T$.
Then, the DFE is given by

$$U_0 = (X^\star, 0) = (\frac{\Lambda}{\mu}, 0)$$

. and the system $\frac{dX}{dt} = F(X, 0)$ becomes

$$\dot{S} = \Lambda - \mu S$$

This equation has a unique equilibrium point

$$X^* = (\frac{\Lambda}{\mu}, 0) \tag{4.4}$$

which is globally asymptotically stable. Therefore, condition (H1) is satisfied. We
now verify the second condition (H2). For model 4.1, we have

$$G(X, Y) = \begin{bmatrix} \beta S(I + I_A) - \gamma E - \mu E p_1 \gamma E - (\mu + \theta + \alpha)I \\ p_2 \gamma E - (\epsilon + \mu)I_A \\ p_3 \gamma E - (\sigma + \mu)Q \\ \alpha I + \epsilon I_A + \sigma Q - \mu R \end{bmatrix}$$

$$D_Y G(X^*, 0) = A = F - V$$

$$= \begin{bmatrix} -(\gamma + \mu) & \beta S_0 & \beta S_0 & 0 & 0 \\ p_1 \gamma & -(\mu + \theta + \alpha) & 0 & 0 & 0 \\ p_2 \gamma & 0 & -(\epsilon + \mu) & 0 & 0 \\ p_3 \gamma & 0 & 0 & -(\sigma + \mu) & 0 \\ 0 & \alpha & \epsilon & \sigma & -\mu \end{bmatrix}$$

Clearly, we see that A is an M-matrix, i,e. all the off-diagonal elements of A are
non-negative.

$$\hat{G}(X, Y) = AY - G(X, Y)$$

$$= \begin{bmatrix} [\beta(I + I_A)](S - S_0) \\ 0 \\ 0 \\ 0 \\ 0 \end{bmatrix}$$

which implies that $\hat{G}(X,Y) \geq 0$ for all $(X,Y) \in \Omega$. Therefore, conditions (H1) and (H2) are satisfied. Hence, disease-free equilibrium is globally asymptotically stable. $\square$

4.6   Stability analysis of EE

4.6.1   Existence of Endemic Equilibrium point

Let us denote the Endemic Equilibrium by $E_1 = (S^*, V^*, E^*, I^*, I_A^*, R^*)$ The Endemic Equilibrium always satisfies:

$$0 = \Lambda - \beta S^*(I^* + I_A^*) - \mu S^*$$
$$0 = \beta S^*(I^* + I_A^*) - \gamma E^* - \mu E^*$$
$$0 = p_1 \gamma E^* - (\alpha + \theta)I^* - \mu I^*$$
$$0 = p_2 \gamma E^* - \epsilon I_A^* - \mu I_A^*$$
$$0 = p_3 \gamma E^* - \sigma Q^* - \mu Q^*$$
$$0 = \alpha I^* + \epsilon I_A^* + \sigma Q^* - \mu R^*$$

(4.5)

which gives

$$S^* = \frac{\Lambda}{\mu + \beta(\frac{\gamma p_2}{\mu + \epsilon} + \frac{\gamma p_1}{\alpha + \theta + \mu})E^*}$$

$$E^* = \frac{\beta \Lambda A - \mu(\mu + \gamma)}{(\mu + \gamma)\beta A}$$

$$I^* = \frac{p_1 \gamma E^*}{\alpha + \theta + \mu}$$

$$I_A^* = \frac{p_2 \gamma E^*}{\epsilon + \mu}$$

$$Q^* = \frac{p_3 \gamma E^*}{\sigma + \mu}$$

$$R^* = \frac{[\frac{p_1 \gamma \alpha}{\alpha + \theta + \mu} + \frac{\epsilon \gamma p_2}{\mu + \epsilon} + \frac{p_3 \gamma \sigma}{\sigma + \mu}]E^*}{\mu}$$

where,

$$A = [\frac{\gamma p_2}{\mu + \epsilon} + \frac{\gamma p_1}{\alpha + \theta + \mu}]$$

4.6.2   Local stability of endemic equilibrium

Theorem 4.6. *The endemic equilibrium E_1 is locally asymptotically stable if $R_0 > 1$, otherwise it is unstable.*

Proof. The Jacobian matrix of the system 4.1 at endemic equilibrium point E_1 is obtained as follows:

$$J_{E1} = \begin{bmatrix} -q & 0 & -\beta S^* & -\beta S^* & 0 & 0 \\ a_{21} & -r & \beta S^* & \beta S^* & 0 & 0 \\ 0 & p_1\gamma & -s & 0 & 0 & 0 \\ 0 & p_2\gamma & 0 & -t & 0 & 0 \\ 0 & p_3\gamma & 0 & 0 & -u & 0 \\ 0 & 0 & \alpha & \epsilon & \sigma & -\mu \end{bmatrix}$$

where

$$q = [\beta(I^* + I_A^*) + \mu]$$
$$r = (\gamma + \mu)$$
$$s = (\mu + \theta + \alpha)$$
$$t = (\epsilon + \mu)$$
$$u = (\sigma + \mu)$$
$$a_{21} = \beta(I^* + I_A^*)$$

Clearly, one eigenvalue of the matrix J_{E1} is negative $-\mu$ and the remaining eigenvalues are the roots of the following Polynomial equation:

$$\lambda^5 + c_4\lambda^4 + c_3\lambda^3 + c_2\lambda^2 + c_1\lambda + c_0 = 0$$

where

$$c_4 = (q + r + s + t + u)$$
$$c_3 = (q + r + s + t + u)^2/2 - (q^2 + r^2 + s^2 + t^2 + u^2)/2 - \beta\gamma S^*(p_1 + p_2)$$
$$c_2 = qr(s + t + u) + (qs + rs)(t + u) + tu(q + r) + \beta\gamma S^*[(a_{21} - q - u)$$
$$(p_1 + p_2) - (sp_2 + tp_1)]$$
$$c_1 = qrs(t + u) + qtu(r + s) + rstu + \beta\gamma S^*(a_{21}s + a_{21}u - qu)(p_1 + p_2)$$
$$- \beta\gamma q S^*(sp_2 + tp_1) - \beta\gamma u S^*(sp_2 + up_1)$$
$$c_0 = qr(s + t + u) + (qs + rs)(t + u) + tu(q + r) + \beta\gamma S^*[(a_{21} - q - u)$$
$$(p_1 + p_2) - (sp_2 + tp_1)]$$

According to the Routh-Hurwitz criterion, the above equation will give negative roots or negative real parts if the following condition is satisfied:

$$c_4 > 0, \begin{vmatrix} c_4 & c_2 \\ 1 & c_3 \end{vmatrix} > 0, \begin{vmatrix} c_4 & c_2 & c_0 \\ 1 & c_3 & c_1 \\ 0 & a_4 & a_2 \end{vmatrix} > 0, \begin{vmatrix} c_4 & c_2 & c_0 & 0 \\ 1 & c_3 & c_1 & 0 \\ 0 & c_4 & c_2 & c_0 \\ 0 & 1 & c_3 & c_1 \end{vmatrix} > 0$$

Hence, the endemic equilibrium point E_1 of the system is locally asymptotically stable when $R_0 > 1$ □

4.7 Dynamic with delay 4.2

The Positivity of the system 4.2 can be proved in a similar way as (Bugalia *et al.*, 2021) and the boundedness of system 4.2 can be proved in a similar way as in Section 4.3.2.

4.7.1 Equilibrium points and their stability

As mentioned by Tipsri and Chinviriyasit (Tipsri and Chinviriyasit, 2014), the equilibrium solutions are the same for the system with and without time delay. Therefore, to obtain the equilibrium points, we use $\tau = 0$. Hence, the Disease-Free and Endemic Equilibrium points of the system 4.2 are the same as obtained in section 4.3.3 and 4.6.1 respectively.

4.7.2 Local stability of disease-free equilibrium point

In this subsection, we will discuss the stability of the system 4.2 around a disease-free equilibrium point. For $\tau > 0$
The Jacobian matrix wrt system 4.2 is given by

$$
\mathrm{J} =
\begin{bmatrix}
-\mu & 0 & -\beta S_0 e^{-\lambda\tau} & -\beta S_0 & 0 & 0 \\
0 & -(\gamma+\mu) & \beta S_0 e^{-\lambda\tau} & \beta S_0 & 0 & 0 \\
0 & p_1\gamma & -(\mu+\theta+\alpha) & 0 & 0 & 0 \\
0 & p_2\gamma & 0 & -(\epsilon+\mu) & 0 & 0 \\
0 & p_3\gamma & 0 & 0 & -(\sigma+\mu) & 0 \\
0 & 0 & \alpha & \epsilon & \sigma & -\mu
\end{bmatrix}
$$

which implies

$$
J_{DFE} =
\begin{bmatrix}
-l_1 & \beta S_0 e^{-\lambda\tau} & \beta S_0 & 0 \\
p_1\gamma & -l_2 & 0 & 0 \\
p_2\gamma & 0 & -l_3 & 0 \\
p_3\gamma & 0 & 0 & -l_4
\end{bmatrix}
$$

Where,
$l_1 = (\gamma+\mu),\ l_2 = (\mu+\theta+\alpha),\ l_3 = (\epsilon+\mu),\ l_4 = \sigma+\mu$

Clearly, two eigenvalues of the matrix J_{DFE} are negative such as $-\mu$ and $-\mu$. The remaining eigenvalues are the roots of the following Polynomial equation.

$$
\lambda^4 + a_3\lambda^3 + a_2\lambda^2 + a_1\lambda + a_0 = 0 \tag{4.6}
$$

where,

$$
\begin{aligned}
a_3 &= -(-l_1 - l_2 - l_3 - l_4) = (l_1 + l_2 + l_3 + l_4) \\
a_2 &= (l_1 + l_2 + l_3 + l_4)^2/2 - (l_1^2 + l_2^2 + l_3^2 + l_4^2)/2 - \beta\gamma S_0 e^{-\lambda\tau}(p_1 + p_2) \\
a_1 &= l_1 l_2 l_3 + l_1 l_2 l_4 + l_1 l_3 l_4 + l_2 l_3 l_4 - \beta\gamma e^{-\lambda\tau} l_2 p_2 S_0 - \beta\gamma e^{-\lambda\tau} l_3 p_1 S_0 \\
&\quad - \beta\gamma l_4 p_1 S_0 - \beta\gamma l_4 p_2 S_0 \\
a_0 &= l_1 l_2 l_3 l_4 - \beta\gamma e^{-\lambda\tau} l_2 l_4 p_2 S_0 - \beta\gamma l_3 l_4 p_1
\end{aligned}
$$

Ruan and Wei's corollary 2.4 (Ruan and Wei, 2003) states that for $t > 0$ if instability arises for a specific value of the delay, a characteristic root of 4.6 must intersect the imaginary axis.

The chereteristic equation can also be written as

$$f(\lambda) = (\lambda^4 + b_3\lambda^3 + b_2\lambda^2 + b_1\lambda + b_0) + e^{-\lambda\tau}(c_3\lambda^3 + c_2\lambda^2 + c_1\lambda + c_0) = 0 \qquad (4.7)$$

For $\tau > 0$, (4.7) is a transcendental chareteristic equation and the roots will be of the form, $\lambda = \eta(\tau) + i\omega(\tau)$, where $\omega > 0$ As explained by Mukandavire (Mukandavire *et al.*, 2007), the roots of a transcendental equation will have positive real parts if and only if it has purely imaginary roots. We will aim to obtain the conditions for which no such purely imaginary root exists for 4.7. These conditions will be then sufficient to conclude that all the roots of 4.7 have negative real parts. Consider, $\lambda = i\omega$ $(\omega > 0)$ is a purely imaginary root of 4.7. Then, 4.7 becomes

$$\omega^4 - ib_3\omega^3 - b_2\omega^2 + ib_1\omega + b_0 + [\cos(\lambda\tau) - i\sin(\lambda\tau)](-ic_3\omega^2 - c_2\omega^3 + ic_1\omega + c_0) = 0$$

Separating real–imaginary parts,

Real :
$$\omega^4 - b_2\omega^2 + b_0 - \cos(\lambda\tau)[c_2\omega^2 - c_0] - \sin(\lambda\tau[c_3\omega^3 - c_1\omega] = 0$$

Complex :
$$-b_3\omega^3 + b_1\omega - \cos(\omega\tau)[c_3\omega^3 - c_1\omega] + \sin(\omega\tau)[c_2\omega^2 - c_0] = 0$$

Squaring both sides of the above two equations and adding we get,

$$\omega^8 + \omega^6(-2b_2 + b_3^2 + c_3^2) + \omega^4(b_2^2 + 2b_0 - 2b_1b_3 + 2c_1c_3 - c_2) + \omega^2(-2b_0b_2 + b_1^2 - c_1^2 + 2c_0c_2) + b_0^2 - c_0^2 = 0$$

Taking $s = \omega^2$. We have

$$s^4 + s^3(-2b_2 + b_3^2 + c_3^2) + s^2(b_2^2 + 2b_0 - 2b_1b_3 + 2c_1c_3 - c_2) + s(-2b_0b_2 + b_1^2 - c_1^2 + 2c_0c_2) + (b_0^2 - c_0^2) = 0 \qquad (4.8)$$

if we assume that

C2 :

$$(-2b_2 + b_3^2 + c_3^2) = g_3 > 0$$
$$(b_2^2 + 2b_0 - 2b_1b_3 + 2c_1c_3 - c_2) = g_2 > 0$$
$$(-2b_0b_2 + b_1^2 - c_1^2 + 2c_0c_2) = g_1 > 0$$
$$(b_0^2 - c_0^2) = g_0 > 0$$

and

$$\begin{vmatrix} g_3 & g_1 \\ 1 & g_2 \end{vmatrix} > 0, \begin{vmatrix} g_3 & g_1 & 0 \\ 1 & g_2 & g_0 \\ 0 & g_3 & g_1 \end{vmatrix} > 0$$

then by Routh–Hurwitz criterion the roots for (4.8) will have negative real parts. However, there does not exist ω such that $s = \omega^2$ is negative. This poses a contradiction. Hence, whenever the conditions in (C2) are true, there does not exist a purely imaginary root of the transcendental equation (4.7). Hence, we have the following theorem.

Theorem 4.7. *Let, $R_0 < 1$ then for $\tau > 0$, the disease-free equilibrium point of system (4.2) is locally asymptotically stable if condition in (C2) is satisfied. Otherwise, the disease-free equilibrium point of the system (4.2) is unstable.*

4.7.3 Local stability of endemic equilibrium point

The Jacobian matrix of the system 4.1 at endemic equilibrium point E_1 is obtained as follows:

$$J_{E1} = \begin{bmatrix} -q & 0 & -\beta S^* e^{-\lambda \tau} & -\beta S^* & 0 & 0 \\ a_{21} & -r & \beta S^* e^{-\lambda \tau} & \beta S^* & 0 & 0 \\ 0 & p_1 \gamma & -s & 0 & 0 & 0 \\ 0 & p_2 \gamma & 0 & -t & 0 & 0 \\ 0 & p_3 \gamma & 0 & 0 & -u & 0 \\ 0 & 0 & \alpha & \epsilon & \sigma & -\mu \end{bmatrix}$$

where

$$q = [\beta(I^* e^{-\lambda \tau} + I_A^*) + \mu]$$
$$r = (\gamma + \mu)$$
$$s = (\mu + \theta + \alpha)$$
$$t = (\epsilon + \mu)$$
$$u = (\sigma + \mu)$$
$$a_{21} = \beta(I^* e^{-\lambda \tau} + I_A^*)$$

Clearly, one eigenvalue of the matrix J_{E1} is negative $-\mu$ and the remaining eigenvalues are the roots of the following Polynomial equation:

$$\lambda^5 + c_4 \lambda^4 + c_3 \lambda^3 + c_2 \lambda^2 + c_1 \lambda + c_0 = 0$$

where

$$c_4 = (q + r + s + t + u)$$

$$c_3 = (q + r + s + t + u)^2/2 - (q^2 + r^2 + s^2 + t^2 + u^2)/2 - \beta\gamma S^* e^{-\lambda\tau}(p_1 + p_2)$$

$$c_2 = qr(s + t + u) + (qs + rs)(t + u) + tu(q + r) + \beta\gamma S^*[(a_{21} - q - u)$$
$$(p_1 + p_2) - (sp_2 + tp_1)]$$

$$c_1 = qrs(t + u) + qtu(r + s) + rstu + \beta\gamma S^*(a_{21}s + a_{21}u - qu)(p_1 + p_2)$$
$$- \beta\gamma q S^*(sp_2 + tp_1) - \beta\gamma u S^* e^{-\lambda\tau}(sp_2 + up_1)$$

$$c_0 = qr(s + t + u) + (qs + rs)(t + u) + tu(q + r) + \beta\gamma S^*[(a_{21} - q - u)$$
$$(p_1 + p_2) - (sp_2 + tp_1)]$$

For $\tau > 0$. The transcendental characteristic equation is given by

$$\lambda^5 + f_4\lambda^4 + f_3\lambda^3 + f_2\lambda^2 + f_1\lambda + f_0 + e^{-\lambda\tau}(j_4\lambda^4 + j_3\lambda^3 + j_2\lambda^2 + j_1\lambda + j_0) = 0 \quad (4.9)$$

the roots will be of the form, $\lambda = \eta(\tau) + i\omega(\tau)$, where $\omega > 0$. As done previously for the local stability of E_0 , we will aim to obtain the conditions for which no purely imaginary root exists for equation (4.9). Let if possible, Equation (4.9) have a purely complex root of the form: $\lambda = i\omega$ Then, (4.9) becomes:

$$i\omega^5 + f_4\omega^4 - if_3\omega^3 - f_2\omega^2 + if_1\omega + f_0 + [\cos(\lambda\tau) - i\sin(\lambda\tau)](j_4\omega^4 - ij_3\omega^3 - j_2\omega^2 + ij\omega + j_0) = 0$$

Separating real–imaginary parts:

Real :

$$F_4\omega^4 - f_2\omega^2 + f_0 + \cos(\lambda\tau)(j_4\omega^4 - j_2\omega^2 j_0) - \sin(\lambda\tau)(j_3\omega^3 - j\omega)$$

Complex :

$$\omega^5 - f_3\omega^3 + f_1\omega - \cos(\lambda\tau)(j_3\omega^3 - j\omega) - \sin(\lambda\tau)(j_4\omega^4 - j_2\omega^2 j_0)$$

Squaring both sides of the above equations and adding we get

$$\omega^1 0 + v_1\omega^8 + v_2\omega^6 + v_3\omega^4 + v_4\omega^2 + + v_5 = 0 \quad (4.10)$$

where,

$$v_1 = f_4^2 - 2f_1 - j_4^2$$
$$v_2 = -2f_4f_2 + 2f_1 + 2j_4j$$
$$v_3 = f_2^2 + 2f_4f_0 - 2f_3f_1 + j_2^2\omega^4 - 2j_4j_0$$
$$v_4 = -2f_2f_0 + f_1^2 - j_2^2 + 2j_3j + 2j_2j_0$$
$$v_5 = f_0^2 - j_0^2$$

Put $s = \omega^2$ in (4.10) we get

$$s^5 + v_1 s^4 + v_2 s^3 + v_3 s^2 + v_4 s + v_5 = 0$$

If we assume $|H_n|$ for $n = 1, 2, 3, 4, 5$, where for each n, H_n is a Hurwitz matrix of order $n * n$, with general form:

$$H_n =$$

$$\begin{bmatrix} v_1 & 1 & 0 & 0 & .... & 0 \\ v_3 & v_2 & v_1 & 1 & .... & 0 \\ v_5 & v_4 & v_3 & v_2 & .... & 0 \\ . & . & . & . & . & . \\ . & . & . & . & . & . \\ . & . & . & . & . & . \\ 0 & 0 & 0 & 0 & 0 & v_n \end{bmatrix} \tag{4.11}$$

with $v_j = 0$ if $j > 5$ or $j < 0$. According to the Routh-Hurwitz criterion, the roots of Equation (4.10) will exhibit negative real parts. Nevertheless, there is no value of ω that can make the expression $s = \omega^2$ negative. This leads to a contradiction. Consequently, the conditions stated in (4.11) are enough to establish that all roots of Equation (4.9) hold negative real parts for $\tau > 0$. As a result, we can state the following theorem.

Theorem 4.8. *Suppose E_1 is an endemic equilibrium point of the system (4.2), it will be locally asymptotically stable for $\tau > 0$ under the condition that each of the seven Hurwitz matrices defined as in (4.11) satisfies two criteria:*

1. The determinant of the matrix, denoted as $|H_n|$, must be greater than zero (i.e., $|H_n| > 0$).

2. The basic reproduction number R_0 must be greater than 1 (i.e., $R_0 > 1$). Otherwise unstable.

4.8 Sensitivity Analysis

In this section, We examine the impact of the parameters used to express the basic reproduction number, R_0, through sensitivity analysis.

This demonstrates that an alteration in these parameters results in an alteration in R_0. It is used to identify the variables with a significant impact on R_0 and determine which ones should be the focus of intervention measures. Sensitivity indices make it possible to quantify the proportional change in a variable when a parameter is altered.

The forward sensitivity index of a variable, with regard to a specific parameter, is used for that.

$$\alpha_\phi^{R_0} = \frac{\partial R_0}{\partial \phi} \frac{\phi}{R_0}$$

where $\phi = [\Lambda,\ \beta,\ \mu,\ \gamma,\ \theta,\ \alpha,\ \epsilon,\ P_1,\ P_2]$. The analytical equation for the sensitivity of R_0 to each parameter it comprises can be calculated using the formula mentioned above. As a result, Figure 4.2 shows the sensitivity index of parameters i.e Λ, β, μ, γ, θ, α, ϵ, P_1, P_2 respectively on R_0. The positive indices indicate a direct relationship between the parameters and R_0, that is if the parameter increases/decrease then the value of R_0 will increase/decrease. Therefore in order to control COVID-19 from the population, we need to reduce the Basic Reproduction number, we can achieve this by reducing the parameters which give positive indices i.e γ, r, β, P_1, P_2 Λ, here birth rate Λ and rate of transmission β are the most sensitive parameters of R_0 In light of the uncontrollable nature of the birth rate, our focus shifts to managing the rate of disease transmission. To achieve this, we must limit our contact rate through measures like quarantine and social distancing. By taking responsible actions and collectively embracing these precautions, we can build a shield of protection against infectious diseases, fostering a healthier and safer society.

Figure 4.2: Forward sensitivity of R_0

Also $\alpha_\beta^{R_0} = +1$ means that if β increase by 1 % than R_0 will also increase by 1 %. The negative indices indicate that there is an inverse relationship between the parameters and R_0, that is if the parameter decreases/increases then the value of R_0 will increase/decrease. μ, θ, α, ϵ have negative indices, among the μ is the highest sensitive if the death rate increase than R_0 decrease. The strength of intervention h has negative indices which imply that if we implement strict intervention measures then R_0 will decrease which will lead to a decrease in the Infected population.

From Figure 4.3, we observe that

- **High β and High γ:** When both the rate of transmission (β) and the rate of transition from exposed to infected (γ) are high, R_0 increases significantly. This indicates a rapid spread of infection due to high transmission rates and quick progression from Exposed to Infected states.

- **Low β and Low γ:** Conversely, when both β and γ are low, R_0 decreases. This suggests better control of the spread as lower transmission rates and slower transition rates reduce the overall number of infections.

- **High β and Low γ:** When the rate of transmission is high but the transition rate is low, R_0 still increases, but less drastically compared to when both are high. This implies that high transmission can be partially mitigated by slower progression to the infected state.

- **Policy Implications:** Effective interventions could aim to reduce β through measures such as social distancing and mask-wearing, while also managing the rate at which exposed individuals become infectious (γ) through timely testing and quarantine measures, thus helping to control the spread of COVID-19.
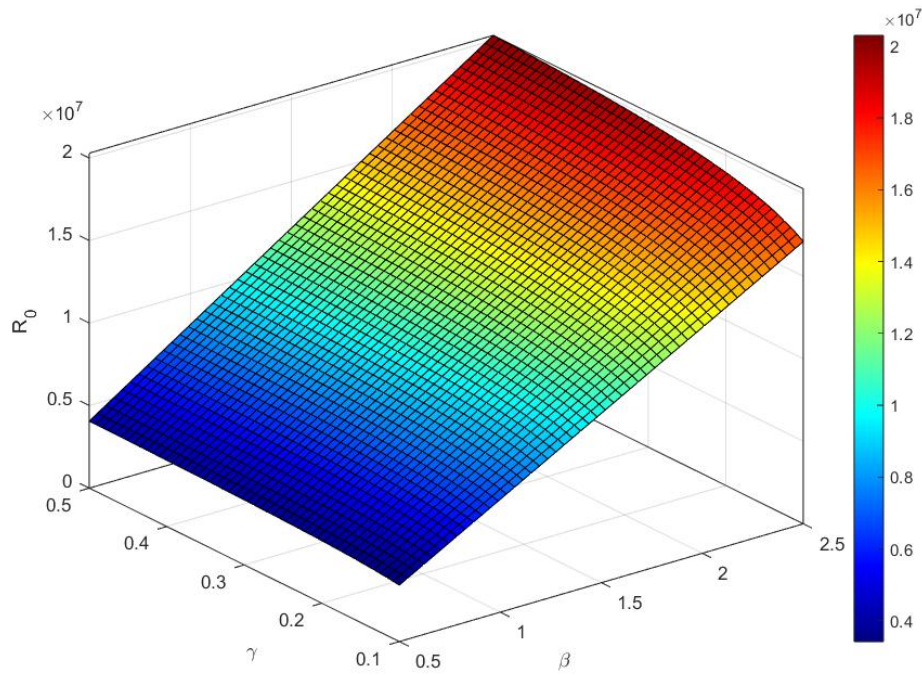
Figure 4.3: The numerical result exhibit that the dependence of R_0 of system on the rate of transmission β and transition from Exposed to Infected population γ

From Figure 4.4, we observe that

- **High β and Low θ:** When the rate of transmission (β) is high and the rate of disease-induced death (θ) is low, R_0 increases significantly.

- **Low β and High θ:** Conversely, when β is low and θ is high, R_0 decreases. This suggests better control of the spread due to lower transmission rates potentially reducing the overall spread.

- **Balancing β and θ:** The relationship highlights the importance of controlling transmission rates and managing disease severity through effective interventions such as vaccination, social distancing, and treatment protocols to reduce R_0.

- **Policy Implications:** Effective interventions could aim to reduce β through measures such as social distancing and mask-wearing, while increasing treatment and care to manage severe cases, thus influencing θ and mitigating the spread of COVID-19.
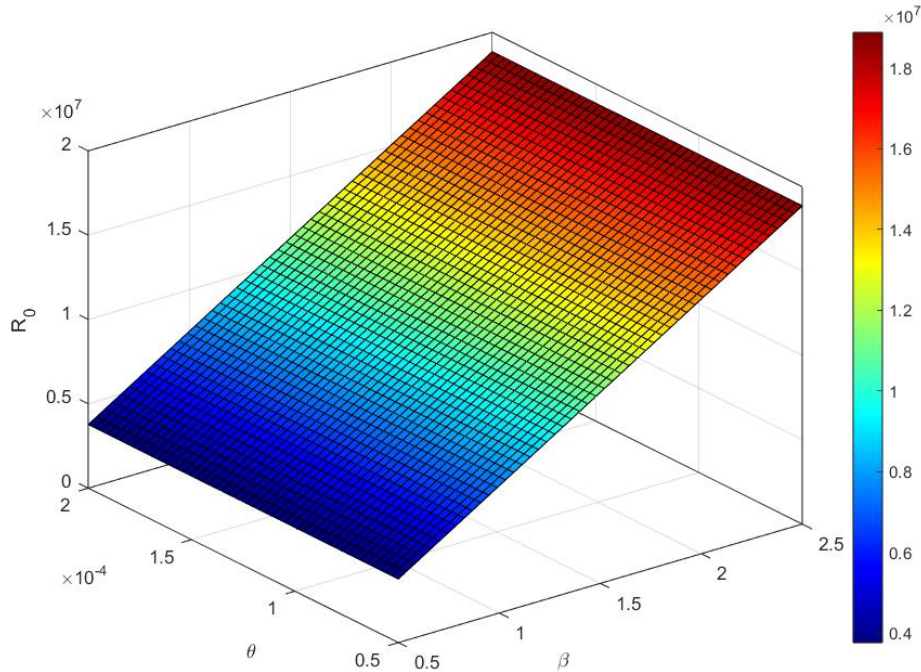
Figure 4.4: The numerical result exhibit that the dependence of R_0 of system on the rate of transmission β and the rate of disease-induced death θ

4.9   Numerical Simulation

For the Numerical Simulation of the proposed model, we illustrate the mathematical findings using the MATLAB program, the value of parameters are listed in the table. Figure 4.5 shows the Variation of $SEII_AQR$ without time delay corresponding to the values of $R_0 > 1$ for different values of initial numbers of each compartment with time $t = 0$ to 100. Figure 4.6 shows the Variation of $SEII_AQR$ without time delay corresponding to the values of $R_0 > 1$ for different values of initial numbers of each compartment with time $t = 0$ to 100
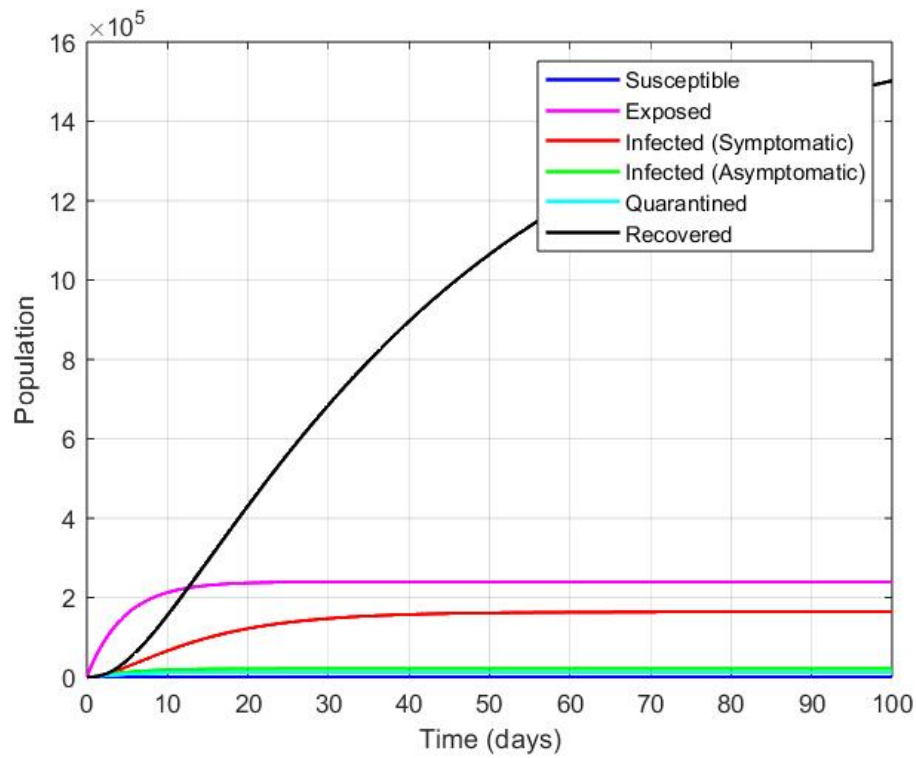
Figure 4.5: Variation of $SEII_AQR$ without time delay corresponding to the values of $R_0 > 1$ for different values of initial numbers of each compartment with time $t = 0$ to 100.
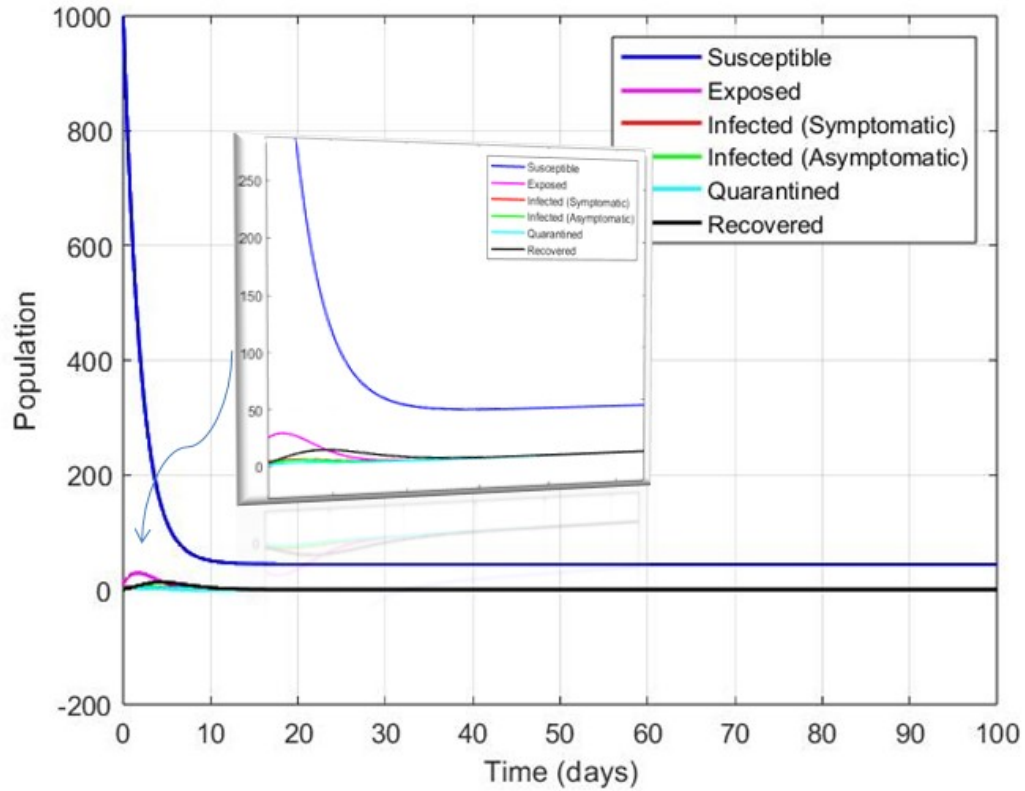
Figure 4.6: Variation of $SEII_AQR$ without time delay corresponding to the values of $R_0 > 1$ for different values of initial numbers of each compartment with time $t = 0$ to 100

By altering the values of tau, the impact of the time delay is observed. In Figures 4.7,4.8,4.9,4.10 we see a Simulation of a system showing a variation in population with the effect of time delay on $SEII_AQR$ when $\tau = 0.5, 3, 5, 7$. From this, we found out that if the time delay τ increases, it means there is a longer delay between the time when an individual becomes exposed and the time they start infecting others. Various precautionary measures will delay the Susceptible from being Exposed and becoming infected.
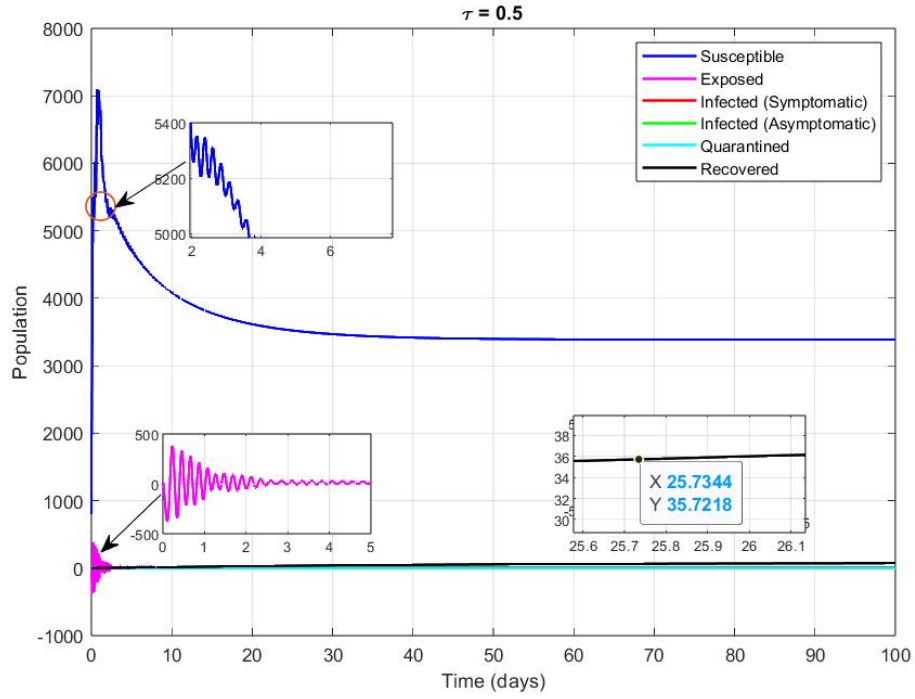
Figure 4.7: Simulation of a system showing the variation of the population with the effect of time delay on $SEII_AQR$ when $\tau = 0.5$
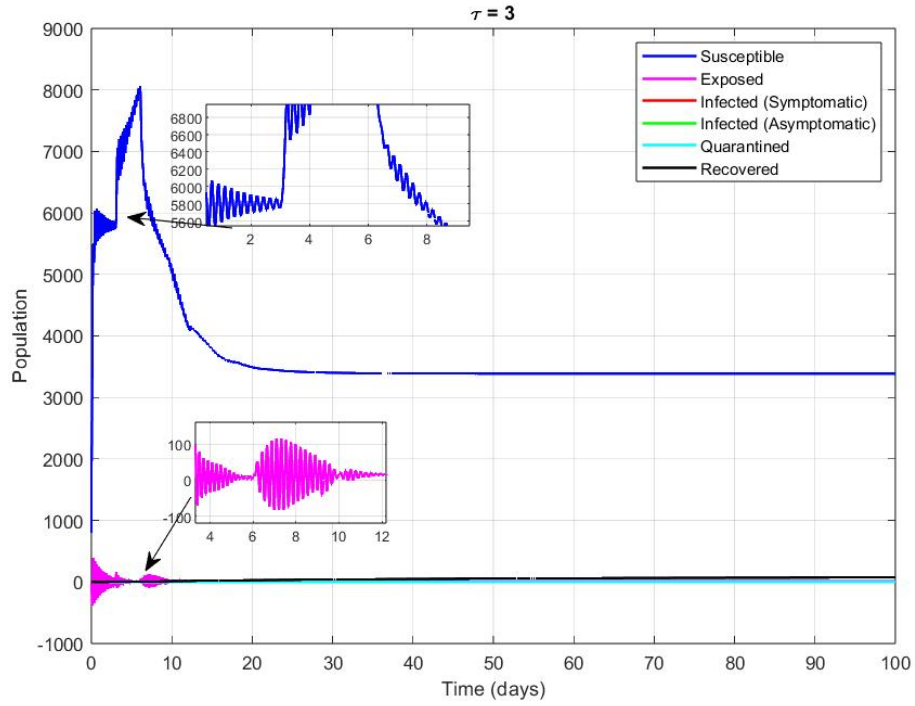
Figure 4.8: Simulation of a system showing the variation of the population with the effect of time delay on $SEII_AQR$ when $\tau = 3$
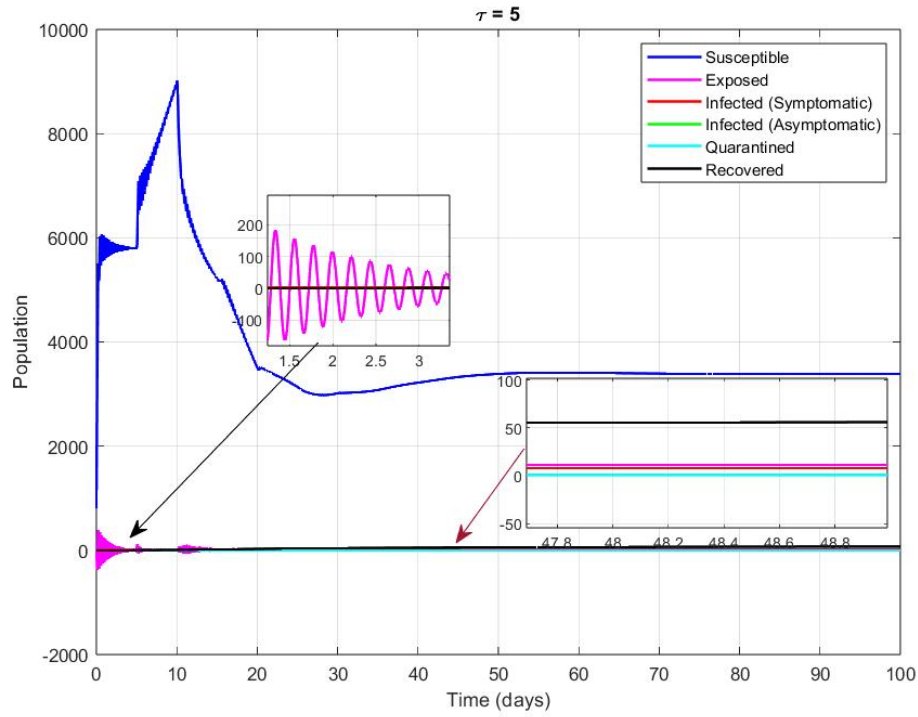
Figure 4.9: Simulation of a system showing the variation of the population with the effect of time delay on $SEII_AQR$ when $\tau = 5$
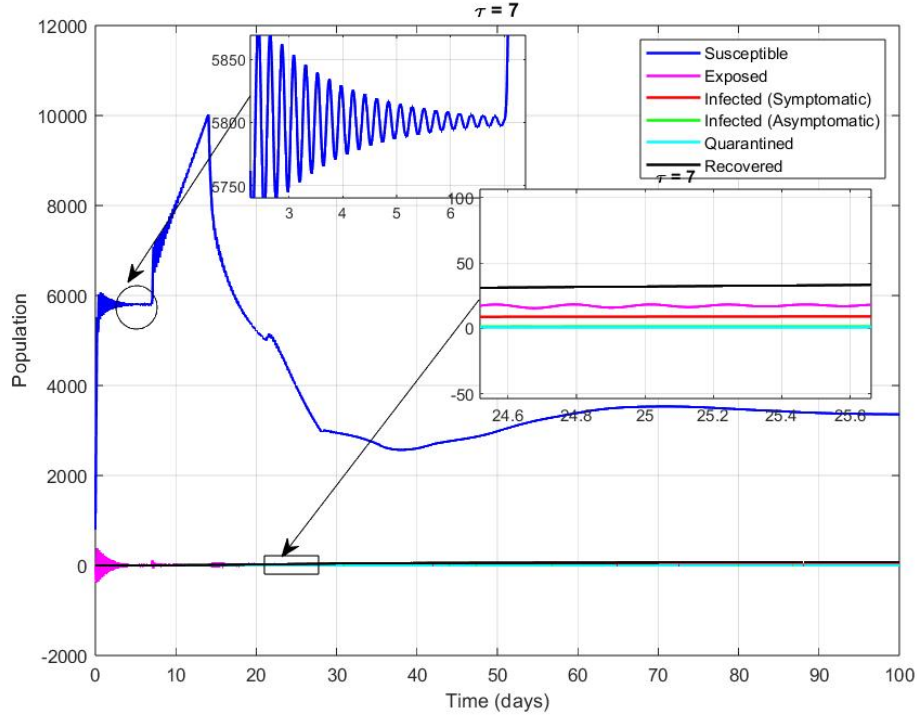
Figure 4.10: Simulation of a system showing the variation of the population with the effect of time delay on $SEII_AQR$ when $\tau = 7$

As τ increases, the number of susceptible individuals will decrease initially. This is because the infection will spread at a slower rate, and more people will move from the susceptible compartment to the exposed compartment due to the delay in transmission.

The number of exposed individuals will increase with an increase in τ. This is because the longer time delay allows more individuals to stay in the exposed compartment before becoming infectious. As a result, the compartment of exposed individuals will grow larger.

The number of symptomatic infected individuals will decrease with an increase in τ. This is because there is a longer period for the infection to spread before individuals become symptomatic and move from the exposed compartment to the infected compartment. With a longer time delay in transmission, more individuals will move from the Exposed compartment to the Asymptomatic Infection compartment instead of becoming symptomatic and moving to the Symptomatic Infected compartment immediately.

The number of people in the Quarantined compartment is likely to initially rise as the time delay *tau* increases. This is because those in the quarantined compartment are those who have been exposed to the virus but are not yet infectious because of the quarantine and the prolonged transmission delay. Instead, they shift from the exposed compartment to the quarantined compartment.

The number of recovered individuals will increase with an increase in τ. This is because the longer time delay allows more individuals to recover before becoming symptomatic and subsequently being quarantined or isolated.

In the initial phase, we see oscillatory behaviour, which arises due to the impact of precautionary measures like social distancing, self-isolation, and personal hygiene. These measures slow down the transmission of the disease, resulting in a longer time before an exposed individual becomes infected. As a result, the dynamics of the disease undergo oscillations, with periods of increasing and decreasing exposed individuals. Due to its influence on the effectiveness of disease control strategies. Our finding can help in setting the timing of control measures, as implementing interventions during periods of high transmission may have a more significant impact on disease control. It is possible to better prepare for and respond to outbreaks by anticipating their time and intensity.

From Figure 4.11 we also see large oscillatory behaviour this is due to the high intensity of transmission as we increase β. Oscillations can lead to fluctuations in the number of infectious individuals over time. Figure 4.12 shows the effect of variations in Transmission Rate β on $SEII_AR$ Model Dynamic.
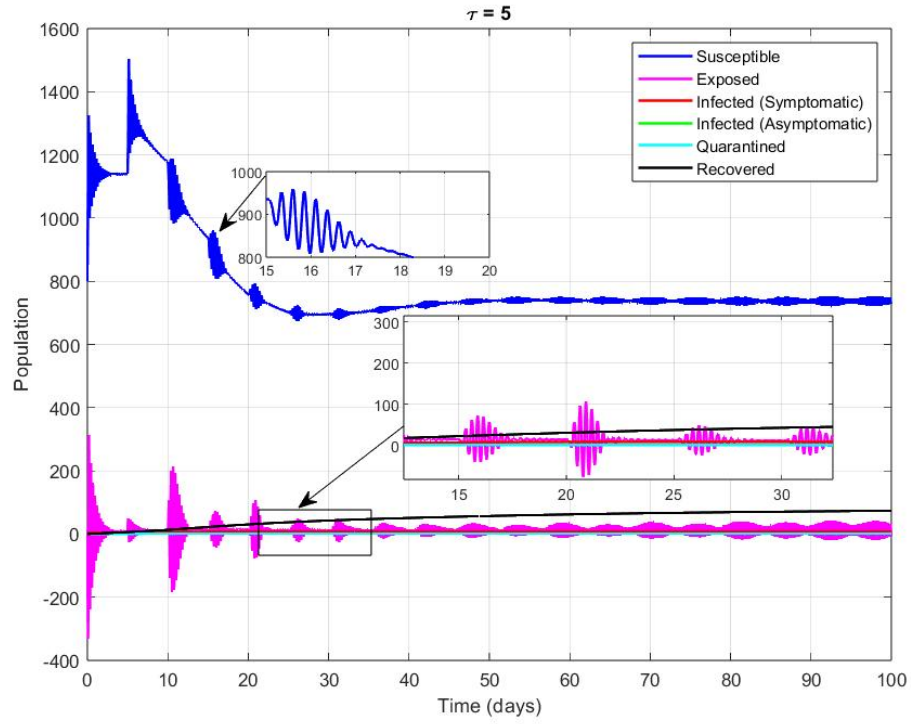
Figure 4.11: Variation of $SEII_AQR$ with effect of time delay when $\tau = 5$ and higher values of β
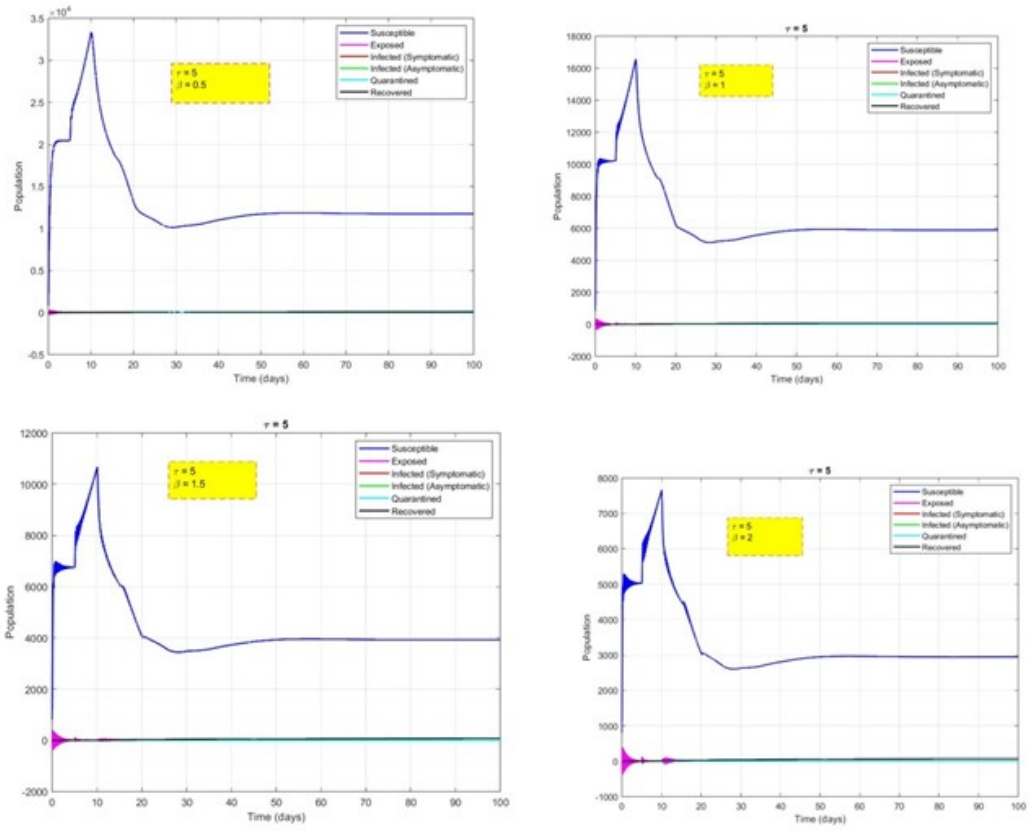
Figure 4.12: Effect of Variations in Transmission Rate β on $SEII_AQR$ Model Dynamics

4.10   Conclusion

In order to curb the COVID-19 disease's rapid spread, a number of preventative measures have been developed because the virus has irreparably affected society as a whole. Lockdowns, social exclusion, and other therapies have all proved effective, but they also hinder the coronavirus's capacity to propagate. It is crucial to appreciate the implications of these delays in order to create efficient pandemic response tactics. In this study, mathematical modelling is investigated, and delay differential equations (DDEs) are used to look into how delays caused by preventative measures affect the dynamics of COVID-19.

We have developed a deterministic compartmental model, denoted as $SEII_AQR$, to characterize the mechanism of disease transmission. The total human population,

denoted as N, is divided into six compartments: Susceptible (S), Exposed (E), Symptomatic Infection (I), Asymptomatic Infection (I_A), Quarantine (Q), and individuals who have either recovered from or succumbed to COVID-19 (R). In light of various precautionary measures, such as social distancing, self-isolation, personal hygiene, mask-wearing, and media awareness, we consider the presence of a delay in the time taken for susceptible individuals to be exposed and potentially infected. To account for this delay caused by precautionary measures, we introduce the parameter τ, representing the extent of the delay in susceptibility to exposure and infection. In other words, τ captures the time lag in disease transmission from infected to susceptible individuals due to the implementation of preventive interventions.

First, we analyze the Dynamics of a non-delayed system 4.1, we explored the presence and stability of two critical points in the model: the Disease-Free Equilibrium (DFE) and the Endemic Equilibrium (EE). Through stability analysis, we determined that the DFE is locally asymptotically stable when the basic reproduction number, denoted as R_0, is less than 1, and it becomes globally asymptotically stable under the same condition that is if $R_0 < 1$. On the other hand, the EE is locally asymptotically stable when R_0 is greater than 1.

Next we Dynamic with delay 4.2, for $\tau > 0$, we derive the expression for Disease-Free Equilibrium (DFE) and the Endemic Equilibrium (EE). We provide stability criteria for both the Disease-Free Equilibrium (DFE) and the Endemic Equilibrium (EE). For $R_0 < 1$, the DFE of the system (4.2) is locally asymptotically stable when the condition in (C2) is satisfied and $\tau > 0$. Conversely, the DFE is unstable for $R_0 > 1$.

Moreover, for E_1, an endemic equilibrium point of the system (4.2), it will be locally asymptotically stable with $\tau > 0$, subject to two conditions being met for each of the seven Hurwitz matrices (H_n) as defined in (4.11). The first condition requires the determinant of the matrix, represented as $|H_n|$, to be greater than zero $(|H_n| > 0)$. The second condition demands that the basic reproduction number, R_0, must be greater than 1 $(R_0 > 1)$. Failure to satisfy these criteria renders the EE unstable. These findings offer crucial insights into the stability properties of both equilibrium points, contributing to a deeper understanding of disease dynamics, especially considering time delays.

We also investigate the impact of various parameters on the basic reproduction number, denoted as R_0, through sensitivity analysis. By examining how changes in

these parameters affect R_0, we aim to identify key variables that significantly influence the transmission of COVID-19 and should be targeted for intervention measures. The forward sensitivity index, denoted as $\alpha_\phi^{R_0}$, is utilized to quantify the proportional change in R_0 with respect to specific parameters, including Λ, β, μ, γ, θ, α, ϵ, P_1, and P_2. The sensitivity indices reveal whether a parameter has a positive or negative relationship with R_0, indicating whether an increase or decrease in the parameter will lead to a corresponding increase or decrease in R_0. Among the parameters with positive indices, β, the rate of disease transmission, and Λ, the birth rate, are the most sensitive to R_0, suggesting that managing disease transmission and limiting contact rates through measures like quarantine and social distancing are crucial in controlling COVID-19. Conversely, parameters with negative indices, such as μ, the death rate, indicate an inverse relationship with R_0, suggesting that increasing intervention measures can lead to a decrease in R_0 and the infected population. Contour plots illustrate the relationship between parameters β and μ and their corresponding values of R_0, highlighting how R_0 varies with changes in these specific parameters and the potential impact on disease transmission. Understanding these dependencies empowers the implementation of targeted interventions aimed at reducing R_0, thus effectively controlling the spread of COVID-19.

In our numerical simulation of the proposed SEIIAQR model using MATLAB, we analyzed the impact of time delay τ and illustrated the findings with Figures 4.5,4.6,4.7,4.8,4.9 and 4.10. As τ increases, there is a longer delay between exposure and infection, caused by precautionary measures. The number of susceptible individuals initially decreases due to slower transmission, while the number of exposed individuals increases with more time for incubation. Symptomatic infected individuals decrease with increased τ, as the infection takes longer to develop symptoms.

Moreover, the number of asymptomatic infected individuals rises due to the longer time delay in transmission, and more exposed individuals move to the asymptomatic compartment. The number of people in quarantine initially increases due to prolonged transmission delay, shifting from the exposed compartment. Additionally, the number of recovered individuals increases, as they have more time to recover before becoming symptomatic.

The model exhibits oscillatory behaviour during the initial phase, influenced by precautionary measures, leading to varying numbers of exposed individuals. Understanding the effects of τ helps in setting optimal timing for control measures to combat

disease transmission effectively. Anticipating outbreak timing and intensity aids in better preparation and response.

Chapter 5

Optimizing SARS-CoV-2 Control Measures: Innovative Reaction-Diffusion Techniques

5.1 Introduction

The COVID-19 pandemic, which emerged in late 2019, has significantly impacted global health, economies, and daily life (H. Lu *et al.*, 2020). After nearly three years, many of the stringent precautionary measures and lockdowns have been lifted, allowing people to resume their regular activities. However, the disease remains a persistent threat due to its ability to spread silently and asymptomatically (Hufnagel *et al.*, 2004). This ongoing risk underscores the need for continued analysis and understanding of COVID-19's transmission dynamics, particularly in how it propagates through time and space.

Understanding how COVID-19 spreads is critical for establishing effective mitigation techniques. Mathematical modelling has emerged as an important tool in this pursuit, providing insights into disease transmission dynamics and directing public health measures. These models assist in predicting the course of the pandemic under various scenarios, assessing the possible impact of control efforts, and guiding resource allocation.

Kermack and McKendrick's groundbreaking work established the basis for utilizing mathematical models to understand the dynamics of infectious diseases (Kermack and McKendrick, 1927). In the context of COVID-19, various mathematical models have been formulated to analyze transmission dynamics in India. Researchers have extended classical models such as SI (Duan *et al.*, 2019), SIS (Y. Xie *et al.*, 2020), and SIR (Sene, 2020) by adding compartments to represent asymptomatic cases, isolated individuals, quarantine measures, protective actions, deaths, lockdowns, hospitalizations, and more (Bajiya *et al.*, 2020; Gupta *et al.*, 2021; Khajanchi and Sarkar, 2020; Mahajan *et al.*, 2020; Ray *et al.*, 2020; Senapati *et al.*, 2021; Tiwari *et al.*, 2020). Cooper et al. (Cooper *et al.*, 2020) analyzed a variant of the well-known susceptible-infected-removed (SIR) model, which does not assume a constant total population and allows the number of susceptible individuals to fluctuate non-monotonically. This innovative SIR model is valuable for assessing the disease's impact due to its predictive capability for COVID-19 spread. Zhou et al. (Zhou *et al.*, 2020) were among the first to apply the SEIR model to estimate epidemiological parameters of the novel Wuhan coronavirus. To estimate the intensity of events and track the virus's dynamic reproduction number simultaneously, Chiang et al. (Chiang *et al.*, 2022) proposed a method combining the Hawkes process with the SEIR model. This approach calculates the infected populations essential for the Hawkes process and considers nonlinear feedback between susceptible and infected populations (Franco, 2020). For the SEIRD model, the feedback phenomena between exposed and infected populations were detailed in (Loli Piccolomini and Zama, 2020). The SEIRD model is particularly akin to a dynamic model for a batch reactor performing an autocatalytic reaction with catalyst deactivation, drawing an analogy between disease transmission and chemical reaction in epidemic and chemical kinetic modelling (Simon, 2020). Hazarika and Gupta (Hazarika and Gupta, 2020) presented a model for forecasting COVID-19 spread using wavelet-coupled random vector functional link networks. Reiner et al. ("Modeling COVID-19 scenarios for the United States", 2021) utilized the SEIR model for scenario analysis in the United States. Xie (G. Xie, 2020) developed a model based on Monte Carlo simulation for COVID-19 spread, with the key feature being the number of infected individuals modelled by a Poisson distribution with the parameter Rt, which could vary across different observation stages.

The COVID-19 pandemic exhibits complex dynamics due to factors like human behaviour, mobility patterns, and varying population densities. This could be mod-

elled using reaction-diffusion model where the infection spreads over space and time, taking into account the movement of individuals and the local interaction rates. As Spatial heterogeneity acknowledges that the population is not uniformly mixed and that the distribution and interactions of individuals vary across different locations.

5.2 Model Formulation

We develop a deterministic compartmental model, denoted as $SEII_AHR$, to describe the mechanism of disease transmission. Let N represent the total human population. This population is divided into six compartments: Susceptible (S), Exposed (E), Symptomatic Infection (I), Asymptomatic Infection (I_A), Hospitalized (H), and those who have either recovered or died from COVID-19 (R). Additionally, we incorporate vital dynamics: the natural human birth rate, denoted by Λ, and the mortality rate, denoted by μ.

Susceptible individuals move to the Exposed compartment upon contact with either Symptomatic (I) or Asymptomatic (I_A) individuals at a transmission rate β.

Our model is adapted to include various intervention techniques. Preventive measures such as lockdowns, media campaigns for awareness, effective hand-washing, social distancing, and mask usage are part of the intervention strategies aimed at slowing disease spread.

The application of these interventions suggests a reduction in the disease transmission rate as reflected in the model parameters. The strength of the intervention, denoted by ψ where $\psi \in [0, 1]$, is considered to decrease the transmission rate. A value of $\psi = 0$ indicates no intervention, while $\psi = 1$ signifies strong intervention.

When interventions are implemented, the parameter β is modified to $(1 - \psi)\beta$. Exposed individuals move to the I, I_A, and H compartments at a rate γ. A fraction of the population transitions from Exposed to Symptomatic at a rate P_1, to Asymptomatic at a rate P_2, and to Hospitalized at a rate P_3.

The term $(1 + b)\sigma H$ indicates that individuals who are hospitalized will recover more quickly and move to the Recovered compartment due to medical treatment. Symptomatic and Asymptomatic individuals recover at rates α and η, respectively. Each compartment may decrease due to natural mortality μ, with the Symptomatic compartment additionally decreasing due to COVID-19-related mortality at a rate θ.

Based on these assumptions, we propose the following model, represented as a system of non-linear differential equations. The schematic diagram is shown in the figure (5.1).
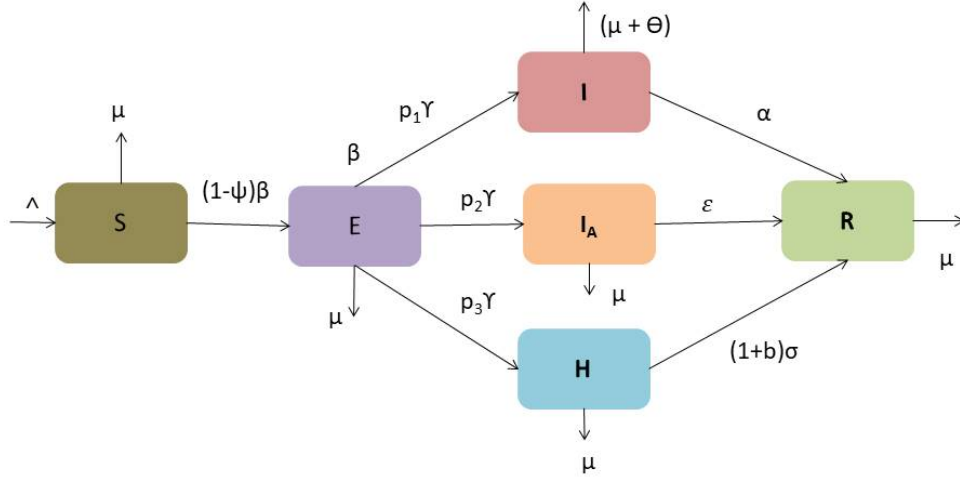
Figure 5.1: Schematic Diagram of $SEII_AHR$

$$\frac{dS}{dt} = \Lambda - (1 - \psi)\beta S(I + I_A) - \mu S,$$

$$\frac{dE}{dt} = (1 - \psi)\beta S(I + I_A) - \gamma E - \mu E,$$

$$\frac{dI}{dt} = p_1\gamma E - (\mu + \theta)I - \alpha I, \tag{5.1}$$

$$\frac{dI_A}{dt} = p_2\gamma E - \epsilon I_A - \mu I_A,$$

$$\frac{dH}{dt} = p_3\gamma E - [(1 + b)\sigma + \mu]H$$

$$\frac{dR}{dt} = \alpha I + \epsilon I_A + [(1 + b)\sigma + \mu]H - \mu R,$$

with nonnegative initial conditions given by

$$S(0) > 0, \ E(0) > 0, \ I(0) > 0, \ I_A > 0, \ H(0) > 0, \ R(0) > 0.$$

All the parameters of the system 5.1 are assumed to be positive for all time $t > 0$.

5.3   Dynamic with Reaction-Diffusion.

The COVID-19 pandemic exhibits complex dynamics due to factors like human behaviour, mobility patterns, and varying population densities. Reaction-diffusion models are well-suited to capture these complexities, providing a more accurate representation of how the virus spreads and evolves over time.

Reaction-diffusion models incorporate both the reaction i.e., local interactions and dynamics of population and diffusion, spatial movement and spread of the Individuals. This dual approach helps in understanding how COVID-19 spreads across different regions over time, providing a spatial-temporal view of the pandemic. Using Eq(5.1) a Reaction-Diffusion model is given as follow

$$\frac{\partial S(x,t)}{\partial t} = D_1 \Delta S + \Lambda - (1-\psi)\beta S(I + I_A) - \mu S, \ x \in \Omega, t > 0$$

$$\frac{\partial E(x,t)}{\partial t} = D_2 \Delta E + (1-\psi)\beta S(I + I_A) - \gamma E - \mu E, \ x \in \Omega, t > 0$$

$$\frac{\partial I(x,t)}{\partial t} = D_3 \Delta I + p_1 \gamma E - (\mu + \theta + \alpha)I, \ x \in \Omega, t > 0 \quad (5.2)$$

$$\frac{\partial I_A(x,t)}{\partial t} = D_4 \Delta I_A + p_2 \gamma E - \epsilon I_A - \mu I_A, \ x \in \Omega, t > 0$$

$$\frac{\partial H(x,t)}{\partial t} = D_5 \Delta H + p_3 \gamma E - [(1+b)\sigma + \mu]H, \ x \in \Omega, t > 0$$

$$\frac{\partial R(x,t)}{\partial t} = D_6 \Delta R + \alpha I + \epsilon I_A + [(1+b)\sigma + \mu]H - \mu R, \ x \in \Omega, t > 0$$

with

$$(S(x,0), E(x,0), I(x,0), I_A(x,0), H(x,0), R(x,0)) = (\zeta_1(x), \zeta_2(x), \zeta_3(x), \zeta_4(x), \zeta_5(x), \zeta_6(x))$$

for $x \in \Omega$ and also satisfy

$$\frac{\partial S}{\partial n} = \frac{\partial E}{\partial n} = \frac{\partial I}{\partial n} = \frac{\partial I_A}{\partial n} = \frac{\partial H}{\partial n} = \frac{\partial R}{\partial n} = 0, \ \ x \in \partial\Omega, t > 0$$

The variables $(S(x,0), E(x,0), I(x,0), I_A(x,0), H(x,0), R(x,0))$ denote the densities of individuals within each compartment at time t and location x. Here, Δ represents the Laplace operator, and D_i (for $i = 1, 2, \ldots, 6$) corresponds to the respective diffusion coefficients. We assume that $D_1 = D_2 = D_3 = D_4 = D_5 = D_6 = D$.

Table 5.1: Parameter Description for $SEII_AHR$

Parameter	Description	Values
Λ	Birth rate	$52000\ year^{-1}$
μ	Death rate	$0.0245\ year^{-1}$
β	Rate of transmission	$1.7399 day^{-1}$
γ	Rate of transition from Exposed to I, I_A, and Q	$0.1923\ day^{-1}$
p_1	Fraction of population moves from Exposed to symptomatic class	0.3362
p_2	Fraction of population moves from Exposed to asymptomatic class	0.4204
p_3	Fraction of population moves from Exposed to quarantine class	0.2434
α	Recovery rate of symptomatic infected class	$0.07\ day^{-1}$
ϵ	Recovery rate of asymptomatic infection	$0.9\ day^{-1}$
σ	Recovery rate of quarantine class	$0.9\ day^{-1}$
θ	Rate of disease-induced death	$0.0001\ day^{-1}$

5.4 Dynamic behaviour of $SEII_AHR$ model with Reaction-Diffusion

We observe that the first five equations in system 5.2 are independent of $R(x,t)$. The resulting reduced system is as follows:

$$\frac{\partial S(x,t)}{\partial t} = D_1\Delta S + \Lambda - (1-\psi)\beta S(I + I_A) - \mu S,\ x \in \Omega, t > 0$$

$$\frac{\partial E(x,t)}{\partial t} = D_2\Delta E + (1-\psi)\beta S(I + I_A) - \gamma E - \mu E,\ x \in \Omega, t > 0$$

$$\frac{\partial I(x,t)}{\partial t} = D_3\Delta I + p_1\gamma E - (\mu + \theta + \alpha)I,\ x \in \Omega, t > 0 \qquad (5.3)$$

$$\frac{\partial I_A(x,t)}{\partial t} = D_4\Delta I_A + p_2\gamma E - \epsilon I_A - \mu I_A,\ x \in \Omega, t > 0$$

$$\frac{\partial H(x,t)}{\partial t} = D_5\Delta H + p_3\gamma E - [(1+b)\sigma + \mu]H,\ x \in \Omega, t > 0$$

with

$$(S(x,0), E(x,0), I(x,0), I_A(x,0), H(x,0)) = (\zeta_1(x), \zeta_2(x), \zeta_3(x), \zeta_4(x), \zeta_5(x))\ for\ x\ in\Omega \qquad (5.4)$$

and satisfy

$$\frac{\partial S}{\partial n} = \frac{\partial E}{\partial n} = \frac{\partial I}{\partial n} = \frac{\partial I_A}{\partial n} = \frac{\partial H}{\partial n} = \frac{\partial R}{\partial n} = 0,\ \ x \in \partial\Omega, t > 0 \qquad (5.5)$$

5.5 Positivity and boundedness

We assume that $D_1 = D_2 = D_3 = D_4 = D_5 = D_6 = D$ and demonstrate the existence and uniqueness of the solution.

Let $X := C(\overline{\Omega}, \mathbb{R}^5)$ be a Banach space equipped with the supremum norm $\|\cdot\|_{\mathbb{X}}$. Define $\mathbb{X}^+ := C(\overline{\Omega}, \mathbb{R}^5_+)$, making $(\mathbb{X}, \mathbb{X}^+)$ a strongly ordered space. Suppose that $\mathbb{T}_1(x)$, $\mathbb{T}_2(x)$, $\mathbb{T}_3(x)$, $\mathbb{T}_4(x)$, $\mathbb{T}_5(x) : C(\overline{\Omega}, \mathbb{R}) \to C(\overline{\Omega}, \mathbb{R})$ are the C_0 semigroups related to $D\Delta - \mu$, $D\Delta - (\gamma + \mu)$, $D\Delta - (\alpha + \theta + \mu)$, $D\Delta - (\epsilon + \mu)$ and $D\Delta - [(1+b)\sigma + \mu]$ dependent on Eq.(5.5) , respectively. It is evident that for every $\phi \in C(\overline{\Omega}, \mathbb{R})$ and $t \geq 0$, we have:

$$\mathbb{T}_1(t)\zeta(x) = e^{-\mu t} \int_\Omega \zeta(s)\Gamma_1(x, t, s)ds,$$

$$\mathbb{T}_2(t)\zeta(x) = e^{-(\gamma+\mu)t} \int_\Omega \zeta(s)\Gamma_1(x, t, s)ds,$$

$$\mathbb{T}_3(t)\zeta(x) = e^{-(\alpha+\theta+\mu)t} \int_\Omega \zeta(s)\Gamma_1(x, t, s)ds,$$

$$\mathbb{T}_4(t)\zeta(x) = e^{-(\epsilon+\mu)t} \int_\Omega \zeta(s)\Gamma_1(x, t, s)ds,$$

$$\mathbb{T}_5(t)\zeta(x) = e^{-[(1+b)\sigma+\mu]t} \int_\Omega \zeta(s)\Gamma_1(x, t, s)ds.$$

where Γ_1 represent the Green functions related to $D\Delta$ depend on Eq. (5.5).
From Martin an Smith (Martin and Smith, 1990) We obtain that $\mathbb{T}_i(t) : C(\overline{\Omega}, \mathbb{R}) \to C(\overline{\Omega}, \mathbb{R})$ $(i = 1, 2, 3, 4, 5)$ stands for strongly positive and compact. For all initial values $\zeta \in \mathbb{X}^+$ and $\mathbb{X} \in \overline{\Omega}$, let $\mathfrak{F} = (\mathcal{F}_1, \mathcal{F}_2, \mathcal{F}_3, \mathcal{F}_4, \mathcal{F}_5)$ be defined as $\mathfrak{F} : \mathbb{X}^+ \to \mathbb{X}$ given by:

$$\mathcal{F}_1(\zeta)(x) = \Lambda - (1 - \psi)\beta\zeta_1(x, 0)[\zeta_3(x, 0) + \zeta_4(x, 0)]$$

$$\mathcal{F}_2(\zeta)(x) = (1 - \psi)\beta\zeta_1(x, 0)[\zeta_3(x, 0) + \zeta_4(x, 0)]$$

$$\mathcal{F}_3(\zeta)(x) = p_1\gamma\zeta_2(x, 0)$$

$$\mathcal{F}_4(\zeta)(x) = p_1\gamma\zeta_2(x, 0)$$

$$\mathcal{F}_5(\zeta)(x) = p_3\gamma\zeta_2(x, 0)$$

Hence equation 5.4-5.5 can be written as

$$\mathbb{Y}(x, t) = \mathbb{T}(t)\zeta(x) + \int_0^t \mathbb{T}(t - s)\mathcal{F}(\mathbb{Y}(x, s)) \, ds,$$

where

$$\mathbb{T}(t) = \mathrm{diag}(\mathbb{T}_1(t), \mathbb{T}_2(t), \mathbb{T}_3(t), \mathbb{T}_4(t), \mathbb{T}_5(t))$$

and

$$\mathbb{Y}(x,t) = (S(x,t), E(x,t), I(x,t), I_A(x,t), H(x,t), R(x,t))$$

. Then, we get the following result.

Theorem 5.1. *For any* $\phi \in \mathbb{X}^+$, *the reaction-diffusion system Eq. (5.4) – (5.5) possesses a unique solution* $\mathbb{Y}(\cdot, t, \phi)$ *with the initial condition* $\mathbb{Y}(\cdot, 0, \phi) = \phi$. *Moreover, the mapping* $\psi(t) : \mathbb{X}^+ \to \mathbb{X}^+$, *defined by* $\psi(t)\phi = (S(\cdot, t, \phi), E(\cdot, t, \phi), I(\cdot, t, \phi), I_A(\cdot, t, \phi), H(\cdot, t, \phi))$ *for all* $x \in \mathbb{X}$ *and* $t \geq 0$, *is point dissipative.*

Proof. For every $\zeta \in \mathbb{X}^+$ and $h > 0$, one has

$$\lim_{h \to 0^+} \frac{1}{h} \operatorname{dist}(hF(\zeta) + \zeta(0), \mathbb{X}^+) = 0$$

. According to Corollary 4 from (Martin and Smith, 1990), $\mathbb{Y}(\cdot, t, \zeta)$ represents a unique mild solution of Eqs. (5.4) - (5.5) on $[0, \tau_\zeta)$, with $\mathbb{Y}(\cdot, 0, \zeta)$ and $\mathbb{Y}(\cdot, t, \zeta) \in \mathbb{X}^+$, where $t_\zeta \leq +\infty$. We then prove that the solution is global. From the system of equation Eq. (5.4) considering the first three equations, we have

$$\frac{\partial}{\partial t}(S(x,t) + E(x,t) + I(x,t) + I_A(x,t) + H(x,t)) = D\Delta(S + E + I + I_A + H) +$$
$$\Lambda - \mu(S + E + I + I_A + H) - \theta I$$
$$- \alpha I - \epsilon I_A - (1+b)\sigma H$$
$$\leq D\Delta(S + E + I + I_A + H) + \Lambda$$
$$- \mu(S + E + I + I_A + H).$$

By comparison principle, for a very small positive number ε there exists $t^* > 0$, $\forall$ $t \geq t^*$, such that $S(x,t) + E(x,t) + I(x,t) + I_A(x,t) + H(x,t) \leq \frac{\Lambda}{\mu} + \varepsilon$, uniformly $\forall$ $x \in \Omega$.

Hence, $S(\cdot, t) \leq \frac{\Lambda}{\mu} + \varepsilon$, $E(\cdot, t) \leq \frac{\Lambda}{\mu} + \varepsilon$, $I(\cdot, t) \leq \frac{\Lambda}{\mu} + \varepsilon$, $I_A(\cdot, t) \leq \frac{\Lambda}{\mu} + \varepsilon$ and $H(\cdot, t) \leq \frac{\Lambda}{\mu} + \varepsilon$.

This indicates that S, E, I, I_A, and H are uniformly bounded. Consequently, $\psi(t) : \mathbb{X}^+ \to \mathbb{X}^+$ is point dissipative. $\qquad \square$

5.6   Basic Reproduction Number R_0

System 5.4 always has Disease Free Equilibrium $E_0(S_0, 0, 0, 0, 0)$ where $S_0 = \frac{\Lambda}{\mu}$ and there exist Endemic Equilibrium $E_1(S^*, E^*, I^*, I_A^*, H^*)$ given by

$$
\begin{aligned}
0 &= \Lambda - (1 - \psi)\beta S^*(I^* + I_A^*) - \mu S^* \\
0 &= (1 - \psi)\beta S^*(I^* + I_A^*) - \gamma E^* - \mu E^* \\
0 &= p_1 \gamma E^* - (\alpha + \theta)I^* - \mu I^* \\
0 &= p_2 \gamma E^* - \epsilon I_A^* - \mu I_A^* \\
0 &= p_3 \gamma E^* - [(1 + b)\sigma + \mu]H^*
\end{aligned}
\tag{5.6}
$$

which gives

$$
\begin{aligned}
S^* &= \frac{\Lambda - (\gamma + \mu E^*)}{\mu} \\
I^* &= \frac{p_1 \gamma E^*}{\alpha + \theta + \mu} \\
I_A^* &= \frac{p_2 \gamma E^*}{\epsilon + \mu} \\
H^* &= \frac{p_3 \gamma E^*}{(1 + b)\sigma + \mu}
\end{aligned}
\tag{5.7}
$$

Furthermore, according to the theory in (W. Wang and Zhao, 2012)

$$
\frac{\partial P_i}{\partial t} = D_i \Delta P_i + \mathcal{F}_i(x, P) - \mathcal{V}_i(x, P), \quad i = 1, 2, 3, 4, 5.
$$

where $P = (E, I, I_A, H, S)^T$.

System (5.4)-(5.5) can be written as

$$
\begin{aligned}
\frac{\partial E(x,t)}{\partial t} &= D_2 \Delta E + (1 - \psi)\beta S(I + I_A) - \gamma E - \mu E, \; x \in \Omega, t > 0 \\
\frac{\partial I(x,t)}{\partial t} &= D_3 \Delta I + p_1 \gamma E - (\mu + \theta + \alpha)I, \; x \in \Omega, t > 0 \\
\frac{\partial I_A(x,t)}{\partial t} &= D_4 \Delta I_A + p_2 \gamma E - \epsilon I_A - \mu I_A, \; x \in \Omega, t > 0 \\
\frac{\partial H(x,t)}{\partial t} &= D_5 \Delta H + p_3 \gamma E - [(1 + b)\sigma + \mu]H, \; x \in \Omega, t > 0 \\
\frac{\partial S(x,t)}{\partial t} &= D_1 \Delta S + \Lambda - (1 - \psi)\beta S(I + I_A) - \mu S, \; x \in \Omega, t > 0
\end{aligned}
\tag{5.8}
$$

$$
\frac{\partial E}{\partial n} = \frac{\partial I}{\partial n} = \frac{\partial I_A}{\partial n} = \frac{\partial H}{\partial n} = \frac{\partial S}{\partial n} = 0, \quad x \in \partial\Omega, t > 0
\tag{5.9}
$$

$$(E(x,0), I(x,0), I_A(x,0), H(x,0), S(x,0)) = (\zeta_2(x), \zeta_3(x), \zeta_4(x), \zeta_5(x), \zeta_1(x)) \; for \; x \in \Omega$$
(5.10)

Therefore we get $\mathcal{F}_i(x, \overline{E_0(0)}) = \begin{bmatrix} (1-\psi)\beta S(I + I_A) \\ 0 \\ 0 \\ 0 \\ 0 \end{bmatrix}$ and

$$\mathcal{V}_i(x, \overline{E_0(0)}) = \begin{bmatrix} (\gamma + \mu)E - D_2\Delta E \\ (\mu + \theta + \alpha)I - p_1\gamma E - D_3\Delta I \\ (\eta + \mu)I_A - p_2\gamma E - D_4\Delta I_A \\ ((1+b)\sigma + \mu)H - p_3\gamma E - D_5\Delta H \\ \beta S(I + I_A) + \mu S - \Lambda - D_1\Delta S \end{bmatrix}$$

$F(x)$, $V(X)$ denoted as

$$F(x) = \left.\frac{\partial \mathcal{F}_i(x, \overline{E_0(x)})}{\partial u_j}\right|_{1 \le i,j \le 4}$$

and

$$V(x) = \left.\frac{\partial \mathcal{V}_i(x, \overline{E_0(x)})}{\partial u_j}\right|_{1 \le i,j \le 3},$$

respectively, where $E_0(x) = (0, 0, 0, 0, S_0)$.
Thus,

$$F(x) = \begin{bmatrix} 0 & (1-\psi)\beta S_0 & (1-\psi)\beta S_0 & 0 \\ 0 & 0 & 0 & 0 \\ 0 & 0 & 0 & 0 \\ 0 & 0 & 0 & 0 \end{bmatrix}$$

and

$$V(x) = \begin{bmatrix} \gamma + \mu - k^2\Delta_2 & 0 & 0 & 0 \\ -p_1\gamma & (\mu + \theta + \alpha) - k^2\Delta_3 & 0 & 0 \\ -p_2\gamma & 0 & \epsilon + \mu - k^2\Delta_4 & 0 \\ -p_3\gamma & 0 & 0 & [(1+b)\sigma + \mu] - k^2\Delta_5 \end{bmatrix}$$

where k is the wave number. $F(x)$ denotes a 4×4 continuous and nonnegative matrix function, while $-V(x)$ represents a 4×4 continuous and cooperative matrix function. According to (W. Wang and Zhao, 2012), the distribution of the total new infections is defined as

$$\int_0^\infty F(x)\mathcal{T}(t)\zeta(x)\,dt,$$

Further, we define

$$[\mathcal{L}(\zeta)](x) = \int_0^\infty F(x)[\mathcal{T}(t)\zeta](x)dt$$

$$= F(x)\int_0^\infty [\mathcal{T}(t)\zeta](x)dt,$$

where $\mathcal{L}$ denotes a positive and continuous operator that maps the initial infection distribution $\zeta(x)$ to the total number of infected individuals produced during the infection period. By the next-generation matrix method, we have

$$R_0 = \frac{(1-\psi)\beta\gamma\Lambda P_1}{\mu(\mu+\gamma)(\alpha+\theta+\mu)} + \frac{(1-\psi)\beta\gamma\Lambda P_2}{\mu(\mu+\epsilon)(\mu+\gamma)}$$

5.7   Uniqueness of DFE and EE

Theorem 5.2. *For $R_0 < 1$, the reaction-diffusion system Eq. (5.4) has only $E_0(S_0, 0, 0, 0)$; whereas for $R_0 > 1$, there exist a unique $E_1(S^*, E^*, I^*, I_A^*, H^*)$, where*

$$S^* = \frac{\Lambda - (\gamma + \mu E^*)}{\mu}$$
$$I^* = \frac{p_1\gamma E^*}{\alpha + \theta + \mu}$$
$$I_A^* = \frac{p_2\gamma E^*}{\epsilon + \mu} \tag{5.11}$$
$$H^* = \frac{p_3\gamma E^*}{(1+b)\sigma + \mu}$$

Proof. Clearly E_0 is unique when $R_0 < 1$. Therefore, we need to prove only for $R_0 > 1$. From Eq. (5.6) we know that

$$S = `\frac{\Lambda - (\gamma + \mu E)}{\mu}, \ I = \frac{p_1\gamma E}{\alpha + \theta + \mu}$$

$$I_A = \frac{p_2\gamma E}{\epsilon + \mu}, \ H = \frac{p_3\gamma E}{(1+b)\sigma + \mu}$$

From second equation of eq(5.6), we have

$$J(E) = (1-\psi)\beta\left(\frac{\Lambda - (\gamma + \mu)E}{\mu}\right)\left[\frac{p_1\gamma E}{\mu + \theta + \alpha} + \frac{p_2\gamma E}{\epsilon + \mu}\right] - (\gamma + \mu)E$$

Since $J(0) = 0$, adding the first two equation of eq(5.6), we have

$$J\left(\frac{\Lambda}{\mu}\right) = -(\gamma + \mu)E = -\Lambda < 0$$

$$
\begin{aligned}
J^{'}(0) &= \frac{(1 - \psi)\beta\gamma\Lambda P_1(\gamma + \mu)}{\mu(\mu + \gamma)(\alpha + \theta + \mu)} + \frac{(1 - \psi)\beta\gamma\Lambda P_2(\gamma + \mu)}{\mu(\mu + \epsilon)(\mu + \gamma)} - (\gamma + \mu) \\
&= \left[\frac{(1 - \psi)\beta\gamma\Lambda P_1}{\mu(\mu + \gamma)(\alpha + \theta + \mu)} + \frac{(1 - \psi)\beta\gamma\Lambda P_2}{\mu(\mu + \epsilon)(\mu + \gamma)} - 1\right](\gamma + \mu) \\
&= (R_0 - 1)(\gamma + \mu) > 0
\end{aligned}
$$

This shows that $J(E) = 0$ exists at least one positive root $E^* \in \left(0, \frac{\Lambda}{\mu}\right)$, this implies that the positive equilibrium of Eq. (5.4) exists. Next, we shall prove E^* is unique. Based on Eq. (5.7) and the following facts

$$(1 - \psi)\beta S^*(I^* + I_A^*) = \gamma E^* + \mu E^* \tag{5.12}$$

we also have $E, I, I_A, H \geq 0$. Therefore, it follows from the above equation

$$J^{'}(E) = (1 - \psi)\beta\left(\frac{\Lambda - (\gamma + \mu)E^*}{\mu}\right)\left[\frac{p_1\gamma}{\mu + \theta + \alpha} + \frac{p_2\gamma}{\epsilon + \mu}\right] - (\gamma + \mu) \tag{5.13}$$

Suppose there exists another positive equilibrium $E_1^{**}(S^{**}, E^{**}, I^{**}, I_A^{**}, H^{**})$, then we have $J^{'}(E_1^{**}) > 0$, which contradicts the inequality. $\qquad\square$

5.8   Local stability of disease-free equilibrium

Let $0 = \mu_1 < \mu_2 < \ldots < \mu_i < \ldots$ be the eigenvalues of $-\Delta$ on Ω with homogeneous Neumann boundary conditions. Let $U(\mu_i)$ denote the eigenfunction space corresponding to μ_i, and let $\{\overline{\omega}_{ij} : j = 1, 2, 3, \ldots, \dim U(\mu_i)\}$ be an orthonormal basis of $U(\mu_i)$. The space $\mathbb{Z}$ can be decomposed as follows:

$$\mathbb{Z} = \oplus_{i=1}^{\infty}\mathbb{Z}_i \quad \text{and} \quad \mathbb{Z}_i = \oplus_{i=1}^{U(\mu_i)}\mathbb{Z}_{ij}$$

,
where

$$\mathbb{Z} = \left\{(E, I, I_A, H, S) \in [C^{'}(\overline{\omega})]^4 : \frac{\partial E}{\partial n} = \frac{\partial I}{\partial n} = \frac{\partial I_A}{\partial n} = \frac{\partial H}{\partial n} = \frac{\partial S}{\partial n} = 0 \ \text{on} \ \partial\Omega\right.$$

, $\mathbb{Z}_{ij} = a\overline{\omega}_{ij} \mid a \in \mathbb{R}^5$. Then, we shall show the local stability of equilibrium as follows.

Theorem 5.3. *The Disease-Free Equilibrium (DFE) E_0 of the reaction-diffusion system described by Eq. (5.4) exhibits local asymptotic stability when $R_0 < 1$.*

Proof. Consider the linearization of the reaction-diffusion system Eq. (5.4) at E_0:

$$\frac{\partial \mathbb{Y}(x,t)}{\partial t} = \mathbb{D}\mathbb{Y}(x,t) + \mathbb{A}(E_0)\mathbb{Y}(x,t),$$

where $\mathbb{Y} = (S, E, I, I_A, H)$, $\mathbb{D} = \mathrm{diag}(D_1, D_2, D_3, D_4, D_5)$ $D_1 = D_2 = D_3 = D_4 = D_5 = D$, and

$$\mathbb{A} = \begin{bmatrix} -\mu & 0 & -(1-\psi)\beta S_0 & -(1-\psi)\beta S_0 & 0 \\ 0 & -(\gamma+\mu) & (1-\psi)\beta S_0 & (1-\psi)\beta S_0 & 0 \\ 0 & p_1\gamma & -(\mu+\theta+\alpha) & 0 & 0 \\ 0 & p_2\gamma & 0 & -(\epsilon+\mu) & 0 \\ 0 & p_3\gamma & 0 & 0 & -[(1+b)\sigma+\mu] \end{bmatrix}$$

Let $\mathcal{L}\mathbb{Y} = \mathbb{D}\mathbb{Y} + \mathbb{A}(E_0)\mathbb{Y}$, and let $\mathbb{Z}_i$ (for $i \geq 1$) be invariant under $\mathcal{L}$. An eigenvalue λ of $\mathcal{L}$ exists if and only if it is an eigenvalue of a matrix $-\mathbb{D}\mu_i + \mathbb{A}(E_0)$ with $i \geq 1$, where there is an eigenvalue in $\mathbb{Z}_i$. In other words, λ must satisfy the following characteristic equation: $\det(\lambda I + \mathbb{D}\mu_i - \mathbb{A}(E_0)) = 0$, where I represents the identity matrix. Therefore, the characteristic equation at E_0 can be specifically expressed as:

$$(\lambda + (\mu + \mu_i D))(\lambda^4 + A_1\lambda^3 + A_2\lambda^2 + A_3\lambda + A_4) = 0. \tag{5.14}$$

Clearly $\lambda_1 = -(\mu + \mu_i D)$ is an eigenvalue of eq (5.14) Therefore the remaining four eigenvalues are the roots of the following equation

$$\lambda^4 + A_1\lambda^3 + A_2\lambda^2 + A_3\lambda + A_4 = 0$$

$$A_1 = (\gamma + \mu) + (\mu + \theta + \alpha) + (\epsilon + \mu) + [(1+b)\sigma + \mu] + 4D\mu_i$$

$$A_2 = (x_1 + x_2 + x_3 + x_4 + 4D\mu_i)^2/2 - ((x_1 + D\mu_i)^2$$
$$+ (x_2 + D\mu_i)^2 + (x_3 + D\mu_i)^2 + (x_4 + D\mu_i)^2)/2$$
$$- (1 - \psi)\beta\gamma S_0(p_1 + p_2)$$

$$A_3 = (x_1 + D\mu_i)(x_2 + D\mu_i)(x_3 + D\mu_i) + (x_1 + D\mu_i)(x_2 + D\mu_i)(x_4 + D\mu_i)$$
$$+ (x_1 + D\mu_i)(x_3 + D\mu_i)(x_4 + D\mu_i) + (x_2 + D\mu_i)(x_3 + D\mu_i)(x_4 + D\mu_i)$$
$$- (1 - \psi)\beta\gamma(x_2 + D\mu_i)p_2 S_0 - (1 - \psi)\beta\gamma(x_3 + D\mu_i)p_1 S_0$$
$$- (1 - \psi)\beta\gamma(x_4 + D\mu_i)p_1 S_0 - (1 - \psi)\beta\gamma(x_4 + D\mu_i)p_2 S_0$$

$$A_4 = (x_1 + D\mu_i)(x_2 + D\mu_i)(x_3 + D\mu_i)(x_4 + D\mu_i) - (1 - \psi)\beta\gamma(x_2 + D\mu_i)(x_4 + D\mu_i)p_2 S_0$$
$$- \beta\gamma(x_3 + D\mu_i)(x_4 + D\mu_i)p_1$$

Where,

$x_1 = (\gamma + \mu)$, $x_2 = (\mu + \theta + \alpha)$, $x_3 = (\epsilon + \mu)$, $x_4 = [(1+b)\sigma + \mu]$ According to the Routh-Hurwitz criterion, the equation above will yield negative roots or roots with negative real parts if the following condition is satisfied:

$$A_1 > 0, \begin{vmatrix} A_1 & A_3 \\ 1 & A_2 \end{vmatrix} > 0, \begin{vmatrix} A_1 & A_3 & 0 \\ 1 & A_2 & A_4 \\ 0 & A_1 & A_3 \end{vmatrix} > 0$$

Hence, the disease-free equilibrium point E_0 of the system is locally asymptotically stable, when $R_0 < 1$. □

Theorem 5.4. *The Endemic Equilibrium E_1 of the reaction-diffusion system Eq. (5.4) is locally asymptotically stable if $R_0 > 1$*

Proof. Consider the linearization of the reaction-diffusion system Eq. (5.4) at E_0:

$$\frac{\partial \mathbb{Y}(x,t)}{\partial t} = \mathbb{D}\mathbb{Y}(x,t) + \mathbb{B}(E_0)\mathbb{Y}(x,t),$$

$$\mathbb{B} = \begin{bmatrix} -q & 0 & -(1-\psi)\beta S^* & -(1-\psi)\beta S^* & 0 \\ a_{21} & -r & (1-\psi)\beta S^* & (1-\psi)\beta S^* & 0 \\ 0 & p_1\gamma & -s & 0 & 0 \\ 0 & p_2\gamma & 0 & -t & 0 \\ 0 & p_3\gamma & 0 & 0 & -u \end{bmatrix}$$

where

$$q = [(1 - \psi)\beta(I^* + I_A^*) + \mu]$$
$$r = (\gamma + \mu)$$
$$s = (\mu + \theta + \alpha)$$
$$t = (\epsilon + \mu)$$
$$u = (\sigma + \mu)$$
$$a_{21} = (1 - \psi)\beta(I^* + I_A^*)$$

Similarly, λ must be a root of $\det(\lambda I + D\mu_i - \mathbb{A}(E_1)) = 0$. Therefore, we can denote the characteristic equation at E_1 as $\lambda^5 + B_4\lambda^4 + B_3\lambda^3 + B_2\lambda^2 + B_1\lambda + B_0 = 0$. where

$$B_4 = (q + r + s + t + u)$$
$$B_3 = (q + r + s + t + u)^2/2 - (q^2 + r^2 + s^2 + t^2 + u^2)/2 - \beta\gamma S^*(p_1 + p_2)$$
$$B_2 = qr(s + t + u) + (qs + rs)(t + u) + tu(q + r) + \beta\gamma S^*[(a_{21} - q - u)$$
$$(p_1 + p_2) - (sp_2 + tp_1)]$$
$$B_1 = qrs(t + u) + qtu(r + s) + rstu + \beta\gamma S^*(a_{21}s + a_{21}u - qu)(p_1 + p_2)$$
$$- \beta\gamma q S^*(sp_2 + tp_1) - \beta\gamma u S^*(sp_2 + up_1)$$
$$B_0 = qr(s + t + u) + (qs + rs)(t + u) + tu(q + r) + \beta\gamma S^*[(a_{21} - q - u)$$
$$(p_1 + p_2) - (sp_2 + tp_1)]$$

According to the Routh-Hurwitz criterion, the above equation will give negative roots or negative real parts if the following condition is satisfied:

$$B_4 > 0, \begin{vmatrix} B_4 & B_2 \\ 1 & B_3 \end{vmatrix} > 0, \begin{vmatrix} B_4 & c_2 & c_0 \\ 1 & B_3 & B_1 \\ 0 & B_4 & B_2 \end{vmatrix} > 0, \begin{vmatrix} B_4 & B_2 & B_0 & 0 \\ 1 & B_3 & B_1 & 0 \\ 0 & c_4 & c_2 & B_0 \\ 0 & 1 & B_3 & B_1 \end{vmatrix} > 0$$

Hence, the endemic equilibrium point E_1 of the system is locally asymptotically stable when $R_0 > 1$ $\qquad\square$

5.8.1   Steady Persistence of COVID-19 under $R_0 > 1$

This subsection examines the uniform persistence of the reaction-diffusion system described by Eq. (5.4). The linearized system is evaluated at $E_0(S_0, 0, 0, 0, 0)$, resulting

in the following linear reaction-diffusion system for E, I, I_A, and H:

$$\frac{\partial E(x,t)}{\partial t} = D\Delta E + (1 - \psi)\beta S_0(I + I_A) - \gamma E - \mu E, x \in \Omega, t > 0$$

$$\frac{\partial I(x,t)}{\partial t} = D\Delta I + p_1\gamma E - (\mu + \theta + \alpha)I, x \in \Omega, t > 0 \tag{5.15}$$

$$\frac{\partial I_A(x,t)}{\partial t} = D\Delta I_A + p_2\gamma E - \epsilon I_A - \mu I_A, x \in \Omega, t > 0$$

$$\frac{\partial H(x,t)}{\partial t} = D\Delta H + p_3\gamma E - [(1 + b)\sigma + \mu]H, x \in \Omega, t > 0$$

$$\frac{\partial E}{\partial n} = \frac{\partial I}{\partial n} = \frac{\partial I_A}{\partial n} = \frac{\partial H}{\partial n} = \frac{\partial R}{\partial n} = 0, \quad x \in \partial\Omega, t > 0 \tag{5.16}$$

Clearly, the above system is a cooperative system. Suppose $E(x,t) = e^{\lambda t}\zeta_2(x)$, $I(x,t) = e^{\lambda t}\zeta_3(x)$, $I_A(x,t) = e^{\lambda t}\zeta_4(x)$, and $H(x,t) = e^{\lambda t}\zeta_5(x)$. Thus, the above system simplifies to

$$\lambda\zeta_2(x) = D\Delta\lambda\zeta_2(x) + (1 - \psi)\beta S_0(\lambda\zeta_3(x) + \lambda\zeta_4(x)) - (\gamma + \mu)\lambda\zeta_2(x), x \in \Omega, t > 0$$

$$\lambda\zeta_3(x) = D\Delta\lambda\zeta_3(x) + p_1\gamma\lambda\zeta_2(x) - (\mu + \theta + \alpha)\lambda\zeta_3(x), x \in \Omega, t > 0 \tag{5.17}$$

$$\lambda\zeta_4(x) = D\Delta\lambda\zeta_4(x) + p_2\gamma\lambda\zeta_2(x) - (\epsilon + \mu)\lambda\zeta_4(x), x \in \Omega, t > 0$$

$$\lambda\zeta_5(x) = D\Delta\lambda\zeta_5(x) + p_3\gamma\lambda\zeta_2(x) - [(1 + b)\sigma + \mu]\lambda\zeta_5(x), x \in \Omega, t > 0$$

$$\frac{\partial\zeta_2}{\partial n} = \frac{\partial\zeta_3}{\partial n} = \frac{\partial\zeta_4}{\partial n} = \frac{\partial\zeta_5}{\partial n} = 0, \quad x \in \partial\Omega \tag{5.18}$$

It follows from Theorem 7.6.1 in (Smith, 1995) that Eq. (5.17) has a principal eigenvalue $\lambda_0(S_0(x))$ with a positive eigenfunction $\zeta(x) = (\zeta_2(x), \zeta_3(x), \zeta_4(x), \zeta_5(x))$. Similar to the argument in (W. Wang and Zhao, 2012) and (L. Zhang et $al.$, 2016), we obtain the lemmas as follows.

Lemma 1: The quantities $(R_0 - 1)$ and the principal eigenvalue $\lambda_0(S_0(x))$ share the same sign. Furthermore, the equilibrium point E_0 is asymptotically stable if $R_0 < 1$.

Lemma 2 : Assume $\mathbb{Y}(\cdot, t, \zeta)$ denotes the solution of the reaction-diffusion system given by Eqs. (5.4)–(5.5) with the initial condition $\mathbb{Y}(\cdot, 0, \zeta) = \zeta \in \mathbb{X}^+$. Additionally

1. For all $\zeta \in \mathbb{X}^+$, $x \in \overline{\Omega}$, and $t > 0$, we have $S(x, t, \zeta) > 0$. Furthermore, there exists a positive number η such that $\liminf_{t \to +\infty} S(x, t, \zeta) \geq \eta$ uniformly for $x \in \overline{\Omega}$.

2. If there exists a time $t_1 > 0$ such that $E(\cdot, t_1, \zeta) \equiv 0, I(\cdot, t_1, \zeta) \equiv 0, I_A(\cdot, t_1, \zeta) \equiv 0$, or $H(\cdot, t_1, \zeta) \equiv 0$, then for all $x \in \overline{\Omega}$ and $t > t_1$, we have $(E(x, t, \zeta), I(x, t, \zeta), I_A(x, t, \zeta), H(x,$
   0.

5.9 Global Stability

We establish global stability for the reaction-diffusion system described by Eq. (5.4) by defining $\zeta(x) = x - 1 - \ln x$. It is evident that $\zeta(x) \geq 0$ for all $x > 0$. Next, we proceed to obtain global stability as follows.

Theorem 5.5. *The Disease-Free Equilibrium (DFE) E_0 of the reaction-diffusion system described by Eq. (5.4) exhibits global asymptotic stability when $R_0 < 1$.*

Proof. From Lemma 1, we ascertain that $\lambda_0(S_0(x)) < 0$ when $R_0 < 1$. This implies the existence of a sufficiently small $\varepsilon_0 > 0$ such that $\lambda_0(S_0(x) + \varepsilon_0) < 0$. Consequently, according to the S-equation of system Eq. (5.4), we have

$$\frac{\partial S(x,t)}{\partial t} \leq D_1 \Delta + \Lambda - \mu S \text{ for } x \in \overline{\Omega}, t > 0.$$

Moreover, there exists a $t_0 > 0$ such that $S(x,t) \leq S_0(x) + \varepsilon_0$ for $x \in \overline{\Omega}$, $t \geq t_0$. Thus, we have:

$$\frac{\partial E(x,t)}{\partial t} \leq D_2 \Delta E + (1-\psi)\beta(S_0(x)+\varepsilon_0)I + (1-\psi)\beta(S_0(x)+\varepsilon_0)I_A - \gamma E - \mu E, \ x \in \Omega, t > 0$$

$$\frac{\partial I(x,t)}{\partial t} \leq D_3 \Delta I + p_1 \gamma E - (\mu + \theta + \alpha)I, \ x \in \Omega, t > 0 \tag{5.19}$$

$$\frac{\partial I_A(x,t)}{\partial t} \leq D_4 \Delta I_A + p_2 \gamma E - \epsilon I_A - \mu I_A, \ x \in \Omega, t > 0$$

$$\frac{\partial H(x,t)}{\partial t} \leq D_5 \Delta H + p_3 \gamma E - [(1+b)\sigma + \mu]H, \ x \in \Omega, t > 0$$

$$\frac{\partial E}{\partial n} = \frac{\partial I}{\partial n} = \frac{\partial I_A}{\partial n} = \frac{\partial H}{\partial n} = \frac{\partial R}{\partial n} = 0, \ \ x \in \Omega, t \geq t_0 \tag{5.20}$$

Let $\zeta(x) = (\zeta_2(x), \zeta_3(x), \zeta_4(x), \zeta_5(x))$ be an eigenfunction of system Eq. (5.17) corresponding to the principal eigenvalue $\lambda_0(S_0(x) + \varepsilon_0) < 0$. There exists a $\zeta_1 > 0$ such that

$$\phi_1(\zeta_2(x), \zeta_3(x), \zeta_4(x), \zeta_5(x)) \geq (E(x,t_0), I(x,t_0), I_A(x,t_0), H(x,t_0))$$

. Furthermore, we get

$$\phi_1(\zeta_2(x), \zeta_3(x), \zeta_4(x), \zeta_5(x))e^{\lambda_0(S_0(x)+\varepsilon_0)(t-t_0)} \geq (E(x,t), I(x,t), I_A(x,t), H(x,t)), \quad \text{for } x \in \Omega, t \geq t_0.$$

Therefore,

$$\lim_{t\to\infty} E(x,t) = 0, \quad \lim_{t\to\infty} I(x,t) = 0, \quad \lim_{t\to\infty} I_A(x,t) = 0, \quad \text{and} \quad \lim_{t\to\infty} H(x,t) = 0,$$

149

uniformly for $x \in \overline{\Omega}$.

This renders the S-equation of the reaction-diffusion system Eq. (5.4) asymptotically stable:

$$\frac{\partial S(x,t)}{\partial t} = D_1\Delta + \Lambda - \mu S.$$

Furthermore, according to Thieme (Thieme, 1992) and Guo et al (Guo *et al.*, 2012), it follows that $\lim_{t\to\infty} S(x,t) = S_0(x)$ uniformly for $x \in \overline{\Omega}$. Hence, E_0 of the reaction-diffusion system Eqs. (5.4)–(5.5) is globally asymptotically stable. $\qquad\square$

5.10   Sensitivity Analysis

In this section, We examine the impact of the parameters used to express the basic reproduction number, R_0, through sensitivity analysis.

This demonstrates that an alteration in these parameters results in an alteration in R_0. It is used to identify the variables with a significant impact on R_0 and determine which ones should be the focus of intervention measures. Sensitivity indices make it possible to quantify the proportional change in a variable when a parameter is altered.

The forward sensitivity index of a variable, with regard to a specific parameter, is used for that.

$$\alpha_\phi^{R_0} = \frac{\partial R_0}{\partial \phi}\frac{\phi}{R_0}$$

where $\phi =[\Lambda,\ \beta,\ \mu,\ \gamma,\ \theta,\ \alpha,\ \epsilon,\ P_1,\ P_2,\ \psi]$. The analytical equation for the sensitivity of R_0 to each parameter it comprises can be calculated using the formula mentioned above. As a result, Figure 5.2 shows the sensitivity index of parameters i.e $\Lambda,\ \beta,\ \mu,$ $\gamma,\ \theta,\ \alpha,\ \epsilon,\ P_1,\ P_2$ respectively on R_0.

The positive indices indicate a direct relationship between the parameters and R_0, that is if the parameter increases/decrease then the value of R_0 will increase/decrease. Therefore in order to control COVID-19 from the population, we need to reduce the Basic Reproduction number, we can achieve this by reducing the parameters which give positive indices i.e $\gamma,\ \beta,\ P_1,\ P_2\ \Lambda$, here birth rate Λ and rate of transmission β are the most sensitive parameters of R_0 In light of the uncontrollable nature of the birth rate, our focus shifts to managing the rate of disease transmission. To achieve this, we must limit our contact rate through measures like quarantine and social distancing. By taking responsible actions and collectively embracing these precautions, we can build a shield of protection against infectious diseases, fostering a healthier

and safer society.Also $\alpha_\beta^{R_0} = +1$ means that if β increase by 1 % than R_0 will also increase by 1 %.

The negative indices indicate that there is an inverse relationship between the parameters and R_0, that is if the parameter decreases/increases then the value of R_0 will increase/decrease. μ, θ, α, ϵ, ψ have negative indices, among the μ is the highest sensitive. The strength of intervention, denoted as ψ, has negative indices. This implies that implementing stringent intervention measures will result in a reduction of the basic reproduction number, R_0. Consequently, a lower R_0 will lead to a decrease in the infected population.

ψ represents the efficacy and strictness of intervention strategies such as social distancing, quarantine, vaccination, and public health policies. When ψ is applied effectively and rigorously, it exerts a downward pressure on R_0. The basic reproduction number, R_0, is a crucial metric in epidemiology that indicates the average number of secondary infections produced by a single infected individual in a fully susceptible population. By reducing R_0, we curtail the spread of the infection, leading to a smaller number of new cases over time. Therefore, stringent intervention measures,
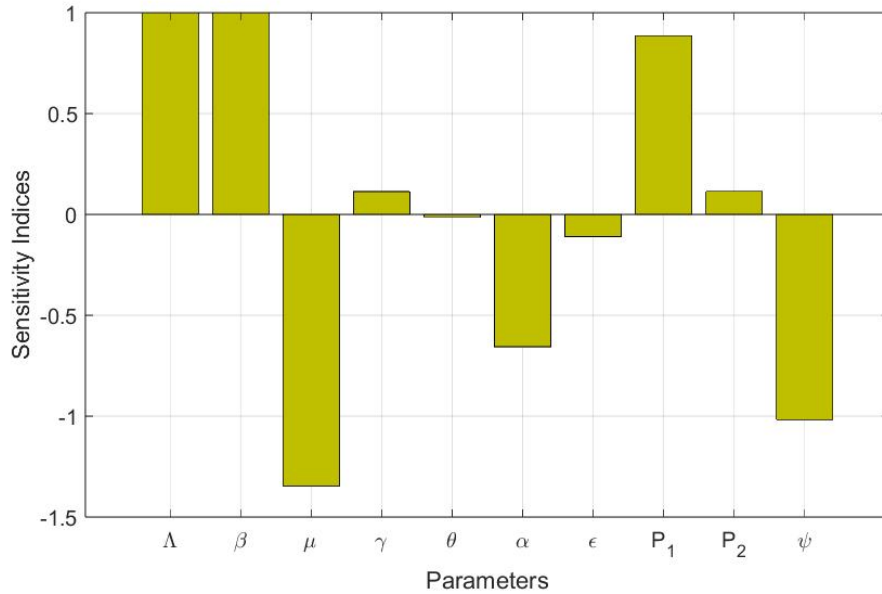
Figure 5.2: Forward sensitivity of R_0.

reflected by a higher negative value of ψ, play a critical role in controlling the outbreak. As R_0 decreases below the threshold of 1, the infection cannot sustain itself

within the population, resulting in a significant decline in the number of active cases and ultimately leading to the containment of the disease.

5.11 Numerical Simulation

For the Numerical Simulation of the proposed model, we illustrate the mathematical findings using the MATLAB program, the value of parameters are listed in the table. Figure 5.3 shows Spatiotemporal evolution of (a) Susceptible $S(t,x)$, (b) Expose $E(t,x)$, (c) Symptomatic Infection $I(t,x)$, (d) Asymptomatic Infection $I_A(t,x)$, (e) Hospitalised $H(t,x)$, (f) Recovered $R(t,x)$.

From Figure 5.4, R_0, β, γ:

- Result: This plot shows how changes in the rate of transmission and the rate of transition from Exposed to infected/hospitalized affect the basic reproduction number.

- Implication: Higher β and higher γ would increase R_0 indicating a faster spread when the transition from Exposed to Hospitalized stage is slow.

In order to reduce the disease spread we need to decrease R_0 by reducing the rate of transmission β which can be done by implementing various precautionary measures such as Social distancing, Personal hygiene and wearing masks. Managing γ through enhancing medical treatment and timely identification and isolation/hospitalisation can significantly help in reducing R_0.
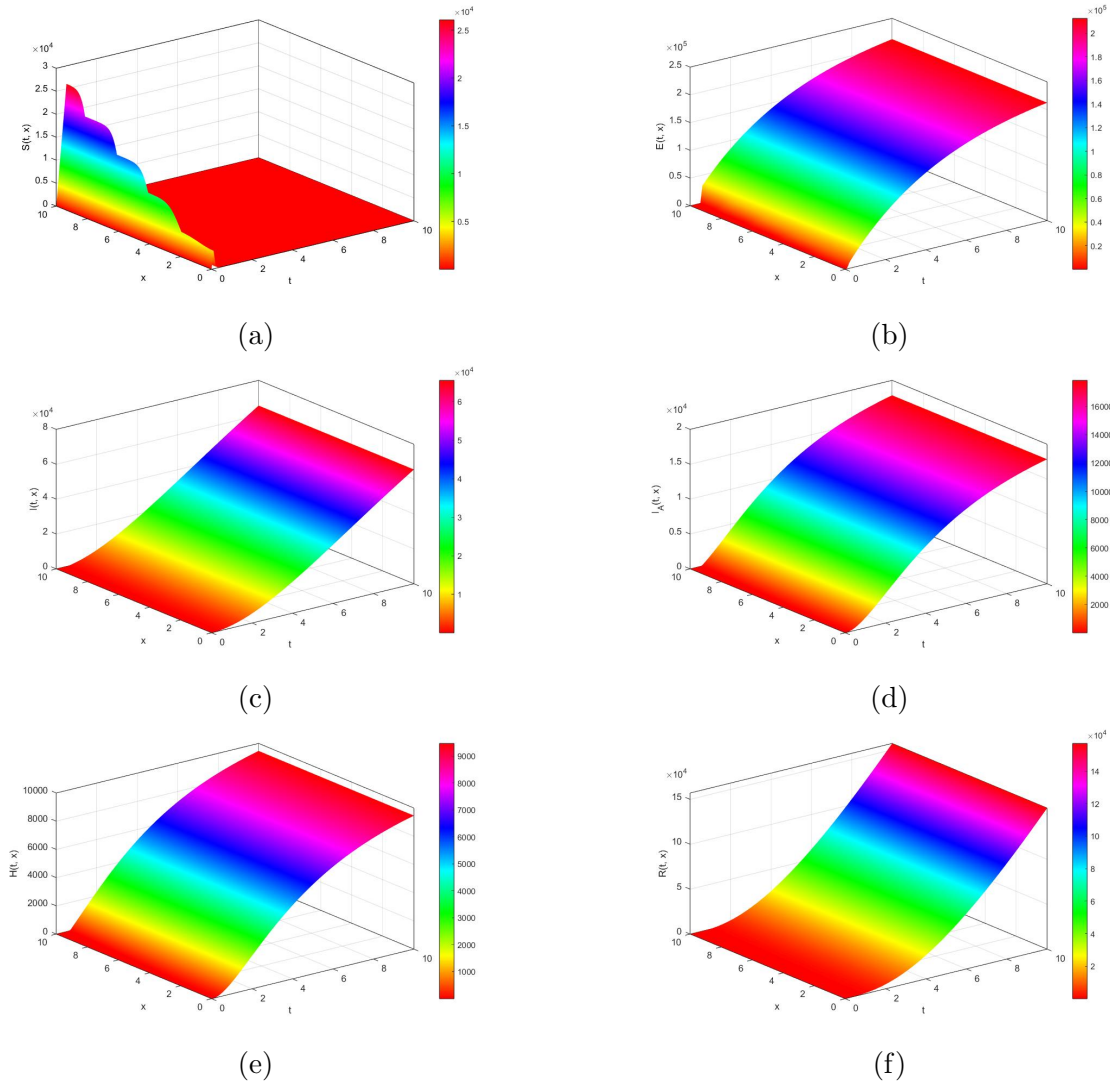
Figure 5.3: Spatiotemporal evolution of (a) Susceptible $S(t, x)$, (b) Expose $E(t, x)$, (c) Symptomatic Infection $I(t, x)$, (d) Asymptomatic Infection $I_A(t, x)$, (e) Hospitalised $H(t, x)$, (f) Recovered $R(t, x)$
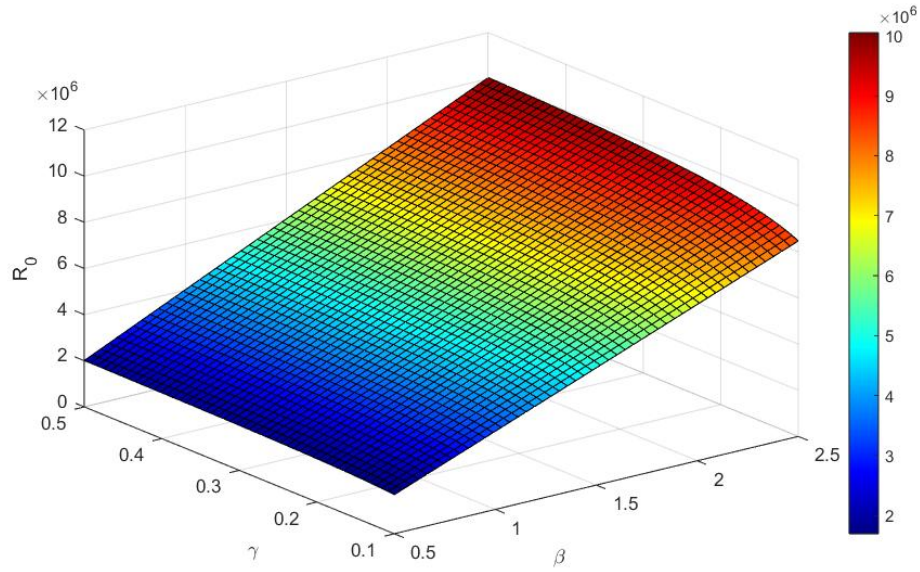
Figure 5.4: The numerical result exhibit that the dependence of R_0 of system on the rate of transmission β and transition of Exposed to Infection/Hospitalize γ.

From Figure 5.5, R_0, β, p_1:

- Result: This plot illustrate the relationship between the rate of transmission β, the fraction of exposed individuals developing symptoms p_1, and R_0.

- Implication: A higher β and higher p_1 would increase R_0, suggesting more symptomatic cases contribute to higher transmission rates.
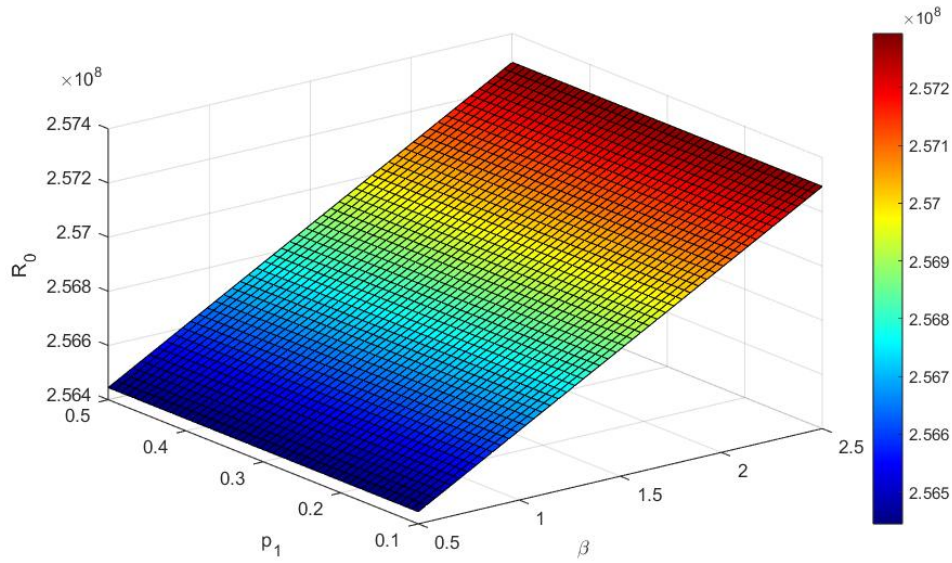
Figure 5.5: The numerical result exhibit that the dependence of R_0 of system on the rate of transmission β and fraction of Exposed developing symptoms p_1.

From Figure 5.6, R_0, β, ψ:

- Result: This plot shows how the rate of transmission and the strength of intervention affect R_0.

- Implication: Stronger interventions (higher ψ) can reduce R_0 even when the transmission rate β is high, highlighting the importance of effective public health measures.
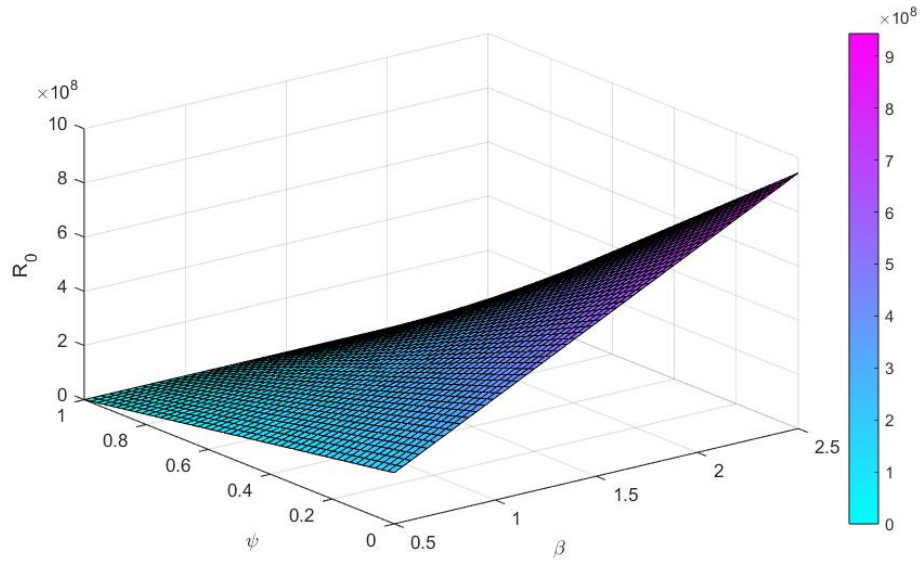
Figure 5.6: The numerical result exhibit that the dependence of R_0 of system on the rate of transmission β and Strength of interventions ψ.

From Figure 5.7, R_0, γ, ψ:

- Result: This plot illustrates the relationship between the rate of transition, the strength of intervention, and R_0.

- Implication: Enhanced interventions ψ combined with faster transitions γ from exposed to hospitalized stages can significantly lower R_0, suggesting a synergistic effect.
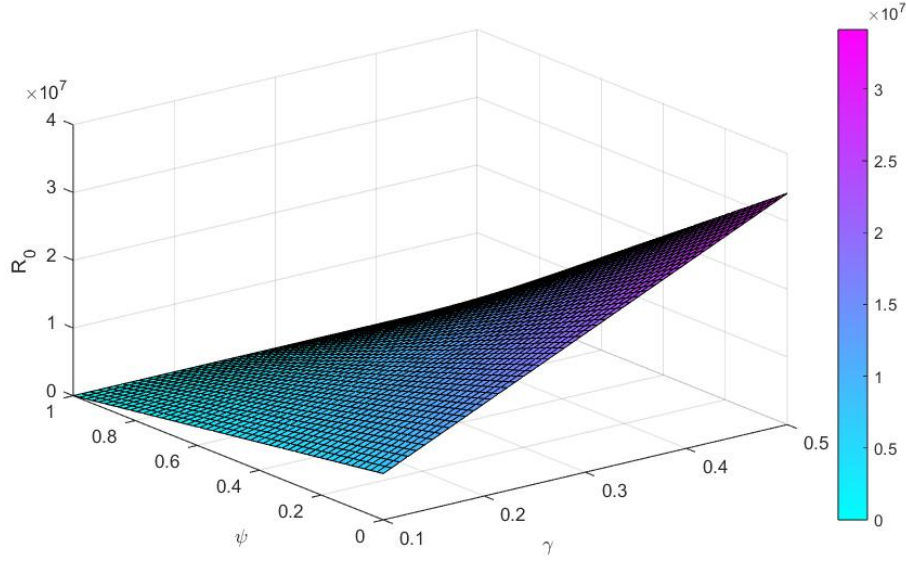
Figure 5.7: The numerical result exhibit that the dependence of R_0 of system on transition of Exposed to Infection/Hospitalize γ and Strength of interventions ψ.

The initial confirmed COVID-19 case in Yangzhou was documented on July 28, 2021, and the outbreak was successfully contained by August 26, 2021. Consequently, the COVID-19 outbreak in Yangzhou lasted for under a month before the situation was completely and promptly controlled. All data regarding COVID-19 in Yangzhou were sourced from the epidemic reports published on the official website of the Yangzhou Commission of Health and were released by the Yangzhou Municipal Government's Press. These data were deidentified and made publicly accessible.

According to the COVID-19 guideline by the National Health Commission (2022), the confirmed cases in Yangzhou comprised 175 (30.7%) classified as mild, 385 (67.5%) as common, and 10 (1.8%) as severe, with the common type having the largest proportion of cases. The period of diagnosis predominantly spanned from July 28 to August 26, with the peak occurring between August 1 and August 14, and the highest daily count of confirmed cases recorded on August 5.

Figure 5.8 illustrates the daily new cases and cumulative cases in Yangzhou, China, from July to September 2021. The parameters were set as follows: $\beta = 0.0065$, $\gamma = 0.05$, $\alpha = 0.004165$, $\epsilon = 0.0714$, $\theta = 0.001$, $\psi = 0.5042$. Given that there were no fatalities in the COVID-19 outbreak in Yangzhou, the parameter μ was set to 0. Additionally, considering the total population of Yangzhou, approximately 4,460,000,

and the initial infection data, the initial conditions were specified as follows: $S(x,0) = 4459996$, $E(x,0) = 1$, $I(x,0) = 1$, $I_A(x,0) = 0$, $Q(x,0) = 0$, $R(x,0) = 0$.
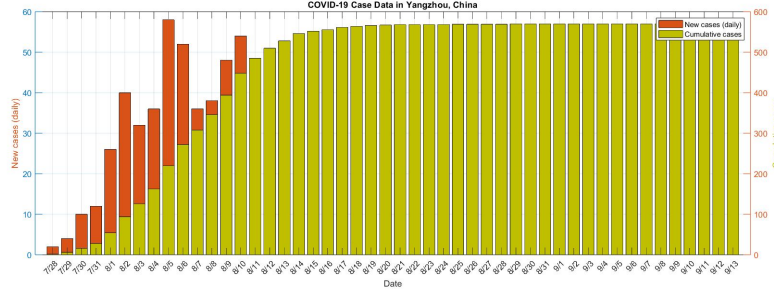
Figure 5.8: the daily new cases and cumulative cases in Yangzhou, China

Based on these initial conditions and parameter values, numerical simulations yielded the data prediction results presented in Figures 5.9 and 5.10. The model-fitting results indicate the following: The basic reproduction number for the COVID-19 outbreak in Yangzhou was calculated to be $R_0 = 2.3651$. The epidemic was projected to reach its peak with 59 new daily confirmed cases on the ninth day, August 5. The total number of infections was estimated to reach 570 cases by the end of the outbreak. Furthermore, the epidemic in Yangzhou was expected to be completely cleared by the 26th day, August 22.
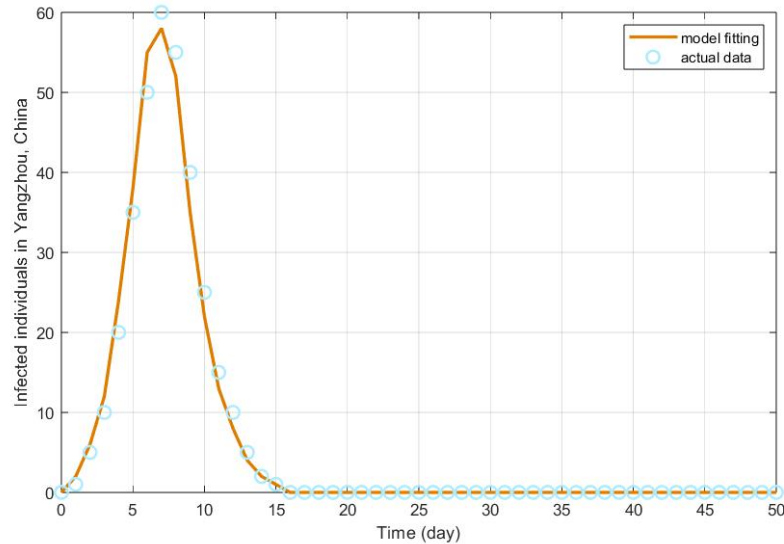
Figure 5.9: Numerical results show prediction of the daily new cases in Yangzhou
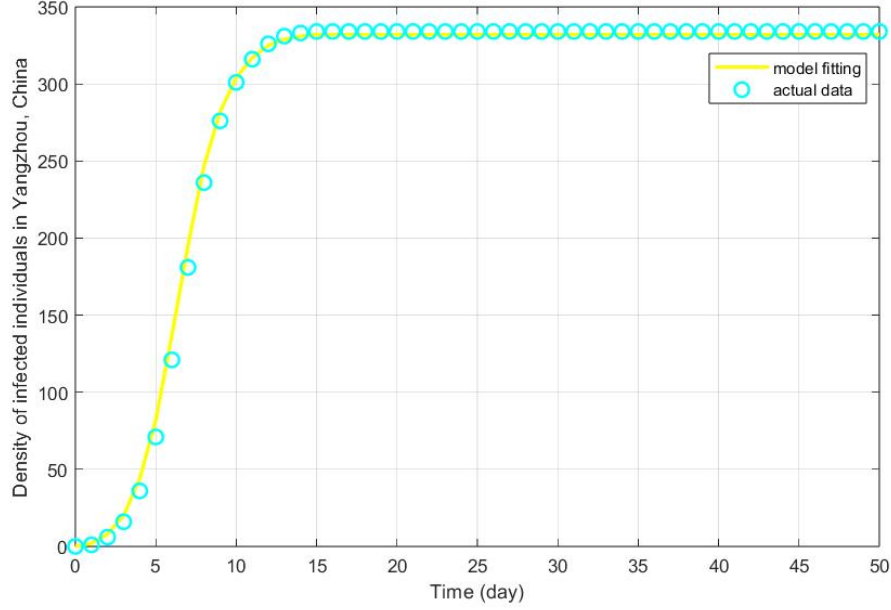
Figure 5.10: Numerical results prediction of the cumulative case in Yangzhou

5.12   Conclusion

The COVID-19 pandemic exhibits complex dynamics due to factors like human be-
haviour, mobility patterns, and varying population densities. The mathematical mod-
elling of COVID-19, $SEII_AHR$ using the Reaction-Diffusion framework has been de-
veloped. It provides a comprehensive understanding of the spatiotemporal dynamics
of the disease and its key influencing parameters.

We discussed the existence and uniqueness of Disease-Free Equilibrium and En-
demic Equilibrium. Stability analysis of the equilibrium points shows Disease Free
Equilibrium is locally asymptotically stable whenever the basic reproduction number,
$R_0 < 1$, and is globally asymptotically stable whenever $R_0 < 1$. Also, Endemic Equi-
librium is locally asymptotically stable whenever the basic reproduction number, R_0
> 1. Steady Persistence of COVID-19 under $R_0 > 1$ of the reaction-diffusion system
described by Eq. (5.4) is also examined.

The analysis of the basic reproduction number R_0 in relation to the transmission
rate β and the transition rate γ from exposed to infected/hospitalized stages, as
illustrated in Figure 5.4, underscores the critical role of these parameters in disease
propagation. Our results indicate that higher values of β and γ significantly elevate

R_0, leading to a faster spread of the infection. Therefore, reducing the transmission rate through measures like social distancing, personal hygiene, and mask-wearing is essential. Additionally, enhancing medical treatment to ensure timely identification, isolation, and hospitalization of exposed individuals can further help in controlling the disease.

Furthermore, Figure 5.5 reveals the impact of the transmission rate β and the fraction of exposed individuals developing symptoms p_1 on R_0. A higher β coupled with a higher p_1 contributes to increased transmission rates, emphasizing the need for effective public health strategies to manage symptomatic cases. Similarly, Figure 5.6 highlights the importance of strong intervention measures (ψ) in reducing R_0 even when the transmission rate is high. This demonstrates that robust public health interventions can significantly mitigate the spread of the virus, regardless of the inherent transmission dynamics.

Additionally, Reaction-Diffusion models can simulate the impact of various intervention strategies such as social distancing, travel restrictions, quarantine measures, and vaccination campaigns. By analyzing these strategies within the model, policymakers can make data-driven decisions on which interventions are most effective in different regions. This approach enhances health responses by forecasting future infection waves, preparing healthcare infrastructures, and implementing timely and suitable actions to mitigate repercussions. Lastly, Figure 5.7 shows the combined effect of the transition rate γ and the strength of interventions ψ on R_0. The findings suggest that enhanced interventions, when paired with faster transitions from exposed to hospitalized stages, can substantially lower R_0. This synergistic effect underscores the importance of an integrated approach that combines public health measures with medical interventions to effectively control the spread of COVID-19. Overall, our study provides valuable insights into the dynamics of COVID-19 and highlights key areas for intervention to reduce the disease's impact on the population.

Chapter 6

Analysis of a Novel Reaction-Diffusion Model for COVID-19: Evaluating Direct and Aerosol Transmission Strategies

6.1 Introduction

The COVID-19 pandemic, caused by the SARS-CoV-2 virus, has highlighted the critical importance of understanding transmission dynamics and developing effective intervention strategies. Traditional compartmental models have provided valuable insights into the disease spread and control measures. However, the spatial heterogeneity and varying modes of transmission, including both direct and aerosol routes, necessitate more sophisticated modelling approaches. This study introduces a novel deterministic $SEII_AA_rR$ reaction-diffusion model that captures the complexities of COVID-19 transmission through both direct contact and aerosol pathways. The model assumes that symptomatic individuals shed more virus than asymptomatic carriers and considers the persistence of the virus in the air for approximately three hours. By incorporating spatial and temporal dynamics, this research aims to provide a comprehensive evaluation of transmission patterns and the effectiveness of various control strategies in different spatial settings.

It is important to recognize that COVID-19 transmission is not limited to direct methods such as coughing, sneezing, and face-to-face communication. Aerosol transmission plays a critical role as well (C. Lu *et al.*, 2020). Aerosols, which are tiny respirable particles smaller than 5–10 μm, can remain airborne and travel significant distances up to 1.5 m and stay up to 3 hours in the air (Anderson *et al.*, 2020). When susceptible individuals inhale these virus-laden aerosols, they immediately become exposed to the virus (Tellier *et al.*, 2019).

Building on the transmission mechanisms of infectious diseases, we explore a novel reaction-diffusion system for COVID-19 that encompasses both direct and aerosol transmission pathways. This comprehensive model allows for an in-depth analysis of the theoretical aspects, enabling us to determine the extinction and persistence thresholds of COVID-19. We further delve into the critical factors influencing the epidemic dynamics of the disease.

Our approach includes performing a detailed stability analysis of the Disease-Free Equilibrium (DFE) and Endemic Equilibrium (EE) both locally and globally. This analysis is crucial for understanding the conditions under which the disease can be eradicated or persists within a population. Additionally, we conduct a global sensitivity analysis on the basic reproduction number R_0, which serves as a pivotal parameter in assessing the potential spread of the virus.

To substantiate our theoretical findings, we implement extensive numerical simulations. These simulations not only corroborate the theoretical calculations but also provide a practical demonstration of the model's accuracy and reliability in predicting the dynamics of COVID-19 transmission. Through this multifaceted approach, we aim to offer valuable insights into the control and mitigation of the ongoing pandemic.

6.2 Model Formulation

We develop a deterministic compartmental model, denoted as $SEII_A A_r R$ (Susceptible, Exposed, Symptomatic infection, Asymptomatic Infection, Aerosol, Recovered), to describe the transmission dynamics of COVID-19. The model includes the following compartments:

- S: Susceptible individuals who are at risk of infection.

- E: Exposed individuals who have been infected but are not yet infectious.

- I: Symptomatic infectious individuals who exhibit symptoms and can transmit the virus.

- I_A: Asymptomatic infectious individuals who do not exhibit symptoms but can still transmit the virus.

- A_r: Aerosol concentration in the environment, which contributes to indirect transmission.

- R: Recovered individuals who have gained immunity and are no longer susceptible.

An assumption made as follows: Transmission Dynamics:

- Symptomatic individuals (I) contribute to direct transmission through contact and also indirectly through the environment by increasing the aerosol concentration (A_r).

- Asymptomatic individuals (I_A) contribute to the direct transmission and to a lesser extent to the aerosol concentration.

- The susceptible population (S) becomes exposed (E) through contact with both symptomatic and asymptomatic individuals, as well as through inhalation of aerosols.

Progression of Disease:

- Exposed individuals (E) transition to either symptomatic (I) or asymptomatic (I_A) infectious states.

- Both symptomatic and asymptomatic individuals eventually recover (R), with different recovery rates.

Aerosol Dynamics:

- The aerosol compartment (A_r) is influenced by contributions from both symptomatic and asymptomatic individuals.

- The aerosol concentration decays over time, reducing the risk of indirect transmission if not continuously replenished.

Susceptible individuals move to the Exposed compartment upon contact with either Symptomatic (I) or Asymptomatic (I_A) individuals at a transmission rate β.

Our model is adapted to include various intervention techniques. Preventive measures such as lockdowns, media campaigns for awareness, effective hand-washing, social distancing, and mask usage are part of the intervention strategies aimed at slowing disease spread.

The application of these interventions suggests a reduction in the disease transmission rate as reflected in the model parameters. The strength of the intervention, denoted by ψ where $\psi \in [0, 1]$, is considered to decrease the transmission rate. A value of $\psi = 0$ indicates no intervention, while $\psi = 1$ signifies strong intervention.

When interventions are implemented, the parameter β is modified to $(1 - \psi)\beta$. Exposed individuals move to the I, I_A, and H compartments at a rate γ. A fraction of the population transitions from Exposed to Symptomatic at a rate P_1, and to Asymptomatic at a rate P_2.

Symptomatic and Asymptomatic individuals recover at rates α and η, respectively. Each compartment may decrease due to natural mortality μ, with the Symptomatic compartment additionally decreasing due to COVID-19-related mortality at a rate θ.

Symptomatic and asymptomatic individuals release virus particles into the air through activities like coughing, sneezing, talking, and breathing. This release is modelled by ϱI and φI_A, where $\varrho > \varphi$ indicates that symptomatic individuals shed more virus particles than asymptomatic ones. The aerosol density also decreases due to natural decay $\Upsilon A_r(x, t)$. Based on these assumptions, we propose the following model, represented as a system of non-linear differential equations. The schematic diagram is shown in the figure (6.1).

$$
\begin{aligned}
\frac{dS}{dt} &= \Lambda - (1 - \psi)\beta S(I + I_A) - \beta_r S A_r - \mu S, \\
\frac{dE}{dt} &= (1 - \psi)\beta S(I + I_A) + \beta_r S A_r - \gamma E - \mu E, \\
\frac{dI}{dt} &= p_1 \gamma E - (\mu + \theta)I - \alpha I, \\
\frac{dI_A}{dt} &= p_2 \gamma E - \epsilon I_A - \mu I_A, \\
\frac{dA_r}{dt} &= \varrho I + \varphi I_A - \Upsilon A_r \\
\frac{dR}{dt} &= \alpha I + \epsilon I_A - \mu R,
\end{aligned}
\tag{6.1}
$$
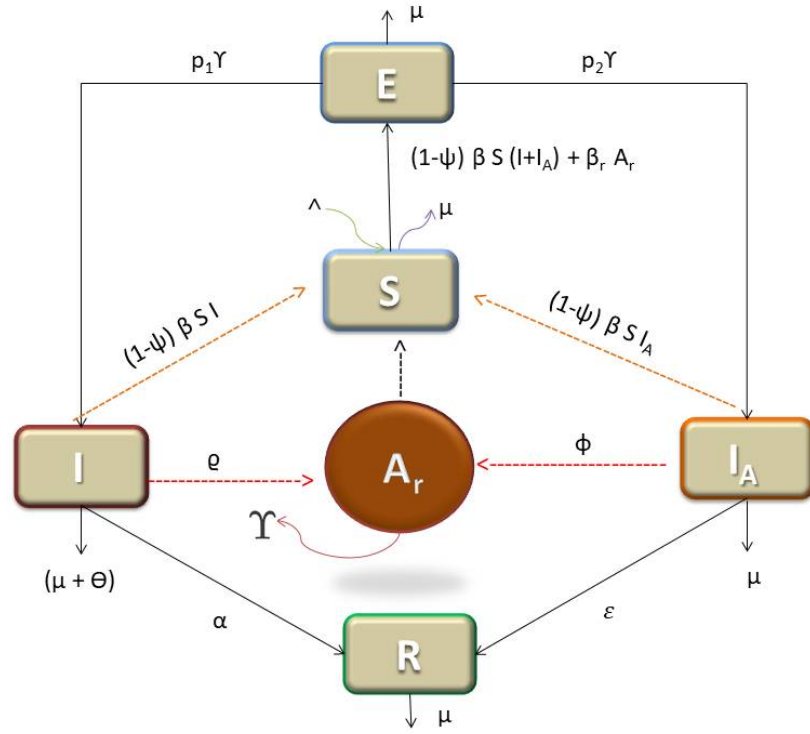
Figure 6.1: Schematic Diagram of $SEII_AHR$

with nonnegative initial conditions given by

$$S(0) > 0, \ E(0) > 0, \ I(0) > 0, \ I_A > 0, \ A_r(0) > 0, \ R(0) > 0.$$

All the parameters of the system (6.1) are assumed to be positive for all time $t > 0$.

6.3 Dynamic with Reaction-Diffusion.

The COVID-19 pandemic exhibits complex dynamics due to factors like human behaviour, mobility patterns, and varying population densities. Reaction-diffusion models are well-suited to capture these complexities, providing a more accurate representation of how the virus spreads and evolves over time.

Reaction-diffusion models incorporate both the reaction i.e., local interactions and dynamics of population and diffusion, spatial movement and spread of the Individuals.

This dual approach helps in understanding how COVID-19 spreads across different regions over time, providing a spatial-temporal view of the pandemic. Using Eq(6.1) a Reaction-Diffusion dynamics is given as follow

Dynamics of Susceptible Individuals $S(t)$

The susceptible individuals are recruited into the population at a constant inflow rate Λ. They decrease due to infection through direct contact at a rate β when they come into contact with infectious (I) and asymptomatic (I_A) individuals, with a reduced transmission rate η for I_A. They also get infected through aerosol transmission at a rate β_r. Additionally, they decrease due to vaccination at a rate δ and natural mortality at a rate μ. Thus, the dynamics of susceptible individuals are given by:

$$\frac{\partial S(x,t)}{\partial t} = D_1 \Delta S + \Lambda - (1 - \psi)\beta S(I + I_A) - \beta_r S A_r - \mu S$$

Dynamics of Exposed Individuals $E(t)$

Exposed individuals are those who have been infected but are not yet infectious. They increase due to infection of both susceptible and vaccinated individuals through direct contact at a rate $(1 - \psi)\beta S(I + I_A)$ and aerosol transmission at a rate $\beta_r S A_r$. They decrease as they transition to the infectious class at a rate γ and due to natural mortality at a rate μ. Thus, the dynamics of exposed individuals are given by:

$$\frac{\partial E(x,t)}{\partial t} = D_2 \Delta E + (1 - \psi)\beta S(I + I_A) + \beta_r S A_r - \gamma E - \mu E$$

Dynamics of Symptomatic Infectious Individuals $I(t)$

Symptomatic infectious individuals arise from the exposed class at a fraction p_1 and transition at a rate γ. They decrease due to disease-induced mortality at a rate θ, recovery at a rate α, and natural mortality at a rate μ. Thus, the dynamics of symptomatic infectious individuals are given by:

$$\frac{\partial I(x,t)}{\partial t} = D_3 \Delta I + p_1 \gamma E - (\mu + \theta + \alpha)I$$

Dynamics of Asymptomatic Infectious Individuals $I_A(t)$

Asymptomatic infectious individuals also arise from the exposed class but at a fraction p_2 and transition at a rate γ. They decrease due to recovery at a rate ϵ and natural mortality at a rate μ. Thus, the dynamics of asymptomatic infectious individuals are given by:

$$\frac{\partial I_A(x,t)}{\partial t} = D_4 \Delta I_A + p_2 \gamma E - \epsilon I_A - \mu I_A$$

Dynamics of Aerosol Density $A_r(x,t)$

Aerosol density $A_r(x,t)$ is affected by the contribution from symptomatic individuals (ϱI) and asymptomatic individuals (φI_A), where $\varrho > \varphi$ indicates that symptomatic individuals contribute more to the aerosol density than asymptomatic individuals. The aerosol density also decreases due to natural decay ($\Upsilon A_r(x,t)$) and spreads out over space via diffusion. Thus, the dynamics of aerosol density are given by:

$$\frac{\partial A_r(x,t)}{\partial t} = D_5 \Delta A_r + \varrho I + \varphi I_A - \Upsilon A_r$$

Dynamics of Recovered Individuals $R(t)$

Recovered individuals increase due to the recovery of both symptomatic and asymptomatic infectious individuals at rates α and ϵ, respectively. They decrease due to natural mortality at a rate μ. Thus, the dynamics of recovered individuals are given by:

$$\frac{\partial R(x,t)}{\partial t} = D_6 \Delta R + \alpha I + \epsilon I_A - \mu R$$

Based on the biological assumptions and the schematic representation of the coronavirus, we develop a mathematical model for the novel coronavirus. This model is expressed as the following six-dimensional system of nonlinear ordinary differential equations (ODEs):

$$\frac{\partial S(x,t)}{\partial t} = D_1 \Delta S + \Lambda - (1-\psi)\beta S(I+I_A) - \beta_r S A_r - \mu S, \ x \in \Omega, t > 0$$

$$\frac{\partial E(x,t)}{\partial t} = D_2 \Delta E + (1-\psi)\beta S(I+I_A) + \beta_r S A_r - \gamma E - \mu E, \ x \in \Omega, t > 0$$

$$\frac{\partial I(x,t)}{\partial t} = D_3 \Delta I + p_1 \gamma E - (\mu + \theta + \alpha)I, \ x \in \Omega, t > 0 \tag{6.2}$$

$$\frac{\partial I_A(x,t)}{\partial t} = D_4 \Delta I_A + p_2 \gamma E - \epsilon I_A - \mu I_A, \ x \in \Omega, t > 0$$

$$\frac{\partial A_r(x,t)}{\partial t} = D_5 \Delta A_r + \varrho I + \varphi I_A - \Upsilon A_r, \ x \in \Omega, t > 0$$

$$\frac{\partial R(x,t)}{\partial t} = D_6 \Delta R + \alpha I + \epsilon I_A + -\mu R, \ x \in \Omega, t > 0$$

with

$$(S(x,0), E(x,0), I(x,0), I_A(x,0), A_r(x,0), R(x,0)) = (\zeta_1(x), \zeta_2(x), \zeta_3(x), \zeta_4(x), \zeta_5(x), \zeta_6(x))$$

for $x \in \Omega$ and also satisfy

$$\frac{\partial S}{\partial n} = \frac{\partial E}{\partial n} = \frac{\partial I}{\partial n} = \frac{\partial I_A}{\partial n} = \frac{\partial A_r}{\partial n} = \frac{\partial R}{\partial n} = 0, \ x \in \partial\Omega, t > 0$$

The variables $(S(x,0), E(x,0), I(x,0), I_A(x,0), A_r(x,0), R(x,0))$ denote the densities of individuals within each compartment at time t and location x. Here, Δ represents the Laplace operator, and D_i (for $i = 1, 2, \ldots, 6$) corresponds to the respective diffusion coefficients. We assume that $D_1 = D_2 = D_3 = D_4 = D_6 = D \neq D_5$.

Table 6.1: Parameter Description for $SEII_AHR$

Parameter	Description	Values
Λ	Birth rate	$52000 \ year^{-1}$
μ	Death rate	$0.0245 \ year^{-1}$
β	Rate of transmission through direct contact	$1.7399 \ day^{-1}$
β_r	Rate of transmission through Aerosol	$0.03 \ day^{-1}$
γ	Rate of transition from Exposed to I, I_A, and Q	$0.1923 \ day^{-1}$
p_1	Fraction of population moves from Exposed to symptomatic class	0.3362
p_2	Fraction of population moves from Exposed to asymptomatic class	0.4204
α	Recovery rate of symptomatic infected class	$0.07 \ day^{-1}$
ϵ	Recovery rate of asymptomatic infection	$0.9 \ day^{-1}$
θ	Rate of disease-induced death	$0.0001 \ day^{-1}$
ψ	Strength of intervention	0.5042
ϱ	Rate at which I shed SARS-CoV-2	$0.03 \ day^{-1}$
φ	Rate at which I_A shed SARS-CoV-2	$0.02 \ day^{-1}$
Υ	Decay rate of a pathogen in the air	$0.02 \ day^{-1}$

6.4 Dynamic behaviour of $SEII_AHR$ model with Reaction-Diffusion

We observe that the first five equations in the system (6.2) are independent of $R(x,t)$. The resulting reduced system is as follows:

$$\frac{\partial S(x,t)}{\partial t} = D_1 \Delta S + \Lambda - (1-\psi)\beta S(I + I_A) - \beta_r S A_r - \mu S, \ x \in \Omega, t > 0$$

$$\frac{\partial E(x,t)}{\partial t} = D_2 \Delta E + (1-\psi)\beta S(I + I_A) - \beta_r S A_r - \gamma E - \mu E, \ x \in \Omega, t > 0$$

$$\frac{\partial I(x,t)}{\partial t} = D_3 \Delta I + p_1 \gamma E - (\mu + \theta + \alpha)I, \ x \in \Omega, t > 0 \qquad (6.3)$$

$$\frac{\partial I_A(x,t)}{\partial t} = D_4 \Delta I_A + p_2 \gamma E - \epsilon I_A - \mu I_A, \ x \in \Omega, t > 0$$

$$\frac{\partial A_r(x,t)}{\partial t} = D_5 \Delta A_r + \varrho I + \varphi I_A - \Upsilon A_r, \ x \in \Omega, t > 0$$

with

$$(S(x,0), E(x,0), I(x,0), I_A(x,0), A_r(x,0)) = (\zeta_1(x), \zeta_2(x), \zeta_3(x), \zeta_4(x), \zeta_5(x)) \; for \; x \, in\Omega \tag{6.4}$$

and satisfy

$$\frac{\partial S}{\partial n} = \frac{\partial E}{\partial n} = \frac{\partial I}{\partial n} = \frac{\partial I_A}{\partial n} = \frac{\partial H}{\partial n} = \frac{\partial R}{\partial n} = 0, \quad x \in \partial\Omega, t > 0 \tag{6.5}$$

6.5 Positivity and boundedness

We assume that $D_1 = D_2 = D_3 = D_4 = D_6 = D \neq D_5$ and demonstrate the existence and uniqueness of the solution.

Let $X := C(\overline{\Omega}, \mathbb{R}^5)$ be a Banach space equipped with the supremum norm $\| \cdot \|_{\mathbb{X}}$. Define $\mathbb{X}^+ := C(\overline{\Omega}, \mathbb{R}^5_+)$, making $(\mathbb{X}, \mathbb{X}^+)$ a strongly ordered space. Suppose that $\mathbb{T}_1(x)$, $\mathbb{T}_2(x)$, $\mathbb{T}_3(x)$, $\mathbb{T}_4(x)$, $\mathbb{T}_5(x) : C(\overline{\Omega}, \mathbb{R}) \to C(\overline{\Omega}, \mathbb{R})$ are the C_0 semigroups related to $D\Delta - \mu$, $D\Delta - (\gamma + \mu)$, $D\Delta - (\alpha + \theta + \mu)$, $D\Delta - (\epsilon + \mu)$ and $D_5\Delta - \Upsilon$ dependent on Eq.(6.5) , respectively. It is evident that for every $\phi \in C(\overline{\Omega}, \mathbb{R})$ and $t \geq 0$, we have:

$$\mathbb{T}_1(t)\zeta(x) = e^{-\mu t} \int_\Omega \zeta(s)\Gamma_1(x,t,s)ds,$$

$$\mathbb{T}_2(t)\zeta(x) = e^{-(\gamma+\mu)t} \int_\Omega \zeta(s)\Gamma_1(x,t,s)ds,$$

$$\mathbb{T}_3(t)\zeta(x) = e^{-(\alpha+\theta+\mu)t} \int_\Omega \zeta(s)\Gamma_1(x,t,s)ds,$$

$$\mathbb{T}_4(t)\zeta(x) = e^{-(\epsilon+\mu)t} \int_\Omega \zeta(s)\Gamma_1(x,t,s)ds,$$

$$\mathbb{T}_5(t)\zeta(x) = e^{-\Upsilon t} \int_\Omega \zeta(s)\Gamma_5(x,t,s)ds.$$

where Γ_1 represent the Green functions related to $D\Delta$ depend on Eq. (6.5).
From Martin an Smith Martin and Smith, 1990 We obtain that $\mathbb{T}_i(t) : C(\overline{\Omega}, \mathbb{R}) \to C(\overline{\Omega}, \mathbb{R})$ $(i = 1, 2, 3, 4, 5)$ stands for strongly positive and compact. For all initial values

$\zeta \in \mathbb{X}^+$ and $\mathbb{X} \in \overline{\Omega}$, let $\mathfrak{F} = (\mathcal{F}_1, \mathcal{F}_2, \mathcal{F}_3, \mathcal{F}_4, \mathcal{F}_5)$ be defined as $\mathfrak{F} : \mathbb{X}^+ \to \mathbb{X}$ given by:

$$\mathcal{F}_1(\zeta)(x) = \Lambda - (1 - \psi)\beta\zeta_1(x, 0)[\zeta_3(x, 0) + \zeta_4(x, 0)] - \beta_r\zeta_1(x, 0)\zeta_5(x, 0)$$

$$\mathcal{F}_2(\zeta)(x) = (1 - \psi)\beta\zeta_1(x, 0)[\zeta_3(x, 0) + \zeta_4(x, 0)] + \beta_r\zeta_1(x, 0)\zeta_5(x, 0)$$

$$\mathcal{F}_3(\zeta)(x) = p_1\gamma\zeta_2(x, 0)$$

$$\mathcal{F}_4(\zeta)(x) = p_1\gamma\zeta_2(x, 0)$$

$$\mathcal{F}_5(\zeta)(x) = \varrho\zeta_3(x, 0) + \varphi\zeta_4(x, 0)$$

Hence equation 6.4-6.5 can be written as

$$\mathbb{Y}(x, t) = \mathbb{T}(t)\zeta(x) + \int_0^t \mathbb{T}(t - s)\mathcal{F}(\mathbb{Y}(x, s))\, ds,$$

where

$$\mathbb{T}(t) = \mathrm{diag}(\mathbb{T}_1(t), \mathbb{T}_2(t), \mathbb{T}_3(t), \mathbb{T}_4(t), \mathbb{T}_5(t))$$

and

$$\mathbb{Y}(x, t) = (S(x, t), E(x, t), I(x, t), I_A(x, t), A_r(x, t), R(x, t))$$

. Then, we get the following result.

Theorem 6.1. *For any $\phi \in \mathbb{X}^+$, the reaction-diffusion system Eq. (6.4) – (6.5) possesses a unique solution $\mathbb{Y}(\cdot, t, \phi)$ with the initial condition $\mathbb{Y}(\cdot, 0, \phi) = \phi$. Moreover, the mapping $\psi(t) : \mathbb{X}^+ \to \mathbb{X}^+$, defined by $\psi(t)\phi = (S(\cdot, t, \phi), E(\cdot, t, \phi), I(\cdot, t, \phi), I_A(\cdot, t, \phi), A_r(\cdot, t, \phi))$ for all $x \in \mathbb{X}$ and $t \geq 0$, is point dissipative.*

Proof. For every $\zeta \in \mathbb{X}^+$ and $h > 0$, one has

$$\lim_{h \to 0^+} \frac{1}{h} \mathrm{dist}(hF(\zeta) + \zeta(0), \mathbb{X}^+) = 0$$

. According to Corollary 4 from Martin and Smith, 1990, $\mathbb{Y}(\cdot, t, \zeta)$ represents a unique mild solution of Eqs. (6.4) - (6.5) on $[0, \tau_\zeta)$, with $\mathbb{Y}(\cdot, 0, \zeta)$ and $\mathbb{Y}(\cdot, t, \zeta) \in \mathbb{X}^+$, where $t_\zeta \leq +\infty$. We then prove that the solution is global. From the system of equation Eq. (6.4) considering the first three equations, we have

$$\frac{\partial}{\partial t}(S(x, t) + E(x, t) + I(x, t) + I_A(x, t)) = D\Delta(S + E + I + I_A) +$$

$$\Lambda - \mu(S + E + I + I_A) - \theta I$$

$$- \alpha I - \epsilon I_A$$

$$\leq D\Delta(S + E + I + I_A) + \Lambda$$

$$- \mu(S + E + I + I_A).$$

By comparison principle, for a very small positive number ε there exists $t^* > 0$, $\forall$ $t \geq t^*$, such that $S(x,t) + E(x,t) + I(x,t) + I_A(x,t) \leq \frac{\Lambda}{\mu} + \varepsilon$, uniformly $\forall$ $x \in \Omega$.

Hence, $S(\cdot,t) \leq \frac{\Lambda}{\mu} + \varepsilon$, $E(\cdot,t) \leq \frac{\Lambda}{\mu} + \varepsilon$, $I(\cdot,t) \leq \frac{\Lambda}{\mu} + \varepsilon$, $I_A(\cdot,t) \leq \frac{\Lambda}{\mu} + \varepsilon$.

This indicates that S, E, I, I_A are uniformly bounded. Consequently, $\psi(t) : \mathbb{X}^+ \to \mathbb{X}^+$ is point dissipative. Similarly, from Eq. (6.4), one has

$$\begin{cases} \frac{\partial A_r(x,t)}{\partial t} \leq D_5 A_r + \varrho(\frac{\Lambda}{\mu} + \varepsilon) + \varphi(\frac{\Lambda}{\mu} + \varepsilon) - \Upsilon A_r, & x \in \Omega, t > t^*, \\ \frac{\partial A_r}{\partial n} = 0, & x \in \partial\Omega, t > 0. \end{cases} \tag{6.6}$$

By comparison principle,

$$\limsup_{t \to +\infty} A_r(x,t) \leq \frac{\varrho(\frac{\Lambda}{\mu} + \varepsilon) + \varphi(\frac{\Lambda}{\mu} + \varepsilon)}{\Upsilon}, \quad \text{uniformly for } \forall x \in \Omega.$$

Therefore, there is $t^* \geq t^*$ such that

$$A_r(x,t) \leq \varrho(\frac{\Lambda}{\mu} + \varepsilon) + \varphi(\frac{\Lambda}{\mu} + \varepsilon), \quad \text{for } \forall t \geq t^*,$$

which implies $A_r(x,t)$ is bounded. Therefore $\psi(t) : X^+ \to X^+$ is point dissipative.

$\square$

6.6 Basic Reproduction Number R_0

System (6.4) always has Disease Free Equilibrium $E_0(S_0, 0, 0, 0, 0)$ where $S_0 = \frac{\Lambda}{\mu}$ and there exist Endemic Equilibrium $E_1(S^*, E^*, I^*, I_A^*, H^*)$ given by

$$\begin{aligned} 0 &= \Lambda - (1-\psi)\beta S^*(I^* + I_A^*) - \beta_r S A_r - \mu S^* \\ 0 &= (1-\psi)\beta S^*(I^* + I_A^*) + \beta_r S A_r - \gamma E^* - \mu E^* \\ 0 &= p_1 \gamma E^* - (\alpha + \theta)I^* - \mu I^* \\ 0 &= p_2 \gamma E^* - \epsilon I_A^* - \mu I_A^* \\ 0 &= \varrho I^* + \varphi I_A^* - \Upsilon A_r^* \end{aligned} \tag{6.7}$$

which gives

$$\begin{aligned} S^* &= \frac{\Lambda - (\gamma + \mu E^*)}{\mu} \\ I^* &= \frac{p_1 \gamma E^*}{\alpha + \theta + \mu} \\ I_A^* &= \frac{p_2 \gamma E^*}{\epsilon + \mu} \\ A_r^* &= \frac{[\frac{\varrho p_1}{(\mu + \theta + \alpha)} + \frac{\varphi p_2}{(\epsilon + \mu)}]}{\Upsilon} \gamma E^* \end{aligned} \tag{6.8}$$

Furthermore, according to the theory in W. Wang and Zhao, [2012]

$$\frac{\partial P_i}{\partial t} = D_i \Delta P_i + \mathcal{F}_i(x, P) - \mathcal{V}_i(x, P), \quad i = 1, 2, 3, 4, 5.$$

where $P = (E, I, I_A, A_r, S)^T$.

System (6.4)-(6.5) can be written as

$$\frac{\partial E(x,t)}{\partial t} = D_2 \Delta E + (1 - \psi)\beta S(I + I_A) + \beta_r S A_r - \gamma E - \mu E, \ x \in \Omega, t > 0$$

$$\frac{\partial I(x,t)}{\partial t} = D_3 \Delta I + p_1 \gamma E - (\mu + \theta + \alpha)I, \ x \in \Omega, t > 0$$

$$\frac{\partial I_A(x,t)}{\partial t} = D_4 \Delta I_A + p_2 \gamma E - \epsilon I_A - \mu I_A, \ x \in \Omega, t > 0 \qquad (6.9)$$

$$\frac{\partial A_r(x,t)}{\partial t} = D_5 \Delta A_r + \varrho I + \varphi I_A - \Upsilon A_r, \ x \in \Omega, t > 0$$

$$\frac{\partial S(x,t)}{\partial t} = D_1 \Delta S + \Lambda - (1 - \psi)\beta S(I + I_A) - \beta_r S A_r - \mu S, \ x \in \Omega, t > 0$$

$$\frac{\partial E}{\partial n} = \frac{\partial I}{\partial n} = \frac{\partial I_A}{\partial n} = \frac{\partial H}{\partial n} = \frac{\partial S}{\partial n} = 0, \quad x \in \partial\Omega, t > 0 \qquad (6.10)$$

$$(E(x,0), I(x,0), I_A(x,0), A_r(x,0), S(x,0)) = (\zeta_2(x), \zeta_3(x), \zeta_4(x), \zeta_5(x), \zeta_1(x)) \ for \ x \in \Omega$$
$$(6.11)$$

Therefore we get $\mathcal{F}_i(x, \overline{E_0(0)}) = \begin{bmatrix} (1 - \psi)\beta S(I + I_A) + \beta_r S A_r \\ 0 \\ 0 \\ 0 \\ 0 \end{bmatrix}$ and

$$\mathcal{V}_i(x, \overline{E_0(0)}) = \begin{bmatrix} (\gamma + \mu)E - D_2 \Delta E \\ (\mu + \theta + \alpha)I - p_1 \gamma E - D_3 \Delta I \\ (\eta + \mu)I_A - p_2 \gamma E - D_4 \Delta I_A \\ \Upsilon A_r - \varrho I - \varphi I_A - D_5 \Delta A_r \\ \beta S(I + I_A) + \mu S - \Lambda - D_1 \Delta S \end{bmatrix}$$

$F(x), V(X)$ denoted as

$$F(x) = \left. \frac{\partial \mathcal{F}_i(x, \overline{E_0(x)})}{\partial u_j} \right|_{1 \le i,j \le 4}$$

and

$$V(x) = \left. \frac{\partial \mathcal{V}_i(x, \overline{E_0(x)})}{\partial u_j} \right|_{1 \le i,j \le 3},$$

respectively, where $E_0(x) = (0, 0, 0, 0, S_0)$.

Thus,

$$F(x) = \begin{bmatrix} 0 & (1-\psi)\beta S_0 & (1-\psi)\beta S_0 & \beta_r S_0 \\ 0 & 0 & 0 & 0 \\ 0 & 0 & 0 & 0 \\ 0 & 0 & 0 & 0 \end{bmatrix}$$

and

$$V(x) = \begin{bmatrix} \gamma+\mu-k^2\Delta_2 & 0 & 0 & 0 \\ -p_1\gamma & (\mu+\theta+\alpha)-k^2\Delta_3 & 0 & 0 \\ -p_2\gamma & 0 & \epsilon+\mu-k^2\Delta_4 & 0 \\ 0 & -\varrho & -\varphi & \Upsilon-k^2\Delta_5 \end{bmatrix}$$

where k is the wave number. $F(x)$ denotes a 4×4 continuous and nonnegative matrix function, while $-V(x)$ represents a 4×4 continuous and cooperative matrix function. According to W. Wang and Zhao, 2012, the distribution of the total new infections is defined as

$$\int_0^\infty F(x)\mathcal{T}(t)\zeta(x)\,dt,$$

Further, we define

$$[\mathcal{L}(\zeta)](x) = \int_0^\infty F(x)[\mathcal{T}(t)\zeta](x)dt$$
$$= F(x)\int_0^\infty [\mathcal{T}(t)\zeta](x)dt,$$

where $\mathcal{L}$ denotes a positive and continuous operator that maps the initial infection distribution $\zeta(x)$ to the total number of infected individuals produced during the infection period. By the next-generation matrix method, we have

$$\begin{aligned} R_0 = & \frac{(1-\psi)\beta\gamma\Lambda P_1}{\mu(\mu+\gamma)(\alpha+\theta+\mu)} + \frac{(1-\psi)\beta\gamma\Lambda P_2}{\mu(\mu+\epsilon)(\mu+\gamma)} \\ & + \frac{\gamma\beta_r\Lambda(\alpha\varphi p_2 + \mu\varrho p_1 + \theta\varphi p_2 + \epsilon\varrho p_1 + \mu\varphi p_2)}{\mu\Upsilon(\mu+\epsilon)(\mu+\gamma)(\alpha+\theta+\mu)} \\ & \triangleq R_{0I} + R_{0I_A} + R_{0A_r} \end{aligned}$$

The biological significance of the quantities R_{0I}, R_{0I_A}, R_{0A_r} can be described as the contributions of Symptomatic Infected individuals, Asymptomatic Infected individuals, and SARS-CoV-2 spread as Aerosols to the basic reproduction number, respectively.

6.7   Uniqueness of DFE and EE

Theorem 6.2. *For $R_0 < 1$, the reaction-diffusion system Eq.(6.4) has only $E_0(S_0, 0, 0, 0)$; whereas for $R_0 > 1$, there exist a unique $E_1(S^*, E^*, I^*, I_A^*, H^*)$, where*

$$S^* = \frac{\Lambda - (\gamma + \mu E^*)}{\mu}$$

$$I^* = \frac{p_1 \gamma E^*}{\alpha + \theta + \mu}$$

$$I_A^* = \frac{p_2 \gamma E^*}{\epsilon + \mu} \tag{6.12}$$

$$A_r^* = \frac{[\frac{\varrho p_1}{(\mu+\theta+\alpha)} + \frac{\varphi p_2}{(\epsilon+\mu)}]}{\Upsilon} \gamma E^*$$

Proof. Clearly E_0 is unique when $R_0 < 1$. Therefore, we need to prove only for $R_0 > 1$. From Eq. (6.6) we know that

$$S = {}'\frac{\Lambda - (\gamma + \mu E)}{\mu}, \ I = \frac{p_1 \gamma E}{\alpha + \theta + \mu}$$

$$I_A = \frac{p_2 \gamma E}{\epsilon + \mu}, \ A_r = \frac{[\frac{\varrho p_1}{(\mu+\theta+\alpha)} + \frac{\varphi p_2}{(\epsilon+\mu)}]}{\Upsilon} \gamma E$$

From second equation of eq(6.6), we have

$$J(E) = (1 - \psi)\beta \left(\frac{\Lambda - (\gamma + \mu)E}{\mu} \right) \left[\frac{p_1 \gamma E}{\mu + \theta + \alpha} + \frac{p_2 \gamma E}{\epsilon + \mu} \right]$$
$$+ \beta_r \left(\frac{\Lambda - (\gamma + \mu)E}{\mu} \right) \left[\frac{[\frac{\varrho p_1}{(\mu+\theta+\alpha)} + \frac{\varphi p_2}{(\epsilon+\mu)}]}{\Upsilon} \gamma E \right] - (\gamma + \mu)E$$

Since $J(0) = 0$, adding the first two equation of eq(**??**), we have

$$J\left(\frac{\Lambda}{\mu} \right) = -(\gamma + \mu)E = -\Lambda < 0$$

$$J'(0) = \frac{(1 - \psi)\beta\gamma\Lambda P_1(\gamma - \mu)}{\mu(\mu + \gamma)(\alpha + \theta + \mu)} + \frac{(1 - \psi)\beta\gamma\Lambda P_2(\gamma - \mu)}{\mu(\mu + \epsilon)(\mu + \gamma)}$$
$$+ \frac{\gamma\beta_r\Lambda(\gamma - \mu)(\alpha\varphi p_2 + \mu\varrho p_1 + \theta\varphi p_2 + \epsilon\varrho p_1 + \mu\varphi p_2)}{\mu\Upsilon(\mu + \epsilon)(\mu + \gamma)(\alpha + \theta + \mu)} - (\gamma - \mu)$$
$$= (R_0 - 1)(\gamma - \mu) > 0$$

174

This shows that $J(E) = 0$ exists at least one positive root $E^* \in \left(0, \frac{\Lambda}{\mu}\right)$, this implies that the positive equilibrium of Eq. (6.4) exists. Next, we shall prove E^* is unique. Based on Eq. (6.8) and the following facts

$$(1 - \psi)\beta S^*(I^* + I_A^*) = \gamma E^* + \mu E^* \tag{6.13}$$

we also have $E, I, I_A, A_r \geq 0$. Therefore, it follows from the above equation

$$
\begin{aligned}
J'(E^*) =&(1 - \psi)\beta \left[\left(\frac{\Lambda - (\gamma + \mu)E^*}{\mu}\right)\left(\frac{p_1\gamma}{\mu + \theta + \alpha} + \frac{p_2\gamma}{\epsilon + \mu}\right) + \left(\frac{p_1\gamma E^*}{\mu + \theta + \alpha} + \frac{p_2\gamma E^*}{\epsilon + \mu}\right)\left(-\frac{\gamma + \mu}{\mu}\right)\right] \\
&+ \beta_r \left[\left(\frac{\Lambda - (\gamma + \mu)E^*}{\mu}\right)\left(\frac{\left(\frac{\varrho p_1}{\mu + \theta + \alpha} + \frac{\varphi p_2}{\epsilon + \mu}\right)}{\Upsilon}\gamma\right) + \left(\frac{\left(\frac{\varrho p_1}{\mu + \theta + \alpha} + \frac{\varphi p_2}{\epsilon + \mu}\right)}{\Upsilon}\gamma E^*\right)\left(-\frac{\gamma + \mu}{\mu}\right)\right] \\
&- (\gamma + \mu)
\end{aligned}
$$

Suppose there exists another positive equilibrium $E_1^{**}(S^{**}, E^{**}, I^{**}, I_A^{**}, A_r^{**})$, then we have $J'(E_1^{**} > 0)$, which contradicts the inequality. $\qquad\square$

6.8 Local stability of disease-free equilibrium

Let $0 = \mu_1 < \mu_2 < \ldots < \mu_i < \ldots$ be the eigenvalues of $-\Delta$ on Ω with homogeneous Neumann boundary conditions. Let $U(\mu_i)$ denote the eigenfunction space corresponding to μ_i, and let $\{\overline{\omega}_{ij} : j = 1, 2, 3, \ldots, \dim U(\mu_i)\}$ be an orthonormal basis of $U(\mu_i)$. The space $\mathbb{Z}$ can be decomposed as follows:

$$\mathbb{Z} = \oplus_{i=1}^{\infty} \mathbb{Z}_i \quad \text{and} \quad \mathbb{Z}_i = \oplus_{i=1}^{U(\mu_i)} \mathbb{Z}_{ij}$$

,
where

$$\mathbb{Z} = \left\{(E, I, I_A, A_r, S) \in [C'(\overline{\omega})]^4 : \frac{\partial E}{\partial n} = \frac{\partial I}{\partial n} = \frac{\partial I_A}{\partial n} = \frac{\partial A_r}{\partial n} = \frac{\partial S}{\partial n} = 0 \text{ on } \partial\Omega\right\}$$

, $\mathbb{Z}_{ij} = a\overline{\omega}_{ij} \mid a \in \mathbb{R}^5$. Then, we shall show the local stability of equilibrium as follows.

Theorem 6.3. *The Disease-Free Equilibrium (DFE) E_0 of the reaction-diffusion system described by Eq. (6.4) exhibits local asymptotic stability when $R_0 < 1$.*

Proof. Consider the linearization of the reaction-diffusion system Eq. (6.4) at E_0:

$$\frac{\partial \mathbb{Y}(x,t)}{\partial t} = \mathbb{D}\mathbb{Y}(x,t) + \mathbb{A}(E_0)\mathbb{Y}(x,t),$$

where $\mathbb{Y} = (S, E, I, I_A, A_r)$, $\mathbb{D} = \text{diag}(D_1, D_2, D_3, D_4, D_5)$ $D_1 = D_2 = D_3 = D_4 = D$, and

$$\mathbb{A} = \begin{bmatrix} -\mu & 0 & -(1-\psi)\beta S_0 & -(1-\psi)\beta S_0 & -\beta_r S_0 \\ 0 & -(\gamma+\mu) & (1-\psi)\beta S_0 & (1-\psi)\beta S_0 & \beta_r S_0 \\ 0 & p_1\gamma & -(\mu+\theta+\alpha) & 0 & 0 \\ 0 & p_2\gamma & 0 & -(\epsilon+\mu) & 0 \\ 0 & 0 & \varrho & \varphi & -\Upsilon \end{bmatrix}$$

Let $\mathcal{L}\mathbb{Y} = \mathbb{D}\mathbb{Y} + \mathbb{A}(E_0)\mathbb{Y}$, and let $\mathbb{Z}_i$ (for $i \geq 1$) be invariant under $\mathcal{L}$. An eigenvalue λ of $\mathcal{L}$ exists if and only if it is an eigenvalue of a matrix $-\mathbb{D}\mu_i + \mathbb{A}(E_0)$ with $i \geq 1$, where there is an eigenvalue in $\mathbb{Z}_i$. In other words, λ must satisfy the following characteristic equation: $\det(\lambda I + \mathbb{D}\mu_i - \mathbb{A}(E_0)) = 0$, where I represents the identity matrix. Therefore, the characteristic equation at E_0 can be specifically expressed as:

$$(\lambda + (\mu + \mu_i D))(\lambda^4 + A_1\lambda^3 + A_2\lambda^2 + A_3\lambda + A_4) = 0. \tag{6.14}$$

Clearly $\lambda_1 = -(\mu + \mu_i D)$ is an eigenvalue of Eq. (6.14) Therefore the remaining four eigenvalues are the roots of the following equation

$$\lambda^4 + A_1\lambda^3 + A_2\lambda^2 + A_3\lambda + A_4 = 0$$

$$A_1 = (\gamma + \mu) + (\mu + \theta + \alpha) + (\epsilon + \mu) + \Upsilon + 4D\mu_i$$

$$A_2 = (x_1 + x_2 + x_3 + x_4 + 4D\mu_i)^2/2 - ((x_1 + D\mu_i)^2$$
$$+ (x_2 + D\mu_i)^2 + (x_3 + D\mu_i)^2 + (x_4 + D\mu_i)^2)/2$$
$$(-(1 - \psi)\beta\gamma S_0)(p_1 + p_2) - \beta_r S_0$$

$$A_3 = (x_1 + D\mu_i)(x_2 + D\mu_i)(x_3 + D\mu_i) + (x_1 + D\mu_i)(x_2 + D\mu_i)(x_4 + D\mu_i)$$
$$+ (x_1 + D\mu_i)(x_3 + D\mu_i)(x_4 + D\mu_i) + (x_2 + D\mu_i)(x_3 + D\mu_i)(x_4 + D\mu_i)$$
$$- (1 - \psi)\beta\gamma(x_2 - \beta_r S_0 + D\mu_i)p_2 S_0 - (1 - \psi)\beta\gamma(x_3 + D\mu_i)p_1 S_0$$
$$- (1 - \psi)\beta\gamma(x_4 + D\mu_i)p_1 S_0 - (1 - \psi)\beta\gamma(x_4 + D\mu_i)p_2 S_0$$

$$A_4 = (x_1 + D\mu_i)(x_2 + D\mu_i)(x_3 + D\mu_i)(x_4 + D\mu_i) - \beta_r S_0 - (1 - \psi)\beta\gamma(x_2 + D\mu_i)(x_4 + D\mu_i)p_2 S_0$$
$$- \beta\gamma(x_3 + D\mu_i)(x_4 + D\mu_i)p_1$$

Where,

$x_1 = (\gamma + \mu)$, $x_2 = (\mu + \theta + \alpha)$, $x_3 = (\epsilon + \mu)$, $x_4 = \Upsilon$ According to the Routh-Hurwitz criterion, the equation above will yield negative roots or roots with negative real parts if the following condition is satisfied:

$$A_1 > 0, \begin{vmatrix} A_1 & A_3 \\ 1 & A_2 \end{vmatrix} > 0, \begin{vmatrix} A_1 & A_3 & 0 \\ 1 & A_2 & A_4 \\ 0 & A_1 & A_3 \end{vmatrix} > 0$$

Hence, the disease-free equilibrium point E_0 of the system is locally asymptotically stable, when $R_0 < 1$. □

Theorem 6.4. *The Endemic Equilibrium E_1 of the reaction-diffusion system Eq. (6.4) is locally asymptotically stable if $R_0 > 1$*

Proof. Consider the linearization of the reaction-diffusion system Eq. (6.4) at E_0:

$$\frac{\partial \mathbb{Y}(x,t)}{\partial t} = \mathbb{D}\mathbb{Y}(x,t) + \mathbb{B}(E_0)\mathbb{Y}(x,t),$$

$$\mathbb{B} = \begin{bmatrix} -q & 0 & -(1 - \psi)\beta S^* & -(1 - \psi)\beta S^* & -\beta_r S^* \\ a_{21} & -r & (1 - \psi)\beta S^* & (1 - \psi)\beta S^* & \beta_r S^* \\ 0 & p_1\gamma & -s & 0 & 0 \\ 0 & p_2\gamma & 0 & -t & 0 \\ 0 & 0 & \varrho & \varphi & -u \end{bmatrix}$$

where

$$q = [(1 - \psi)\beta(I^* + I_A^*) + \beta A_r^* + \mu]$$

$$r = (\gamma + \mu)$$

$$s = (\mu + \theta + \alpha)$$

$$t = (\epsilon + \mu)$$

$$u = \Upsilon$$

$$a_{21} = (1 - \psi)\beta(I^* + I_A^*) + \beta_r S^*$$

Similarly, λ must be a root of $\det(\lambda I + D\mu_i - \mathbb{A}(E_1)) = 0$. Therefore, we can denote the characteristic equation at E_1 as $\lambda^5 + B_4\lambda^4 + B_3\lambda^3 + B_2\lambda^2 + B_1\lambda + B_0 = 0$. where

$$B_4 = (q + r + s + t + u)$$

$$B_3 = (q + r + s + t + u)^2/2 - (q^2 + r^2 + s^2 + t^2 + u^2)/2 - \beta\gamma S^*(p_1 + p_2)$$

$$B_2 = qr(s + t + u) + (qs + rs)(t + u) + tu(q + r) + \beta\gamma S^*[(a_{21} - q - u)$$
$$(p_1 + p_2) - (sp_2 + tp_1)]$$

$$B_1 = qrs(t + u) + qtu(r + s) + rstu + \beta\gamma S^*(a_{21}s + a_{21}u - qu)(p_1 + p_2)$$
$$- \beta\gamma qS^*(sp_2 + tp_1) - \beta\gamma uS^*(sp_2 + up_1)$$

$$B_0 = qr(s + t + u) + (qs + rs)(t + u) + tu(q + r) + \beta\gamma S^*[(a_{21} - q - u)$$
$$(p_1 + p_2) - (sp_2 + tp_1)]$$

According to the Routh-Hurwitz criterion, the above equation will give negative roots or negative real parts if the following condition is satisfied:

$$B_4 > 0, \begin{vmatrix} B_4 & B_2 \\ 1 & B_3 \end{vmatrix} > 0, \begin{vmatrix} B_4 & c_2 & c_0 \\ 1 & B_3 & B_1 \\ 0 & B_4 & B_2 \end{vmatrix} > 0, \begin{vmatrix} B_4 & B_2 & B_0 & 0 \\ 1 & B_3 & B_1 & 0 \\ 0 & c_4 & c_2 & B_0 \\ 0 & 1 & B_3 & B_1 \end{vmatrix} > 0$$

Hence, the endemic equilibrium point E_1 of the system is locally asymptotically stable when $R_0 > 1$ □

6.8.1 Steady Persistence of COVID-19 under $R_0 > 1$

This subsection examines the uniform persistence of the reaction-diffusion system described by Eq. (6.4). The linearized system is evaluated at $E_0(S_0, 0, 0, 0, 0)$, resulting

in the following linear reaction-diffusion system for E, I, I_A, and A_r:

$$\frac{\partial E(x,t)}{\partial t} = D\Delta E + (1-\psi)\beta S_0(I + I_A) + \beta_r S_0 A_r - \gamma E - \mu E, x \in \Omega, t > 0$$

$$\frac{\partial I(x,t)}{\partial t} = D\Delta I + p_1\gamma E - (\mu + \theta + \alpha)I, x \in \Omega, t > 0 \tag{6.15}$$

$$\frac{\partial I_A(x,t)}{\partial t} = D\Delta I_A + p_2\gamma E - \epsilon I_A - \mu I_A, x \in \Omega, t > 0$$

$$\frac{\partial A_r(x,t)}{\partial t} = D_5\Delta A_r + \varrho I + \varphi I_A - \Upsilon A_r, x \in \Omega, t > 0$$

$$\frac{\partial E}{\partial n} = \frac{\partial I}{\partial n} = \frac{\partial I_A}{\partial n} = \frac{\partial A_r}{\partial n} = \frac{\partial R}{\partial n} = 0, \quad x \in \partial\Omega, t > 0 \tag{6.16}$$

Clearly, the above system is a cooperative system. Suppose $E(x,t) = e^{\lambda t}\zeta_2(x)$, $I(x,t) = e^{\lambda t}\zeta_3(x)$, $I_A(x,t) = e^{\lambda t}\zeta_4(x)$, and $A_r(x,t) = e^{\lambda t}\zeta_5(x)$. Thus, the above system simplifies to

$$\lambda\zeta_2(x) = D\Delta\lambda\zeta_2(x) + (1-\psi)\beta S_0(\lambda\zeta_3(x) + \lambda\zeta_4(x)) - (\gamma + \mu)\lambda\zeta_2(x), x \in \Omega, t > 0$$

$$\lambda\zeta_3(x) = D\Delta\lambda\zeta_3(x) + p_1\gamma\lambda\zeta_2(x) - (\mu + \theta + \alpha)\lambda\zeta_3(x), x \in \Omega, t > 0 \tag{6.17}$$

$$\lambda\zeta_4(x) = D\Delta\lambda\zeta_4(x) + p_2\gamma\lambda\zeta_2(x) - (\epsilon + \mu)\lambda\zeta_4(x), x \in \Omega, t > 0$$

$$\lambda\zeta_5(x) = D\Delta\lambda\zeta_5(x) + \varrho\zeta_3(x) + \varphi\zeta_4(x) - \Upsilon\zeta_5(x), x \in \Omega, t > 0$$

$$\frac{\partial\zeta_2}{\partial n} = \frac{\partial\zeta_3}{\partial n} = \frac{\partial\zeta_4}{\partial n} = \frac{\partial\zeta_5}{\partial n} = 0, \quad x \in \partial\Omega \tag{6.18}$$

It follows from Theorem 7.6.1 in Smith, 1995 that Eq. (6.17) has a principal eigenvalue $\lambda_0(S_0(x))$ with a positive eigenfunction $\zeta(x) = (\zeta_2(x), \zeta_3(x), \zeta_4(x), \zeta_5(x))$. Similar to the argument in W. Wang and Zhao, 2012 and L. Zhang *et al.*, 2016, we obtain the lemmas as follows.

Lemma 1: The quantities $(R_0 - 1)$ and the principal eigenvalue $\lambda_0(S_0(x))$ share the same sign. Furthermore, the equilibrium point E_0 is asymptotically stable if $R_0 < 1$.

Lemma 2 : Assume $\mathbb{Y}(\cdot, t, \zeta)$ denotes the solution of the reaction-diffusion system given by Eqs. (6.4)–(6.5) with the initial condition $\mathbb{Y}(\cdot, 0, \zeta) = \zeta \in \mathbb{X}^+$. Additionally

1. For all $\zeta \in \mathbb{X}^+$, $x \in \overline{\Omega}$, and $t > 0$, we have $S(x, t, \zeta) > 0$. Furthermore, there exists a positive number η such that $\liminf_{t \to +\infty} S(x, t, \zeta) \geq \eta$ uniformly for $x \in \overline{\Omega}$.

2. If there exists a time $t_1 > 0$ such that $E(\cdot, t_1, \zeta) \equiv 0$, $I(\cdot, t_1, \zeta) \equiv 0$, $I_A(\cdot, t_1, \zeta) \equiv 0$, or $A_r(\cdot, t_1, \zeta) \equiv 0$, then for all $x \in \overline{\Omega}$ and $t > t_1$, we have $(E(x, t, \zeta), I(x, t, \zeta), I_A(x, t, \zeta), A_r(x$
   0.

6.9 Global Stability

We establish global stability for the reaction-diffusion system described by Eq. (6.4) by defining $\zeta(x) = x - 1 - \ln x$. It is evident that $\zeta(x) \geq 0$ for all $x > 0$. Next, we proceed to obtain global stability as follows.

Theorem 6.5. *The Disease-Free Equilibrium (DFE) E_0 of the reaction-diffusion system described by Eq. (6.4) exhibits global asymptotic stability when $R_0 < 1$.*

Proof. From Lemma 1, we ascertain that $\lambda_0(S_0(x)) < 0$ when $R_0 < 1$. This implies the existence of a sufficiently small $\varepsilon_0 > 0$ such that $\lambda_0(S_0(x) + \varepsilon_0) < 0$. Consequently, according to the S-equation of system Eq. (6.4), we have

$$\frac{\partial S(x,t)}{\partial t} \leq D_1 \Delta + \Lambda - \mu S \text{ for } x \in \overline{\Omega}, t > 0.$$

Moreover, there exists a $t_0 > 0$ such that $S(x,t) \leq S_0(x) + \varepsilon_0$ for $x \in \overline{\Omega}$, $t \geq t_0$. Thus, we have:

$$\begin{aligned}
\frac{\partial E(x,t)}{\partial t} &\leq D_2 \Delta E + (1-\psi)\beta(S_0(x) + \varepsilon_0)I + (1-\psi)\beta(S_0(x) + \varepsilon_0)I_A \\
&\quad + \beta(S_0(x) + \varepsilon_0)A_r - (\gamma - \mu)E, \ x \in \Omega, t > 0
\end{aligned} \tag{6.19}$$

$$\frac{\partial I(x,t)}{\partial t} \leq D_3 \Delta I + p_1 \gamma E - (\mu + \theta + \alpha)I, \ x \in \Omega, t > 0 \tag{6.20}$$

$$\frac{\partial I_A(x,t)}{\partial t} \leq D_4 \Delta I_A + p_2 \gamma E - \epsilon I_A - \mu I_A, \ x \in \Omega, t > 0$$

$$\frac{\partial A_r(x,t)}{\partial t} \leq D_5 \Delta A_r + \varrho I + \varphi I_A - \Upsilon A_r, \ x \in \Omega, t > 0$$

$$\frac{\partial E}{\partial n} = \frac{\partial I}{\partial n} = \frac{\partial I_A}{\partial n} = \frac{\partial A_r}{\partial n} = \frac{\partial R}{\partial n} = 0, \ \ x \in \Omega, t \geq t_0 \tag{6.21}$$

Let $\zeta(x) = (\zeta_2(x), \zeta_3(x), \zeta_4(x), \zeta_5(x))$ be an eigenfunction of system Eq. (6.17) corresponding to the principal eigenvalue $\lambda_0(S_0(x) + \varepsilon_0) < 0$. There exists a $\zeta_1 > 0$ such that

$$\phi_1(\zeta_2(x), \zeta_3(x), \zeta_4(x), \zeta_5(x)) \geq (E(x,t_0), I(x,t_0), I_A(x,t_0), A_r(x,t_0))$$

. Furthermore, we get

$$\phi_1(\zeta_2(x), \zeta_3(x), \zeta_4(x), \zeta_5(x))e^{\lambda_0(S_0(x)+\varepsilon_0)(t-t_0)} \geq (E(x,t), I(x,t), I_A(x,t), A_r(x,t)), \quad \text{for } x \in \Omega, t \geq t_0$$

Therefore,

$$\lim_{t\to\infty} E(x,t) = 0, \quad \lim_{t\to\infty} I(x,t) = 0, \quad \lim_{t\to\infty} I_A(x,t) = 0, \quad \text{and} \quad \lim_{t\to\infty} A_r(x,t) = 0,$$

uniformly for $x \in \overline{\Omega}$.

This renders the S-equation of the reaction-diffusion system Eq. (6.4) asymptotically stable:

$$\frac{\partial S(x,t)}{\partial t} = D_1 \Delta + \Lambda - \mu S.$$

Furthermore, according to Thieme Thieme, 1992 and Guo et al Guo *et al.*, 2012, it follows that $\lim_{t \to \infty} S(x,t) = S_0(x)$ uniformly for $x \in \overline{\Omega}$. Hence, E_0 of the reaction-diffusion system Eqs. (6.4)–(6.5) is globally asymptotically stable.   □

6.10   Sensitivity Analysis

In this section, We examine the impact of the parameters used to express the basic reproduction number, R_0, through sensitivity analysis.

This demonstrates that an alteration in these parameters results in an alteration in R_0. It is used to identify the variables with a significant impact on R_0 and determine which ones should be the focus of intervention measures. Sensitivity indices make it possible to quantify the proportional change in a variable when a parameter is altered.

The forward sensitivity index of a variable, with regard to a specific parameter, is used for that.

$$\alpha_\phi^{R_0} = \frac{\partial R_0}{\partial \phi} \frac{\phi}{R_0}$$

where $\phi = [\Lambda, \beta, \mu, \gamma, \theta, \alpha, \epsilon, P_1, P_2, \psi, \varrho, \varphi, \Upsilon, \beta_r]$. The analytical equation for the sensitivity of R_0 to each parameter it comprises can be calculated using the formula mentioned above. As a result, Figure 6.2 shows the sensitivity index of parameters i.e $\Lambda, \beta, \mu, \gamma, \theta, \alpha, \epsilon, P_1, P_2, \psi, \varrho, \varphi, \Upsilon, \beta_r$ respectively on R_0.

The positive indices indicate a direct relationship between the parameters and R_0, that is if the parameter increases/decrease then the value of R_0 will increase/decrease. Therefore in order to control COVID-19 from the population, we need to reduce the Basic Reproduction number, we can achieve this by reducing the parameters which give positive indices i.e $\gamma, \beta, P_1, P_2 \Lambda, \beta_r, \varrho, \varphi$.

β (**Rate of Direct Transmission**): This parameter represents the rate at which susceptible individuals become infected through direct contact with infectious individuals. It includes interactions such as physical touch, droplets from coughs or sneezes, and close proximity interactions. Since direct transmission is a primary pathway for the spread of COVID-19, the sensitivity index for β is typically high. This implies

that small changes in the rate of direct transmission can significantly impact R_0. Therefore, measures such as social distancing, mask-wearing, and reducing gatherings are crucial to lowering β and consequently R_0.
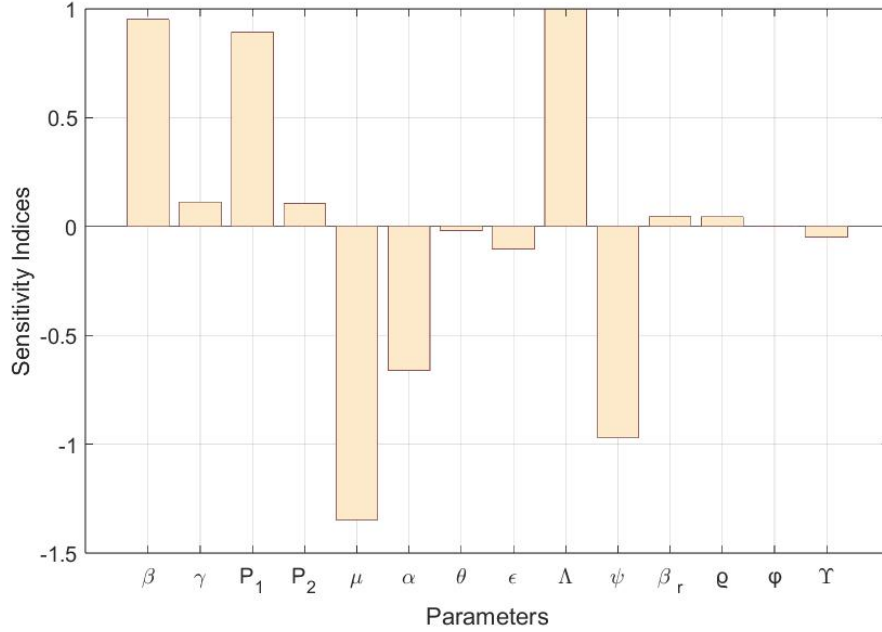
Figure 6.2: Forward sensitivity of R_0.

β_r **(Transmission Through Aerosol):** This parameter signifies the rate of transmission through aerosols, which are tiny particles that can remain suspended in the air for extended periods and travel longer distances. Aerosol transmission is particularly important in enclosed spaces with poor ventilation. Although β_r might have a lower sensitivity index compared to β, it still plays a significant role in the overall transmission dynamics. The sensitivity index $\beta > \beta_r$ indicates that direct transmission has a more substantial impact on R_0 compared to aerosol transmission. Nevertheless, improving indoor ventilation, using air filtration systems, and encouraging outdoor activities can help reduce β_r and its contribution to R_0. The negative indices indicate that there is an inverse relationship between the parameters and R_0, that is if the parameter decreases/increases then the value of R_0 will increase/decrease.

In summary, reducing R_0 requires a multifaceted approach that targets both β and β_r, with a greater emphasis on reducing direct transmission due to its higher

sensitivity index. This combined effort will contribute to controlling the spread of COVID-19 within the population.

Now for the negative indices, we have μ, θ, α, ϵ, ψ, and Υ. These parameters have an inverse relationship with R_0, meaning that if these parameters increase, the value of R_0 will decrease, thereby contributing to the control of COVID-19 within the population.

ψ **(Strength of Intervention):** This parameter represents the effectiveness and strength of interventions implemented to control the spread of the virus. Interventions can include a wide range of measures such as lockdowns, travel restrictions, quarantine protocols, and mass vaccination campaigns. A higher value of ψ indicates stronger and more effective interventions. Since ψ has a negative index, increasing the strength of interventions will lead to a reduction in R_0. This highlights the importance of robust public health measures and policies in mitigating the spread of COVID-19. For example, effective contact tracing, widespread testing, and timely quarantine can significantly reduce transmission rates and bring down R_0.

Υ **(Rate of Decay of Pathogen SARS-CoV-2):** This parameter signifies the rate at which the virus decays or becomes inactive in the environment. Factors influencing Υ include temperature, humidity, exposure to sunlight, and the presence of disinfectants. A higher rate of decay means that the virus does not survive long outside a host, reducing the likelihood of transmission. Enhancing the rate of decay through environmental controls, such as regular disinfection of surfaces, improving hygiene practices, and utilizing UV light in public spaces, can effectively reduce R_0. The negative index associated with Υ indicates that increasing the rate of decay will contribute to lowering the basic reproduction number.

Other parameters such as μ (death rate), α (recovery rate of I) and ϵ (recovery rate of I_A) also play vital roles. Enhancing these parameters through better healthcare, vaccination strategies, and supportive policies will further aid in reducing R_0.

6.11 Numerical Simulation

For the Numerical Simulation of the proposed model, we illustrate the mathematical findings using the MATLAB program.
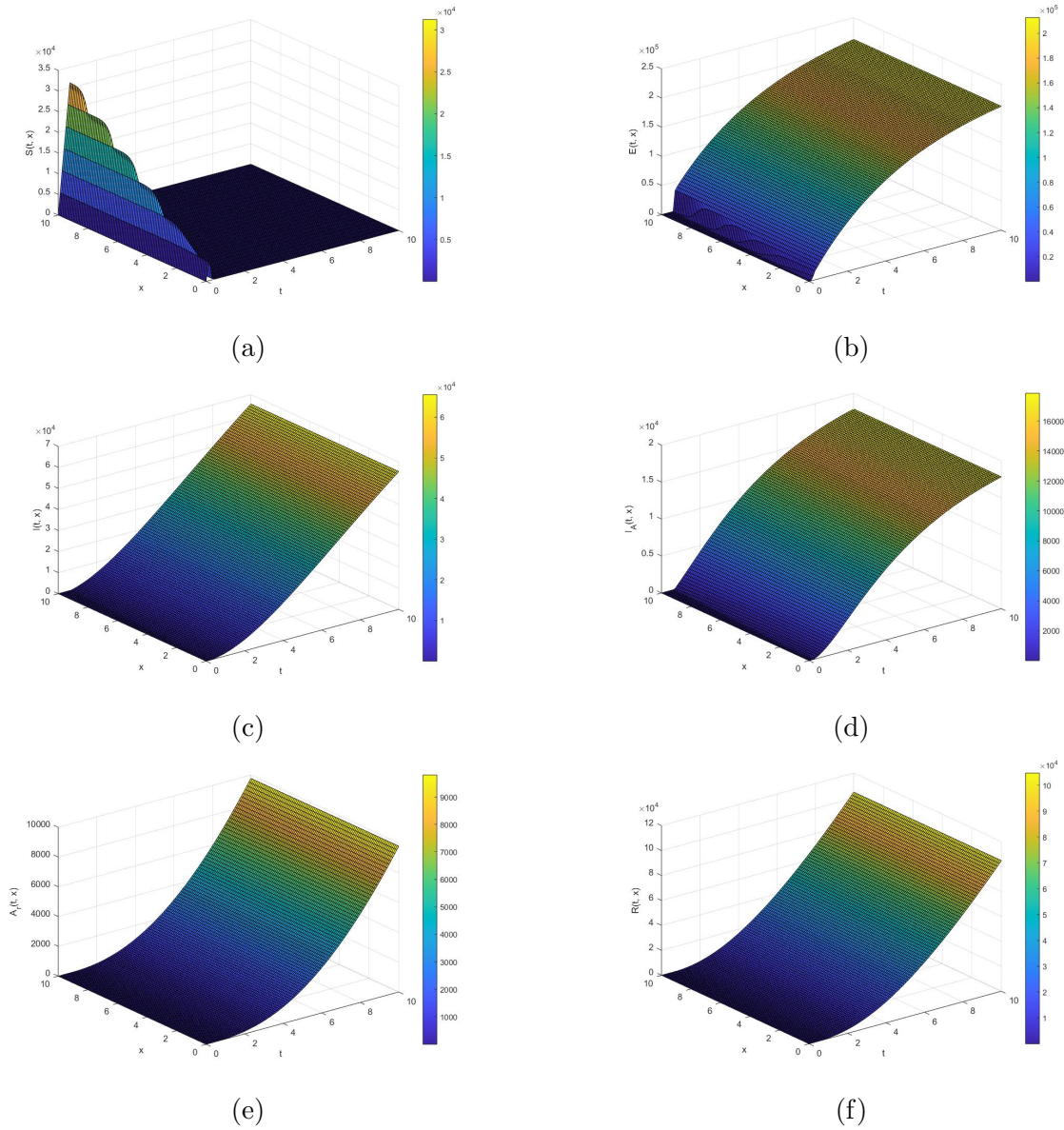
Figure 6.3: Spatiotemporal evolution of (a) Susceptible $S(t,x)$, (b) Expose $E(t,x)$, (c) Symptomatic Infection $I(t,x)$, (d) Asymptomatic Infection $I_A(t,x)$, (e) Aerosol $A_r(t,x)$, (f) Recovered $R(t,x)$

Figure 6.3 shows Spatiotemporal evolution of (a) Susceptible $S(t,x)$, (b) Expose $E(t,x)$, (c) Symptomatic Infection $I(t,x)$, (d) Asymptomatic Infection $I_A(t,x)$, (e) Aerosol $A_r(t,x)$, (f) Recovered $R(t,x)$.

The impact of various parameters on the basic reproduction number (R_0) can

be elucidated through several key groupings. From Figure 6.4, when examining R_0, β (rate of transmission through direct contact), and ψ (strength of intervention), it becomes evident that a high transmission rate and low intervention strength result in a high R_0, indicating an elevated spread of infection. Conversely, when the transmission rate is low and intervention strength is high, R_0 is significantly reduced, suggesting better control of the spread. This emphasizes the importance of effective interventions in reducing direct contact transmission. Stronger interventions can significantly lower R_0, even in scenarios with high transmission rates.
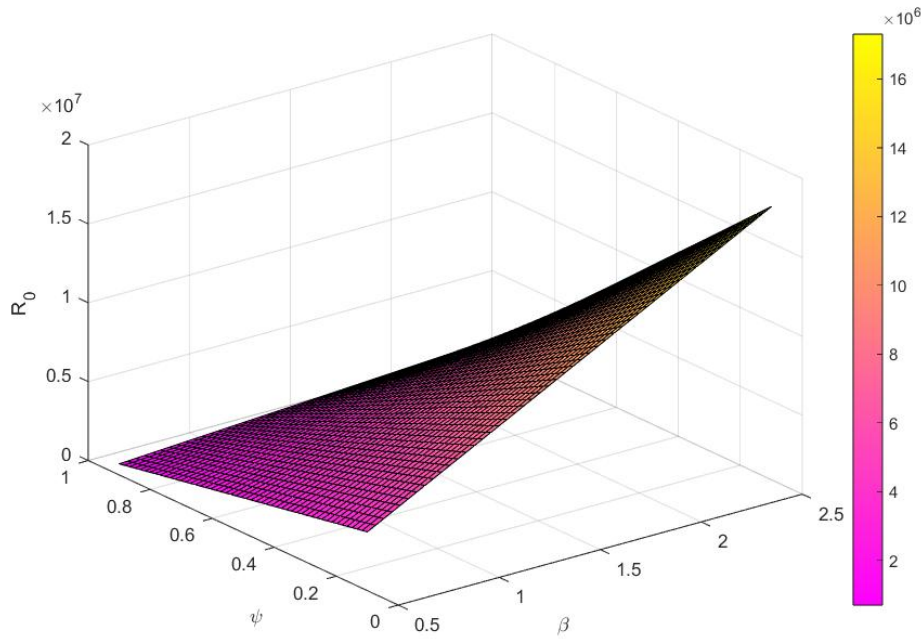
Figure 6.4: The numerical result exhibit that the dependence of R_0 of system on the rate of transmission β and Strength of intervention ψ.

In the context of R_0, β_r (rate of transmission through aerosol), and φ (rate at which asymptomatic individuals shed SARS-CoV-2), higher values of these parameters lead to a higher R_0, indicating a greater spread of infection (Figure 6.5). Lower values, on the other hand, result in a lower R_0. This grouping highlights the critical role of asymptomatic individuals in spreading the virus through aerosols. Measures to reduce aerosol transmission, such as mask mandates and improved ventilation, can significantly lower R_0.
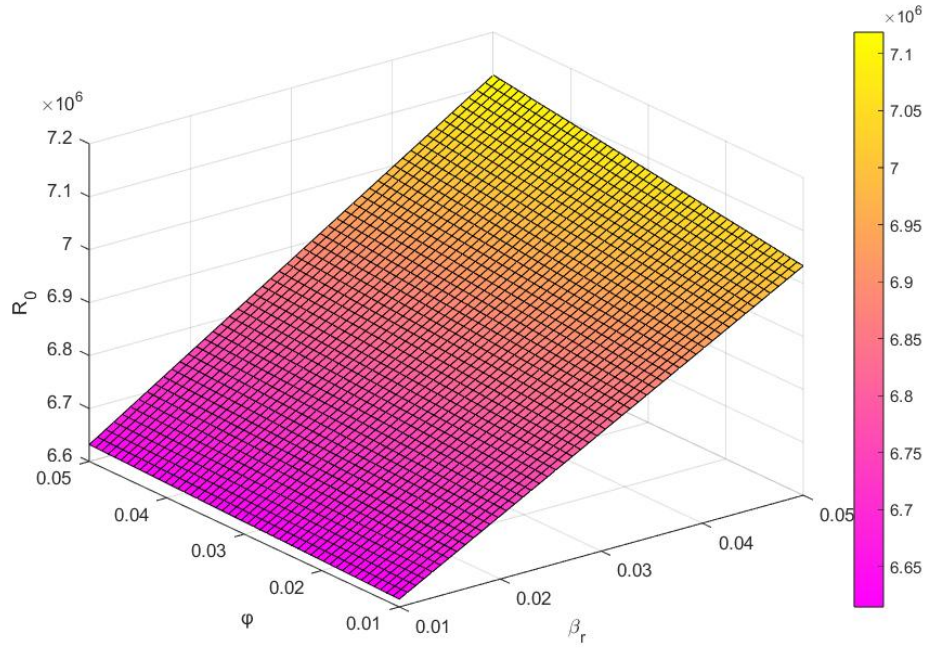
Figure 6.5: The numerical result exhibit that the dependence of R_0 of system on the rate of transmission through aerosol β_r and rate at which Asymptomatic infected individual shed SARS-CoV-2 φ.

From Figure 6.6, β (direct transmission), and β_r (aerosol transmission) together, high values of both parameters result in a very high R_0, indicating a high potential for outbreaks. Lower values suggest better control. This underscores the combined effect of direct and aerosol transmission on the spread of COVID-19, highlighting the need for interventions targeting both pathways to effectively reduce R_0.
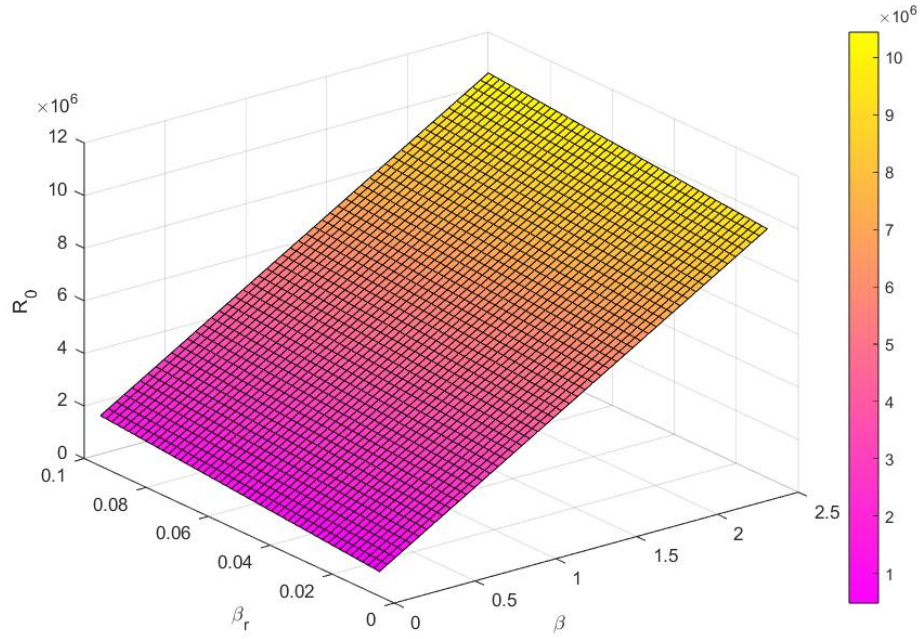
Figure 6.6: The numerical result exhibit that the dependence of R_0 of system on the rate of direct transmission β and rate of aerosol transmission β_r.

The impact of symptomatic individuals on the spread of the virus is evident when examining R_0, p_1 (fraction of the population moving from exposed to symptomatic class), and ϱ (rate at which symptomatic individuals shed SARS-CoV-2) (Figure 6.7). Higher values of these parameters lead to a higher R_0, while lower values result in a lower R_0. This grouping shows that a higher fraction of exposed individuals becoming symptomatic and shedding the virus significantly increases R_0. Reducing the shedding rate through treatment or isolation of symptomatic individuals can help lower R_0.
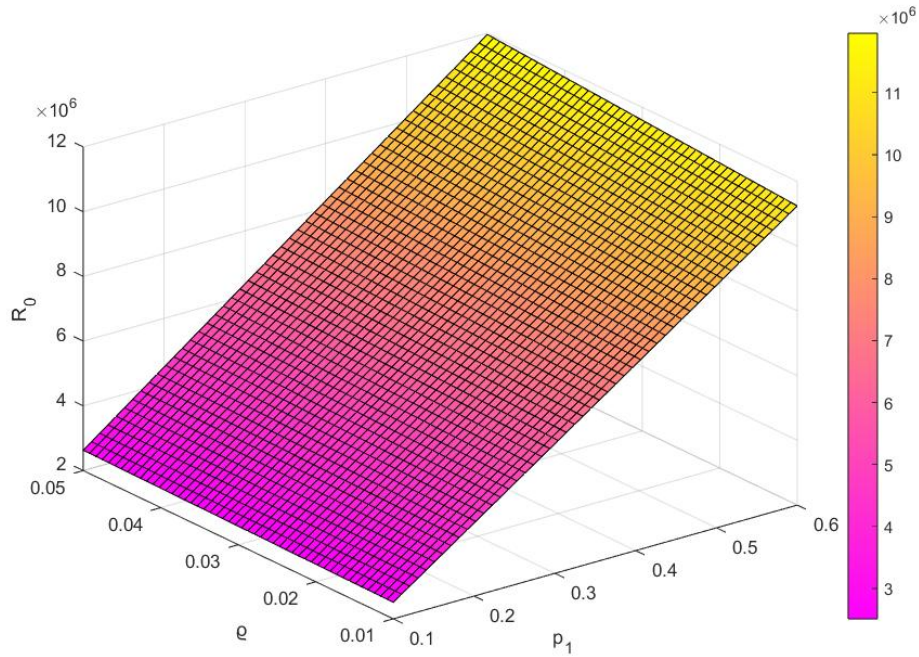
Figure 6.7: The numerical result exhibits that the dependence of R_0 of system on fraction of Exposed individual exhibit symptoms p_1 and rate at which Symptomatic infected individual shed SARS-CoV-2 ϱ.

Similarly, the role of asymptomatic individuals in transmission is highlighted by R_0, p_2 (fraction of the population moving from exposed to asymptomatic class), and φ (rate at which asymptomatic individuals shed SARS-CoV-2) (Figure 6.8). Higher values of these parameters lead to a higher R_0, while lower values result in a lower R_0. Managing asymptomatic individuals through testing and isolation is crucial for controlling the spread of the virus.
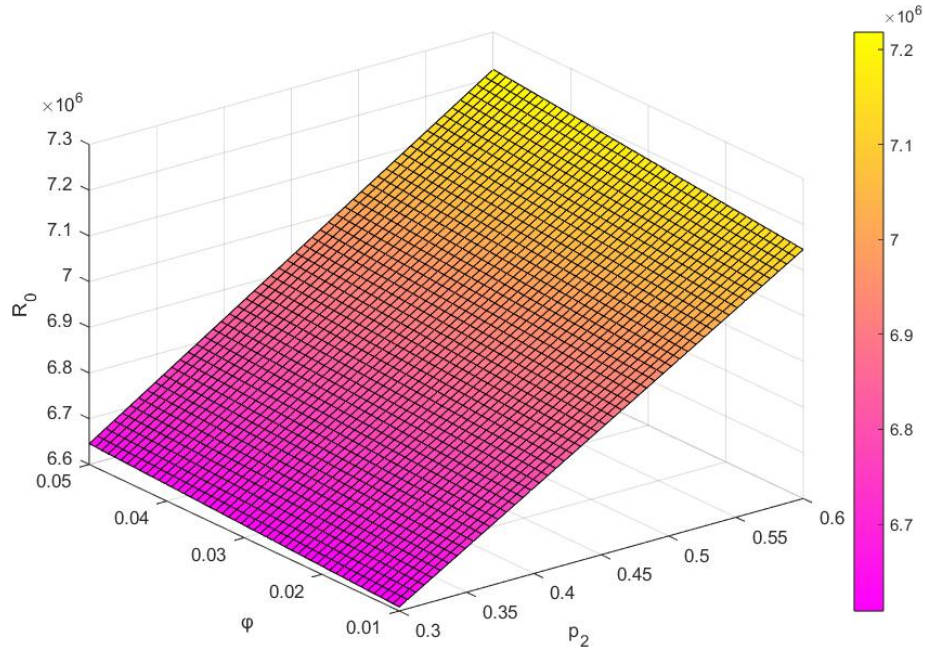
Figure 6.8: The numerical result exhibits that the dependence of R_0 of the system on a fraction of Exposed individuals becoming infected but do not show symptoms p_1 and the rate at which Asymptomatic infected individual shed SARS-CoV-2 φ.

Finally, the environmental factors influencing the spread of COVID-19 are evident in the grouping of R_0, φ (rate at which asymptomatic individuals shed SARS-CoV-2), and Υ (decay rate of the pathogen in the air) (Figure 6.9). Higher shedding rates from asymptomatic individuals and a slower decay rate of the virus in the air significantly increase R_0. Improving ventilation and air filtration systems to increase the decay rate of the pathogen can help reduce R_0.
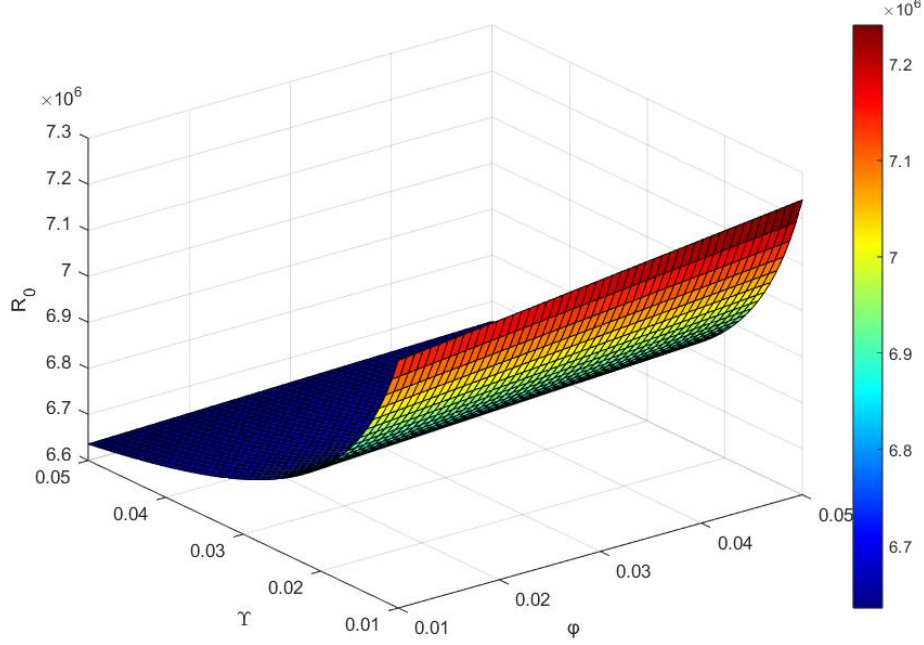
Figure 6.9: The numerical result exhibit that the dependence of R_0 of system on the rate at which Asymptomatic infected individual shed SARS-CoV-2 φ and the rate at which SARS-CoV-2 decay in the air Υ

6.12 Conclusion

This study has presented a comprehensive evaluation of COVID-19 dynamics using a deterministic $SEII_AA_rR$ reaction-diffusion model, incorporating both direct and aerosol transmission routes. By accounting for spatial heterogeneity and the prolonged airborne presence of SARS-CoV-2, the model offers nuanced insights into the spread of the virus across different regions. The assumption that symptomatic individuals shed more virus than asymptomatic carriers underscores the importance of targeted interventions.

We discussed the existence and uniqueness of Disease-Free Equilibrium and Endemic Equilibrium. Stability analysis of the equilibrium points shows Disease Free Equilibrium is locally asymptotically stable whenever the basic reproduction number, $R_0 < 1$, and is globally asymptotically stable whenever $R_0 < 1$. Also, Endemic Equilibrium is locally asymptotically stable whenever the basic reproduction number,

$R_0 > 1$. The steady Persistence of COVID-19 under $R_0 > 1$ of the reaction-diffusion system described by Eq. (6.4) is also examined.

Our findings emphasize that spatially targeted strategies, such as localized lockdowns and enhanced ventilation in high-risk areas, can significantly mitigate the spread of COVID-19. Specifically, our research highlights several key interventions that can effectively reduce the basic reproduction number, R_0, even in scenarios with high transmission rates (β).

First, we found that stronger interventions, characterized by higher values of ψ, can significantly reduce R_0. This indicates that robust public health measures, such as stringent lockdowns or movement restrictions in hotspot regions, are crucial in controlling the spread of the virus.

Second, reducing the shedding rate (ϱ) through effective treatment or isolation of symptomatic individuals plays a vital role in lowering R_0. This underscores the importance of prompt diagnosis and isolation of infected individuals to minimize the virus's presence in the community.

Third, managing asymptomatic individuals through regular testing and isolation is essential in controlling the spread of COVID-19. By identifying and isolating asymptomatic carriers, we can significantly reduce the virus shed (φ) by these individuals, thereby lowering the overall transmission potential.

Lastly, improving ventilation and air filtration systems to increase the decay rate of the pathogen in the air (Υ) is a critical intervention. Enhancing indoor air quality in public spaces, workplaces, and residential areas can help reduce the concentration of viral particles in the air, thereby decreasing the risk of airborne transmission and contributing to a lower R_0.

In summary, our findings suggest that a combination of spatially targeted lockdowns, effective isolation of symptomatic and asymptomatic individuals, and improvements in indoor air quality are essential strategies to mitigate the spread of COVID-19. These interventions, when implemented together, can significantly reduce the basic reproduction number and control the outbreak, even in the presence of high transmission rates.

This novel modelling approach highlights the critical role of integrating spatial and temporal dimensions in understanding and controlling infectious disease outbreaks, providing a valuable tool for policymakers and public health officials in managing current and future pandemics.

Chapter 7

Conclusions

This thesis has explored various facets of COVID-19 dynamics and control strategies through a series of interconnected studies, each building on the last to provide a comprehensive understanding of how to combat the pandemic effectively. Chapter 1 presents a general introduction to the COVID-19 pandemic and the role of mathematical modelling in understanding its spread and control.

Chapter 2 delved into the mathematical modelling of vaccination strategies against SARS-CoV-2, focusing on assessing coverage and efficacy. Our findings demonstrated the critical role of achieving high vaccination coverage and ensuring effective vaccines. By reducing the basic reproduction number R_0 and the number of infections, these strategies were shown to be paramount in mitigating the impact of COVID-19. The model highlighted that without substantial vaccine coverage and efficacy, the virus would continue to pose a significant threat.

Building on this foundation, Chapter 3 investigated the broader dynamics of SARS-CoV-2, incorporating various intervention strategies alongside vaccination. By combining measures such as social distancing and mask-wearing with vaccination efforts, we found a substantial decrease in the virus's transmission rate. This chapter underscored the necessity of a multifaceted approach, demonstrating that a synergistic combination of interventions is crucial for effectively curbing the spread of COVID-19 and protecting public health.

Chapter 4 expanded our understanding by examining the impact of precautionary measures on COVID-19 transmission through a Delay Differential Equation (DDE) approach. This model incorporated the notion of time delay introduced by interventions, such as social distancing and self-isolation, which postpone the transmission of the disease. Our analysis revealed that prompt and sustained implementation of

these measures is vital for reducing transmission rates. Delays in taking action can significantly increase infection rates, highlighting the importance of timely and proactive responses.

In Chapter 5, we introduced innovative reaction-diffusion techniques to optimize SARS-CoV-2 control measures. Recognizing that in the real world, populations cannot be considered homogenous, we incorporated heterogeneity to make our model more realistic. By acknowledging the diverse characteristics of different regions and populations, the model provided a more nuanced understanding of disease dynamics. This approach demonstrated that customized strategies based on local conditions could enhance the effectiveness of control measures, paving the way for more targeted interventions.

Chapter 6 presented a novel reaction-diffusion model to evaluate the dynamics of direct and aerosol transmission of COVID-19. Building on existing knowledge that SARS-CoV-2 can be transmitted through aerosols, with virus particles smaller than 5 micrometres remaining airborne for up to 3 hours and travelling more than 1.5 meters, we developed a model that emphasized the significant role of aerosol transmission, particularly in enclosed spaces. Strategies aimed at improving ventilation and air filtration, alongside traditional direct transmission interventions, were shown to be critical in mitigating overall transmission. This comprehensive model underscored the necessity of integrated approaches that address both direct and aerosol pathways to effectively control the virus's spread.

In conclusion, the chapters of this thesis collectively contribute to a deeper understanding of COVID-19 dynamics and the effectiveness of various intervention strategies. The mathematical models developed and analyzed provide valuable insights for public health policymakers, emphasizing the importance of a multifaceted approach in combating the pandemic. By integrating vaccination strategies, timely precautionary measures, and innovative modelling techniques, this research offers a robust framework for optimizing SARS-CoV-2 control and informs future responses to similar public health crises.

Bibliography

Abbas, M., Asghar, M., and Guo, Y. (2022). "Decision-making analysis of minimizing the death rate due to covid-19 by using q-rung orthopair fuzzy soft bonferroni mean operator". *Journal of Fuzzy Extensions and Applications*, **3(3)**, 231–248.

Acuna-Zegarra, M. A., Santana-Cibrian, M., and Velasco-Hernandez, J. X. (2020). "Modeling behavioral change and COVID-19 containment in mexico: A trade-off between lockdown and compliance". *Mathematical Biosciences*, **325**, 108370. https://doi.org/10.1016/j.mbs.2020.108370

Adelman, K., La Porta, A., Santangelo, T. J., Lis, J. T., Roberts, J. W., and Wang, M. D. (2002). "Single molecule analysis of rna polymerase elongation reveals uniform kinetic behavior". *Proceedings of the National Academy of Sciences*, **99(21)**, 13538–13543.

Agrawal, S., et al. (2020). "Covid-19 epidemic: Unlocking the lockdown in india (working paper)" [https://covid19.iisc.ac.in/wp-content/uploads/2020/04/Report-1-20200419-UnlockingTheLockdownInIndia.pdf].

Aguiar, M., Anam, V., Blyuss, K. B., Estadilla, C. D. S., Guerrero, B. V., Knopoff, D., Kooi, B. W., Srivastav, A. K., Steindorf, V., and Stollenwerk, N. (2022). "Mathematical models for dengue fever epidemiology: A 10-year systematic review". *Physics of Life Reviews*, **40**, 65–92.

Alemzewde, A., et al. (2023). "Mathematical model and analysis on the impacts of vaccination and treatment in the control of the covid-19 pandemic with optimal control" (A. Shafiq, Ed.). *Journal of Applied Mathematics*, 1–15.

Anastassopoulou, C., Russo, L., Tsakris, A., and Siettos, C. (2020). "Data-based analysis, modelling and forecasting of the COVID-19 outbreak". *PloS One*, **15(3)**, e0230405. https://doi.org/10.1371/journal.pone.0230405

Anderson, E., Turnham, P., Griffin, J., et al. (2020). "Consideration of the aerosol transmission for covid-19 and public health". *Risk Analysis*, **40(5)**, 902–907.

Anggriani, N., Ndii, M., Amelia, R., et al. (2022). "A mathematical covid-19 model considering asymptomatic and symptomatic classes with waning immunity". *Alexandria Engineering Journal*, **61**, 113–124.

Avila-Vales, E., and Pérez, Á. G. (2019). "Dynamics of a time-delayed sir epidemic model with logistic growth and saturated treatment". *Chaos, Solitons and Fractals*, **127**, 55–69.

Babus, A., Das, S., and Lee, S. (2023). "The optimal allocation of covid-19 vaccines". *Economics Letters*, **224**, Article 111008.

Bacaër, N. (2011). *A short history of mathematical population dynamics* (1st). Springer London.

Bajiya, V. P., Bugalia, S., and Tripathi, J. P. (2020). "Mathematical modeling of covid-19: Impact of non-pharmaceutical interventions in india". *Chaos: An Interdisciplinary Journal of Nonlinear Science*, **30(11)**, 113143.

Banerjee, S. (2021). *Mathematical modeling: Models, analysis and applications*. CRC Press.

Bernoulli, D. (1760). "Essai d'une nouvelle analyse de la mortalité causée par la petite vérole, et des avantages de l'inoculation pour la prévenir". *Histoire de l'Acad., Roy. Sci.(Paris) avec Mem*, 1–45.

Boldog, P., Tekeli, T., Vizi, Z., Denes, A., Bartha, F. A., and Rost, G. (2020). "Risk assessment of novel coronavirus COVID-19 outbreaks outside china". *Journal of Clinical Medicine*, **9(2)**. https://doi.org/10.3390/jcm9020571

Brauer, F. (2017). "Mathematical epidemiology: Past, present, and future". *Infectious Disease Modelling*, **2(2)**, 113–127. https://doi.org/10.1016/j.idm.2017.02.001

Buck, C. (1988). *The challenge of epidemiology: Issues and selected readings* (Vol. 505). Pan American Health Organization.

Bugalia, S., Tripathi, J. P., and Wang, H. (2021). "Mathematical modeling of intervention and low medical resource availability with delays: Applications to covid-19 outbreaks in spain and italy". *Mathematical Biosciences and Engineering*, **18(5)**, 5865–5920.

Carcione, J. M., Santos, J. E., Bagaini, C., and Ba, J. (2020). "A simulation of a covid-19 epidemic based on a deterministic seir model". *Frontiers in public health*, **8**, 230.

Castillo-Chavez, C. (2002). "On the computation of r. and its role on global stability carlos castillo-chavez*, zhilan feng, and wenzhang huang". *Mathematical approaches for emerging and reemerging infectious diseases: an introduction*, **1**, 229.

Chan, V. W.-S., Chiu, P. K.-F., Yee, C.-H., Yuan, Y., Ng, C.-F., and Teoh, J. Y.-C. (2020). "A systematic review on covid-19: Urological manifestations, viral rna detection and special considerations in urological conditions". *World journal of urology*, 1–12.

Chatterjee, K., Chatterjee, K., Kumar, A., and Shankar, S. (2020). "Healthcare impact of covid-19 epidemic in india: A stochastic mathematical model". *Medical Journal Armed Forces India*, **76**, 147–155. https://doi.org/10.1016/j.mjafi.2020.03.022

Chen, H., Guo, J., Wang, C., Luo, F., Yu, X., Zhang, W., Li, J., Zhao, D., Xu, D., Gong, Q., et al. (2020). "Clinical characteristics and intrauterine vertical transmission potential of covid-19 infection in nine pregnant women: A retrospective review of medical records". *The lancet*, **395(10226)**, 809–815.

Chen, T., Rui, J., Wang, Q., Zhao, Z., Cui, J., and Yin, L. (2020). "A mathematical model for simulating the phase-based transmissibility of a novel coronavirus". *Infectious Diseases of Poverty*, **9**, 24. https://doi.org/10.1186/s40249-020-00640-3

Chen, X., and Yu, B. (2020). "First two months of the 2019 coronavirus disease (COVID-19) epidemic in china: Real-time surveillance and evaluation with a second derivative model". *Glob Health Res Policy*, **5**, 7. https://doi.org/10.1186/s41256-020-00137-4

Chhetri, B., Vamsi, D., Prakash, D., et al. (2022). "Age structured mathematical modeling studies on covid-19 with respect to combined vaccination and medical treatment strategies". *Computational and Mathematical Biophysics*, **10**, 281–303.

Chiang, W.-H., Liu, X., and Mohler, G. (2022). "Hawkes process modeling of covid-19 with mobility leading indicators and spatial covariates". *International journal of forecasting*, **38(2)**, 505–520.

Chinazzi, M., and Davis, J. T. (2020). "The effect of travel restrictions on the spread of the 2019 novel coronavirus (COVID-19) outbreak". *Science*, **368(6489)**, eaba9757. https://doi.org/10.1126/science.aba9757

Choi, S., and Ki, M. (2020). "Estimating the reproductive number and the outbreak size of COVID-19 in korea". *Epidemiol Health*, **42**, e2020011. https://doi.org/10.4178/epih.e2020011

Cohen, J., and Normile, D. (2020). New sars-like virus in china triggers alarm.

Colavita, F., Lapa, D., Carletti, F., Lalle, E., Messina, F., Giombini, E., Quartu, S., Vairo, F., Ippolito, G., and Capobianchi, M. R. (2020). "Sars-cov-2 isolation from ocular secretions of a patient with covid-19 in italy with prolonged viral rna detection". *Annals of Internal Medicine*. https://doi.org/10.7326/M20-1176

Cooper, I., Mondal, A., and Antonopoulos, C. G. (2020). "A sir model assumption for the spread of covid-19 in different communities". *Chaos, Solitons and Fractals*, **139**, 110057.

COVID, W. (19). Vaccine tracker and landscape. 2021.

Creech, C. B., Walker, S. C., and Samuels, R. J. (2021). "Sars-cov-2 vaccines". *Jama*, **325(13)**, 1318–1320.

Das, A., Dhar, A., Kundu, A., and Goyal, S. (2020). "Covid-19: Analysis of a modified seir model, a comparison of different intervention strategies and projections for india" [http://dx.doi.org/10.1101/2020.06.04.20122580].

Das, D., Khajanchi, S., and Kar, T. (2019). "Influence of multiple re-infections in tuberculosis transmission dynamics: A mathematical approach". *2019 8th International Conference on Modeling Simulation and Applied Optimization (ICMSAO)*, 1–5. https://doi.org/10.1109/ICMSAO.2019.8880397

Das, D., Khajanchi, S., and Kar, T. (2020a). "The impact of the media awareness and optimal strategy on the prevalence of tuberculosis". *Applied Mathematics and Computation*, **366**, 124732. https://doi.org/10.1016/j.amc.2019.124732

Das, D., Khajanchi, S., and Kar, T. (2020b). "Transmission dynamics of tuberculosis with multiple re-infections". *Chaos, Solitons and Fractals*, **130**, 109450. https://doi.org/10.1016/j.chaos.2019.109450

Diekmann, O., and Heesterbeek, J. A. P. (2000). *Mathematical epidemiology of infectious diseases: Model building, analysis and interpretation* (Vol. 5). John Wiley and Sons.

Diekmann, O., Heesterbeek, J. A. P., and Metz, J. A. J. (1990). "On the definition and the computation of the basic reproduction ratio r 0 in models for infectious diseases in heterogeneous populations". *Journal of mathematical biology*, **28**, 365–382.

Dong, L., Tian, J., He, S., Zhu, C., Wang, J., Liu, C., and Yang, J. (2020). "Possible vertical transmission of sars-cov-2 from an infected mother to her newborn". *JAMA*, **323(18)**, 1846–1848.

Duan, M., Chang, L., and Jin, Z. (2019). "Turing patterns of an si epidemic model with cross-diffusion on complex networks". *Physica A: statistical mechanics and its applications*, **533**, 122023.

Eikenberry, S., Muncuso, M., Iboi, E., Phan, T., Kostelich, E., Kuang, Y., et al. (2020). "To mask or not to mask: Modeling the potential for face mask use by the general public to curtail the covid-19 pandemic". *Infectious Disease Modelling*, **5**, 293–308. https://doi.org/10.1016/j.idm.2020.04.001

Eikenberry, S. E., Mancuso, M., Iboi, E., Phan, T., Eikenberry, K., Kuang, Y., and et al. (2020). "To mask or not to mask: Modeling the potential for face mask use by the general public to curtail the COVID-19 pandemic". *Infect Dis Model*, **5**, 293–308. https://doi.org/10.1016/j.idm.2020.04.001

Fanelli, D., and Piazza, F. (2020). "Analysis and forecast of COVID-19 spreading in china, italy and france". *Chaos, Solitons and Fractals*. https://doi.org/10.1016/j.chaos.2020.109761

Ferretti, L., Wymant, C., Kendall, M., Zhao, L., Nurtay, A., Abeler-Dorner, L., and et al. (2020). "Quantifying SARS-CoV-2 transmission suggests epidemic control with digital contact tracing". *Science*, **368(6491)**. https://doi.org/10.1126/science.abb6936

Franco, E. (2020). "A feedback sir (fsir) model highlights advantages and limitations of infection-dependent mitigation strategies". *arXiv preprint arXiv:2004.13216*.

Fuk-Woo, C., et al. (2020). "Novel coronavirus indicating person-to-person transmission: A study of a family cluster". *The Lancet*, **395**, 514–523. https://doi.org/10.1016/S0140-6736(20)30154-9

Galli, M., Zardini, A., Gamshie, W., Santini, S., Tsegaye, A., Trentini, F., Marziano, V., Guzzetta, G., Manica, M., d'Andrea, V., et al. (2023).

Ganyani, T., Kremer, C., Chen, D., Torneri, A., Faes, C., Wallinga, J., and et al. (2020). "Estimating the generation interval for coronavirus disease (COVID-19) based on symptom onset data, march 2020". *Euro Surveillance*, **25(17)**. https://doi.org/10.2807/1560-7917.ES.2020.25.17.2000257

Goel, K., Kumar, A., and Nilam. (2020). "Nonlinear dynamics of a time-delayed epidemic model with two explicit aware classes, saturated incidences, and treatment". *Nonlinear Dynamics*, **101(3)**, 1693–1715.

Guo, Z., Wang, F.-B., and Zou, X. (2012). "Threshold dynamics of an infective disease model with a fixed latent period and non-local infections". *Journal of Mathematical Biology*, **65(6-7)**, 1387–1410.

Gupta, M., Mohanta, S. S., Rao, A., Parameswaran, G. G., Agarwal, M., Arora, M., Mazumder, A., Lohiya, A., Behera, P., Bansal, A., et al. (2021). "Transmission dynamics of the covid-19 epidemic in india and modeling optimal lockdown exit strategies". *International Journal of Infectious Diseases*, **103**, 579–589.

Halloran, M. E. (2001). "Concepts of transmission and dynamics". *Epidemiologic methods for the study of infectious diseases*, **56**, 85–96.

Han, Q., Lin, Q., Ni, Z., and You, L. (2020). "Uncertainties about the transmission routes of 2019 novel coronavirus". *Influenza and Other Respiratory Viruses*, **14(4)**, 470.

Hauser, A., Counotte, M. J., Margossian, C. C., Konstantinoudis, G., Low, N., Althaus, C. L., and et al. (2020). "Estimation of SARS-CoV-2 mortality during the early stages of an epidemic: A modelling study in hubei, china and northern italy" [Preprint]. https://doi.org/10.1101/2020.03.04.20031104

Hauser, A., Counotte, M. J., Margossian, C. C., Konstantinoudis, G., Low, N., Althaus, C. L., and Riou, J. (2020). "Estimation of sars-cov-2 mortality during the early stages of an epidemic: A modeling study in hubei, china, and six regions in europe". *PLoS medicine*, **17(7)**, e1003189.

Hazarika, B. B., and Gupta, D. (2020). "Modelling and forecasting of covid-19 spread using wavelet-coupled random vector functional link networks". *Applied Soft Computing*, **96**, 106626.

Hellewell, J., Abbott, S., Gimma, A., Bosse, N. I., Jarvis, C. I., Russell, T. W., and et al. (2020). "Feasibility of controlling COVID-19 outbreaks by isolation of cases and contacts". *The Lancet Global Health*, **8(4)**, E488–E496. https://doi.org/10.1016/s2214-109x(20)30074-7

Hethcote, H. W. (2000). "The mathematics of infectious diseases". *SIAM Review*, **42(4)**, 599–653. https://doi.org/10.1137/S0036144500371907

Hethcote, H. W. (1989). Three basic epidemiological models. In *Applied mathematical ecology* (pp. 119–144). Springer.

Holshue, M. L., DeBolt, C., Lindquist, S., Lofy, K. H., Wiesman, J., Bruce, H., Spitters, C., Ericson, K., Wilkerson, S., Tural, A., et al. (2020). "First case of 2019 novel coronavirus in the united states". *New England journal of medicine*, **382(10)**, 929–936.

Hou, C., Chen, J., Zhou, Y., Hua, L., Yuan, J., He, S., and et al. (2020). "The effectiveness of quarantine of wuhan city against the corona virus disease 2019 (COVID-19): A well-mixed seir model analysis". *Journal of Medical Virology.* https://doi.org/10.1002/jmv.25827

Hu, Z., Cui, Q., Han, J., Wang, X., Sha, W. E. I., and Teng, Z. (2020). "Evaluation and prediction of the COVID-19 variations at different input population and quarantine strategies, a case study in guangdong province, china". *International Journal of Infectious Diseases*, **95**, 231–240. https://doi.org/10.1016/j.ijid.2020.04.010

Hufnagel, L., Brockmann, D., and Geisel, T. (2004). "Forecast and control of epidemics in a globalized world". *Proceedings of the national academy of sciences*, **101(42)**, 15124–15129.

Imai, N., et al. (2020). "Estimating the potential total number of novel coronavirus cases in wuhan city, china". https://www.preventionweb.net/news/view/70092

Jones, W. H., et al. (1868). "Hippocrates collected works i". *Cambridge Harvard University Press. Retrieved on March*, **25**, 2008.

Kai, D., and Guy-PhilippeGoldstein. (2020). "Universal masking is urgent in the COVID-19 pandemic: Seir and agent based models, empirical validation,policy recommendations".

Kendall, D. G. (1956). "Deterministic and stochastic epidemics in closed populations". *Proceedings of the Third Berkeley Symposium on Mathematical Statistics and Probability, 1954–1955*, **4**, 149–165.

Kermack, W. O., and McKendrick, A. G. (1927). "A contribution to the mathematical theory of epidemics". *Proceedings of the royal society of london. Series A, Containing papers of a mathematical and physical character*, **115(772)**, 700–721.

Khajanchi, S., Das, D., and Kar, T. (2018). "Dynamics of tuberculosis transmission with exogenous reinfections and endogenous reactivation". *Physica A: Statistical Mechanics and its Applications*, **497**, 52–71. https://doi.org/10.1016/j.physa.2018.01.088

Khajanchi, S., Sarkar, K., and Mondal, J. (2020). "Dynamics of the covid-19 pandemic in india". *arXiv preprint arXiv:2005.06286.* https://doi.org/10.48550/arXiv.2005.06286

Khajanchi, S., Bera, S., and Roy, T. K. (2021). "Mathematical analysis of the global dynamics of a htlv-i infection model, considering the role of cytotoxic t-lymphocytes". *Mathematics and Computers in Simulation*, **180**, 354–378.

Khajanchi, S., and Sarkar, K. (2020). "Forecasting the daily and cumulative number of cases for the covid-19 pandemic in india". *Chaos: An interdisciplinary journal of nonlinear science*, **30(7)**, 071101.

Khasteh, M., Refahi Sheikhani, A., and Shariffar, F. (2022). "A novel numerical approach for distributed order time fractional covid-19 virus model". *Journal of Applied Research in Industrial Engineering*, **9(4)**, 442–453.

Killerby, M. E., Biggs, H. M., Midgley, C. M., Gerber, S. I., and Watson, J. T. (2020). "Middle east respiratory syndrome coronavirus transmission". *Emerging infectious diseases*, **26(2)**, 191.

Kissler, S. M., Tedijanto, C., Goldstein, E., Grad, Y. H., and Lipsitch, M. (2020). "Projecting the transmission dynamics of SARS-CoV-2 through the postpandemic period". *Science*, **368(6493)**, 860–868. https://doi.org/10.1126/science.abb5793

Koo, J. R., Cook, A. R., Park, M., and Sun, Y. (2020). "Interventions to mitigate early spread of SARS-CoV-2 in singapore: A modelling study". *The Lancet Infectious Diseases*. https://doi.org/10.1016/S1473-3099(20)30162-6

Korobeinikov, A., and Wake, G. C. (2002). "Lyapunov functions and global stability for sir, sirs, and sis epidemiological models". *Applied Mathematics Letters*, **15(8)**, 955–960.

Kot, M. (2001). *Elements of mathematical ecology*. Cambridge University Press.

Kraemer, M. U. G., Yang, C.-H., Gutierrez, B., Wu, C.-H., Klein, B., Pigott, D. M., and et al. (2020). "The effect of human mobility and control measures on the COVID-19 epidemic in china". *Science*, **368(6490)**, 493–497. https://doi.org/10.1126/science.abb4218

Kucharski, A. J., Russell, T. W., Diamond, C., Liu, Y., Edmunds, J., Funk, S., Eggo, R. M., Sun, F., Jit, M., Munday, J. D., et al. (2020). "Early dynamics of transmission and control of covid-19: A mathematical modelling study". *The lancet infectious diseases*, **20(5)**, 553–558.

Kumar, A., and Nilam. (2019). "Stability of a delayed sir epidemic model by introducing two explicit treatment classes along with nonlinear incidence rate and holling type treatment". *Computational and Applied Mathematics*, **38(3)**, 130.

Kumar, V. M., Pandi-Perumal, S. R., Trakht, I., and Thyagarajan, S. P. (2021). "Strategy for covid-19 vaccination in india: The country with the second highest population and number of cases". *npj Vaccines*, **6(1)**, 60.

Kuniya, T. (2020). "Prediction of the epidemic peak of coronavirus disease in japan, 2020". *Clinical Medicine*. https://doi.org/10.3390/jcm9030789

Kuznetsov, Y. A., and Kuznetsov, Y. A. (2004). "Numerical analysis of bifurcations". *Elements of applied bifurcation theory*, 505–585.

La Salle, J., and Lefschetz, S. (1961). *Stability by liapunov's direct method*. Academic Press.

La Salle, J. P. (1976). *The stability of dynamical systems*. SIAM.

Li, L., Yang, Z., Dang, Z., Meng, C., Huang, J., Meng, H., and et al. (2020). "Propagation analysis and prediction of the COVID-19". *Infectious Disease Modelling*, **5**, 282–292. https://doi.org/10.1016/j.idm.2020.03.002

Li, L., Yang, Z., Dang, Z., Meng, C., Huang, J., Meng, H., Wang, D., Chen, G., Zhang, J., Peng, H., et al. (2020). "Propagation analysis and prediction of the covid-19". *Infectious Disease Modelling*, **5**, 282–292.

Li, M. Y., and Muldowney, J. S. (1995). "Global stability for the seir model in epidemiology". *Mathematical biosciences*, **125(2)**, 155–164.

Li, Q., Guan, X., Wu, P., Wang, X., Zhou, L., Tong, Y., and et al. (2020). "Early transmission dynamics in wuhan, china, of novel coronavirus-infected pneumonia". *New England Journal of Medicine*, **382**, 1199–1207. https://doi.org/10.1056/NEJMoa2001316

Li, R., Pei, S., Chen, B., Song, Y., Zhang, T., Yang, W., and Shaman, J. (2020). "Substantial undocumented infection facilitates the rapid dissemination of novel coronavirus (sars-cov-2)". *Science*, **368(6490)**, 489–493.

Li, R., Pei, S., Chen, B., Song, Y., Zhang, T., Yang, W., and et al. (2020). "Substantial undocumented infection facilitates the rapid dissemination of novel coronavirus (COVID-19)". https://doi.org/10.1101/2020.02.14.20023127

Li, Y.-D., Chi, W.-Y., Su, J.-H., Ferrall, L., Hung, C.-F., and Wu, T.-C. (2020). "Coronavirus vaccine development: From sars and mers to covid-19". *Journal of biomedical science*, **27**, 1–23.

Lin, X., and Wang, H. (2012). "Stability analysis of delay differential equations with two discrete delays". *Canadian applied mathematics quarterly*, **20(4)**, 519–533.

Liu, L., Wei, Q., Alvarez, X., Wang, H., Du, Y., Zhu, H., Jiang, H., Zhou, J., Lam, P., Zhang, L., et al. (2011). "Epithelial cells lining salivary gland ducts are early target cells of severe acute respiratory syndrome coronavirus infection in the upper respiratory tracts of rhesus macaques". *Journal of virology*, **85(8)**, 4025–4030.

Liu, Y., Ning, Z., Chen, Y., Guo, M., Liu, Y., Gali, N. K., Sun, L., Duan, Y., Cai, J., Westerdahl, D., et al. (2020). "Aerodynamic characteristics and rna concentration of sars-cov-2 aerosol in wuhan hospitals during covid-19 outbreak (preprint)".

Liu, Z., Magal, P., Seydi, O., and Webb, G. (2020a). "Predicting the cumulative number of cases for the covid-19 epidemic in china from early data". *arXiv preprint arXiv:2002.12298*. https://doi.org/10.48550/arXiv.2002.12298

Liu, Z., Magal, P., Seydi, O., and Webb, G. (2020b). "A COVID-19 epidemic model with latency period". *Infectious Disease Modelling*. https://doi.org/10.1016/j.idm.2020.03.003

Liu, Z., Magal, P., Seydi, O., and Webb, G. (2020c). "Predicting the cumulative number of cases for the COVID-19". https://doi.org/10.1101/2020.03.11.20034314

Loli Piccolomini, E., and Zama, F. (2020). "Monitoring italian covid-19 spread by a forced seird model". *PloS one*, **15(8)**, e0237417.

Lotfi, M., Hamblin, M. R., and Rezaei, N. (2020). "Covid-19: Transmission, prevention, and potential therapeutic opportunities". *Clinica chimica acta*, **508**, 254–266.

Lu, C., Liu, X., and Jia, Z. (2020). "2019-ncov transmission through the ocular surface must not be ignored". *Lancet*, **395(10224)**, e39.

Lu, C. W., Liu, X. F., and Jia, Z. (2020). "2019-ncov transmission through the ocular surface must not be ignored". *The Lancet*, **395(10224)**, e39.

Lu, H., Stratton, C. W., and Tang, Y.-W. (2020). "Outbreak of pneumonia of unknown etiology in wuhan, china: The mystery and the miracle". *Journal of medical virology*, **92(4)**, 401.

Magal, P., and Webb, G. (2020). "Predicting the number of reported and unreported cases for the COVID-19 epidemic in south korea, italy, france and germany". https://doi.org/10.1101/2020.03.21.20040154

Mahajan, A., Sivadas, N. A., and Solanki, R. (2020). "An epidemic model sipherd and its application for prediction of the spread of covid-19 infection in india". *Chaos, Solitons and Fractals*, **140**, 110156.

Maier, B. F., and Brockmann, D. (2020). "Effective containment explains subexponential growth in recent confirmed COVID-19 cases in china". *Science*, **368(6492)**, 742–746. https://doi.org/10.1126/science.abb4557

Mandal, M., Jana, S., Nandi, S. K., Khatua, A., Adak, S., and Kar, T. K. (2020). "A model based study on the dynamics of COVID-19: Prediction and control". *Chaos, Solitons, and Fractals*, 109889. https://doi.org/10.1016/j.chaos.2020.109889

Mandal, S., Bhatnagar, T., and Arinaminpathy, N. (2020). "Prudent public health intervention strategies to control the coronavirus disease 2019 transmission in india: A mathematical model-based approach". *Indian Council of Medical Research*. https://doi.org/10.4103/ijmr.IJMR_504_20

Martin, R., and Smith, H. (1990). "Abstract functional-differential equations and reaction-diffusion systems". *Transactions of the American Mathematical Society*, **321(1)**, 1–44.

Mathieu, E., Ritchie, H., Ortiz-Ospina, E., Roser, M., Hasell, J., Appel, C., Giattino, C., and Rodés-Guirao, L. (2021). "A global database of covid-19 vaccinations". *Nature human behaviour*, **5(7)**, 947–953.

"Modeling covid-19 scenarios for the united states". (2021). *Nature medicine*, **27(1)**, 94–105.

Mohammed, I., Nauman, A., Paul, P., Ganesan, S., Chen, K.-H., Jalil, S. M. S., Jaouni, S. H., Kawas, H., Khan, W. A., Vattoth, A. L., Al-Hashimi, Y. A., Fares, A., Zeghlache, R., and Zakaria, D. (2022). "The efficacy and effectiveness of the covid-19 vaccines in reducing infection, severity, hospitalization, and mortality: A systematic review". *Human vaccines and immunotherapeutics*, **18(1)**, 2027160. https://doi.org/10.1080/21645515.2022.2027160

Msemburi, W., Karlinsky, A., Knutson, V., Aleshin-Guendel, S., Chatterji, S., and Wakefield, J. (2023). "The who estimates of excess mortality associated with the covid-19 pandemic". *Nature*, **613(7942)**, 130–137.

Mukandavire, Z., Garira, W., and Chiyaka, C. (2007). "Asymptotic properties of an hiv/aids model with a time delay". *Journal of Mathematical Analysis and Applications*, **330(2)**, 916–933.

Munayco, C. V., Tariq, A., Rothenberg, R., Soto-Cabezas, G. G., Reyes, M. F., Valle, A., et al. (2020). "Early transmission dynamics of COVID-19 in a southern hemisphere setting: Lima-peru: February 29th-march 30th, 2020". *Infectious Disease Modelling*. https://doi.org/10.1016/j.idm.2020.05.001

Muniz-Rodriguez, K., Fung, I. C.-H., Ferdosi, S. R., Ofori, S. K., Lee, Y., Tariq, A., and et al. (2020). "Severe acute respiratory syndrome coronavirus 2 transmission potential, iran, 2020". *Emerging Infectious Diseases*, **26(8)**. https://doi.org/10.3201/eid2608.200536

Nadim, S., Ghosh, I., and Chattopadhyay, J. (2020). "Short-term predictions and prevention strategies for covid-2019: A model based study". *arXiv preprint arXiv:2003.08150*. https://doi.org/10.48550/arXiv.2003.08150

Nagy, A., and Alhatlani, B. (2021). "An overview of current covid-19 vaccine platforms". *Computational and structural biotechnology journal*, **19**, 2508–2517.

Naqvi, A. A. T., Fatima, K., Mohammad, T., Fatima, U., Singh, I. K., Singh, A., Atif, S. M., Hariprasad, G., Hasan, G. M., and Hassan, M. I. (2020). "Insights into sars-cov-2 genome, structure, evolution, pathogenesis and therapies: Structural genomics approach". *Biochimica et Biophysica Acta (BBA)-Molecular Basis of Disease*, **1866(10)**, 165878.

Ngonghala, C. N., Iboi, E., Eikenberry, S., Scotch, M., MacIntyre, C. R., Bonds, M. H., and et al. (2020). "Mathematical assessment of the impact of nonpharmaceutical interventions on curtailing the 2019 novel Coronavirus". *Mathematical Biosciences*, **325**, 108364. https://doi.org/10.1016/j.mbs.2020.108364

Ngonghala, C., Iboi, E., Eikenberry, S., Scotch, M., and Gumel, A. (2019). "Mathematical assessment of the impact of non-pharmaceutical interventions on curtailing the 2019 novel coronavirus". *Mathematical Biosciences*, **325**, 108364. https://doi.org/10.1016/j.mbs.2020.108364

Núñez-Delgado, A. (2020). "What do we know about the sars-cov-2 coronavirus in the environment?" *Science of the Total Environment*, **727**, 138647.

Omori, R., Mizumoto, K., and Chowell, G. (2020). "Changes in testing rates could mask the novel coronavirus disease (COVID-19) growth rate". *International Journal of Infectious Diseases*, **94**, 116–118. https://doi.org/10.1016/j.ijid.2020.04.021

Organization, W. H., et al. (2020a). "Coronavirus disease 2019 (covid-19): Situation report, 73".

Organization, W. H., et al. (2020b). *Infection prevention and control during health care when novel coronavirus (ncov) infection is suspected: Interim guidance, 25 january 2020* (tech. rep.). World Health Organization.

Organization, W. H., et al. (2020c). "Naming the coronavirus disease (covid-19) and the virus that causes it". *Brazilian Journal of Implantology and Health Sciences*, **2(3)**.

Organization, W. H., et al. (2021). "Status of covid-19 vaccines within who eul/pq evaluation process. 2021". *Available from:[cited 2022 February 1]*.

Organization, W. H. (2023). "Who research agenda for hand hygiene in health care 2023–2030: Summary".

Penn, M., and Donnelly, C. (2023). "Asymptotic analysis of optimal vaccination policies". *Bulletin of Mathematical Biology*, **85**, 15.

Perc, M., Miksic, N., Slavinec, M., and Stozer, A. (2020). "Forecasting covid-19". *Frontiers in Physics*, **8**, 127. https://doi.org/10.3389/fphy.2020.00127

Perko, L. (2013). *Differential equations and dynamical systems* (Vol. 7). Springer Science and Business Media.

Pulla, P. (2020). "Covid-19: India imposes lockdown for 21 days and cases rise". *BMJ*, **368**. https://doi.org/10.1136/bmj.m1251.

Rai, R., Khajanchi, S., Tiwari, P., Venturino, E., and Misra, A. (2021). "Impact of social media advertisements on the transmission dynamics of covid-19 pandemic in india". *Journal of Applied Mathematics and Computing*. https://doi.org/10.1007/s12190-021-01507-y

Ray, D., Salvatore, M., Bhattacharyya, R., Wang, L., Du, J., Mohammed, S., Purkayastha, S., Halder, A., Rix, A., Barker, D., et al. (2020). "Predictions, role of interventions and effects of a historic national lockdown in india's response to the covid-19 pandemic: Data science call to arms". *Harvard data science review*, **2020(Suppl 1)**.

Rezapour, S., Mohammadi, H., and Samei, M. E. (2020). "Seir epidemic model for covid-19 transmission by caputo derivative of fractional order". *Advances in difference equations*, **2020(1)**, 1–19.

Rm, A. (1991). "Infectious diseases of humans". *Aust J Public Health*, **16**, 208–212.

Roosa, K., Lee, Y.-H., Luo, R., Kirpich, A., Rothenberg, R., Hyman, J. M., and et al. (2020a). "Real-time forecasts of the COVID-19 epidemic in china from february 5th to february 24th, 2020". *Infectious Disease Modelling*, **5**, 256–263. https://doi.org/10.1016/j.idm.2020.02.002

Roosa, K., Lee, Y.-H., Luo, R., Kirpich, A., Rothenberg, R., Hyman, J. M., and et al. (2020b). "Short-term forecasts of the COVID-19 epidemic in guangdong and zhejiang, china: February 13-23, 2020". *Journal of Clinical Medicine*, **9(2)**, 596. https://doi.org/10.3390/jcm9020596

Ross, R. (1916). "An application of the theory of probabilities to the study of a priori pathometry. part i". *Proceedings of the Royal Society of London. Series A,*

Containing Papers of a Mathematical and Physical Character, **92(638)**, 204–230. https://doi.org/10.1098/rspa.1916.0007

Ross, R., and Hudson, H. (1917a). "An application of the theory of probabilities to the study of a priori pathometry. part ii". *Proceedings of the Royal Society of London. Series A, Containing Papers of a Mathematical and Physical Character*, **93(650)**, 212–225. https://doi.org/10.1098/rspa.1917.0014

Ross, R., and Hudson, H. (1917b). "An application of the theory of probabilities to the study of a priori pathometry. part iii". *Proceedings of the Royal Society of London. Series A, Containing Papers of a Mathematical and Physical Character*, **93(650)**, 225–240. https://doi.org/10.1098/rspa.1917.0015

Ruan, S., and Wei, J. (2003). "On the zeros of transcendental functions with applications to stability of delay differential equations with two delays". *Dynamics of Continuous Discrete and Impulsive Systems Series A*, **10**, 863–874.

Samui, P., Mondal, J., and Khajanchi, S. (2020). "A mathematical model for covid-19 transmission dynamics with a case study of india". *Chaos, Solitons and Fractals*, **140**, 110173. https://doi.org/10.1016/j.chaos.2020.110173

Sanche, S., Lin, Y. T., Xu, C., Romero-Severson, E., Hengartner, N., and Ke, R. (2020). "High contagiousness and rapid spread of severe acute respiratory syndrome coronavirus 2". *Emerging Infectious Diseases*, **26(7)**. https://doi.org/10.3201/eid2607.200282

Sanghera, J., Pattani, N., Hashmi, Y., Varley, K. F., Cheruvu, M. S., Bradley, A., and Burke, J. R. (2020). "The impact of sars-cov-2 on the mental health of healthcare workers in a hospital setting—a systematic review". *Journal of occupational health*, **62(1)**, e12175.

Santarpia, J. L., Rivera, D. N., Herrera, V., Morwitzer, M. J., Creager, H., Santarpia, G. W., Crown, K. K., Brett-Major, D. M., Schnaubelt, E., Broadhurst, M. J., et al. (2020). "Transmission potential of sars-cov-2 in viral shedding observed at the university of nebraska medical center". *MedRxiv*.

Sarkar, K., Khajanchi, S., and Nieto, J. (2020). "Modeling and forecasting of the covid-19 pandemic in india". *Chaos, Solitons and Fractals*, **139**, 110049. https://doi.org/10.1016/j.chaos.2020.110049

Scarabel, F., Pellis, L., Bragazzi, N. L., and Wu, J. (2020). "Canada needs to rapidly escalate public health interventions for its COVID-19 mitigation strategies". *Infectious Disease Modelling*. https://doi.org/10.1016/j.idm.2020.03.004

Senapati, A., Rana, S., Das, T., and Chattopadhyay, J. (2021). "Impact of intervention on the spread of covid-19 in india: A model based study". *Journal of Theoretical Biology*, **523**, 110711.

Sene, N. (2020). "Sir epidemic model with mittag–leffler fractional derivative". *Chaos, Solitons and Fractals*, **137**, 109833.

Shekatkar, S., et al. (2020). "Indsci-sim: A state-level epidemiological model for india" [https://indscicov.in/indscisim].

Shiferaw, K., and Lemecha, O. (2022). "Mathematical modeling for covid-19 transmission dynamics: A case study in ethiopia". *Results in Physics*, **34**, 105191.

Shim, E., Tariq, A., Choi, W., Lee, Y., and Chowell, G. (2020). "Transmission potential and severity of COVID-19 in south korea". *International Journal of Infectious Diseases*, **93**, 339–344. https://doi.org/10.1016/j.ijid.2020.03.031

Simon, C. M. (2020). "The sir dynamic model of infectious disease transmission and its analogy with chemical kinetics". *PeerJ Physical Chemistry*, **2**, e14.

Singh, A., and Arquam, M. (2022). "Epidemiological modeling for covid-19 spread in india with the effect of testing". *Physica A: Statistical Mechanics and its Applications*, **592**, 126774.

Smith, H. L. (1995). *Monotone dynamical systems: An introduction to the theory of competitive and cooperative systems: An introduction to the theory of competitive and cooperative systems*. American Mathematical Soc.

Stafford, E., Dimitrov, D., Ceballos, R., Campelia, G., and Matrajt, L. (2023). "Retrospective analysis of equity-based optimization for covid-19 vaccine allocation". *PNAS Nexus*, **2**, Article pgad283.

Sun, T., and Weng, D. (2020). "Estimating the effects of asymptomatic and imported patients on COVID-19 epidemic using mathematical modeling". *Journal of Medical Virology*. https://doi.org/10.1002/jmv.25939

Sweilam, N., Al-Mekhlafi, S., Mohammed, Z., and Baleanu, D. (2020). "Optimal control for variable order fractional hiv/aids and malaria mathematical models with multi-time delay". *Alexandria Engineering Journal*, **59(5)**, 3149–3162.

Tang, B., Bragazzi, N., Li, Q., Tang, S., Xiao, Y., and Wu, J. (2020). "An updated estimation of the risk of transmission of the novel coronavirus (2019-ncov)". *Infectious Disease Modelling*, **5**, 248–255. https://doi.org/10.1016/j.idm.2020.02.001

Tang, B., Wang, X., Li, Q., Bragazzi, N. L., Tang, S., Xiao, Y., and Wu, J. (2020). "Estimation of the transmission risk of the 2019-ncov and its implication for public health interventions". *Journal of clinical medicine*, **9(2)**, 462.

Tang, B., Wang, X., Li, Q., Bragazzi, N. L., Tang, S., Xiao, Y., and et al. (2020). "Estimation of the transmission risk of the 2019-ncov and its implication for public health interventions". *Journal of Clinical Medicine*, **9(2)**, 462. https://doi.org/10.3390/jcm9020462

Tellier, R., Li, Y., Cowling, B., et al. (2019). "Recognition of aerosol transmission of infectious agents: A commentary". *BMC Infectious Diseases*, **19(1)**, 1–9.

Thieme, H. R. (1992). "Convergence results and a poincaré-bendixson trichotomy for asymptotically autonomous differential equations". *Journal of mathematical biology*, **30(7)**, 755–763.

Thompson, R. N. (2020). "Novel coronavirus outbreak in wuhan, china, 2020: Intense surveillance is vital for preventing sustained transmission in new locations". *Journal of Clinical Medicine*, **9(2)**, 498. https://doi.org/10.3390/jcm9020498

Tipsri, S., and Chinviriyasit, W. (2014). "Stability analysis of seir model with saturated incidence and time delay". *International Journal of Applied Physics and Mathematics*, **4(1)**, 42.

Tiwari, V., Deyal, N., and Bisht, N. S. (2020). "Mathematical modeling based study and prediction of covid-19 epidemic dissemination under the impact of lockdown in india". *Frontiers in Physics*, **8**, 586899.

To, K. K.-W., Tsang, O. T.-Y., Yip, C. C.-Y., Chan, K.-H., Wu, T.-C., Chan, J. M.-C., Leung, W.-S., Chik, T. S.-H., Choi, C. Y.-C., Kandamby, D. H., et al. (2020). "Consistent detection of 2019 novel coronavirus in saliva". *Clinical Infectious Diseases*, **71(15)**, 841–843.

Tobías, A. (2020). "Evaluation of the lockdowns for the sars-cov-2 epidemic in italy and spain after one month follow up". *Science of the Total Environment*, **725**, 138539.

Van den Driessche, P., and Watmough, J. (2002). "Reproduction numbers and sub-threshold endemic equilibria for compartmental models of disease transmission". *Mathematical biosciences*, **180(1-2)**, 29–48.

van den Driessche, P., and Watmough, J. (2008). Further notes on the basic reproduction number. In *Mathematical epidemiology* (pp. 159–178). Springer Berlin Heidelberg. https://doi.org/10.1007/978-3-540-78911-6_6

Van Doremalen, N., Bushmaker, T., Morris, D. H., Holbrook, M. G., Gamble, A., Williamson, B. N., Tamin, A., Harcourt, J. L., Thornburg, N. J., Gerber, S. I., et al. (2020). "Aerosol and surface stability of sars-cov-2 as compared with sars-cov-1". *New England journal of medicine*, **382(16)**, 1564–1567.

Venkatesh, A., Ankamma Rao, M., and Vamsi, D. (2023). "A comprehensive study of optimal control model simulation for covid-19 infection with respect to multiple variants". *Communications in Mathematical Biology and Neuroscience*, **75**, 1–33.

Verity, R., Okell, L. C., Dorigatti, I., and Winskill, P. (2020). "Estimates of the severity of COVID-19 disease". https://doi.org/10.1101/2020.03.09.20033357

Wang, C., Liu, L., Hao, X., Guo, H., Wang, Q., Huang, J., He, N., Yu, H., Lin, X., Pan, A., et al. (2020). "Evolving epidemiology and impact of non-pharmaceutical interventions on the outbreak of coronavirus disease 2019 in wuhan, china". *MedRxiv*, 2020–03.

Wang, M.-Y., Zhao, R., Gao, L.-J., Gao, X.-F., Wang, D.-P., and Cao, J.-M. (2020). "Sars-cov-2: Structure, biology, and structure-based therapeutics development". *Frontiers in cellular and infection microbiology*, **10**, 587269.

Wang, W., and Zhao, X.-Q. (2012). "Basic reproduction numbers for reaction-diffusion epidemic models". *SIAM Journal on Applied Dynamical Systems*, **11(4)**, 1652–1673.

Willman, M., Kobasa, D., and Kindrachuk, J. (2019). "A comparative analysis of factors influencing two outbreaks of middle eastern respiratory syndrome (mers) in saudi arabia and south korea". *Viruses*, **11(12)**, 1119.

World Health Organization. (2020). Advice on the use of masks in the context of COVID-19. https://www.who.int/publications/i/item/advice-on-the-use-ofmasks-in-the-community-during-home-care-and-in-healthcare-settings-in-the-context-of-the-novel-coronavirus-(2019-ncov)-outbreak

World Health Organization. (2024). Covid-19 epidemiological update: Edition 167. https://www.who.int/publications/m/item/covid-19-epidemiological-update-edition-167

Wu, J. T., Leung, K., and Leung, G. M. (2020). "Nowcasting and forecasting the potential domestic and international spread of the 2019-ncov outbreak originating in Wuhan, China: A modelling study". *The Lancet*, **395(10225)**, 689–697. https://doi.org/10.1016/s0140-6736(20)30260-9

Wu, J., Leung, K., and Leung, G. (2020). "Nowcasting and forecasting the potential domestic and international spread of the 2019-ncov outbreak originating in wuhan, china: A modelling study". *The Lancet*, **395**, 689–697. https://doi.org/10.1016/S0140-6736(20)30260-9

Xie, G. (2020). "A novel monte carlo simulation procedure for modelling covid-19 spread over time". *Scientific reports*, **10(1)**, 13120.

Xie, Y., Wang, Z., Lu, J., and Li, Y. (2020). "Stability analysis and control strategies for a new sis epidemic model in heterogeneous networks". *Applied Mathematics and Computation*, **383**, 125381.

Yang, Z., Zeng, Z., Wang, K., Wong, S. S., Liang, W., Zanin, M., and et al. (2020). "Modified SEIR and AI prediction of the epidemics trend of COVID-19 in china under public health interventions". *Journal of Thoracic Disease*, **12(3)**, 165. https://doi.org/10.21037/jtd.2020.02.64

Zhang, L., Wang, Z.-C., and Zhang, Y. (2016). "Dynamics of a reaction–diffusion waterborne pathogen model with direct and indirect transmission". *Computers and Mathematics with Applications*, **72(1)**, 202–215.

Zhang, Y.-Z., and Holmes, E. C. (2020). "A genomic perspective on the origin and emergence of sars-cov-2". *Cell*, **181(2)**, 223–227.

Zhao, S., Lin, Q., Ran, J., Musa, S. S., Yang, G., Wang, W., and et al. (2020). "Preliminary estimation of the basic reproduction number of novel coronavirus (2019-ncov) in china, from 2019 to 2020: A data-driven analysis in the early phase of the outbreak". *International Journal of Infectious Diseases*, **92**, 214–217. https://doi.org/10.1016/j.ijid.2020.01.050

Zhao, S., Musa, S. S., Lin, Q., Ran, J., Yang, G., Wang, W., and et al. (2020). "Estimating the unreported number of novel coronavirus (2019-nCoV) cases in China in the first half of january 2020: A data-driven modelling analysis of the early outbreak". *Journal of Clinical Medicine*, **9(2)**. https://doi.org/10.3390/jcm9020388

Zhao, Z., Niu, Y., Luo, L., Hu, Q., Yang, T., Chu, M., Chen, Q., Lei, Z., Rui, J., Song, C., et al. (2021). "The optimal vaccination strategy to control covid-19: A modeling study in wuhan city, china".

Zhou, T., Liu, Q., Yang, Z., Liao, J., Yang, K., Bai, W., Lu, X., and Zhang, W. (2020).
    "Preliminary prediction of the basic reproduction number of the wuhan novel
    coronavirus 2019-ncov". *Journal of Evidence-Based Medicine*, **13(1)**, 3–7.

Zhu, Y., and Chen, Y. Q. (2021). "On a statistical transmission model in analysis of
    the early phase of covid-19 outbreak". *Statistics in Biosciences*, **13(1)**, 1–17.

Zhu, Y., and Chen, Y. Q. (2020). "On a statistical transmission model in analysis
    of the early phase of COVID-19 outbreak". *Statistics in Biosciences*. https:
    //doi.org/10.1007/s12561-020-09277-0

BIO-DATA OF THE CANDIDATE

Personal Information:

Name   : Joan Laldinpuii

Father's name   : Lalhmangaiha

Mother's name : PC Lalhnehthangi

Date of Birth   : 24.03.1998

Nationality   : Indian

Gender   : Female

Present Address : Salem Veng, Lunglei, Mizoram

Email   : jodi.slem@gmail.com

Academic Records:

EXAMINATION	BOARD/UNIVERSITY	YEAR	PERCENTAGE/CGPA
H.S.L.C	M.B.S.E	2013	73 %
H.S.S.L.C	M.B.S.E	2015	68 %
B.Sc Mathematics	M.Z.U	2018	85.42 % (Topper)
M.Sc Mathematics	M.Z.U	2020	9.261 CGPA (Gold Medallist)

(JOAN LALDINPUII)

LIST OF PUBLICATIONS

1. Jamal Hussain and Joan Laldinpuii (2023)." Mathematical Modelling for Mitigating Covid-19", *IEEE* 11th *Region 10 Humanitarian Technology Conference (R10-HTC)*, 1160-1167.

2. Jamal Hussain and Joan Laldinpuii (2024), "Vaccination Strategies Against SARS-CoV-2: Evaluating the Impact of Coverage and Efficacy Using a Mathematical Model", *Modeling Earth Systems and Environment*.
   DOI: https://doi.org/10.1007/s40808-024-02110-3.(Impact Factor: 3.0)

3. Jamal Hussain and Joan Laldinpuii (2024). " Optimizing Intervention Strategies for SARS-CoV-2 Control: A Reaction-Diffusion Approach", *High Technology Letters*, DOI:10.37896/HTL30.6/10928.

4. Jamal Hussain and Joan Laldinpuii (2024), "Mathematical Modelling of Covid-19 with Vaccination", *High Technology Letters*,
   DOI: 10.37896/HTL30.6/1093.

5. Jamal Hussain and Joan Laldinpuii, "Quantifying the Impact of Precautionary Measure: A Delay Differential Equation of COVID-19 Spread", *Advance and Applications in Mathematical Science*. (Accepted)

6. Jamal Hussain and Joan Laldinpuii, "Unraveling the Dynamics of SARS-CoV-2: A Mathematical Model Investigating Vaccination Impact and Intervention Strategies", *Advance and Applications in Mathematical Science*. (Accepted)

7. Jamal Hussain and Joan Laldinpuii, "Evaluating the Effectiveness of COVID-19 Precautions: A Delay Differential Equation Approach ", *Journal of Xidian University*. (Accepted)

CONFERENCES/ SEMINARS/ WORKSHOPS

1. Presented a paper "A Mathematical Model of Coronavirus Disease (Covid-19) with Vaccination" in the 1st *International Conference on Advance in Science* organized by Gargaon College Science Forum and IQAC, Gargaon College in collaboration with CSIR-NEIST on 5th and 6th May, 2020.

2. Attended *One week training program on Mathematical Modelling and Computing* organized by Mizoram University, Aizawl-796 004, Mizoram on 26th April to 2nd May, 2022.

3. Presented a paper " Mathematical Modelling for Mitigating Covid-19" in the 11th *IEEE Humanitarian Technology Conference* organized by IEE Gujarat Section at Marwadi University, Rajkot, India on 16th-18th October, 2023.

4. Attended *National Workshop on Role of Mathematical Modeling in Environment (NWRMME-2023)* organized by Mizoram University, Aizawl-796 004, Mizoram during 18th-19th May, 2023.

5. Presented a paper "A Mathematical Model of Coronavirus Disease(COVID-19) containing Vaccination compartment" in the *National Conference on Recent Developments in Mathematics and Computer Science* organized by Mizoram Mathematics Research Association on 13th-14th March, 2023.

PARTICULARS OF THE CANDIDATE

NAME OF CANDIDATE	Joan Laldinpuii
DEGREE	DOCTOR OF PHILOSOPHY
DEPARTMENT	MATHEMATICS AND COMPUTER SCIENCE
TITLE OF THESIS	MATHEMATICAL MODELLING OF COVID-19(SARS-CoV-2) PANDEMIC
DATE OF ADMISSION	: 05.11.2020

APPROVAL OF RESEARCH PRO-
POSAL

1. DRC	: 22/10/2021
2. BOS	: 25/10/2021
3. SCHOOL BOARD	: 29/10/2021
MZU REGISTRATION NO.	: 1501456
Ph. D. REGISTRATION NO.	: MZU/Ph.D./1701 of 05.11.2020
EXTENSION (IF ANY)	: NIL

Prof. M. Sundararajan,

(Head of Department)

Dept. Maths. and Comp. Sc.,

Mizoram University, Mizoram.

ABSTRACT

MATHEMATICAL MODELLING OF
COVID-19(SARS-CoV-2) PANDEMIC

AN ABSTRACT SUBMITTED IN PARTIAL FULFILLMENT OF
THE REQUIREMENTS FOR THE DEGREE OF
DOCTOR OF PHILOSOPHY

JOAN LALDINPUII
MZU REGISTRATION NUMBER : 1501456
Ph.D. REGISTRATION NO: MZU/Ph.D./1701 of 05.11.2020

DEPARTMENT OF MATHEMATICS AND COMPUTER
SCIENCE
SCHOOL OF PHYSICAL SCIENCES
AUGUST, 2024

ABSTRACT

MATHEMATICAL MODELLING OF COVID-19(SARS-CoV-2)
PANDEMIC

BY

JOAN LALDINPUII

Department of Mathematics and Computer Science

Supervisor : Prof. Jamal Hussain

Submitted

In partial fulfillment of the requirement of the Degree of Doctor of

Philosophy in Mathematics of Mizoram University, Aizawl.

ABSTRACT

The COVID-19 pandemic, caused by the SARS-CoV-2 virus, has posed unprecedented challenges globally, affecting millions of lives and overwhelming healthcare systems. The necessity for effective intervention strategies has driven researchers to employ various approaches, including mathematical modelling, to predict and mitigate the spread of the virus. This thesis aims to explore and develop mathematical models that can offer insights into the dynamics of the virus and the impact of different control measures.

The Objectives of this Research are given bellow:

- To study the stability of various Mathematical Models.

- To study the effect of delay created by precautionary measures.

- To study the effect of Diffusion on various Models.

The thesis is structured into seven chapters, each building on the previous one to provide a comprehensive analysis of COVID-19 dynamics and intervention strategies.

Chapter 1: *General Introduction* This chapter presents a general introduction to the COVID-19 pandemic and the role of mathematical modelling in understanding its spread and control.

Chapter 2: *Mathematical Modeling of Vaccination Strategies Against SARS-CoV-2: Assessing Coverage and Efficacy* This chapter provided a comprehensive analysis of various vaccination strategies against SARS-CoV-2 using our proposed $SVEII_AR$ model. The results demonstrated that higher vaccination coverage and efficacy significantly reduce the basic reproduction number R_0 and the number of infections. The model highlights the critical role of vaccination in controlling the spread of COVID-19, emphasizing that achieving high coverage and ensuring effective vaccines are paramount for mitigating the pandemic's impact.

Chapter 3: *Investigating SARS-CoV-2 Dynamics: The Role of Vaccination and Intervention Strategies* This chapter delved into the dynamics of SARS-CoV-2 by incorporating various intervention measures. The $SVEII_AR$ model revealed

that combining vaccination with other interventions, such as social distancing and mask-wearing, substantially decreases the transmission rate. This synergistic approach underscores the necessity of a multifaceted strategy to effectively curb the virus's spread and protect public health.

Chapter 4: *Evaluating Precautionary Measures in COVID-19 Spread: A Delay Differential Equation Approach* This chapter explored the impact of precautionary measures on COVID-19 transmission using delay differential equations. The findings illustrated how delays in implementing measures can lead to significant increases in infection rates. Conversely, prompt and sustained interventions are critical in reducing transmission. The delay differential equation $SEII_AQR$ model provided valuable insights into the timing and effectiveness of various precautionary measures, offering a framework for timely decision-making in pandemic response.

Chapter 5: *Optimizing SARS-CoV-2 Control Measures: Innovative Reaction-Diffusion Techniques* This chapter focused on optimizing control measures for SARS-CoV-2. The model demonstrated how spatial heterogeneity and diffusion processes influence the spread of the virus. By incorporating these factors, the model provided a more nuanced understanding of disease dynamics, highlighting the importance of tailored interventions based on regional characteristics. This approach paves the way for more targeted and effective control strategies.

Chapter 6: *Analysis of a Novel Reaction-Diffusion Model for COVID-19: Evaluating Direct and Aerosol Transmission Strategies* In the final analytical chapter, a novel reaction-diffusion $SEII_AHR$ model was developed to evaluate the dynamics of direct and aerosol transmission of COVID-19. The model revealed that aerosol transmission plays a significant role in the spread of the virus, especially in enclosed spaces. Strategies focusing on improving ventilation and air filtration, alongside traditional direct transmission interventions, were shown to be critical in mitigating overall transmission. This comprehensive model emphasizes the need for integrated approaches addressing both direct and aerosol pathways.

Chapter 7: *Conclusion* This chapter provides a summary and conclusions of the thesis, synthesizing the findings from each chapter and discussing their implications for future research and public health policy.

Throughout this thesis, I have aimed to offer valuable insights for public health policymakers, emphasizing the importance of a multifaceted approach in combating the pandemic. By integrating vaccination strategies, timely precautionary measures, and innovative modelling techniques, this research provides a robust framework for optimizing SARS-CoV-2 control and informs future responses to similar public health crises.